Red Sea Intermediate Water in the Greater Agulhas Current System

Raymond E. Roman

Thesis Presented for the Degree of

DOCTOR OF PHILOSOPHY

in the Department of Oceanography

UNIVERSITY OF CAPE TOWN

July 2007

Acknowledgements

I would like to thank Prof. J.R.E Lutjeharms for his constructive criticism and guidance. Special thanks are also extended to my family who has been incredible support to me. Them in combination with the fact that there is a God that answers prayers have made it possible for me to progress this far. I like to acknowledge J. Karstenzen for making available the matlab scripts of the method used in this thesis. Unpublished data made available by NIOZ (MARE and ACSEX cruises) is gratefully acknowledged as well as financial support from the National Research Foundation.

Table of contents

List of Figures **Page**

Abstract

Despite its small formation volume, Red Sea Intermediate Water (RSIW) has been observed as far south as the Agulhas Retroflection where it is involved in inter-ocean exchange. The spreading and contribution of RSIW has been established previously by combining all available hydrographic data. Considering the variable seasonal formation of RSIW and complex circulations patterns along its path south one would expect variable input of RSIW into the Agulhas Current system. Such variation in input cannot be established by combining all available data and can only be looked at using synoptic hydrographic sections. This is the aim of this thesis. To this aim a multi-parameter water mass analysis was used to establish the water mass content of RSIW along 36 hydrographic sections in the greater Agulhas Current system. In setting up the source water mass matrix a second question arose concerning the vertical spreading range of RSIW when North Indian Deep Water (NIDW), which is also defined as a oxygen poor water mass, was included in the source water matrix.

Results showed the smallest input of RSIW comes from east of Madagascar. In terms of variability, the maximum RSIW contribution differed by more than a 100% between different sections at the southern tip of Madagascar. Although slightly smaller, this variability was also observed in the northern and southern mouth of the Mozambique Channel. Variability in the maximum RSIW contribution strongly correlated with the net transport of RSIW. This variability in the maximum water mass content and net transport of RSIW were observed as far south as the southern Agulhas Current. Differences in the transport and maximum contribution along the Agulhas Current were in some cases more than a 100%. It was thus concluded that the transport of RSIW along the Agulhas Current is highly variable making any estimates of transport for more than a singular hydrographic section impossible. In terms of the maximum density level, RSIW spreading appears in some cases to lie as deep as the $\sim\sigma_n$=27.70 even when NIDW was introduced into the source water matrix. Although RSIW was detected as deep as the 27.7 surface, it was found that the bulk of the high salinity, low oxygen water was assigned as NIDW. In some cases all the high salinity, low oxygen water present was NIDW. We thus conclude that not all high salinity, low oxygen water in the south-west Indian Ocean is RSIW.

Chapter 1
Introduction

Red Sea Intermediate Water in the Greater Agulhas Current System

Global climate change has received a great deal of attention in recent times due to its potential catastrophic impacts. The ocean through the global thermohaline circulation is a major component of the global climate system and therefore of critical importance. South of Africa this involves the exchange of water masses between the Indian and Atlantic Oceans in the Agulhas Current Retroflection region. Relatively salty warm surface and intermediate waters are transferred from the Indian Ocean to the relatively cooler fresher Atlantic Ocean whilst there is an inflow of relatively cooler and fresher North Atlantic Deep water into the Indian Ocean at deeper levels from the Atlantic Ocean. The transfer of Indian Ocean water occurs in the form filaments and mesoscale eddies shed by the Agulhas Current. This Agulhas leakage of Indian Ocean water has been shown to stimulate and stabilize the northern overturning circulation of the Atlantic Ocean that results in the formation of North Atlantic Deep Water (Weijer et al., 1999, 2000). Red Sea Intermediate Water, the warmest and most saline intermediate water in the southwest Indian Ocean has been shown as a contributor of salt and heat to the south-east Atlantic and is therefore of some importance (You et al., 2003).

Red Sea Intermediate Water: Source region and source water characteristics

The Red Sea, a rift valley (~2000 km long and on average <300 km wide) separating Africa and Asia (figure 1), is characterised as having one of the most saline surface waters in the world ocean with salinities reaching 41 psu in the northern part of the basin. This high salinity water is formed as a result of excess evaporation over precipitation (~2.06 m yr^{-1}), negligible river inflow and restricted exchange with the open ocean (Morcos, 1970; Privett, 1959; Bower et al., 2000; Jean-Baptiste et al., 2004; Sofianos et al., 2002). The flow parallel to the main axis is composed of a wind and thermohaline driven upper layer and a deep thermohaline driven system which are separated by a strong pycnocline. Exchange between these two layers is restricted to winter-time deep convection at the northern end and upwelling over the whole area (Woelk and Quadfasel, 1996).Tracer studies, however, would suggest that even the subsurface circulation is largely affected by the seasonal modulation of the monsoon (Eshel et al., 1994).

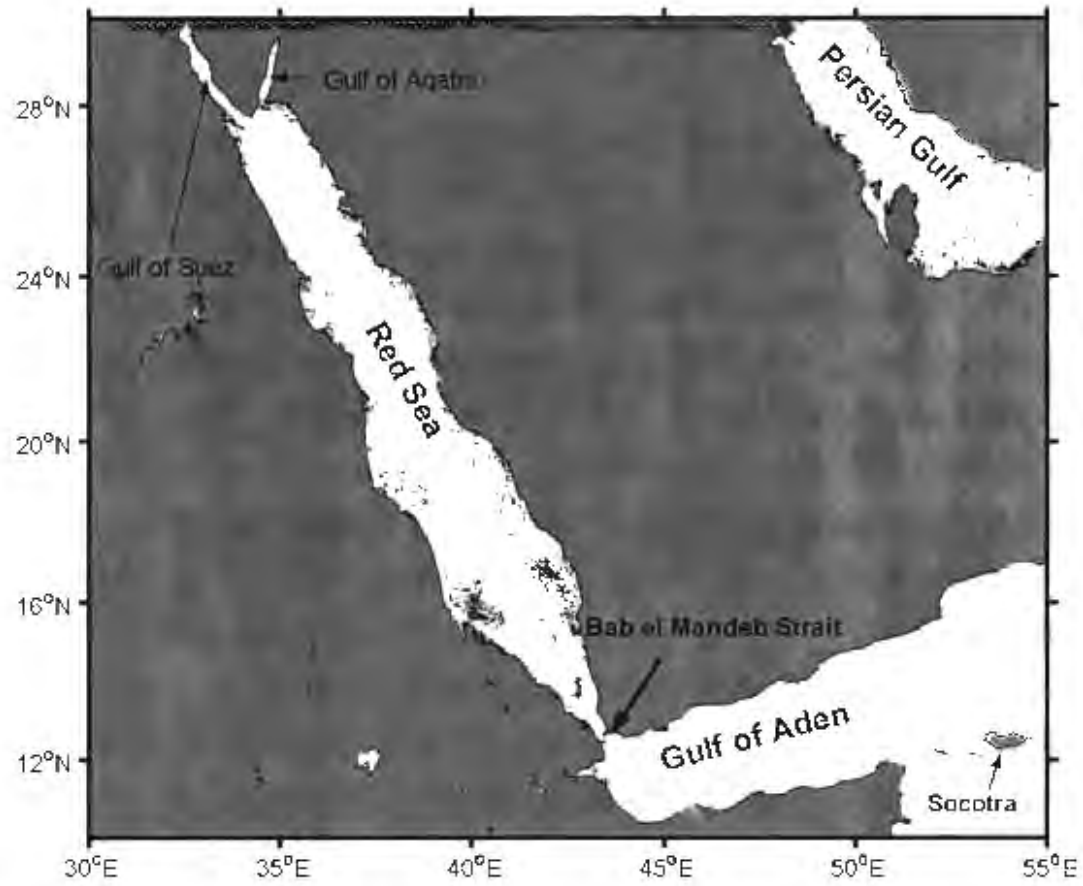

Figure 1: Geographical map of the Red Sea

The formation of Red Sea Intermediate Water occurs in the northern Red Sea mostly during the winter months. Annual estimates of the formation rate varying from 0.06 Sv to 0.16 Sv (Wyrtki, 1974; Maillard, 1974; Cember, 1988; Eshel et al., 1994; Jean-Baptist et al., 2004). Winter-cooled, high density outflows from the Gulf of Suez and Aqaba flow down the continental slope southward filling the deep basin of the Red Sea. These then upwell in the south (Cember, 1988; Woelk and Quadfasel, 1996; Jean-Baptiste et al., 2004).

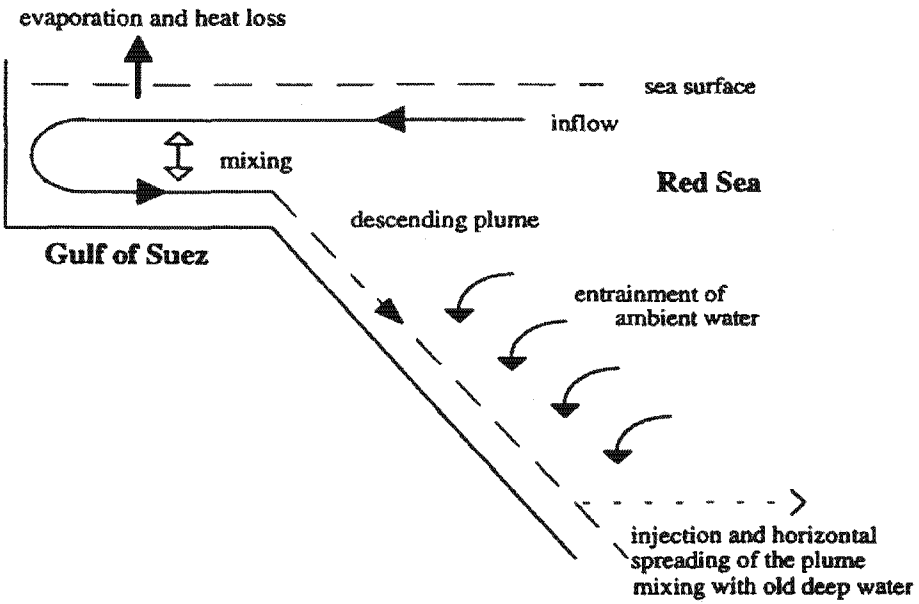

Figure 2: Schematic of the processes involved in wintertime deep water formation in the northern Red Sea (Woelk and Quadfasel, 1996)

The Red Sea's only connection with the open ocean is through Bab el Mandab Strait into the Gulf of Aden-Indian Ocean (figure 1). The shallow Hanish Sill (~137 m) just north of the Strait however prevents any free communication between the deep water of the Red Sea and that of the open ocean (Woelk and Quadfasel, 1996). According to Murray and Johns (1997) the flow through the Strait is is two layered for most of the winter consisting of a deep outflow which extends ~75 m off the bottom and a surface inflow overlying it. In summer the flow changes to a three layer flow structure with a surface outflow (~upper 20 m), a thick intermediate inflow of cold low salinity water and a weak deep outflow (lowest 25 m) that occasionally vanishes. The outflow of Red Sea Intermediate Water (RSIW) through the Bab el Mandeb Strait into the Gulf of Aden varies seasonally and intra-seasonally as a result of the monsoon wind and buoyancy fluxes. The transport of RSIW drops to very low levels in summer (mean ~0.05 Sv, 1 Sv = 10^6 m^3s^{-1}) stopping altogether for brief periods. During the winter months the transport of RSIW reaches a maximum (mean ~0.6 Sv). Strong intra-seasonal variability is however observed during this period with the outflow varying between 0.2 and >0.7 Sv on time scales of several days up to a month (Murray and Johns, 1997).

As the outflows descends from the sill depth of ~150 m along two channels it entrains less dense, fresher Gulf of Aden water and reached a neutral buoyancy in the western part of the Gulf in multiple, intermediate depth, high salinity layers which are centred around 600 m. Different mixing histories along the two bathymetric channels have been thought to cause this multilayered structure (Bower et al., 2000). In summer the outflow waters equilibrate upstream of where the bathymetric channels empty into the Tadjura Rift whereas in winter this occurs where the channels empty into the Rift. This occurs between the potential density range 27.0 and 27.5 (Bower et al., 2002, 2005). The product waters formed in winter also differs slightly from that formed in summer. In winter the outflow waters are warmer and saltier compared to summer. This difference is not attributed to differences in the Red Sea; rather it is as a result of a change in the mixing regime (Bower et al., 2000). Once in the Gulf of Aden, RSIW is strongly influenced by cyclonic and anti-cyclonic eddies. RSIW gets entrained in these eddies and modified via mixing with less saline Indian Ocean water (Bower et al., 2000; Bower et al., 2002). In the eastern half of the Gulf RSIW is concentrated in a single thick layer centred on the potential density level ~27.2 (Bower et al., 2000).

RSIW in the Indian Ocean

As RSIW leaves the Gulf of Aden it spreads into the Indian via the Socotra Passage and around Socotra Island. During the winter monsoon RSIW spreads into the Indian Ocean mainly through the Socotra Passage, down the African continental slope (Schott and Fischer, 2000; Beal et al., 2000). This pattern seems to change during the summer monsoon with the RSIW inflow into the Somali Basin coming from the east. This means that RSIW rounds Socotra Island rather than flowing through the passage (Fisher et al., 1996). During this period RSIW flows southward, principally toward the interior of the Indian Ocean whilst RSIW along the western boundary re-circulates northwards through the Socotra Passage (Fisher et al., 1996; Beal et al., 2003). Beal et al. (2003) have speculated that this stemming of the export of RSIW at the western boundary occurs during the late summer monsoon when the Somali Current runs deep. The outflow of RSIW via these routes into the Indian Ocean has been shown to occur at least partially in the form of lenses or anti-cyclonic eddies (Shapiro and Maschanov, 1991; Shapiro et al., 1994; DiMarco et al., 2002; Chapman et al., 2003). During the winter months, north of 2°S RSIW seems to hug the African continental

slope very closely whereas south of here it has been found to become separated from the slope. RSIW however still crosses the equator close to the western boundary at a depth of about 750 m (Quadfasel and Schott, 1982). Beal et al. (2000) have pointed out that south of the equator near 5°S RSIW occurs at temperatures between 4-8°C and is generally found between 700 to 1000 m.

As RSIW moves from its source southward (figure 3) it continually mixes with Antarctic Intermediate Water (AAIW) which has its source further south and Indonesian Intermediate Water (IIW) with its source at the Pacific-Indonesian Throughflow (You, 1998). This southward spreading into the greater Agulhas Current System occurs mostly on the western boundary of the basin.

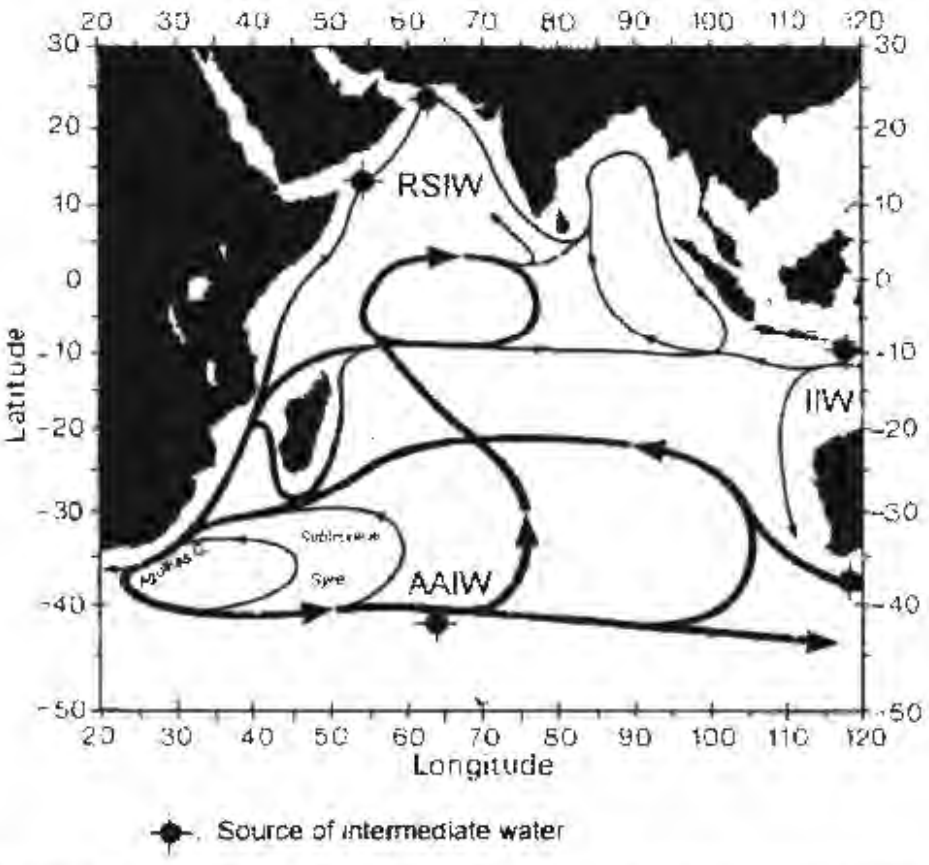

Figure 3: Schematic of the intermediate circulation in the Indian Ocean (You, 1998)

The greater Agulhas Current System

Flow regime in the greater Agulhas Current System

The subtropical gyre in the southwest Indian Ocean with the Agulhas Current on its western boundary has the strongest flow of any of the other two southern hemisphere oceans (Quartly and Srokosz, 2002; Stramma and Lutjeharms, 1997). The Agulhas Current has three source regions namely the Mozambique Channel, the East Madagascar Current and water coming from the east that forms part of a recirculation cell in the southwest corner on the Indian Ocean. Most of the estimated 70 Sv transported by the Agulhas Current comes from water that recirculates northwards in the western and central parts of the Indian Ocean Basin (Gordon et al., 1987; Stramma and Lutjeharms, 1997). The northward branching water comes from the Agulhas Return Current that at the Agulhas Retroflection transports around 54 Sv whilst around 76°E the transport eastward is only 15 Sv (Veronis, 1973; Stramma, 1992; Stramma and Lutjeharms, 1997, Lutjeharms and Ansorge, 2001).

The flow field in the Mozambique Channel has been unclear until recently and has now been shown to be dominated by large southward moving anti-cyclones and smaller cyclones (de Ruijter et al., 2002 and Chapman et al., 2003). The anti-cyclonic eddies appear to be over 300 km wide and penetrate right to the bottom. These eddies propagate at an average speed of 4.5 km/day and there is typically a train of 3 anti-cyclonic eddies present in the channel at any one time (de Ruijter et al., 2002; Schouten et al., 2003). The volume transport through the channel across its narrowest part has remarkably large variations that range between 20 Sv northwards to 60 Sv southwards. Anti-cyclones are usually formed in this region when the current regime is strong (Ridderinkhof and de Ruijter, 2003). It has been suggested by Schouten et al. (2003) that these eddies are caused by Rossby waves with a periodicity of about 90 days. It has however been observed (Schott et al., 1988; Quadfasel and Swallow, 1986) that the dominant period is around 50 days making it unclear how these waves interact to form these eddies. On average 4 anti-cyclonic eddies are formed each year (Schouten et al., 2003).

Across the narrowest part of the Mozambique Channel close to the African continental slope, the Mozambique Undercurrent flows northwards at two different depths namely at intermediate and deep levels (1500 and 2500 m) (Ridderinkhof and de Ruijter, 2003). Calculations in the southern part of the channel showed it carried roughly 5 Sv of Atlantic origin water into the channel of which the intermediate depth water was mostly Antarctic Intermediate Water (AAIW) whilst at its deeper level it carried North Atlantic Deep Water (NADW) (de Ruijter et al., 2002). The average flow based on current meter observations through the narrowest section is 14 Sv southward. (Ridderinkhof and de Ruijter, 2003). This is similar to the eddy induced transport of about 15 Sv calculated by de Ruijter et al. (2002).

The East Madagascar Current is fed by the South Equatorial Current (SEC) which flows westward around 17-25°S. The SEC current bifurcates when it reaches Madagascar into a northern and a southern branch around 20°S (Chapman et al., 2003). The southern branch of the East Madagascar Current has a width of <120 km (Lutjeharms et al., 1981, Swallow et al., 1988; Chapman et al., 2003). Most studies put transport of the current around 20 Sv (Warren, 1981; Swallow et al., 1988; Schott et al., 1988; Donohue and Toole, 2003). Water from both the northern and southern branches of the East Madagascar Current (EMC) reaches the Agulhas Current proper. In the case of the former it occurs via the Mozambique Channel within eddies moving down the channel (DiMarco et al., 2002). From previous publications the flow of water from the southern branch of the EMC to the Agulhas Current is less clear. Schott et al. (1988) have indicated that the EMC rounds the southern end of the island and flows westward as a stream. The flow at the southern termination has been pictured by Tchernia (1980); supported by hydrographic data (Gründlingh, 1993) and surface drifter data (Shenoi et al., 1999) as flowing up the west coast of the island turning anti-clockwise at the northern end of the Mozambique Channel after which its joins the Mozambique Current. Other possibilities are that it flows due west to the African shelf and then turn south to the Agulhas Current or that it never reaches the African coast but retroflects in the vicinity of the Madagascar ridge as satellite remote-sensing would suggest (Gründlingh 1987, 1993; Lutjeharms, 1988; DiMarco et al., 2000). Conditions associated with the Agulhas Current that allows it to retroflect are the background eastward flow, conservation of potential vorticity and bottom topography (de Ruijter and Boudra, 1985; Ou and de Ruijter, 1986; de Ruijter

et al., 1999; Matano, 1996). In the case of the EMC the background flow is to the west which means that any Retroflection would be localised and probably result in the formation of anti-cyclonic eddies (de Ruijter et al., 2004). These eddies have been observed using satellite remote sensing (Lutjeharms and Machu, 2000) and from hydrographic observations (de Ruijter et al., 2004). De Ruijter et al. (2004) found that anti-cyclonic eddies are associated with a cyclonic eddy with a central jet between the two. Each of these eddies had a diameter of about 250 km. They also show that the water associated with anti-cyclones comes from the oceanic side of the current whilst the water from the cyclone is from the inshore part of the EMC. Between April 1995 and June 2000 they identified 17 dipoles each feeding about 8 Sv of EMC water per dipole into the Agulhas Retroflection region assuming each is roughly the same size as the one sample during the Agulhas Current Sources Experiment (ACSEX) cruise. The south-westward movement of these dipoles and their interaction with the Agulhas Retroflection have been shown to result in an extreme early reflection of the Agulhas Current (de Ruijter et al., 2004).

The Agulhas Current

The main axis of flow for the Agulhas Current is southwest along the continental slope of the east and south coast of South Africa. Harris (1972) has reported that a front in both hydrographic properties and acceleration potential separates the inner and outer portions of the Agulhas Current. Water shoreward of the front was inferred to come from the Mozambique Channel whilst the offshore cooler, fresher, high oxygen waters came from the East Madagascar Current and the recirculation cell in the southwest Indian Ocean. This observation has also been highlighted in other studies (Menanché, 1963; DiMarco et al., 2002). In the northern Agulhas Current (27-34°S) the current flows along a narrow continental shelf and steep continental slope where it exhibits minimal meandering (Gründlingh, 1983). The passage of a Natal Pulse (Lutjeharms and Roberts, 1988) can however result in the current meandering more than 100 km offshore. The passage of Natal Pulses ranges from 5-20 days at 32°S (Beal and Bryden, 1999). In the absence of these pulses the mean current core is at the surface some 20 km offshore at 32°S (Beal and Bryden 1997). The steady flow observed in the northern Agulhas Current changes south of Port Elizabeth. Here the shelf widens and the current flows in a meandering fashion (Lutjeharms et al., 1989; van der Vaart and de Ruijter, 2001).

Farther downstream the current separates from the shelf and retroflects with the majority of the water flowing eastward as the Agulhas Return Current (Lutjeharms and van Ballegooyen, 1988; van der Vaart and de Ruijter, 2001). As explained above this Retroflection in the current occurs as a result of the conservation of potential vorticity, bottom topography and the prevailing eastward flow. The position of the Retroflection is highly variable and lies between 10 and 21°E (Lutjeharms and Gordon, 1987). The eastward flowing Agulhas Return Current meanders significantly partly due to topographical features like the Agulhas Plateau (Lutjeharms and van Ballegooyen, 1984; Quartly and Srokosz, 2002). The current terminates finally between 66°E and 70°E (Lutjeharms and Ansorge, 2001).

Although the majority of water in the Agulhas Current System is carried back into the Indian Ocean as part of the subtropical gyre, approximately 9 Sv at intermediate level alone carried into the Atlantic Ocean annually as a result of the Retroflection occluding and forming Agulhas rings that move off into the south Atlantic Ocean (Boebel et al., 2003). This process of ring shedding is controlled upstream by Natal Pulses that move down the current (van Leeuwen et al., 2000). On average 4 to 5 rings are shed annually (Byrne et al., 1995; Schouten et al., 2002). The rings are on average 200 km in diameter and have been observed to merge, split, deform and to reconnect with the Agulhas Retroflection (Olson and Evans 1986; Lutjeharms and Valentine 1988; Schouten et al., 2000; Boebel et al., 2003). Slightly smaller (120 km diameter) cyclones interact with these rings in the southeastern Cape Basin or "Cape Cauldron" resulting in vigorous mixing and stirring taking place (Boebel et al., 2003). Leakage from the Indian Ocean to the Atlantic Ocean also occurs on a much smaller scale in the form of filaments (Lutjeharms and Cooper, 1996). Model studies have shown that this leaking Indian Ocean water plays an important role in the Atlantic meridional overturning circulation (Weijer et al., 1999, 2001).

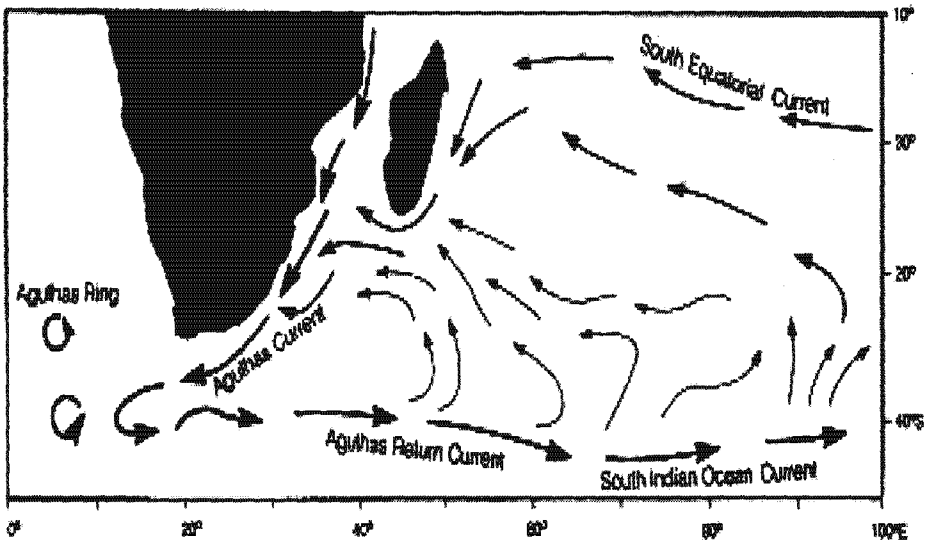

Figure 4: Schematic of the greater Agulhas Current System (Lutjeharms and Ansorge, 2001)

RSIW in the greater Agulhas Current System

What do we know or what has been proposed?

Mozambique Channel

Chapman et al. (2003) have suggested that RSIW crosses the equator as individual boluses which are mixed into the background near the Comores, raising the salinity. This high salinity water then crosses the Davie Ridge in anti-cyclonic eddies formed at the northern part of the Mozambique Channel. These anti-cyclonic eddies dominate most of the southward flow in the channel. Along the southward path of these eddies isopycnal mixing occurs between RSIW in the eddy cores and Antarctic Intermediate Water present in the Mozambique Undercurrent (de Ruijter et al., 2002). On average 4 anti-cyclonic eddies move through the Mozambique Channel annually (Schouten et al., 2003). You et al. (2003) has indicated that RSIW contributes between 20-30% (on $\sigma_n > 27.45$; σ_n = neutral density surface) of intermediate water that passes through the Mozambique Channel and feeds into the Agulhas Current. Beal et al. (2000) have in turn suggested this value to be only around 6-7%. This large difference in the source water mass contribution is primarily due to the fact that the two studies have two different source regions. The source region used in Beal et al. (2000) is much closer to the actual source of RSIW in the eastern part of the Gulf of Aden, which results in a much more saline RSIW source water type. In fact, in their study they showed that through mixing the RSIW contribution at the position where You et al. (2003) defined

it was only 40% of the total water mass content. Taking this into account the two results seems comparable. The lower contribution of RSIW on the upper density levels seen in You et al. (2003) suggests a greater interaction of RSIW with AAIW and IIW. Indications are that water coming through the Mozambique Channel contributes primarily to the inshore portion of the Agulhas Current (Harris, 1972; Gordon et al., 1987; DiMarco et al., 2002).

East Madagascar Current

The southward flow of RSIW does not exclusively occur through the Mozambique Channel as low oxygen, high salinity water, has also been found within the East Madagascar Current (Donohue and Toole, 2003). Float data presented by Chapman et al. (2003) do not support this finding. It has to be noted however that the level at which the lowest oxygen occurred is much deeper than the 800-900 m depth of the float data. You et al. (2003) have indicated a RSIW contribution on σ_n = 27.55 of above 10%. This neutral density surface is somewhat deeper than the maximum 900 m depth of floats. This contribution is however considerably smaller than that observed in the Mozambique Channel (You et al., 2003; Beal et al., 2000). Above this level their calculations concur with that of Chapman et al. (2003) that little or no RSIW is found in the East Madagascar Current. The low oxygen, high nutrient water found east of Madagascar seems to be concentrated in the East Madagascar Current and not offshore (Donohue and Toole, 2003).

Agulhas Current

South of the Mozambique Channel, RSIW has been observed as part of the Agulhas Current proper as a filament (Toole and Warren, 1993) and as individual lenses in other parts of the South Indian Ocean as far south as 28°S (Gründlingh, 1985; Donohue and Toole, 2003). Although there is a general net southward movement of RSIW in the Agulhas Current, Donohue et al. (2000) claim some part of it is transported northwards again by means of the Agulhas Undercurrent. The transport of RSIW down the northern section of the Agulhas Current is restricted to the landward side of the current with AAIW on the outside (Gordon et al., 1987; Beal and Bryden, 1999). In the northern part of the Agulhas Current, RSIW contributed 6-7% to the intermediate water as defined by Beal et al. (2000) which resulted in a 0.95 Sv RSIW

transport off the east coast of South Africa (Beal et al., 2000; Beal and Bryden, 1999). This transport result was similar to the influx of product water at their source region resulting in their hypothesis that whatever RSIW is mixed into the Indian Ocean is eventually exported at the western boundary. Further south, RSIW has been traced as far as the Agulhas Current Retroflection region and has also been observed in rings that have been shed into the Cape Basin of the South Atlantic Ocean (Gordon et al., 1987; Valentine et al., 1993; van Aken et al., 2003). Thus despite its small formation volume RSIW contributes to the supply of heat and salt that stimulates and stabilizes the meridional overturning cell in the Atlantic (Weijer et al., 1999; 2001). Between 4 and 5 rings are shed each year by the Agulhas Current (Byrne et al, 1995; Schouten et al., 2000). At the Retroflection You et al. (2003) have indicated a RSIW contribution of between 10-20%. This is slightly higher than that observed by Beal et al. (2000) if you consider the source water type used by You et al. (2003) is considered to represent only 40% of the source water type used by Beal et al. (2000).

In the Cape Basin, the intermediate water from the Indian Ocean is quickly dissociated from the rings where it is blended with water from the South Atlantic Current and the tropical Atlantic (McDonagh et al., 1999; Schouten et al., 2000). The RSIW source characteristics are thus rapidly obscured by the vigorous mixing which takes place there (Boebel et al., 2003). Transport measurements of intermediate water masses calculated by You et al. (2003) indicate a net transport of 0.3±1 Sv of RSIW eastward down the Agulhas Current at 20°E. In their section across the south east Atlantic RSIW is responsible for 0.4±1 Sv of the total transport. Not all RSIW in the Agulhas Current is transferred into the South Atlantic as some patches of RSIW can still be seen spreading along the Agulhas Return Current (You, 1998).

From the evidence above it would appear that RSIW spreading in the Indian Ocean and more specifically in the south west Indian Ocean have been fairly well described and quantified. Some questions however still remain unresolved that previous studies could not address. These questions are detailed in the following section.

Chapter 2

Key Questions

1) **What is the flow pattern of RSIW in the greater Agulhas System and is the flow intermittent?**

Both You et al. (2003) and Beal et al. (2000) have used a combination of all the available hydrographic data to determine the general spreading path of RSIW. Beal et al. (2000) used a simple mixing model in which RSIW is defined as a single water type using only its salinity characteristic over the density range 27.0 to 27.6. Their two-end-member mixing model consisted only of RSIW and AAIW, excluding IIW (or Banda Intermediate Water as they have referred to it) since its salt input was unresolvable from zero when compared to its salinity when it leaves the Indian Ocean, assuming this happens via the Agulhas Current. You (1998) and You et al. (2003) on the other hand have used up to 6 or 7 parameters (temperature, salinity, oxygen, silicates, phosphates, nitrates and potential vorticity) to define their water masses which included IIW. Instead of a examining a single water type over the entire density range in which it is found they computed the influence of RSIW on a number of density surfaces using several water types. Their model thus seems to be more robust than that used by Beal et al. (2000) and could help resolve the influence of IIW. On the other hand, You et al.'s density range was much smaller than that of Beal et al. (2000) and in most cases the maximum contribution of RSIW seemed to occur on the deepest density surface which means that the RSIW layer was not fully resolved. When comparing the results from Beal et al. (2000) with the maximum contributions from You et al. (2003) and taking into account the difference in the water mass definitions discussed above, the spreading pathways and water mass contributions are comparable.

Both the models of Beal et al. (2000) and You et al. (2003) have serious shortcomings. It has been mentioned in several papers that RSIW spreading in the Indian Ocean occurs at least partially in the form of boluses or lenses (Shapiro et al., 1994; DiMarco et al., 2002). Whilst combining all the available hydrographic data, as done by both Beal et al. (2000) and You et al. (2003) would give a good idea of the spreading paths it cannot resolve temporally varying features such as these. Also the influence of Mozambique eddies(which dominate the southward flow in the Mozambique Channel) on the transport of RSIW as events or as distinct lenses cannot be established in this way. This possible intermittency of the presence of RSIW is an important aspect of its role and can only be determined by using synoptic

hydrographic data. By comparing synoptic sections at similar geographical positions with each other and with other sections further upstream this possible intermittency of RSIW in the Agulhas Current System will be investigated by quantifying the RSIW contribution along the individual hydrographic sections.

2) What is the full spreading range of RSIW in the south-west Indian Ocean?

The range over which RSIW spreads in the Indian Ocean is somewhat difficult to establish. Warren et al. (1966) have noted RSIW influence over the potential density range 27.0 to 27.66 or a neutral density range of about 27.15 to 27.8. Its core in the southern Indian Ocean at 32°S has been reported to lie as deep as 27.6 ($\sim\sigma_n$=27.8) whilst in the northern Indian Ocean it has been reported to lie as shallow as 27.2 ($\sim\sigma_n$ =27.25). This change can be attributed to much more vigorous mixing taking place between RSIW, IIW and AAIW above the 27.6 density level. Beal et al. (2000) in their study have used the potential density range 27.0-27.6 ($\sim\sigma_n$ =27.125-27.7) whilst Donohue and Toole (2003) have reported RSIW influence between the potential density range 27.0 and 27.7 ($\sim\sigma_n$ =27.125-27.8). However, with a maximum neutral density level of 27.7-27.8, warm oxygen poor North Indian Deep Water (NIDW) as defined by Beal et al. (2003) and reported to lie below the neutral density level 27.6 needs to be considered as a possible source water mass. Wyrtki (1971) supports the idea of introducing NIDW, as just below this level there are a phosphate and nitrate maxima in the northern Indian Ocean. These maxima do not have their origin in the Red Sea but in the northern Indian Ocean and are formed as a result of nutrient regeneration (Wyrtki, 1971; You, 2000). Also considering dianeutral upwelling in the northern Indian Ocean at this level this water mass might have some influence within the RSIW layer (You, 1999).

Characteristics of NIDW

NIDW as defined by Beal et al. (2003) is generally understood to be upwelled Circumpolar Deep Water that enters the Arabian Basin from the south (Toole and Warren, 1993; Warren, 1992). The water mass was classified as having a high salinity, low oxygen and high nutrients (Warren and Johnson, 1992; Spencer et al., 1982; Mantyla and Reid, 1995). Its high salinity and low oxygen is obtained as a result of vertical mixing with intermediate level water masses (Warren 1992, You

1999). Warren (1992) identified this water mass as lying roughly between 1500 to 3500 m which would put its upper potential density level around 27.7 (σ_n =27.8) which is slightly lower than that indicated by Beal et al. (2003). Wyrtki (1971) has indicated the phosphate and nitrate maxima to lie between the potential density range 27.6 and 27.8 (σ_n =27.7-27.8). Along the I07 World Ocean Circulation Experiment (WOCE) section (figure 5.1) the nitrate maximum is situated just below the 27.7 neutral density surface which would make it safe to assume that the upper range of NIDW lies from around 27.6 as indicated in Beal et al. (2003). Since NIDW gets its high salinity (and temperature), low oxygen signature from RSIW/PGW it would be safe to say that the range of influence of RSIW would thus be much deeper than the maximum 27.55 neutral density surface used by You et al. (2003) in line with observations in Donohue and Toole (2003) in the southern Indian Ocean.

NIDW spreading in the south-west Indian Ocean

Figures below give some indication of the spreading of NIDW as defined by Beal et al. (2003) by means of the nitrate maximum. In the Indian Ocean the nitrate maximum that is found below the neutral density 27.7 (figure 5(a)) shaols to just below the 27.6 level at the Mascarene Plateau. South of the Mascarene Plateau (figure 5(b)) we observe the intrusion of southern Indian Ocean water masses just below the 27.8 neutral density level resulting in a double nitrate and phosphate maximum. This nitrate maximum just below the 27.6 neutral density level is also observed in sections just north of the narrowest part of the Mozambique Channel (figure 5(c)) and at the southern mouth of the channel (figure 5(d)). Along the section at the southern mouth the oxygen minimum is now lying much deeper and the nitrate maximum co-inside (figures 5(d) and 5(e)). In most cases along this section the salinity maximum is also found at this level. This is in contrast to what is observed just north of the Mozambique Channel where the oxygen minimum and intermediate salinity maximum are separate from the nutrient maximum. Further south this nutrient maximum layer is described in some detail by Toole and Warren (1993) as lying a few hundred meters below the AAIW at around 1500 or roughly on the neutral density surface 27.7. They do not assign a specific name to this layer but indicate more extreme core values to have come from the north with more moderate values coming from the south.

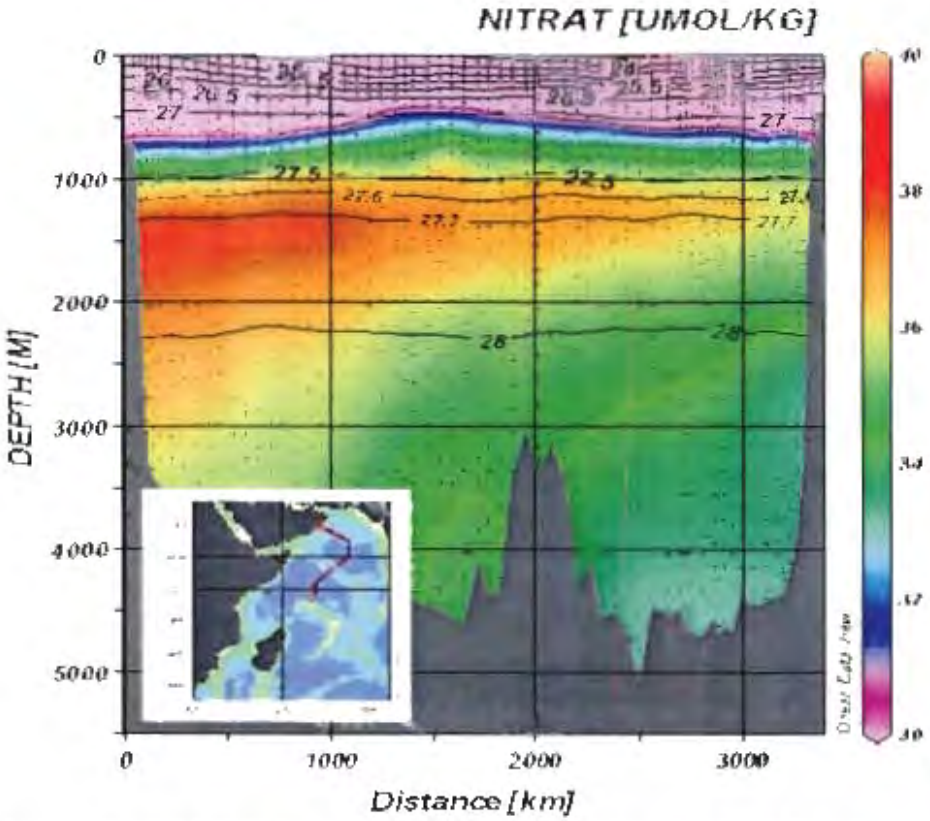

Figure 5(a): Distribution of dissolved nitrate in µmol/kg along the section shown in inserted map

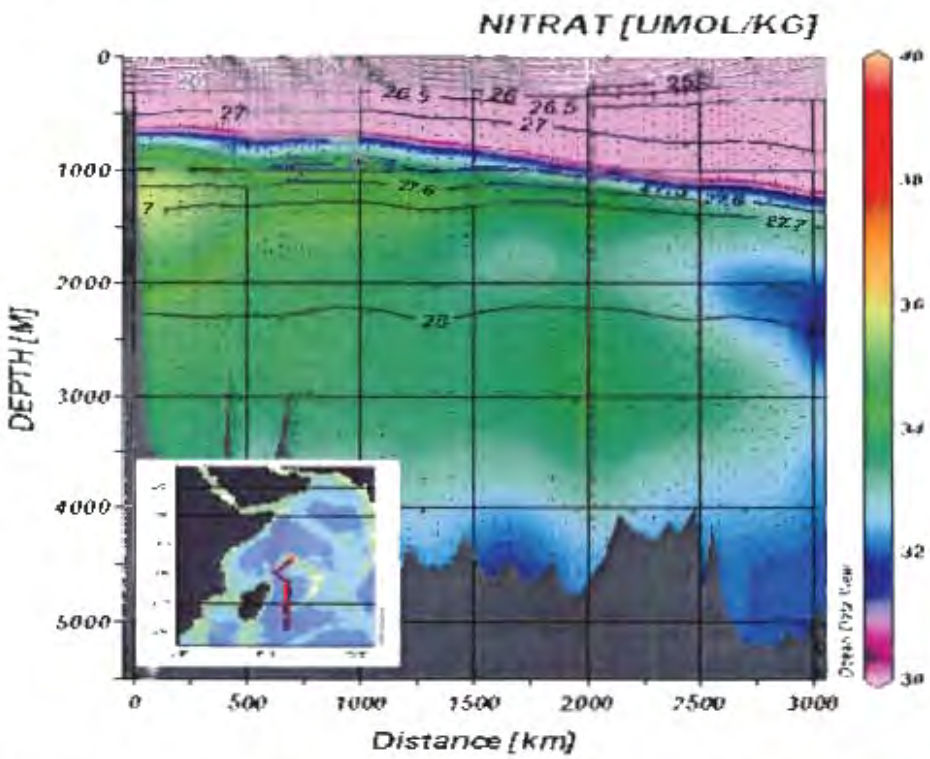

Figure 5(b): Distribution of dissolved nitrate in µmol/kg along the section shown in inserted map

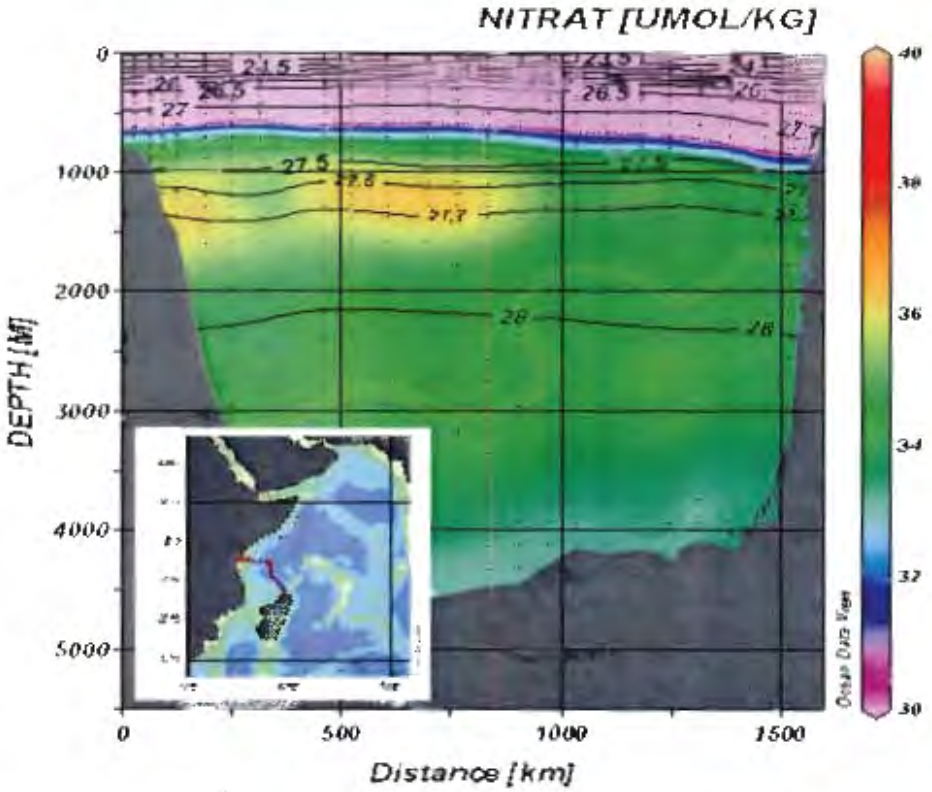

Figure 5(c): Distribution of dissolved nitrate in μmol/kg along the section shown in inserted map

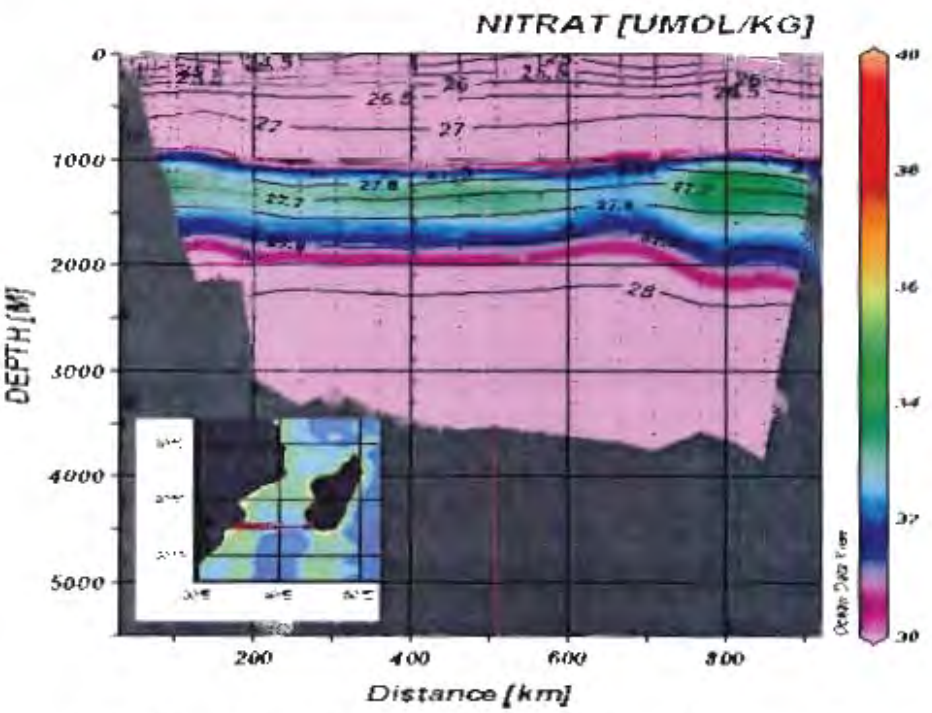

Figure 5(d). Distribution of dissolved nitrate in μmol/kg along the section shown in inserted map

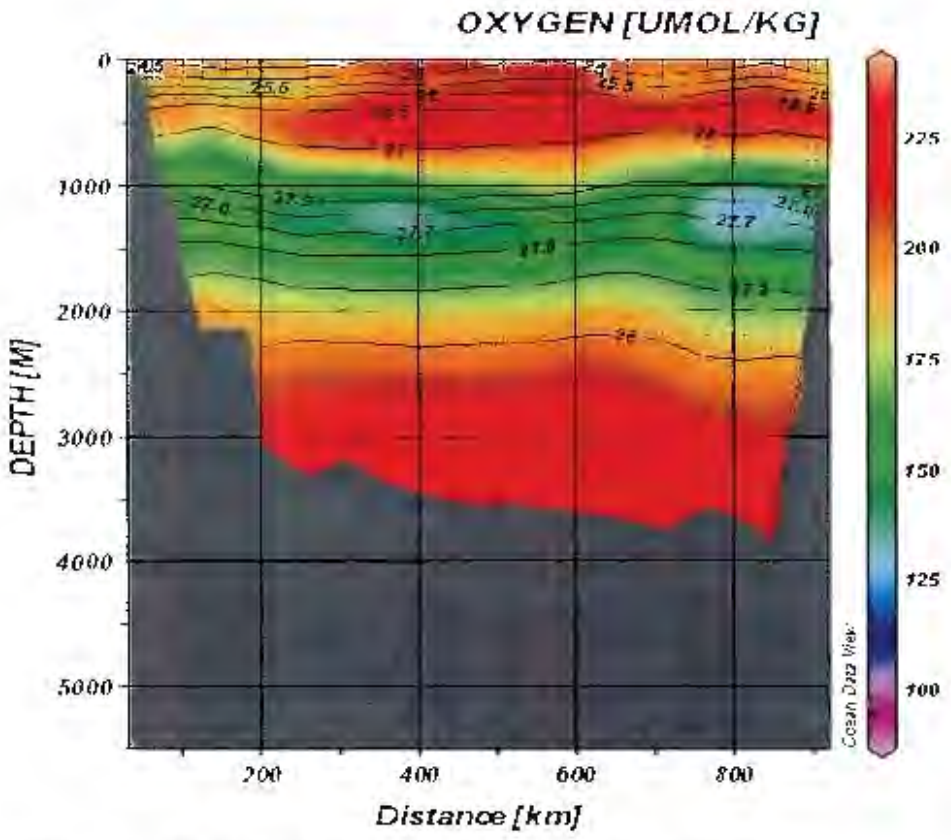

Figure 5(e): Distribution of dissolved oxygen in µmol/kg

It would thus seem that RSIW does spread below the maximum 27.55 neutral density level used in You et al. (2003). If this is the case, it is unclear what the full density range would be if NIDW is considered at the deepest density level of RSIW. Both RSIW and NIDW have a salinity maximum and oxygen minimum relative to other water masses in their density range and in conjunction with diaeutral upwelling it would make it difficult to separate these two water masses when simply using salinity or oxygen. Until now all low oxygen, high salinity water in the south west Indian Ocean has mostly been termed RSIW even on neutral density surfaces as deep as 27.7. It could thus be possible that NIDW could have been wrongly attributed as RSIW. This leaves us with the questions about what the full range of RSIW is in the south western Indian Ocean and would this result in the reclassification of previously observed high salinity, low oxygen water. Also, if RSIW spreading does reach this deep the complete quantification of RSIW transport is yet to be established using the much more robust method used in You et al. (2003) since their study did not take into account the full spreading range.

Chapter 3
Data and Methods

The data used in this study comprise both historic and modern bottle data collected within the region of the greater Agulhas Current system. The historic data were obtained from the National Ocean Data Centre database and included such cruises as the Agulhas Retroflection Cruise (ARC) completed in 1983 and historical sections of the Mozambique Channel completed in the 1960's. The modern data comprised all World Ocean Circulation (WOCE) cruise lines (I03, I04, I05w, I05p, I06, SR02, A12) in the greater Agulhas Current region, data collected during the Mixing of Agulhas Rings Experiment (MARE) I, MARE II and data collected during the Agulhas Current Sources Experiment (ACSEX) I, ACSEX II and ACSEX III cruises. The individual cruise tracks and station positions are shown in figures 6, 14, 24 and 31. The cruise tracks of the MARE were through a singule ring that was sampled twice roughly five months apart. The cruises were sub-divided into four regions, namely the northern source regions (regions A and B), the northern Agulhas Current (region C) and the southern Agulhas Current and Retroflection region (region D) (figure 6).

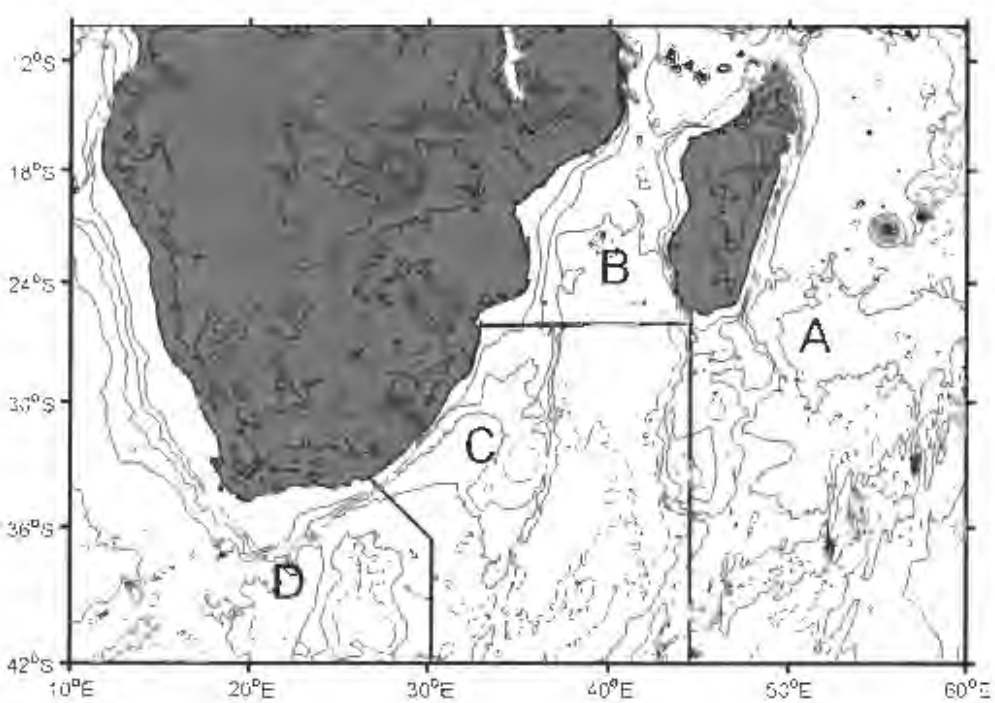

Fig 6: Map showing the regional sub-divisions of the Agulhas Current System

The linear system of equations which are solved for the relative contributions of all the source water types for each data point can be expressed as:

$$Gx - d = R$$

where G contains the matrix of parameter values that define the water types, d the vector containing the data, x the relative contributions of the water samples and R the vector with the residuals. In order to make parameters of incommensurable units comparable, normalization of the source water matrix is necessary which is obtained by normalizing the elements in G by the whole range of each parameter in G. This can be written as

$$G'_{ji} = (G_{ji} - \overline{G}_j)/\sigma_j$$

where

$$\overline{G}_j = 1/n \sum_{i=1}^{n} G_{ji}$$

and

$$\sigma_j = \sqrt{1/n \sum_{i=1}^{n} (G_{ji} - \overline{G}_j)^2}$$

All variables are unfortunately not equally reliable due to differences in instrumental or analytical accuracy and/or high environmental variability. To account for this each parameter is weighted using:

$$W_j = \sigma_j^2 / \delta_{j\max}$$

where $\delta_{j\max}$ is the maximum of the water mass variances of parameter j (Tomczak and Large, 1989). For a more detailed description of the OMP analysis methodology the reader is referred to Tomczak and Large (1989), Poole and Tomczak (1999) and Tomczak (1999). In this study a total of seven parameters were utilized to describe the individual source water types: temperature, salinity, oxygen, phosphate, nitrate, silicate and potential vorticity (see Table 1). In order to take into account nutrient regeneration the following equations were used to calculate the initial phosphate and NO (Broecker, 1974) using a Redfield ratio of 175 (Broecker and Takahashi, 1985) for the ARC and WOCE cruises:

$$PO_4^{\circ} = PO_4 - (O^{sat}_2 - O_2)/Re$$

$$NO = 9NO_3 + O_2$$

This increases the number of conservative parameters as suggested by You (1998) along with temperature and salinity. However, to retain the vertical resolution of the MARE I, MARE II and ACSEX I cruises, non-conservative phosphate and nitrate had to be used because of the limited number of oxygen samples that were analyzed on those cruises. It is assumed that this will have minimal effect on our results since according to You (1998) water mass spreading occurs at a far greater rate than nutrient regeneration.

Source water matrix

You et al. (2003) has indicated intermediate source water masses in the south Indian Ocean to be RSIW, south Indian Antarctic Intermediate Water (siAAIW), Drake Passage Antarctic Intermediate Water (dAAIW), Indonesian Intermediate Water (IIW) and a transformation end member of these sources, Atlantic Antarctic Intermediate Water (aAAIW) over the neutral density range 27.25 and 27.55. This range is based exclusively on the spreading of the AAIW core in the Indian Ocean. Beal et al. (2003) have indicated the spreading range of RSIW to be between $\sim\sigma_n$=27.1 and 27.6. This is almost similar to the range used by You (1998). Some studies suggest the range to be greater, but Wyrtki (1971) indicate that in the source region this would include the phosphate and nitrate rich waters below $\sim\sigma_n$=27.60 which do not have their origin in the Red Sea but in the northern Indian Ocean. At the shallow end of the density range ($\sim\sigma_n$=27.25) You et al. (2003) have shown RSIW to add little to the water mass mixture in the south-west Indian Ocean. For the sake of comparison it is assumed that this is the upper range of RSIW in the south-west Indian Ocean. It was also decided for that reason to keep the maximum density level at $\sim\sigma_n$=27.55 which is only slightly shallower than the maximum $\sim\sigma_n$=27.6. Although the two boundary density surfaces of this analysis are kept similar to that of You et al. (2003) the source water matrix is slightly different to that of You (1998, 2003) as it is found that along the sections under investigation aAAIW could be excluded. You (2002) argued that aAAIW must be included when looking at a basin-wide water

mass mixing scheme. It does not represent a water mass volume but is apparently needed by the mixing model. However with the introduction of the overlaying and underlying central and deep water masses this water mass was not required by the mixing model I used. These water masses did not form part of You (2002) source water matrix.

Data used to define the above-mentioned intermediate water masses in their respective source regions were obtained from the National Ocean Data Centre (NODC) database. RSIW source water types were defined in the area 51-55°E and 12-15°N just north of the Socotra Passage through which it flows into the Indian Ocean on the $\sim\sigma_n$=27.25 and $\sim\sigma_n$=27.55 surfaces (Table 1). This area does not extend as far east as the source region used by You (1998) whose area extended into the Arabian basin to include the influence of Persian Gulf intermediate water. Schott and Fisher (2000) have however shown the main route for RSIW into the Indian Ocean to be through the Socotra Passage during the winter monsoon when the outflow of RSIW is at it strongest and not around it as the source region used by You (1998) suggests (his Figure 3) and thus the smaller source region. Noted however is that You (1998) included a shallower density surface $\sim\sigma_n$=27.125 on which Persian Gulf water would have some influence and would probably necessitated the larger source region.

The source water types for siAAIW and dAAIW were defined in the source regions 60-64°E and 30-40°S for siAAIW and from 50 to 60°W just north of the Subtropical Convergence for dAAIW on $\sim\sigma_n$=27.25, $\sim\sigma_n$=27.40 and $\sim\sigma_n$=27.55 (Table1). The source region for siAAIW coincided with the region where the youngest AAIW in the western central Indian Ocean was found by Fine (1993) using CFC analysis. dAAIW has its origins in the South Pacific and enters the Atlantic through the northern Drake Passage after which it is modified in the Falkland Loop (McCarthy, 1977; Piola and Gordon, 1989; You, 2002) where it is defined in this study. The above two water mass definitions do not differ dramatically from that used by You et al. (2003). IIW has its origins in the deep basins of the Indonesian archipelago and was defined in the geographic box 110-120°E and 8-15°S on $\sim\sigma_n$=27.25 and $\sim\sigma_n$=27.55 (Table 1). Whilst this geographic box is similar to that defined by You (1998) and used in You et al. (2003), source water definitions are considerably different. The source water

type described in these two studies is slightly warmer and saltier which is described as North Indian Intermediate Water (NIIW) by Bray et al. (1997) and Wijffels et al. (2002). This water mass (NIIW) is formed north of the equator through mixing of marginal sea (RSIW) outflows and cross-equatorial intermediate water flow (IIW and AAIW) (Wijffels et al., 2002; You, 1998).

In order for the system of equations to be over-determined the number of source water types used to establish the relative contribution of each of the source water masses cannot exceed the number of parameters. The ten water types described above would thus make the system of just seven parameters under-determined. Furthermore large mass conservation residuals around $\sim\sigma_n$=27.25 and $\sim\sigma_n$=27.55 from initial tests of our method over the density range 27.25-27.55 suggested the inclusion of Indian Ocean Central Water (ICW) or Upper Circumpolar Deep Water (UCDW) and North Indian Deep Water (NIDW) in some of the hydrographic sections. This is understandable since ICW overlay all the intermediate water masses in the southern Indian Ocean whilst UCDW and NIDW are overlaid by the intermediate water masses. To accommodate for this the range over which RSIW spreads in the Indian Ocean ($\sim\sigma_n$=27.25-27.70) was split into two ranges $\sim\sigma_n$=27.25-27.40 (above the AAIW minimum) and $\sim\sigma_n$=27.40-27.70 (below the AAIW minimum) reducing the number of source water types needed for each range. This was not always sufficient along some sections and it was decided that along the sections where ICW or UCDW was necessary for inclusion in the source water matrix, IIW would be defined only on $\sim\sigma_n$=27.25 in the shallower density range whilst siAAIW on $\sim\sigma_n$=27.55 would be excluded from the source water matrix over the neutral density range 27.40-27.70. This seemed feasible since according to You et al. (2003), siAAIW contributes only a small amount of the water mass fraction compared to dAAIW on this density level and the fact that IIW is almost exclusively found on $\sim\sigma_n$=27.25 whilst being almost absent below this density level in this region. Mass conservation residuals indicating how well the defined source water masses represent the actual water masses show this assumption was feasible. The above assumption was also tested by reducing the density range $\sim\sigma_n$=27.25-27.55 into two ranges namely $\sim\sigma_n$=27.25-27.40 and $\sim\sigma_n$=27.4-27.55 using all the source water definitions within the ranges and in order to make sure it made no difference to the RSIW source water mass fraction. Along the

sections where either ICW or UCDW were included, IIW made up less than 5% of the water mass fraction over the entire range or was totally absent and could thus be excluded from the water mass matrix. This was also the case along MARE I and II sections.

UCDW west of Madagascar was defined in the same region as dAAIW upon the neutral density surface on which its characteristic oxygen minimum surface (σ_n =27.8) is found whereas for east of Madagascar it was defined in the same geographic area as siAAIW. This is based on You (2000) showing most of the deep water in the Natal Valley flowing in from the west whilst east of Madagascar its origins are in the south. NIDW was defined in the Arabian Basin in the geographical box 10-20°N and 55-70°E on σ_n =27.75 more or less where the phosphate and nitrate maximums are found. It is assumed that You (2000) was correct in his assumption that NIDW is simply aged UCDW and this water mass was only included when using non-conservative nitrate and phosphate i.e. when oxygen was a limiting parameter, thus reducing the number of conservative variables. The use of non-conservative parameters would introduce an error due to the biological effect that is implicitly reflected in the residual term. In order to make all sections comparable this calculation was done for all the sections under investigation. This calculation is also useful in comparing the full range of RSIW spreading with that of previous publications that did not use the conservative variables initial phosphate and NO. ICW was defined on σ_n =27.0 using data collected along the WOCE I5 cruise track. Mass conservation residuals for the individual sections are not shown, but all fell within 1% of the water mass conservation percentage. The only exceptions to this were along some sections that extended to the Sub-Tropical Convergence. All the source water definitions are shown in Table 1.

After its percentage contribution at each data point had been determined the transport of RSIW was calculated using geostrophic calculations for the ARC, WOCE and MARE sections whilst for the ACSEX sections the more accurate Lowered Acoustic Doppler Current Profiler (LADCP) measurements was used. In order to take the possible patchy distribution of RSIW into account the transport of RSIW at each station had to be calculated separately. For the sections along which geostrophic

calculations was used, the transport at each station was simply the average value between two points. The geostrophic transport associated with the first and last stations was assumed to be that calculated for the first and last station pairings. The transport at each station within the chosen neutral density range was then multiplied with the average RSIW contribution of the corresponding stations for the specified density range.

Tables

Table 1: Source water type definitions using potential temperature, salinity, oxygen, silicate, NO, initial phosphate and potential vorticity as well as the parameter weight

Water type on neutral density	Θ(°C)	S	O_2 (µmol/kg)	H_4SiO_4 (µmol/kg)	NO (µmol/kg)	$PO_4°$ (µmol/kg)	PV ($x10^8 s^{-3}$)
ICW (27.0)	9	34.69	212	10.0	389	1.04	0.110
siAAIW (27.25)	6.8	34.57	206	16.6	441.2	1.21	0.103
siAAIW (27.40)	4.5	34.36	210	33.0	490	1.53	0.080
siAAIW (27.55)	3.51	34.40	192	49.0	489.9	1.45	0.062
dAAIW (27.25)	4.40	34.17	297	10.3	509	1.55	0.090
dAAIW (27.40)	3.46	34.20	278	20.0	535	1.65	0.050
dAAIW (27.55)	2.78	34.30	233	42.0	509	1.66	0.061
RSIW (27.25)	12.01	35.75	24.1	42.3	298	1.15	0.035
RSIW (27.55)	9.09	35.48	19.9	74.9	336.7	1.34	0.025
IIW (27.25)	6.89	34.61	85.3	72.6	403.9	1.38	0.030
IIW (27.55)	4.65	34.60	91.9	105.9	425.8	1.43	0.017
UCDW (27.80) Atlantic Ocean	2.53	34.55	170	74	490.4	1.56	0.043
UCDW (27.80) Indian Ocean	2.67	34.58	176	65.4	490	1.60	0.040
NIDW (27.80)	5.10	35.03	39	110	384.8	1.49	0.020
Weight	42	42	4.8	1.57	5.92	1.8	4.34

Chapter 4
Results

4.1) Region A: East and south of Madagascar

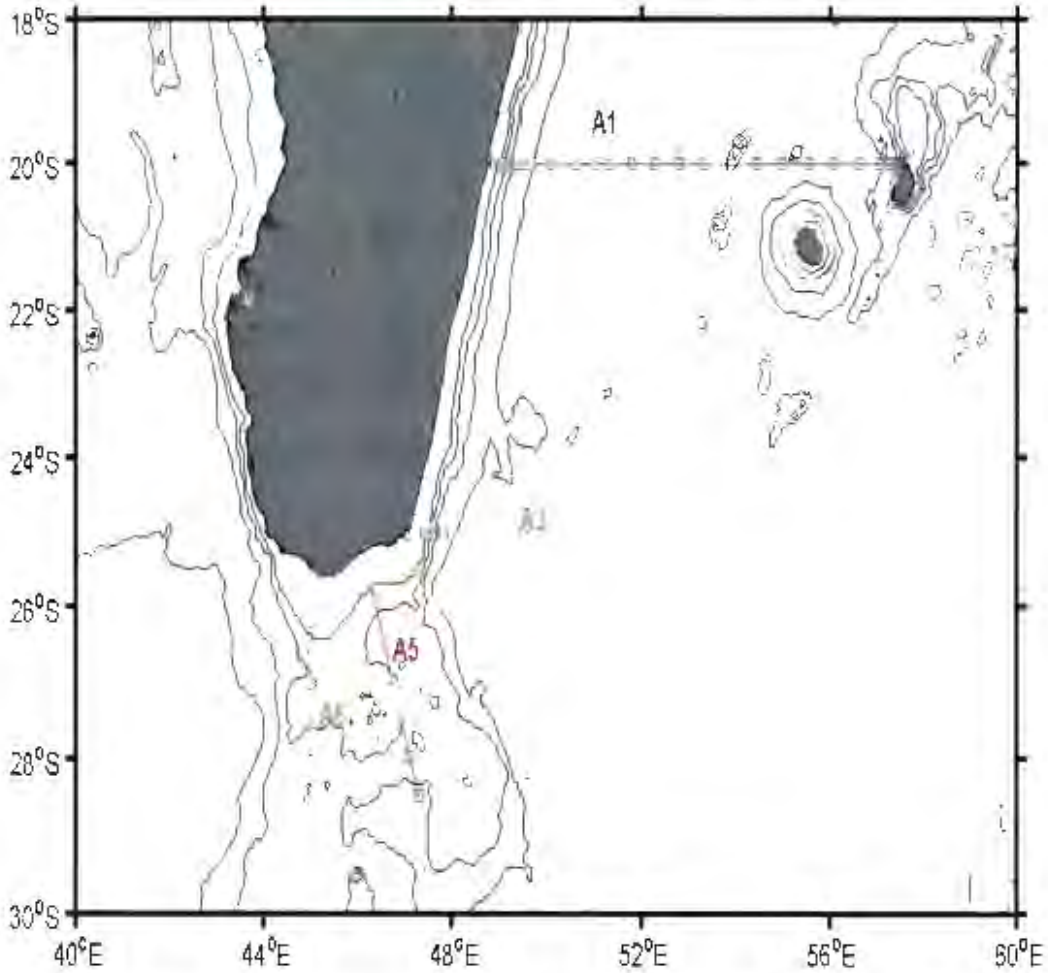

Fig 7: Map showing the individual cruise tracks of the hydrographic sections investigated in region A. Sections A1 and A2 were completed as part of WOCE whereas sections A3 to A6 were completed as part of ACSEX II

4.1) Region A (East of Madagascar)

WOCE sections

Section A1 (WOCE 103 line) (see figure 7)

This section runs along 20°S where the South Equatorial Current bifurcates northward and southward at the coast to form the East Madagascar Current. Surface currents did not reveal a strong southward boundary current as the section was too close to the South Equatorial bifurcation latitude. The strongest velocities along this section were instead associated with a weak surface trapped offshore cyclonic eddy centred at 50°E (Donohue and Toole, 2003). The circulation patterns described above can clearly be seen in the isohalines and isotherms with the cyclonic eddy observed about 120 km offshore (figure 8(ii)). At intermediate depths the high salinity, low oxygen minimum water core normally associated with RSIW appears 400-600 km offshore below the potential density level 27.25 (figure 8(ii)).

Along this section two high content RSIW cores were observed at the upper part of the density range 27.4-27.7 (figure 8(i)b) that were situated between 400-550 km offshore and around 900 km offshore. In these cores RSIW contributed between 15-20% of the water mass mixture in the samples. The core at 450-550 km coincided with the high salinity, low oxygen core whilst the core observed around 900 km does not show this strong correlation (see figures 8(i)b and 8(ii)). When NIDW was introduced into the source water matrix RSIW still contributed 15-20% of the water samples with the highest RSIW contribution cores still observed around 450-600 km offshore and 850 km offshore. LADCP measurements indicate the flow to be southward at the two data points where the RSIW core mixing fraction is between 15-20% whilst between these two data points the flow is northward (Donohue and Toole, 2003). This above 10% mixing fraction or contribution is consistent with what You et al. (2003) calculated for the neutral density surface 27.40 for this region. In the density range 27.25-27.4 (figure 8(i)a) the RSIW content was less than 10% of the water sample in three cores which are associated with the underlying RSIW layer (figures 8(i)a and b). In terms of it spreading range the RSIW core is found to move southward above the neutral density level 27.64 (around 1200 m). Its range of influence does however reach down to the maximum neutral density level of 27.68 in both matrix configurations.

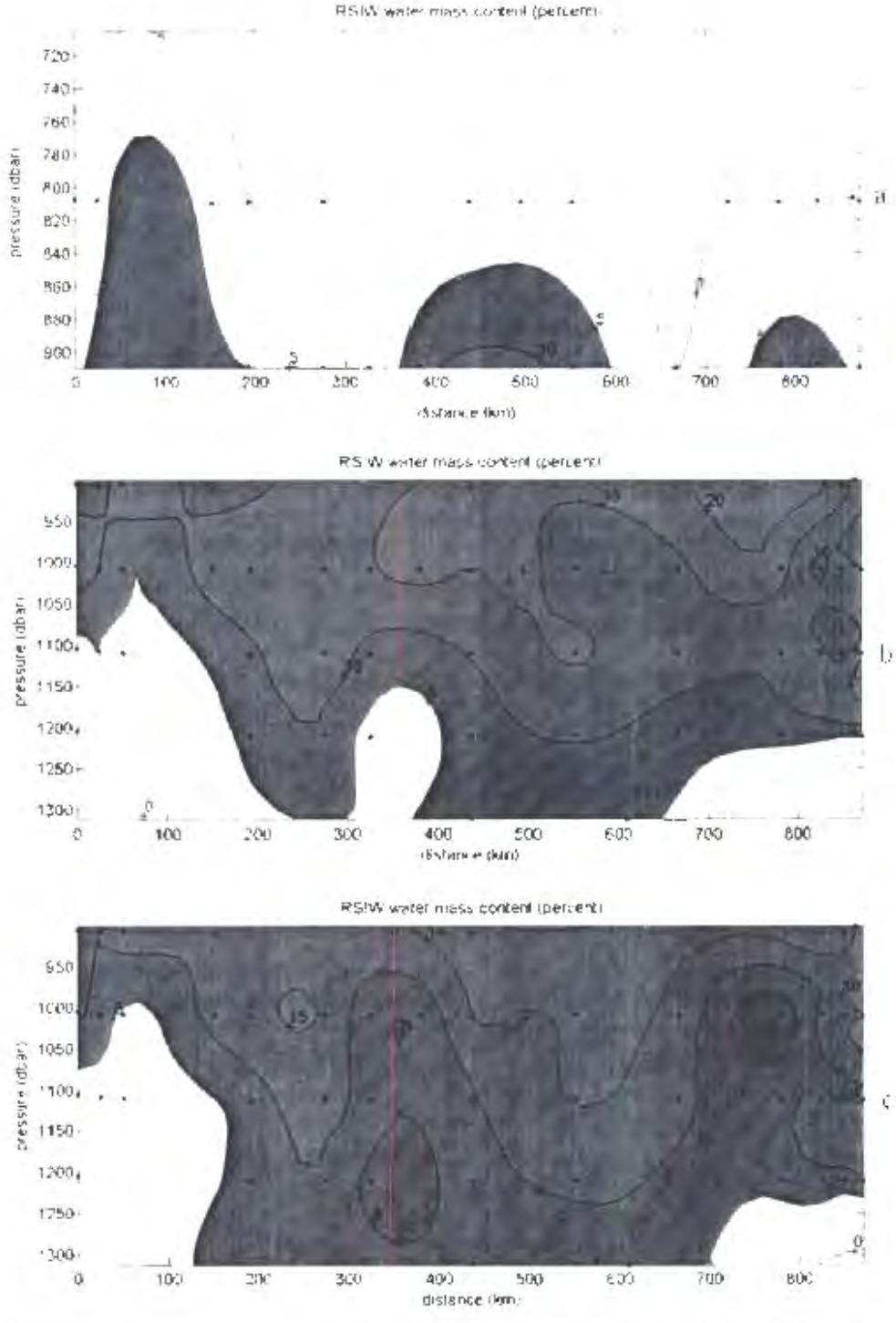

Fig 8 (i): a) RSIW contribution over the density range σ_n=27.25-27.40 (b) RSIW contribution without NIDW in the source water matrix over the range σ_n=27.40-27.70 (c) RSIW contribution with NIDW in the source water matrix over the range σ_n=27.40-27.70 along section A1 (see figure 7). Dots indicate bottle sample locations.

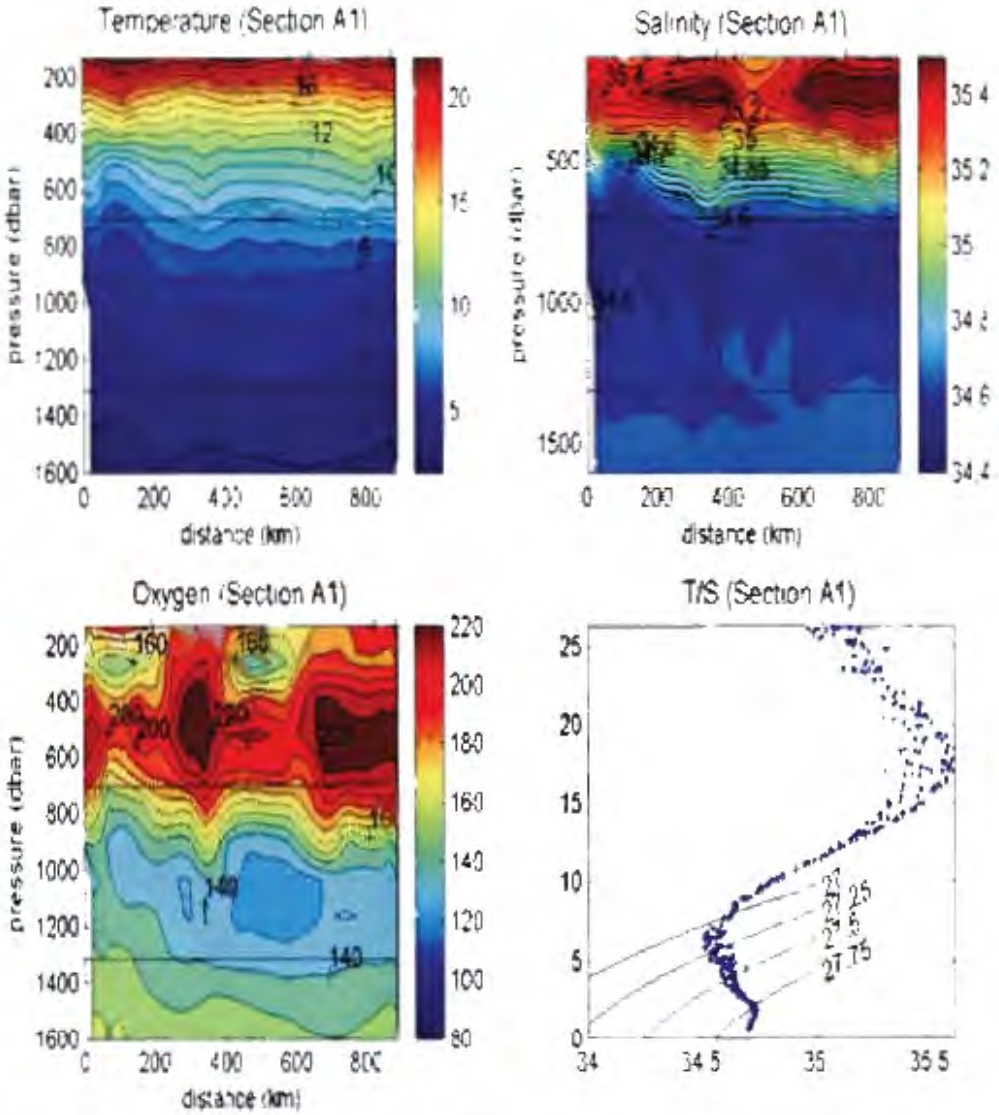

Fig 8 (ii): Property plots along section A1 (see figure 7) of temperature, salinity, oxygen and a T/S plot

Section A2 (WOCE I04east) (see figure 7)

This section at the southern tip of Madagascar crossed a well-developed East Madagascar Current with observed surface currents reaching 80 cm/s (Donohue and Toole, 2003). The current is clearly shown in the downward slope in the isotherms and isohalines (figure 9(ii)) from the slope to about a 100 km offshore. Further offshore the upward slope in the isotherms and isohalines is consistent with the strong northward flow shown in Donohue and Toole (2003) which they have associated with a cyclonic eddy. This difference in the flow regime compared to the previous section is also accompanied by a shift in the property distributions. The position of the oxygen minimum and salinity maximum are now observed along the Madagascar slope as opposed to offshore. As would be expected the salinity minimum also appears fresher than that observed along section A1 indicating stronger southern influence (figure 9(ii)).

The distribution pattern of RSIW within the density range 27.40-27.70 indicates two separate cores situated along the Madagascar slope and around 200 km offshore (figure 9(i)b). The core along the slope is associated with the East Madagascar Current whilst the offshore core appears to be associated with a cyclonic eddy (Donohue and Toole, 2003). Along the slope, RSIW at its core contributes between 15-20% of the water sample whilst offshore (around 200 km offshore) it contributes only 10-15% of the water sample. However when NIDW is introduced into the water mass matrix, the RSIW core along the slope contributing only slightly less than 15% to the water mass mixture of the sample (figure 8(i)c). Offshore it still contributes 10-15% to the water mass mixture of the sample at around 1000 m. This finding is consistent with You et al. (2003). NIDW was, however, not part of the source water matrix in You et al. (2003) was and we found it to contribute 20% of the water mass mixture centred on the neutral density surface 27.6 (between 1050 and 1100 m) along the Madagascar slope. It would thus appear that most of the high temperature, high salinity and low oxygen water found along the East Madagascar slope is NIDW as opposed to RSIW as indicated by Donohue and Toole (2003). Over the density range 27.25-27.40 RSIW contributed just less than 10% (figure 8(i)c) of the water sample at it core along the Madagascar slope. More over, much of the high salinity, low oxygen water seen in the T/S around the potential density level 27.25 and above (figure 8(ii)) is found to be IIW which is also described as a low oxygen, high salinity water mass

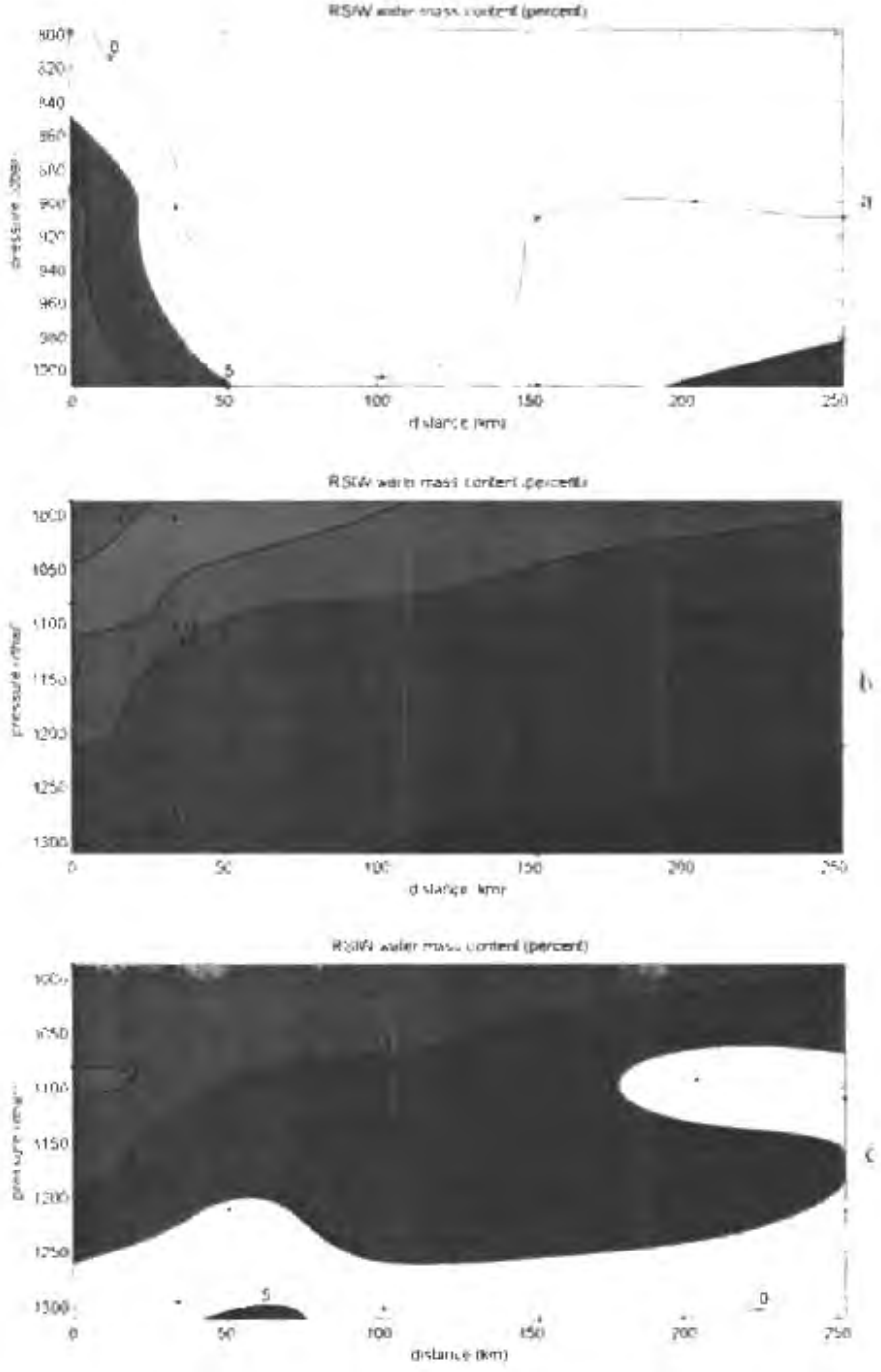

Fig 9 (1): a) RSIW contribution over the density range σ_θ=27.25-27.40 (b) RSIW contribution without NIDW in the source water matrix over the range σ_θ=27.40-27.70 c) RSIW contribution with NIDW in the source water matrix over the range σ_θ=27.40-27.70 along section A2 (see figure 7). Dots indicate bottle sample locations.

ASCEX II cruise sections

Section A3 (see figure 7)

This east-west section was occupied along the same latitude as the previous section. However, the flow regime was slightly different than the flow along section A3 in that there was no offshore eddy. The flow regime is clearly depicted in the slopes of the isotherms and isohalines (figure 10b). Similar to section A2, an oxygen minimum was observed along the Madagascar slope but indications from the T/S diagram indicate very little to no RSIW (figure 10b). Due to limited bottle samples the maximum density in our chosen density range for this section was only 27.49 which meant CDW and NIDW could be excluded from the source water mass matrix. Initial runs over density range 27.40- 27.70 indicated that we could also exclude dAAIW water types on the neutral density surfaces 27.4 and 27.55 from the water mass matrix. Results from the revised source water mass matrix show that RSIW content in the water samples collected was less than 5% (figure 10a) which would support the previous findings that the East Madagascar Current transports small or negligible amounts of RSIW into the greater Agulhas Current System above the neutral density 27.55 (You et al., 2003). The higher oxygen minimum in this density range (figure 10b) compared with the previous hydrographic section correlates well with the slightly lower water mass contribution. The sparse vertical resolution does however make any concrete conclusions impossible.

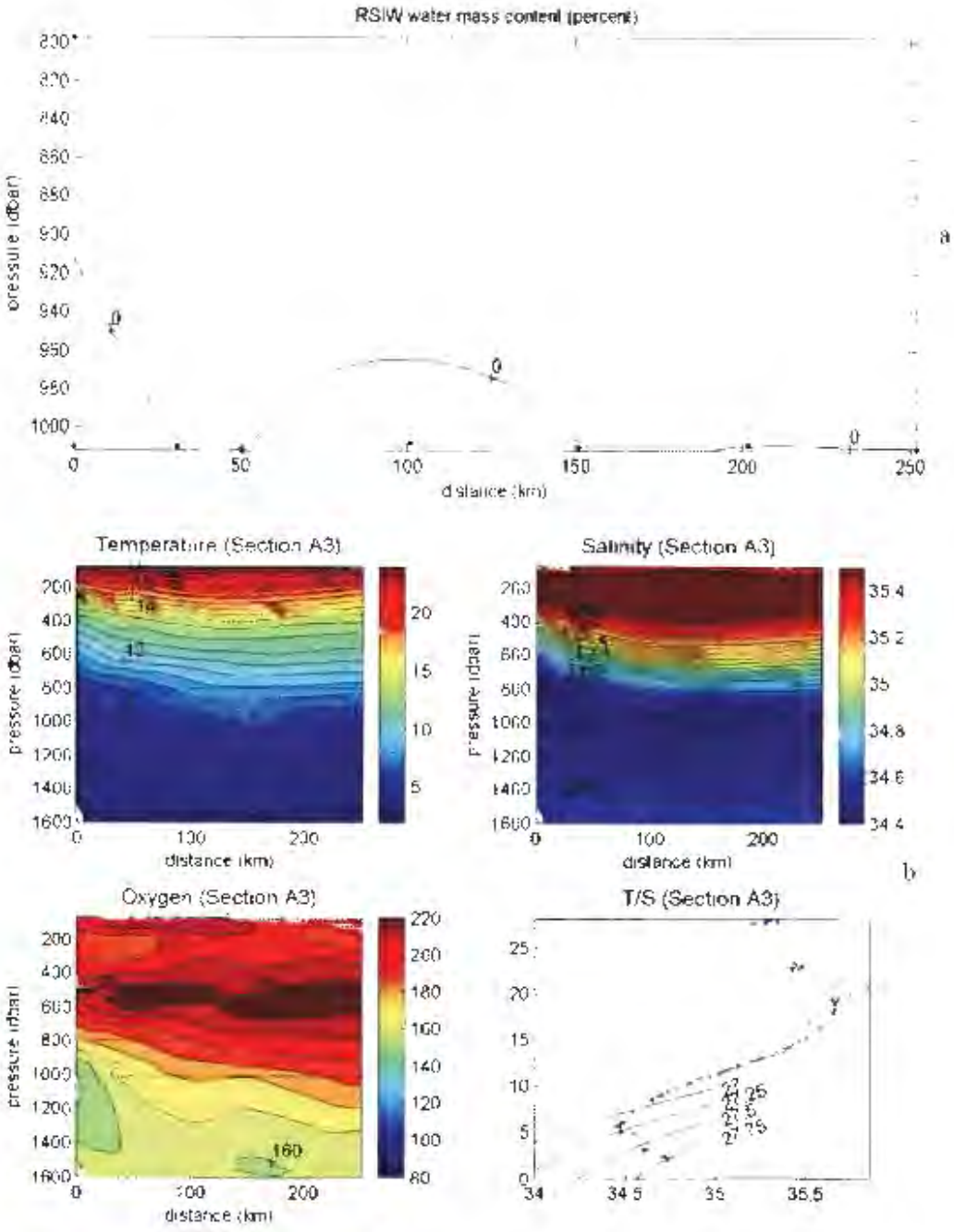

Fig 10: a) RSIW contribution over the density range 27.25-27.485 and (b) property plots of temperature, salinity, oxygen and a T/S plot along section A3 (see figure 7). Dots indicate bottle sample locations.

Section A4 (see figure 7)

The flow regime displayed by the isotherms and isohalines for section A4 (figure 11c) show a boundary current flowing south west and offshore north eastward flow. No RSIW was detected in the density range 27.25-27.40 and could thus not be contoured consistent with low RSIW contributions observed in the abovementioned section where it contributed at most less than 5% of the water mass mixture of the samples. The T/S diagram on the other hand would suggest that RSIW is present within this density range (figure 11c). As in the case of section A2 this high salinity water was found to be IIW. Over the density range 27.40-27.70 RSIW at its core contributed between 15-20% of the water sample concentrated close to the continental slope (figure 11a). In contrast with sections A1 and A2, RSIW contributed at most 7% to the water samples along the slope when NIDW was included in the source water matrix. This is a significant reduction in its contribution that was not observed along the other two sections. As was the case along section A3, RSIW influence is observed as deep as the neutral density surface 27.64 which was the deepest neutral surface within the deeper neutral density range.

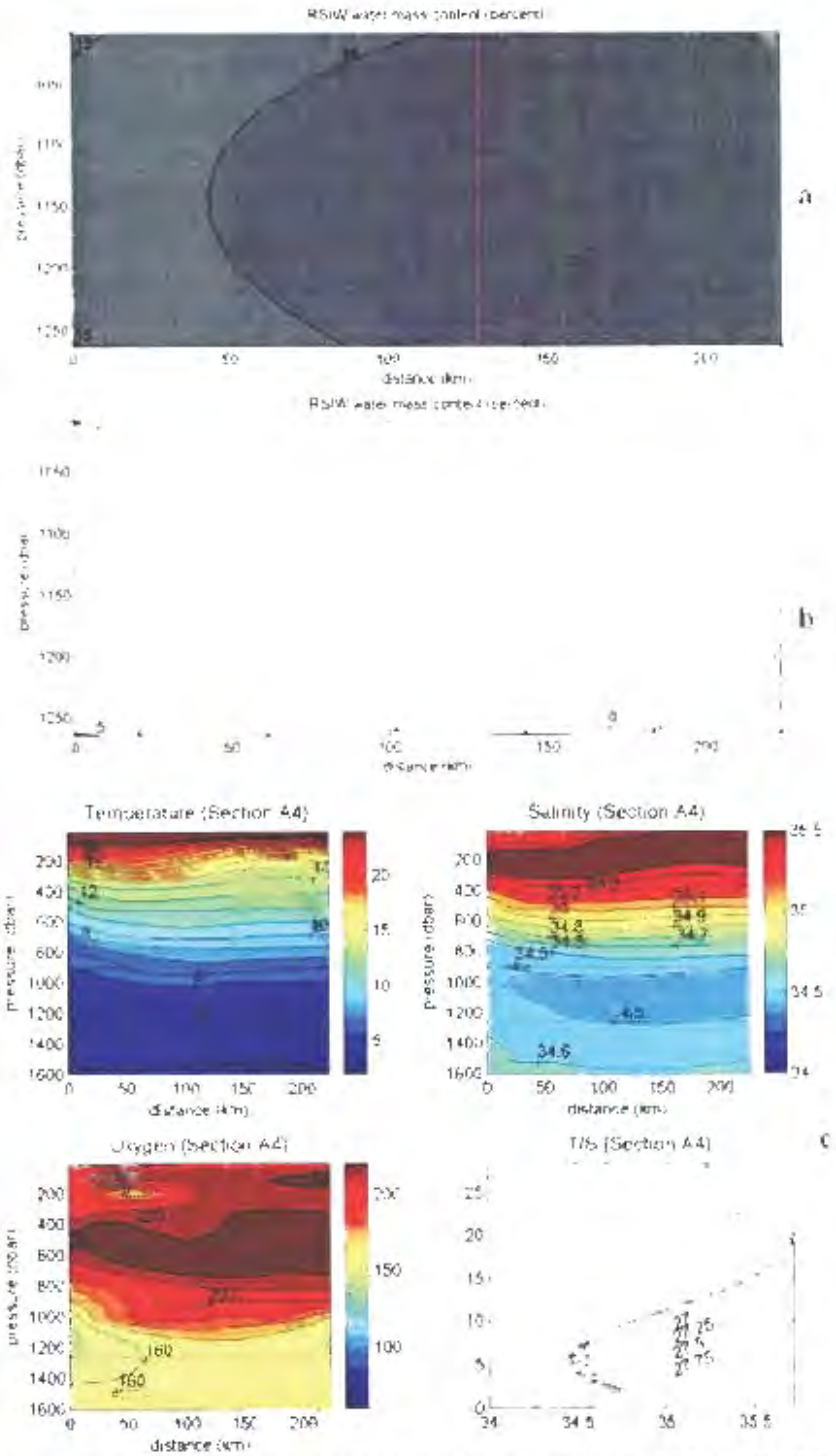

Fig 11: a) RSIW contribution over the density range σ_n=27.40-27.70 (b), RSIW contribution with NIDW included over the range σ_n=27.40-27.70 (c), and property distributions of temperature, salinity oxygen with a T/S plot along section A4 (see figure 7). Dots indicate bottle sample locations.

Section A5 (see figure 7)

The downward slope of the isotherms and isohalines along the slope suggest a strong East Madagascar Current flowing in a south west direction (figure 12(ii)). The upward slope in the isolines further offshore suggests easterly flow further offshore. As was the case along the other sections at the southern tip of Madagascar, a salinity maximum and oxygen minimum is observed along the slope (figure 12(ii)). Similar to section A4 RSIW at its most concentrated over the density range 27.40-27.70 contributed between 15-20% of the water sample along the continental slope. Its distribution appears layer-like in that it is observed in all the offshore stations in which it contributed 5-10% of the water sample (figure 12(i)b). Consistent with section A4 the contribution from RSIW was much reduced in this density range when NIDW was introduced into the source water mass matrix. With the introduction of NIDW the RSIW contribution was reduced to around 6% along the slope with a second core observed around 250 km offshore (figure 12(i)c). Unlike section A4, RSIW is detectable in density range 27.25-27.40 but contributing less than 5% of the water samples collected (figure 12(i)a). This would be consistent with what is observed in the T/S diagram (figure 12 (ii)). Like all of the previous sections, the influence of RSIW (RSIW content >5%) is observed below the 27.6 neutral density level for both source water mass configurations.

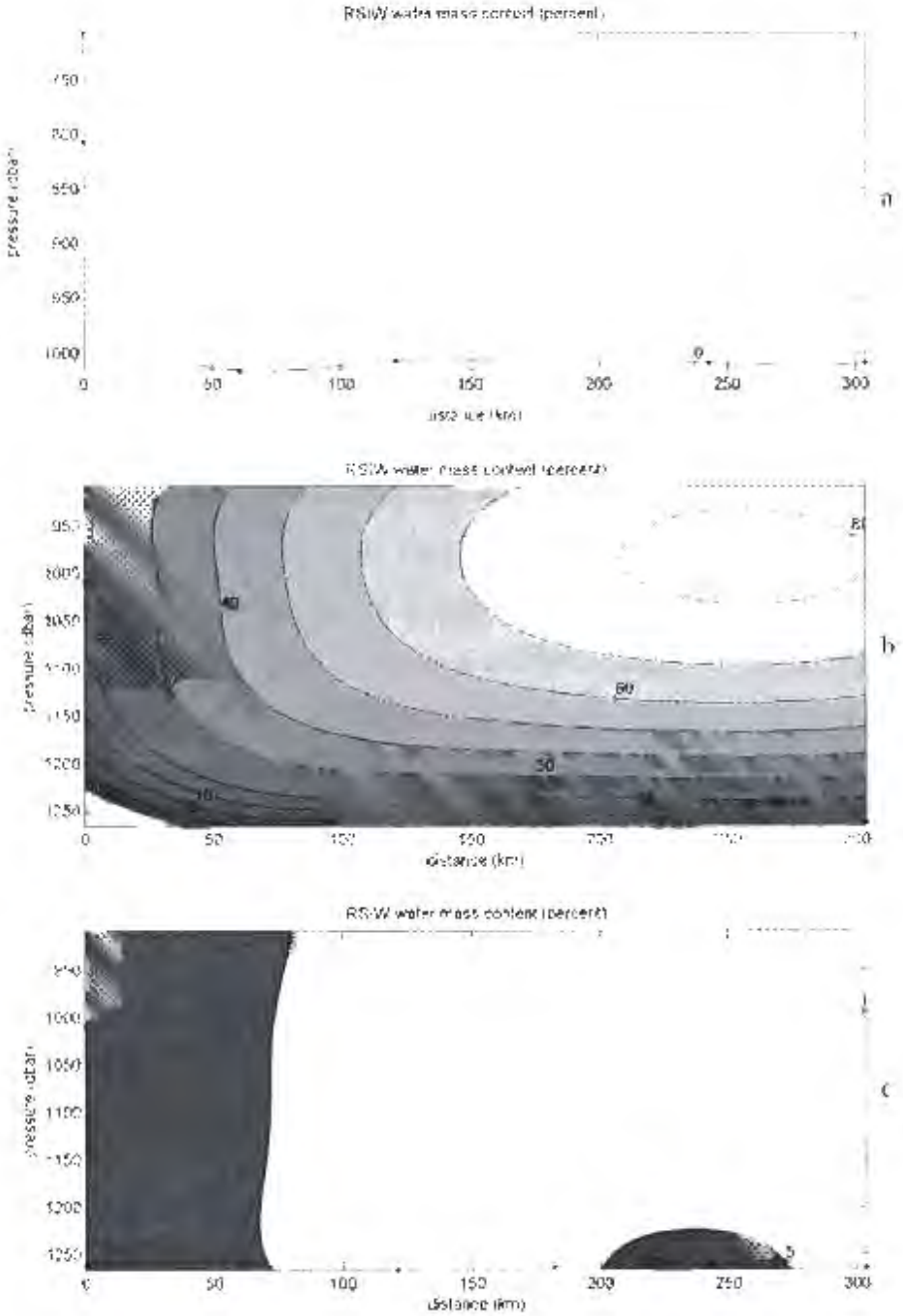

Fig 12 (i): a) RSIW contribution over the density range σ_θ=27.25-27.40 (b) RSIW contribution without NIDW in the source water matrix over the range σ_θ=27.40-27.70 (c) RSIW contribution with NIDW in the source water matrix over the range σ_θ=27.40-27.70 along section A5 (see figure 7). Dots indicate bottle sample locations.

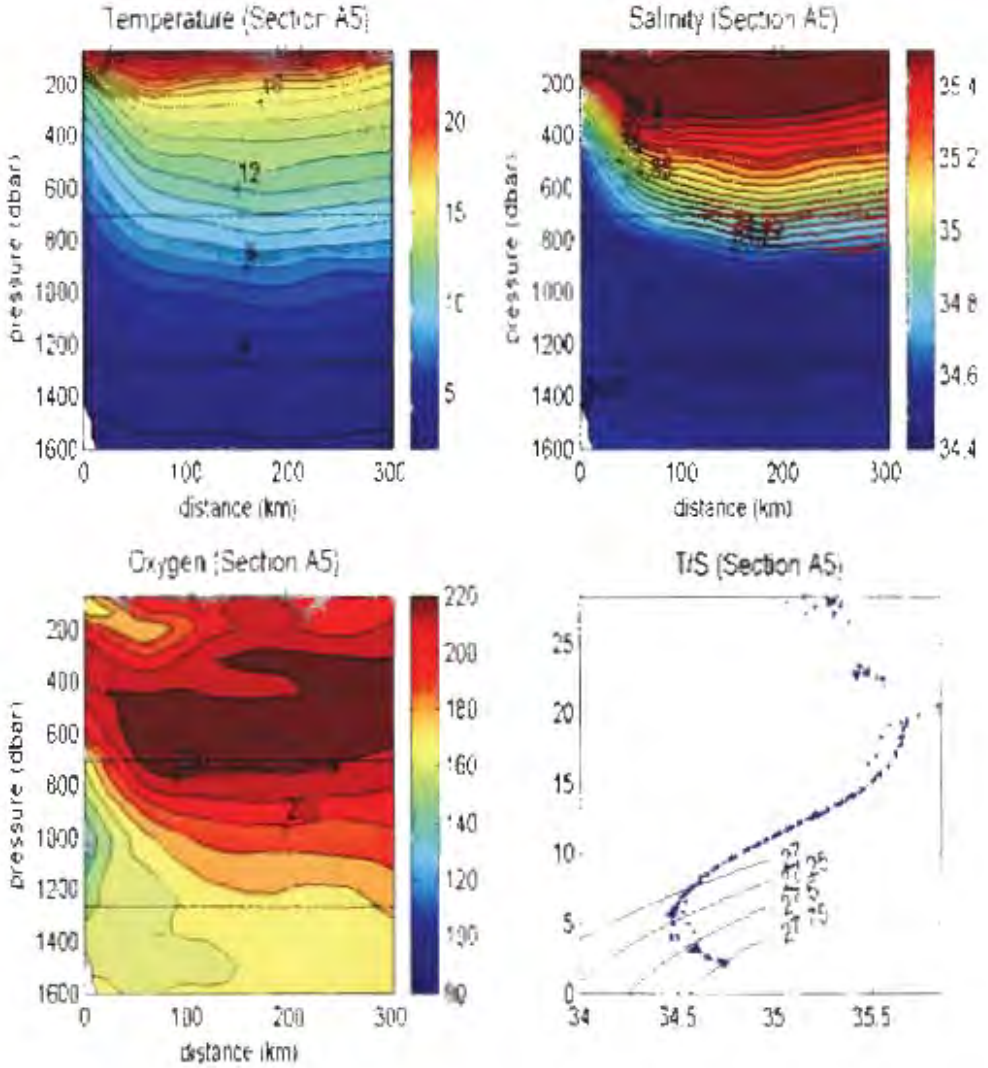

Fig 12 (ii): Property plots along section A5 (see figure 7) of temperature, salinity, oxygen and a T/S plot

Section A6 (see figure 7)

As in the case of the above section the isotherms and isohalines for this section suggest a boundary current at intermediate level moving westward with the offshore flow being eastward. Also consistent with the other sections an intermediate salinity maximum and oxygen minimum is observed along the slope (figure 13 (ii)). This north south section shows a very similar picture as all the other sections described above with a RSIW core found close to the continental slope and constituting between 15-20% of the water sample over the density range 27.40-27.70 (figure 13 (i)b). Unlike the abovementioned two sections and consistent with sections A1 and A2, RSIW still contributed between 10-15% of the water sample at its core even when NIDW is introduced into the source water matrix. Little to no (RSIW content = <5%) RSIW is detected over density range 27.25-27.40 (figure 13 (i)a) which is consistent with what was found along most sections east of Madagascar. The somewhat higher salinity observed in the T/S diagram (figure 13 (ii)) within this density range was in fact found to be IIW (not shown). The maximum RSIW penetration (RSIW content = <5%) for this section also went beyond the 27.6 neutral density level for both source water mass configurations (figures 13(i) b and c).

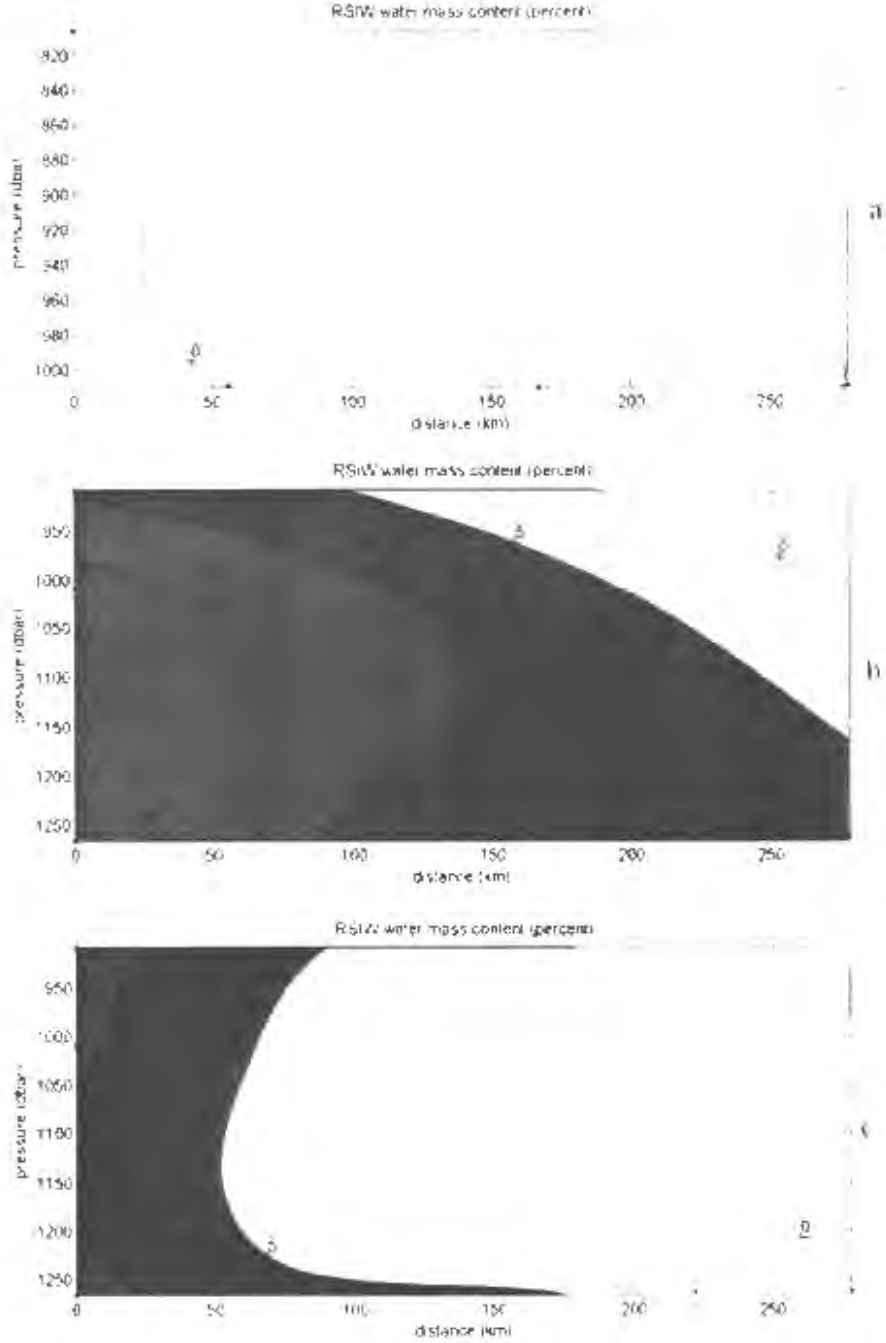

Fig 13 (i): a) RSIW contribution over the density range σ_θ=27.25-27.40 (b) RSIW contribution without NIDW in the source water matrix over the range σ_θ=27.40-27.70 (c) RSIW contribution with NIDW in the source water matrix over the range σ_θ=27.40-27.70 along section A6 (see figure 7). Dots indicate bottle sample locations.

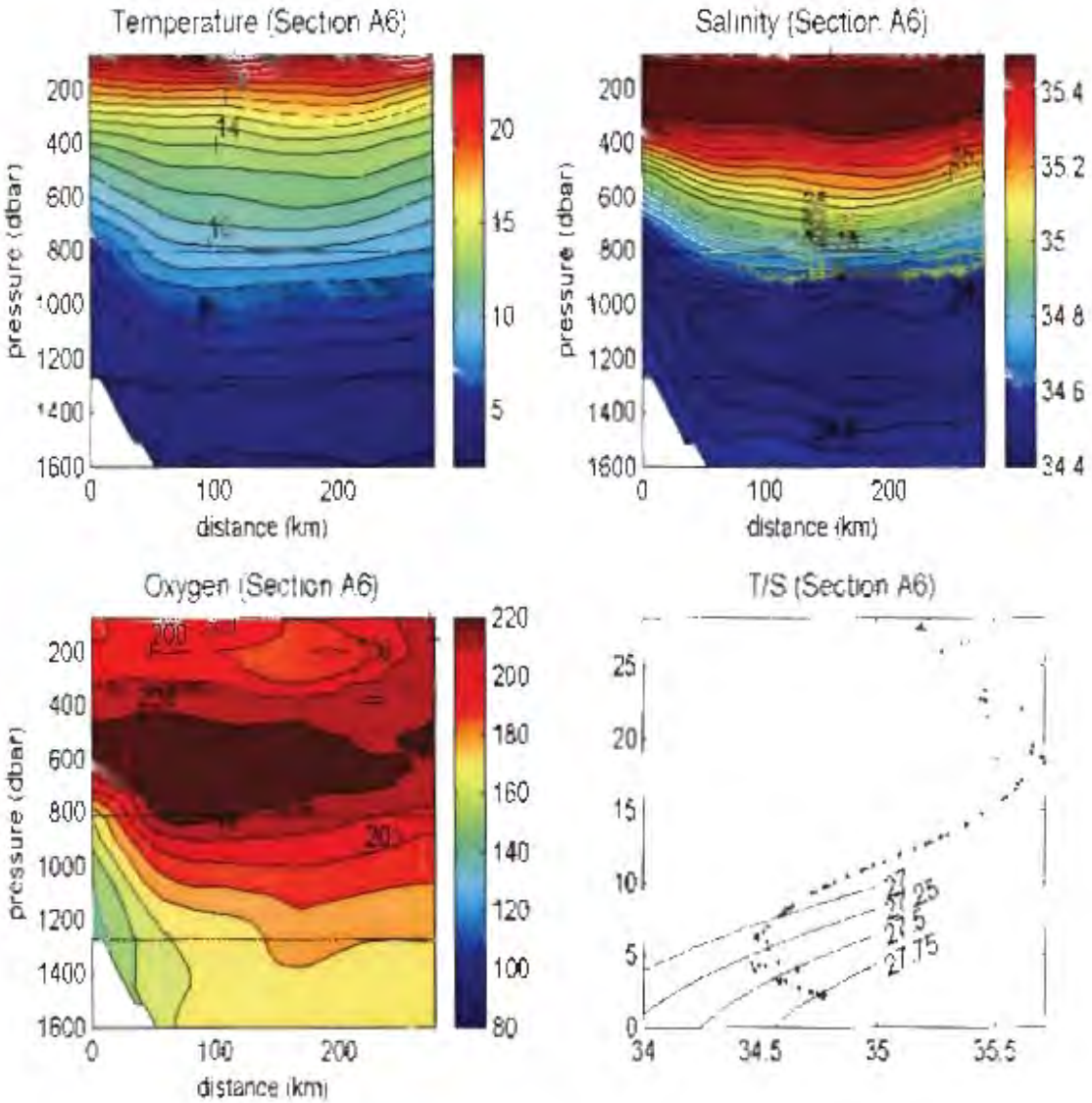

Fig 13 (ii): Property plots along section A6 (see figure 7) of temperature, salinity, oxygen and a T/S plot

4.2) Region B: Mozambique Channel

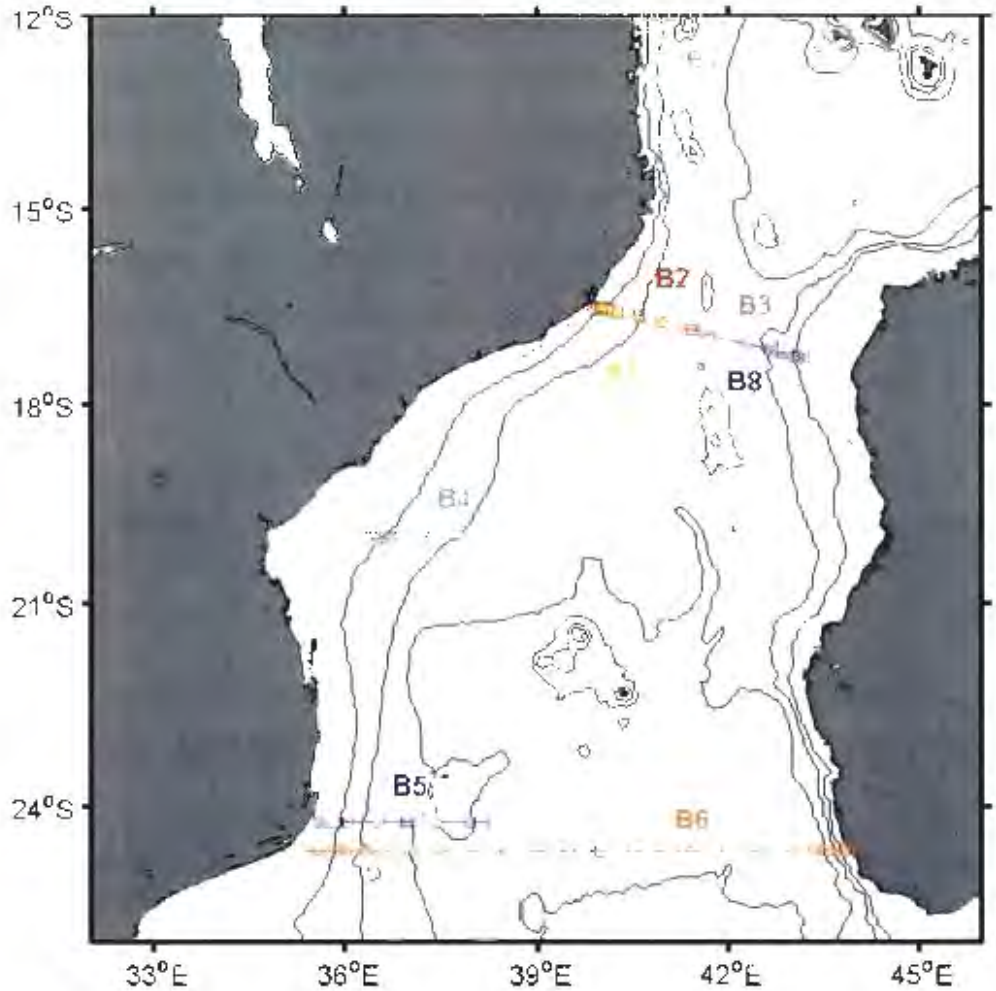

Fig 14: Shows the cruise tracks of the individual sections in the Mozambique Channel. Sections B1 to B5 were completed as part of the ACSEX I cruise; section B6 is a WOCE cruise and sections B7 and B8 were completed as part of the ACSEX III cruise.

4.2) Region B (Mozambique Channel)

Source Water mass matrix

As explained in the methods section (Chapter 3) non-conservative phosphate and nitrate was used for sections B1 to B5 instead of the conservative parameters initial phosphate and NO. This necessitated the inclusion of NIDW into the water-mass matrix. Because of the limited number of parameters it is assumed that siAAIW is the major AAIW in the Indian Ocean or at least in the Mozambique Channel (You et al., 2003) and dAAIW was excluded from the water mass matrix. Mass conservation residuals indicated the sole use of UCDW as defined in the Atlantic as sufficient and that UCDW as defined in the Indian Ocean can be excluded from the source water type matrix south of the narrowest part of the Mozambique Channel. This is consistent with the flow pattern of deep water as indicated in You (2000).

As a test we compared RSIW contributions obtained from using non-conservative phosphate and nitrate to that obtained from using conservative phosphate and nitrate for samples in which the oxygen parameter was not limited (not shown below). Results showed similar water mass contributions. The assumption that water mass regeneration occurs at a much slower rate than water mass spreading does seem to be feasible and would thus allow for comparisons with other sections using initial phosphate and NO. For sections B6 and B9 conservative initial PO and NO is reintroduced as parameters of the source water mass matrix. No nitrate measurements was made along sections B7 and B8 so neither nitrate or NO was part of the source water matrix.

Historic sections

Most of historic sections (completed in the 1960's) in the Mozambique Channel was placed in the addendum. The reason for this was that although they provided some indication as to the maximum contribution of RSIW their wide station spacing (sometimes >100 km) made them less useful.

Section B1 (see figure 14)

This section just north of the narrowest part of the Mozambique Channel extended only 80 km offshore. LADCP measurements in de Ruijter et al. (2002) show the surface flow to be southward as the slightly downward slope in the isotherms and isohalines suggests (figure 15(i)c). Two distinct RSIW cores are observed along this section around 28 km offshore of the African continental slope. In the shallow core (around 900 m) RSIW contributes greater than 30% of the water sample whilst in the deeper core it contributes just less than 25% of the water sample (figure 15(i)b). This water mass mixing fraction is similar to that indicated in You et al. (2003). Their results indicated values higher than 30% in the Mozambique Channel on the neutral density surface 27.55. The shallow RSIW core lies within the oxygen minimum layer and occurs where there is a downwelling in the phosphate and nitrate concentration for this layer. The deeper RSIW core co-insided with the salinity maximum and somewhat lower phosphate and nitrate values at 1200 m around 28 km offshore (figures 15(i)b, c and 15(ii)).

Unlike observations east of Madagascar, RSIW at its core contributed 25-30% of the water sample over the neutral density range 27.25-27.40 just off the continental slope (figure 15(i)a). This core co-insided with a upwelling of the oxygen minimum at this position (figure 14(i)c). In terms of its neutral density range RSIW still contributed over 20% to the water mass fraction on the neutral density surface 27.69 even with NIDW as part of the source water mass matrix. Along the I02 WOCE section completed just north of this section RSIW was found to be associated with an anti-cyclonic eddy (DiMarco et al., 2002). Since this section only extended 80 km offshore this cannot be ruled out. Sea surface height anomalies shown in de Ruijter et al. (2002) do however not suggest this. The net transport of RSIW across this short section for both density ranges was -1.67 Sv.

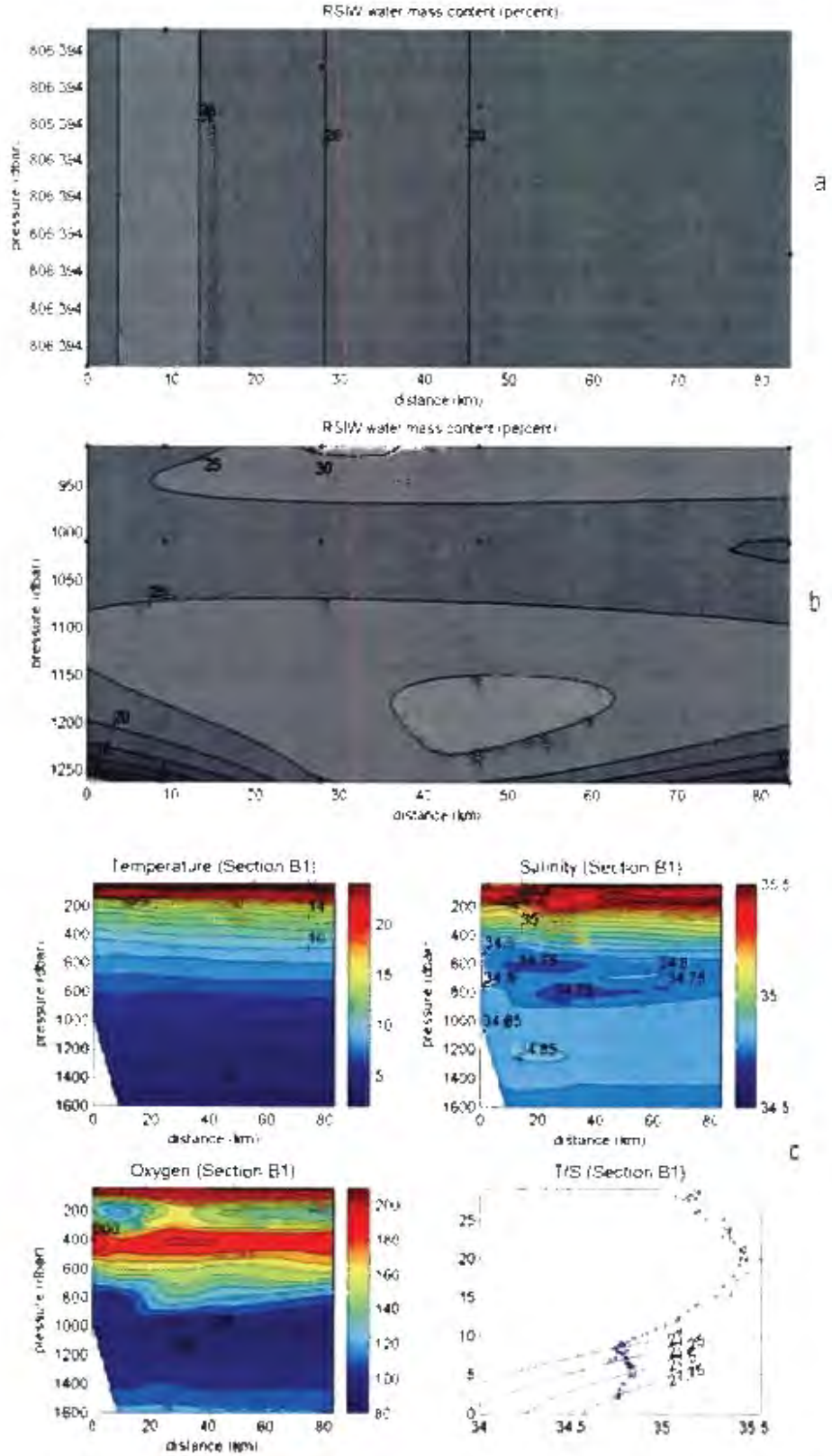

Fig 15(i): a) RSIW contribution over the two density ranges 27.25-27.40 (b) 27.40-27.70 and (c) property distributions of temperature, salinity oxygen with a T/S plot (c) along section B1 (see figure 14). Dots indicate bottle sample locations

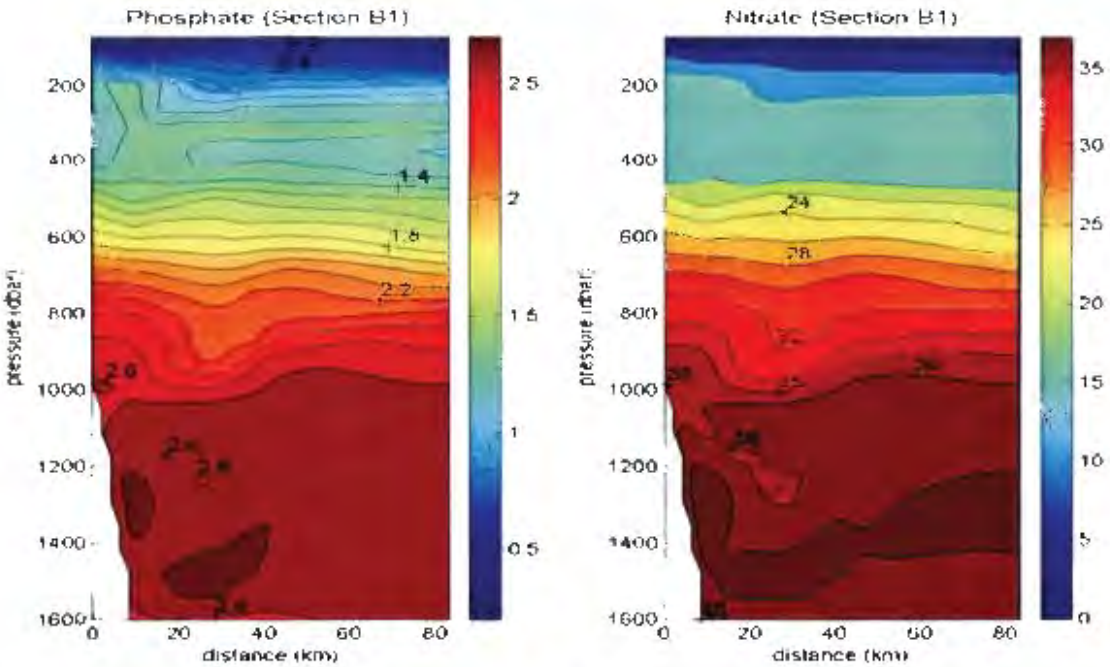

Figure 15(ii): Distribution of dissolved phosphate and nitrate along section B1 (see figure 14)

Section B2 (see figure 14)

This section across the narrowest part of Mozambique Channel from the Mozambique coast to the middle of the channel crossed the southward flowing limb of a anti-cyclonic eddy (de Ruijter et al., 2002) shown in the slightly downward slope of the isotherms and isohalines (figure 16(i)c). It needs to be noted here that the geographical distance covered in the lower density range is slightly shorter than that of the upper density range. Station 1 is not represented in the lower density range because it did not reach into the deeper density range.

Two RSIW cores are observed in both neutral density ranges 27.25-27.40 and 27.40-27.70 which could be considered as just two separate cores over the complete density range (figure 16(i) a and b). The RSIW cores are situated just west and east of the strongest southward flow associated within the anti-cyclonic eddy. The western core appears to be more strongly associated with the extreme oxygen minimum whilst the RSIW core in the middle of the channel co-insided with both the salinity maximum and somewhat less extreme oxygen minimum (figure 16(i)c). At these positions there is also a downwelling in the phosphate and nitrate values (figure 16(ii)). The source water mass contribution of RSIW in the middle of the channel was between 25-30% of the water sample whilst in the RSIW core close to the African continental slope it contributed just below 30% of the water sample. As was the case in the above section the most saline water was found below the neutral density surface 27.66 (just below 1200 m) in the centre of the channel suggesting considerable mixing in the upper part of the chosen intermediate density range (figure 16(i)c). The RSIW cores are however found within the 27.25-27.55 neutral density range whilst the full range of RSIW can be considered to be deeper than the maximum neutral density of 27.69. Across this section the net RSIW transport was -2.62 Sv.

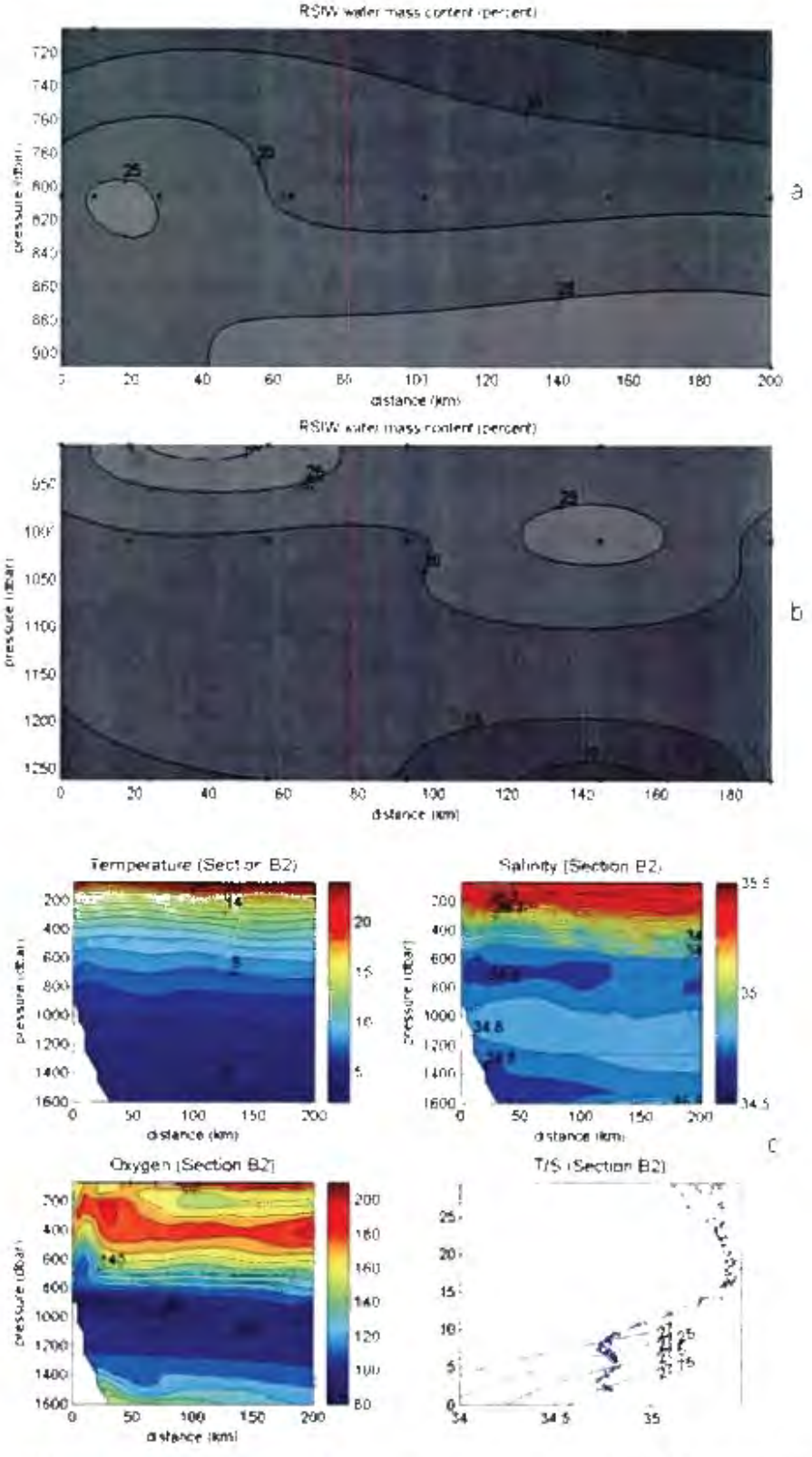

Fig 16(i): a) RSIW contribution over the two density ranges 27.25-27.40 (b) 27.40-27.70 and (c) property distributions of temperature, salinity oxygen with a T/S plot (c) along section B2 (see figure 14). Dots indicate bottle sample locations.

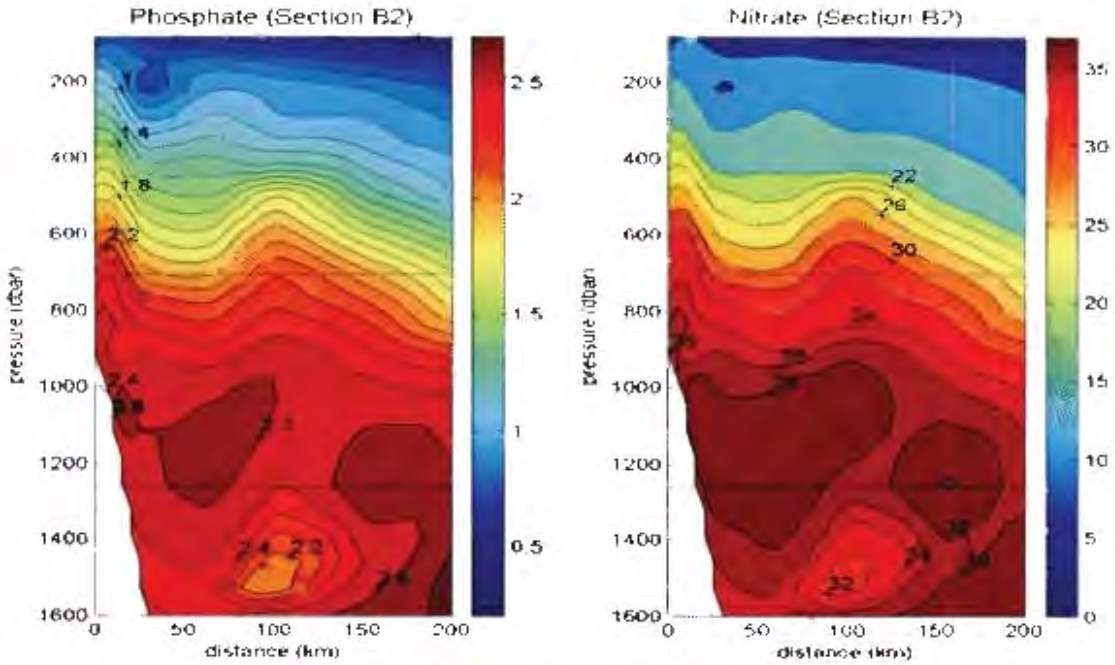

Figure 16(ii): Distribution of dissolved phosphate and nitrate along section B2 (see figure 14)

Section B3 (see figure 14)

This section completes the cross section of the narrowest part Mozambique Channel from just east of the middle of the channel to the Madagascar coast. It covers mostly the northward flowing limb of the anti-cyclone mentioned above and is shown by the upward slope of the isolines (figure 17(i)c) as well as in the LADCP measurements in de Ruijter et al. (2002). Along this section it is shown that RSIW does indeed flow close to the Madagascar slope where it contributed greater than 30% of the water sample. This is similar to what was found by You et al. (2003) centred just below the neutral density surface 27.40 (figure 17(i)b). This is slightly higher than the 25-30% observed along the western half of the channel where the lowest oxygen values were observed (figure 17(i)c). Since the flow at the level at which RSIW is found is slightly northward it is likely that this water came from the African slope and circulated with the anti-cyclone. Although it would appear as if the highest RSIW contribution is no longer associated with the most saline, oxygen depleted water -which is now found in the middle of the channel- actual values indicate the middle only to be more saline by 0.004 psu and the difference in oxygen concentration being about 1.4 µmol/l. It needs to be noted however that the phosphate and nitrate concentrations are slightly higher at the position of the oxygen minimum and salinity maximum when compared to the eastern section (figures 17(i) b, c and 17(ii)). The RSIW contribution at this position (middle of the channel) was however still in excess of 20%.

Station 1 along this section represents the strongest northward flow according to de Ruijter et al. (2002) which would indicate that the highest RSIW contributions were circulating around the outside part of ring. Contrary to the higher contribution in the eastern half in the lower density range we observe a lower maximum contribution in the eastern half of the channel over the density range 27.25-27.40 compared to the western part with RSIW contributing slightly less than the 25-30% observed western half of the channel. In this density range the maximum water sample contribution of RSIW was 20-25% (figure 17(i)a). Although observed as separate cores in this density range they are in fact associated with the underlying RSIW layer observed in the deeper density range. The maximum range of RSIW influences stretched beyond the maximum 27.68 neutral density level. The net transport of RSIW along this northward flowing limb of the anticyclone was 1.21 Sv.

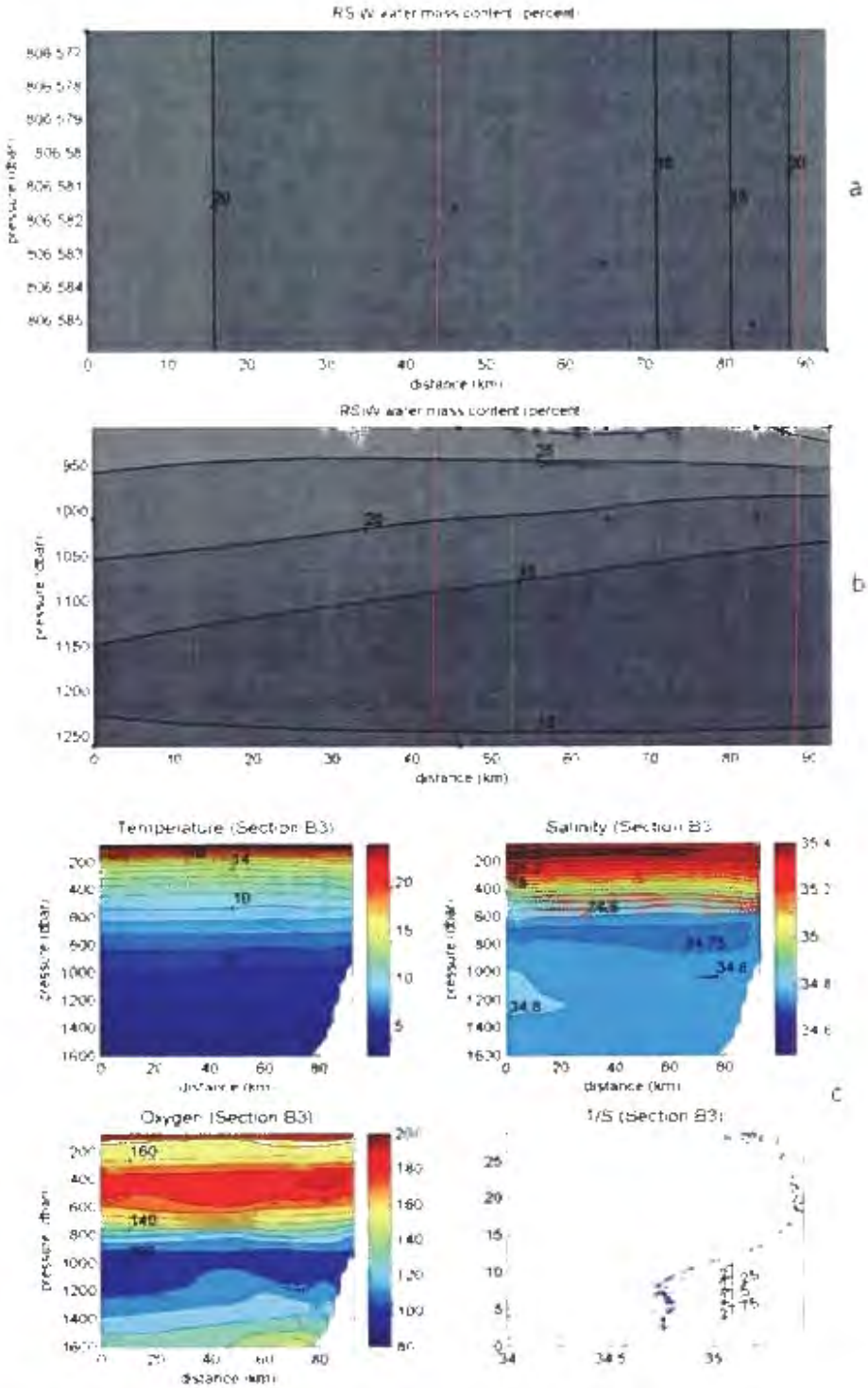

Fig 17(i): a) RSIW contribution over the two density ranges 27.25-27.40 (b) 27.40-27.70 and (c) property distributions of temperature, salinity oxygen with a T/S plot (c) along section B3 (see figure 14). Dots indicate bottle sample locations

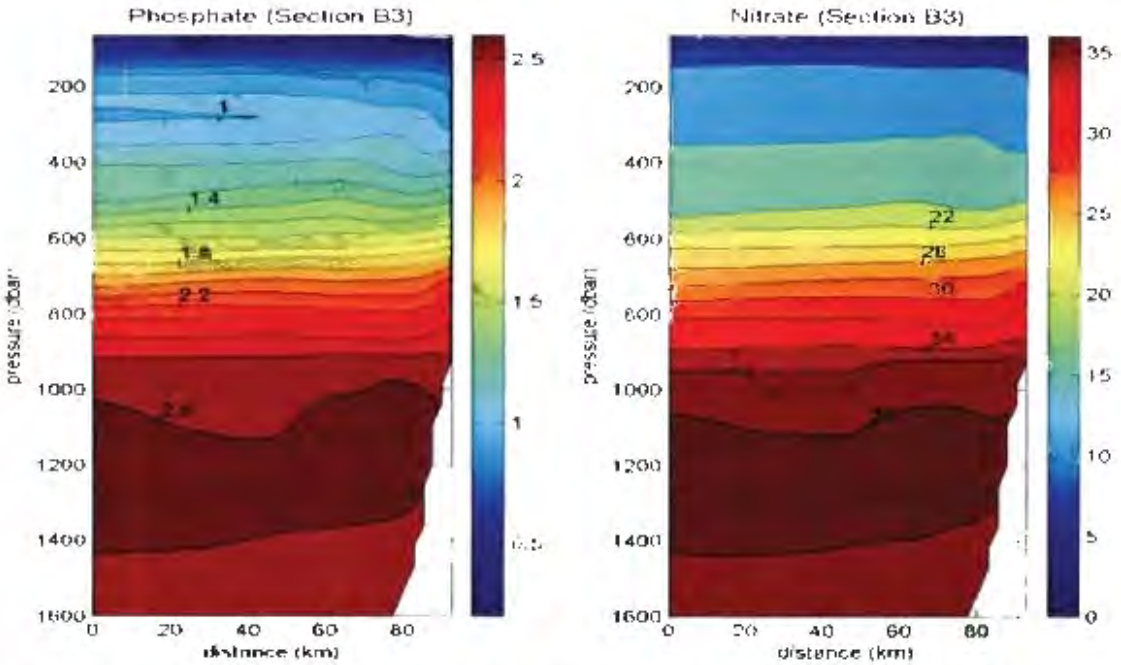

Figure 17(ii): Distribution of dissolved phosphate and nitrate along section B3 (see figure 14)

Section B4 (see figure 14)

According to the flow regime described in de Ruijter et al. (2002) and shown in the downward slope in the isolines (figure 18(i)c), this section crossed the southward flowing limb of an anti-cyclone situated just off the coast of Mozambique. Along this section two RSIW cores are observed (over the combined density range) about 100 km from the continental shelf where RSIW contributed close to 30% of the water sample and about 275 km offshore where it contributed 20-25% of the water sample in the density range 27.25-27.40 (figure 18(i) a and b). This is the first section along which the highest water sample contribution of RSIW is observed in the upper (27.25-27.40 as suppose to 27.40-27.70) density range. The core at a 100 km offshore is also clearly visible in the intermediate salinity maximum and oxygen minimum (figure 18(i)c). Unlike in previous sections we don't observe the strong downwelling in the phosphate and nitrate concentrations at the position of the RSIW core (figure 18(ii)). It needs to be noted however that there is a slight reduction in the nitrate maximum along this section compared to that further north.

From the surface currents shown in de Ruijter et al. (2002) it would appear as if these cores are on the landward and offshore side of the strongest southward flow associated with the anti-cyclone similar to what was observed in the northern Mozambique Channel. Also the RSIW maximum contribution value found in the landward core is consistent with that observed and associated with the anti-cyclonic eddy in the northern part of the Mozambique Channel (sections B2 and B3). As was the case in the above sections RSIW influence appears to reach beyond the 27.68 maximum level. Along this section the net transport of RSIW amounted to -1.89 Sv which is slightly lower than that across the southward flowing limb of the anti-cyclone in the northern Mozambique Channel. The cross section of this anti-cyclonic eddy does however not appear to stretch to the middle (de Ruijter et al., 2002) of the eddy which could account for the difference.

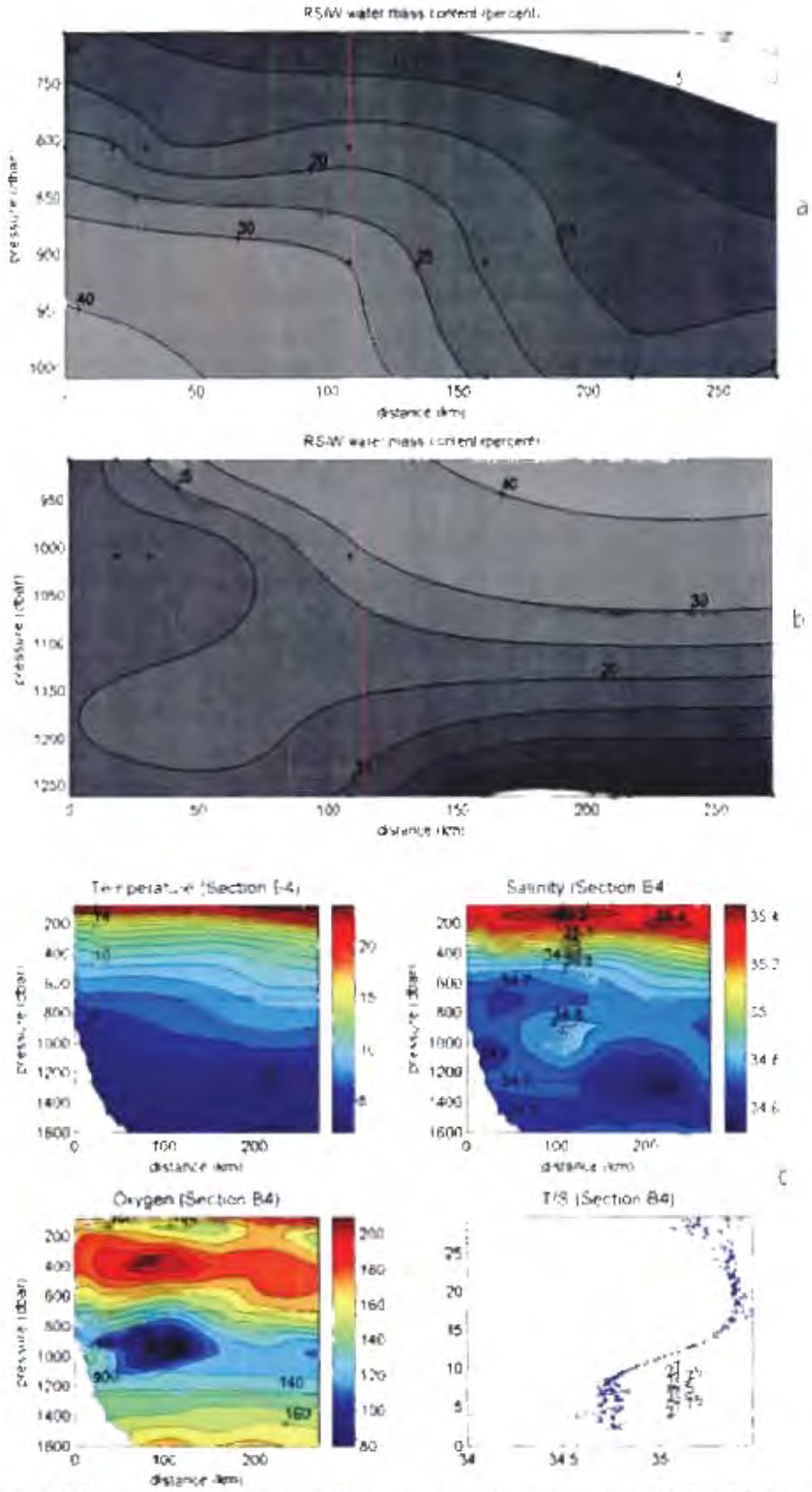

Fig 18(i): (a) RSIW contribution over the two density ranges 27.25-27.40 (b) 27.40-27.70 and (c) property distributions of temperature, salinity oxygen with a T/S plot (c) along section B4 (see figure 14). Dots indicate bottle sample locations.

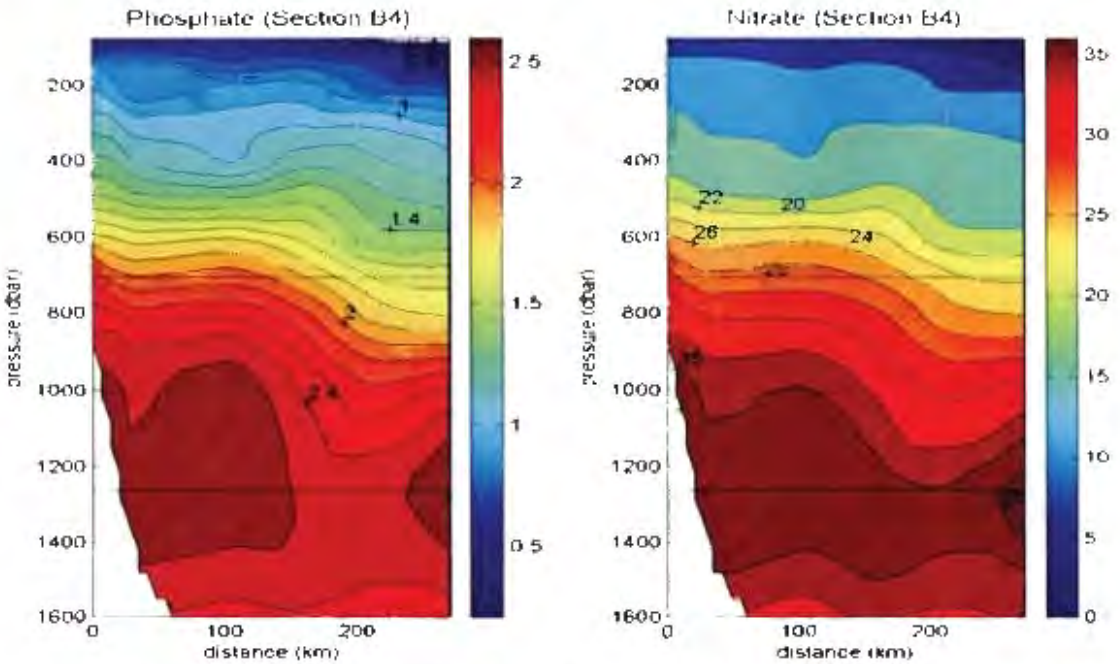

Figure 18(ii): Distribution of dissolved phosphate and nitrate along section B4 (see figure 14)

Section B5 (see figure 14)

Completed at the southern exit of the Mozambique Channel this section, as was the case in the above section, partially crossed an anti-cyclonic eddy (de Ruijter et al., 2002). Along this section RSIW at its core contributed 25-30% of the water sample on the outside half of the eddy (figure 19(i)b and figure 19(i)c) according to the flow regime depicted in de Ruijter et al. (2002). This core as would be expected was associated with the salinity maximum and oxygen minimum as well as a slight downwelling in the phosphate and nitrate concentrations (figure 19(i) c and 19(ii)). The extreme oxygen minimum however now lies deeper and to the west of the maximum RSIW contribution at which position RSIW contributed 20% of the water sample. At this position there is also a downwelling in the phosphate and nitrate concentrations (figure 19(ii)). The core is observed in the neutral density range 27.40-27.70 as oppose to the 27.25-27.40 range along the abovementioned section. Compared with other sections in the channel very little RSIW was found along the continental slope outside the eddy. The flow along the slope was shown to be slightly northward in de Ruijter et al. (2002) using LADCP measurements. This is also shown in the slightly downward slope in the isotherms with the salinity section (figure 18(i) c) showing the water along the slope to be mostly fresh AAIW. This finding supports that of de Ruijter et al. (2002) that eddies in the Mozambique Channel are the carriers of RSIW towards the Agulhas Current.

In contrast to the other sections further north in the Mozambique Channel it is found that the water sample contribution of RSIW in the density range 27.25-27.40 is considerably reduced compared to that observed in the density range 27.40-27.70. It now mirrors observations east of Madagascar when comparing the upper and lower density ranges. Its contribution to the water sample was however still in excess of 15% 250 km offshore. This is still considerably higher than was found east of Madagascar. The maximum neutral density level upon which RSIW was detected was 27.60 where it contributed just over 5% along the slope. Across this section the net transport of RSIW was only -0.76 Sv, considerably lower than the sections further north of it.

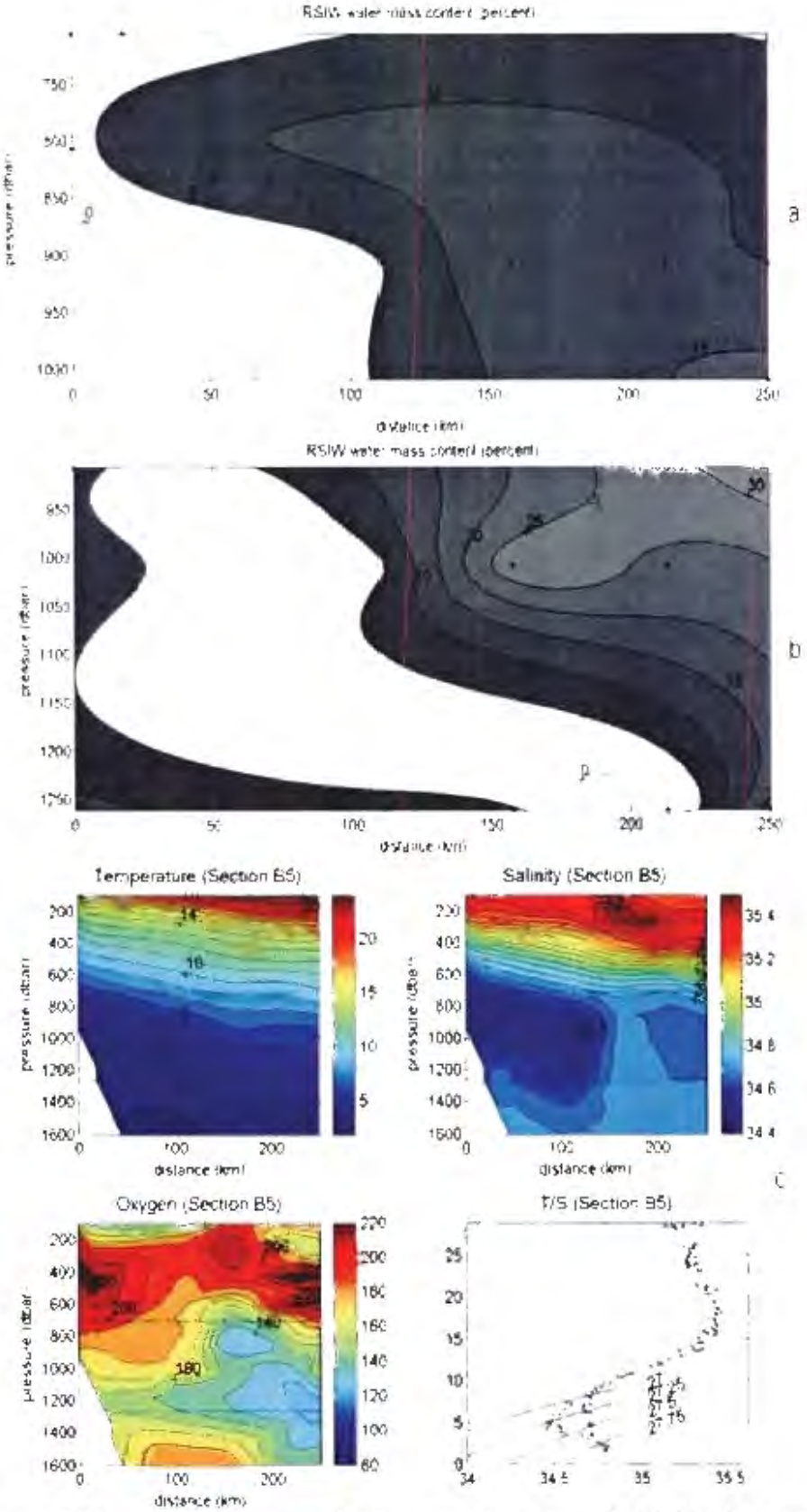

Fig 19(i): a) RSIW contribution over the two density ranges 27.25-27.40 (b) and 27.40-27.70 and (c) property distributions of temperature, salinity oxygen with a T/S plot (c) along section B5 (see figure 14). Dots indicate bottle sample locations

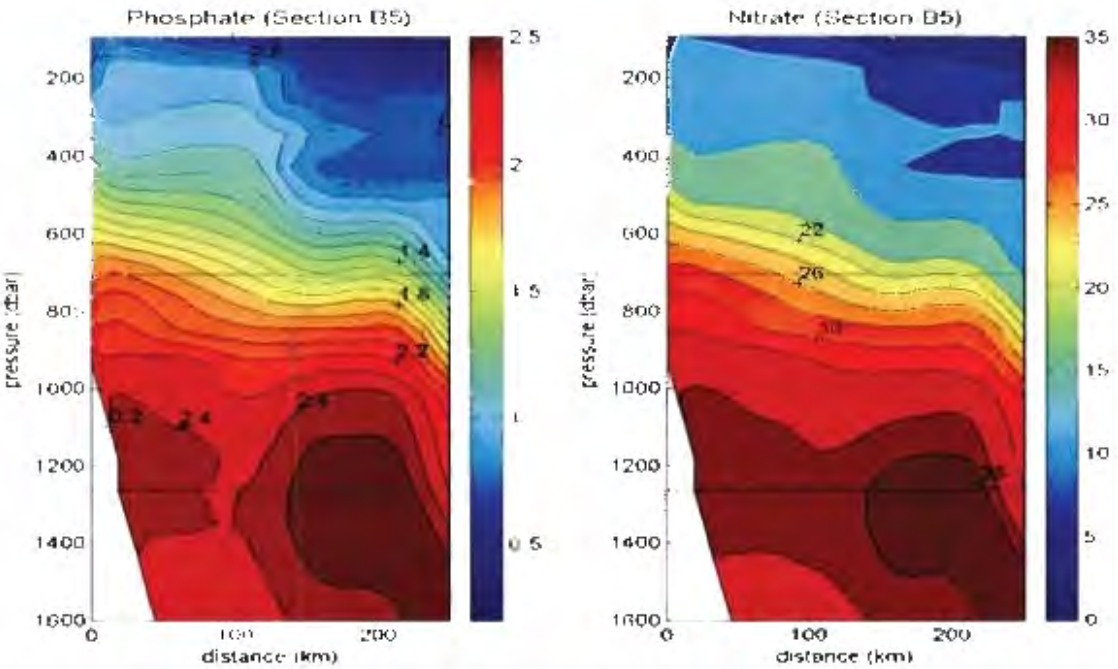

Figure 19(ii): Distribution of dissolved phosphate and nitrate along section B5 (see figure 14)

Section B6 (WOCE section I04, see figure 14)

In this section across the southern mouth of the Mozambique Channel the flow is dominated by two cyclonic eddies (Donohue and Toole, 2003; DiMarco et al., 2002). These two features are shown in the doming of the isotherms and isohalines at about 50 km and around 600 km from the African slope (figure 20(ii)). Considering the salinity distribution it would appear as if the RSIW was concentrated mostly outside these eddies. This pattern is also clearly seen in the oxygen distribution with the lowest oxygen concentrations found outside the cyclones (figure 20(i)). Along this section potential vorticity constraints did not allow for the most saline water along the African continental slope to be included because it was a bottom value. To overcome this problem another data point with the same values as the deepest water sample was included, the only difference being that it was 5 m deeper. It is assumed this would not have any effect since we do not expect drastic changes in the parameter values over such a short distance.

Similar to the abovementioned section we find that RSIW in density range 27.25-27.40 is much reduced compared to sections further north. In this density range two separate cores are observed; one along the African continental slope and another along the Madagascar slope with RSIW contributing around 10% of the water sample (figure 20(i) a). These cores do however not appear to be independent from the underlying RSIW. In the density range 27.40-27.70 RSIW contributed between 20-25% of the water sample in three separate cores which were separated by the two cyclonic eddies (figure 20(i)b, 20(ii)). This is slightly less than the 25-30% in the abovementioned section completed just north of this one. However when NIDW is introduced into the source water matrix resulting in a more direct comparison with the above section, RSIW contributed only between 15-20% of the water sample in a core situated in the southward limb of the cyclonic eddy along the slope. In the southward limb of the offshore cyclonic eddy it only contributed 10-15% of the water sample. This is much reduced from the 25-30% in the above section but similar to that observed along section B15 (figure 52 in addendum) at the southern exit of the Mozambique Channel. The net transport of RSIW across this section was only -0.45 Sv which as the water sample fraction is lower than that calculated for section B5 around the same latitude. It needs to be noted however that section B5 does not cross the whole channel and that RSIW is not confined to the western half of the channel as

indicated along this section and section B15 in the addendum. In terms of the neutral density range we now observe a considerable change between the two source water mass configurations not previously seen in the channel. RSIW now seem to be mostly constricted above the 27.55 neutral density level in the western part of the channel whilst in the eastern part it reached as deep as 27.68.

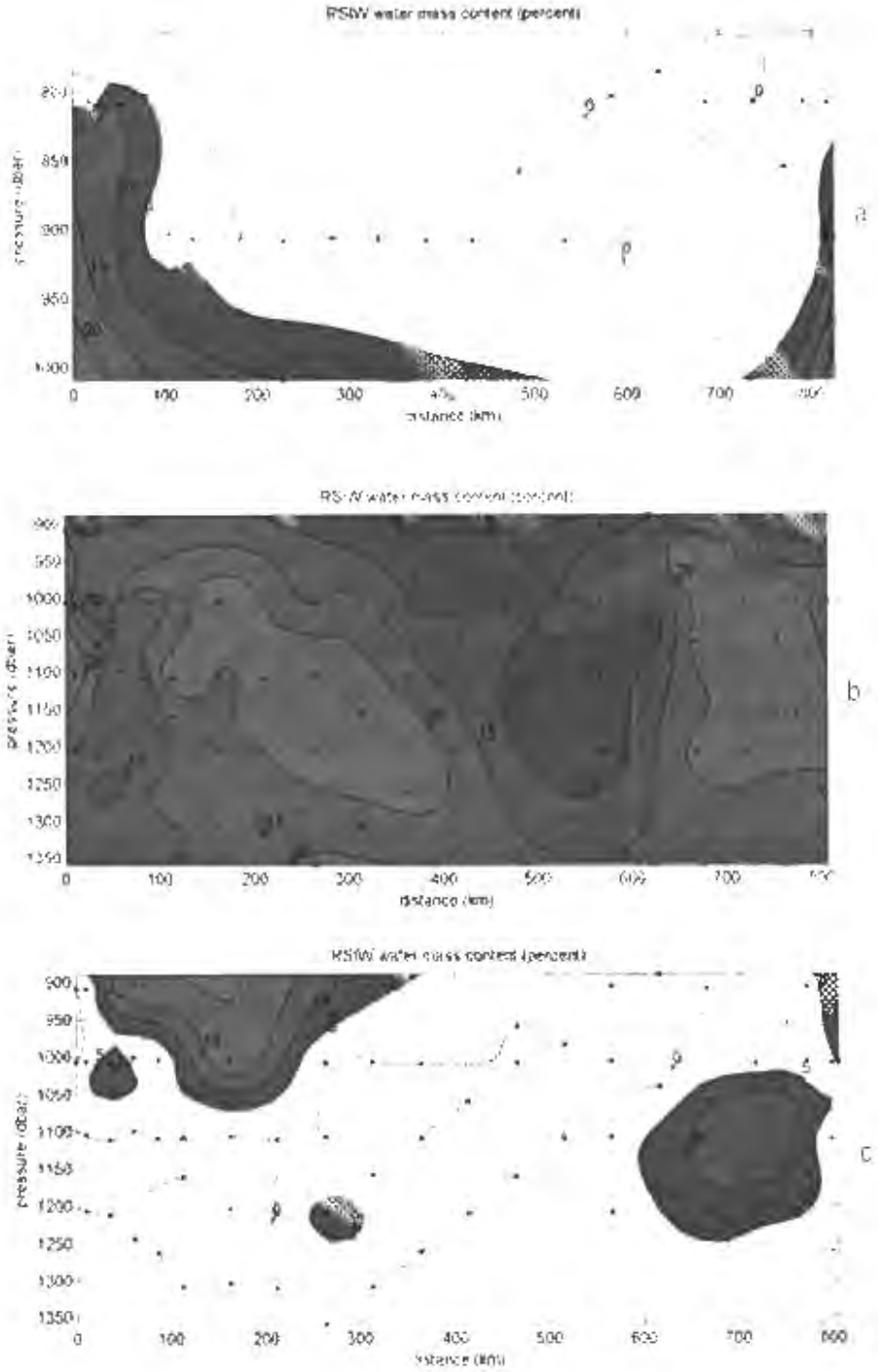

Fig 20 (i): a) RSIW contribution over the density range σ_n=27.25-27.40 (b) RSIW contribution without NIDW in the source water matrix over the range σ_n=27.40-27.70 (c) RSIW contribution with NIDW in the source water matrix over the range σ_n=27.40-27.70 along section B6 (see figure 14). Dots indicate bottle sample locations.

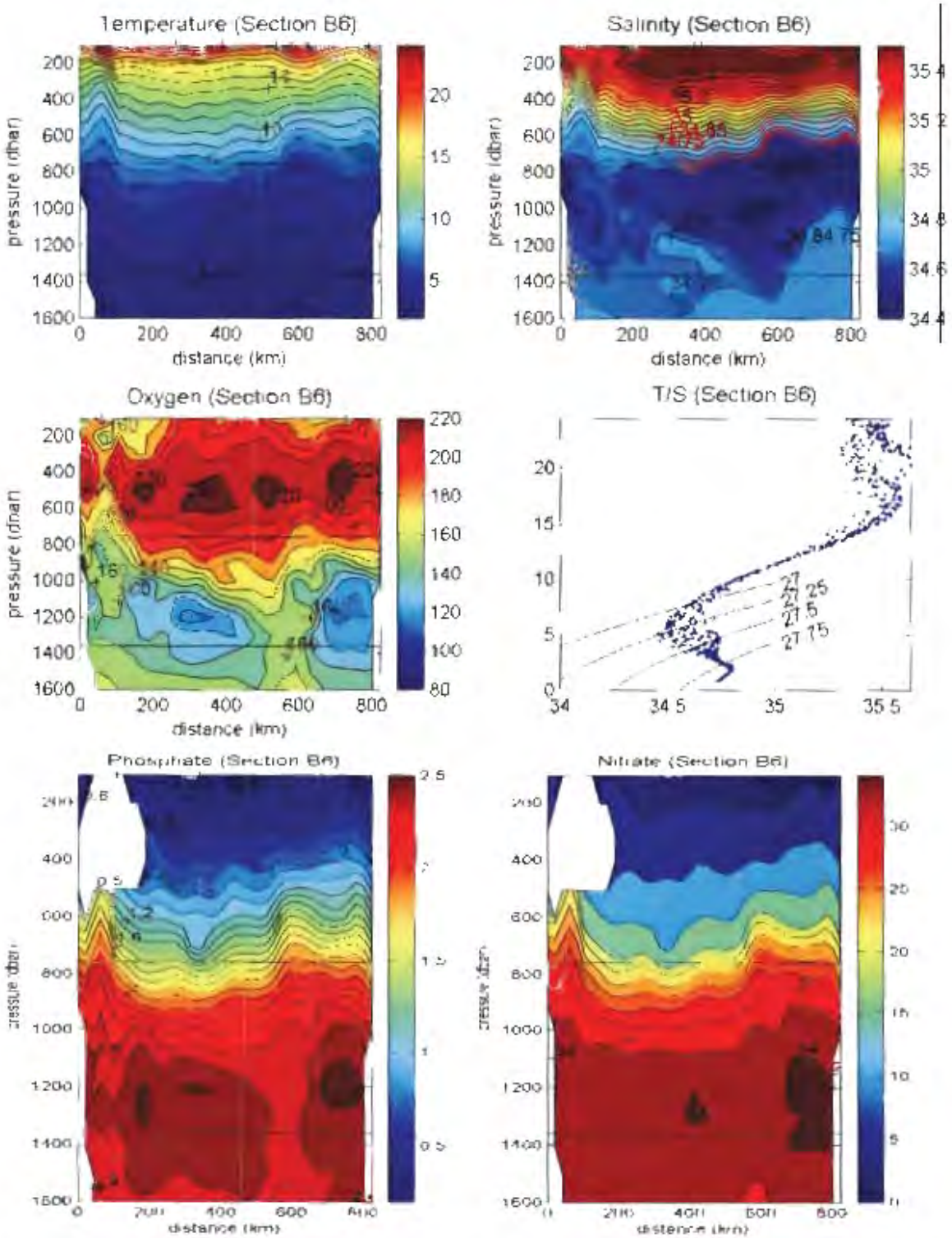

Fig 20 (ii): Property plots along section B6 (see figure 14) of temperature, salinity, oxygen, phosphate, nitrate and a T/S plot

ACSEX III cruise sections

Section B7 (see figure 14)

This section, similar to section B2, crossed the narrowest part of the Mozambique Channel from the African coast to the middle of the channel and shows a very similar RSIW distribution pattern even though the flow pattern is different. Across the narrowest part of the channel the flow is now weak cyclonic (Ridderinkhof and de Ruijter, 2003) compared to the anti-cyclonic flow observed along sections B2 and B3 of which this section crosses mostly the weak northward flowing part. This cyclonic flow is also observed in the upward slope of the isotherms (figure 21(ii)). Unlike section B2 this section does not extend to the middle of the channel.

Despite all the differences, RSIW as was the case along section B2, contributed 25-30% to the water sample at its core over the density range 27.40-27.70 (figure 21(i)c) which was flowing both southward and northward all be it sluggishly (Ridderinkhof and de Ruijter, 2003). However when NIDW was excluded from the source water matrix (figure 21(i)b), the RSIW core appeared to be also flowing sluggishly northward. In this matrix configuration the RSIW content is slightly higher amounting to 30-40% of the water sample. Different to section B2 however, the highest contribution values are not observed over density range 27.25-27.40. The highest RSIW contribution in this density range was between 15-20% of the water sample in what appeared to be a layer distribution (figure 21(i)a). The layer is however not distinct and formed part of the RSIW layer observed in the lower density range. The net RSIW transport across this section is only -0.58 Sv which is much reduced but still southward as was the case along section B2.

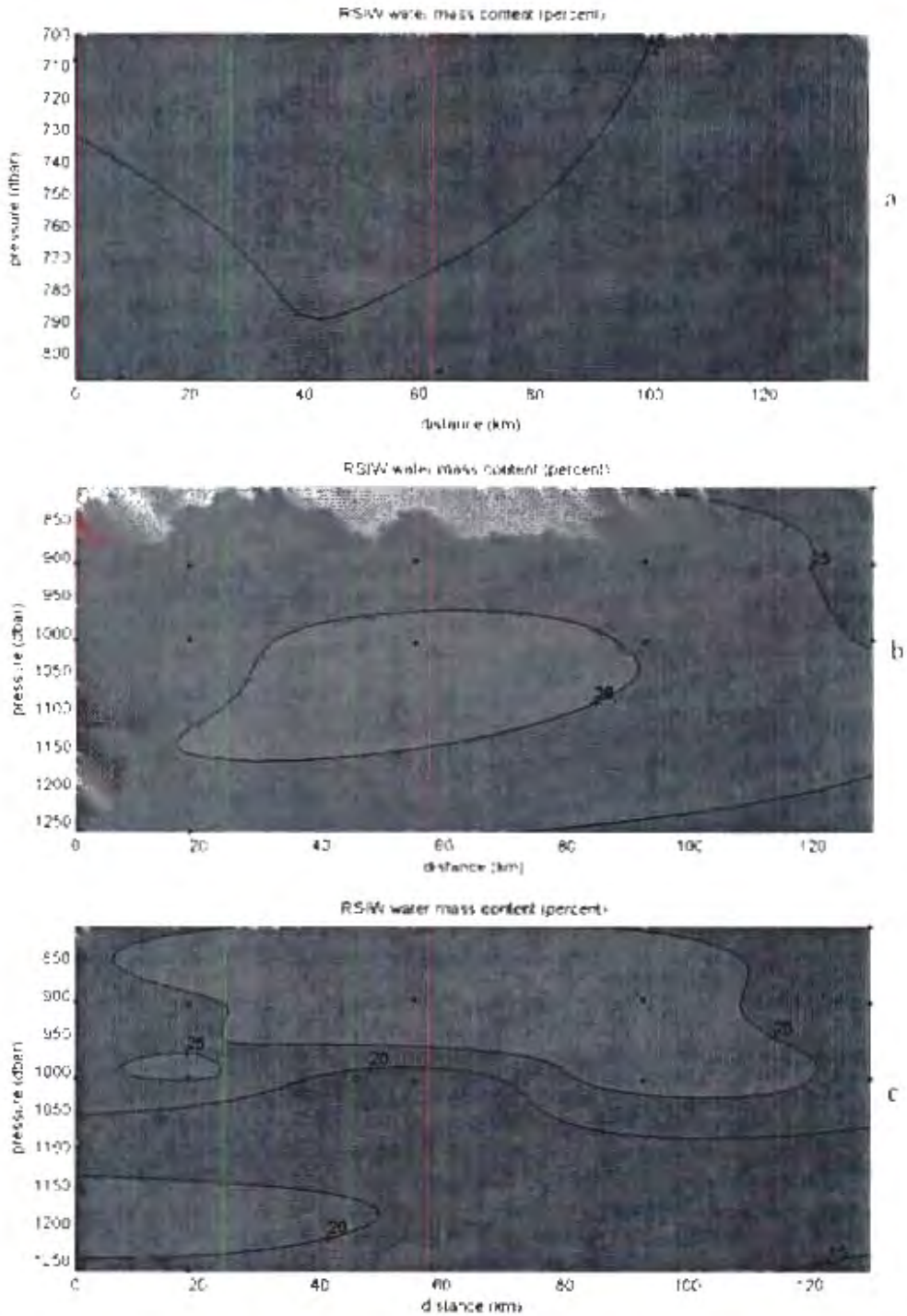

Fig 21 (i): a) RSIW contribution over the density range σ_n=27.25-27.40 (b) RSIW contribution without NIDW in the source water matrix over the range σ_n=27.40-27.70 (c) RSIW contribution with NIDW in the source water matrix over the range σ_n=27.40-27.70 along section B7 (see figure 14). Dots indicate bottle sample locations.

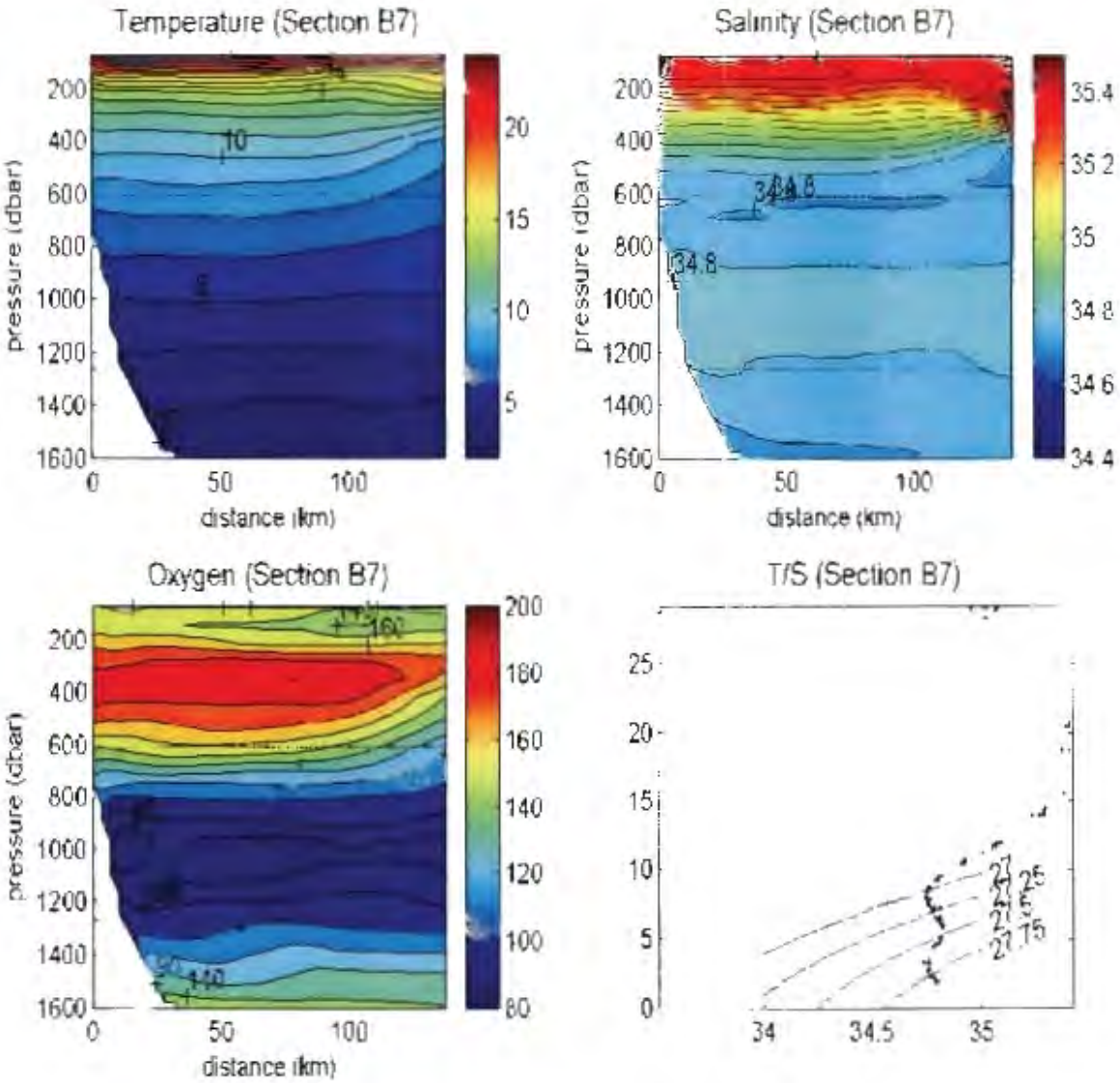

Fig 21 (ii): Property plots along section B7 (see figure 14) of temperature, salinity, oxygen and a T/S plot

Section B8 (see figure 14)

Crossing the southward flowing limb of the abovementioned cyclonic eddy as shown in the downward slope of the isohalines and isotherms (figure 22(ii)) this section covered the same line as section B3 except that it extended further west to the middle of the Mozambique Channel. A single RSIW core is observed along the Madagascar slope in which the RSIW content was 25-30% of the water sample in the density range 27.40-27.70 (figure 22(i)e). This is slightly less than the 30-40% contribution along section B3. It has to be noted that the flow along the Madagascar slope is now southward compared to the slightly northward flow in the case of section B3 (Ridderinkhof and de Ruijter, 2003).

Offshore the RSIW distribution appears layer like. The core observed in the middle of the channel along section B2 is not evident along this section. The contribution of RSIW was slightly higher and more in line with what was observed along section B3 when NIDW is excluded from the source water matrix with maximum RSIW contributing being 30-40% in several water samples (figure 21(i)b). The distribution of the high content RSIW water is however much greater along this section. Over the density range 27.25-27.40 the highest RSIW core is observed along the Madagascar slope where RSIW contributes 20-25% of the water sample at its core (figure 21(i)a). This is not an individual core but formed part of the layer just below it. Across this section the net transport of RSIW amounted only to -0.96 Sv which as in the above case was less and in the opposite direction of the previously measured transport along section B3.

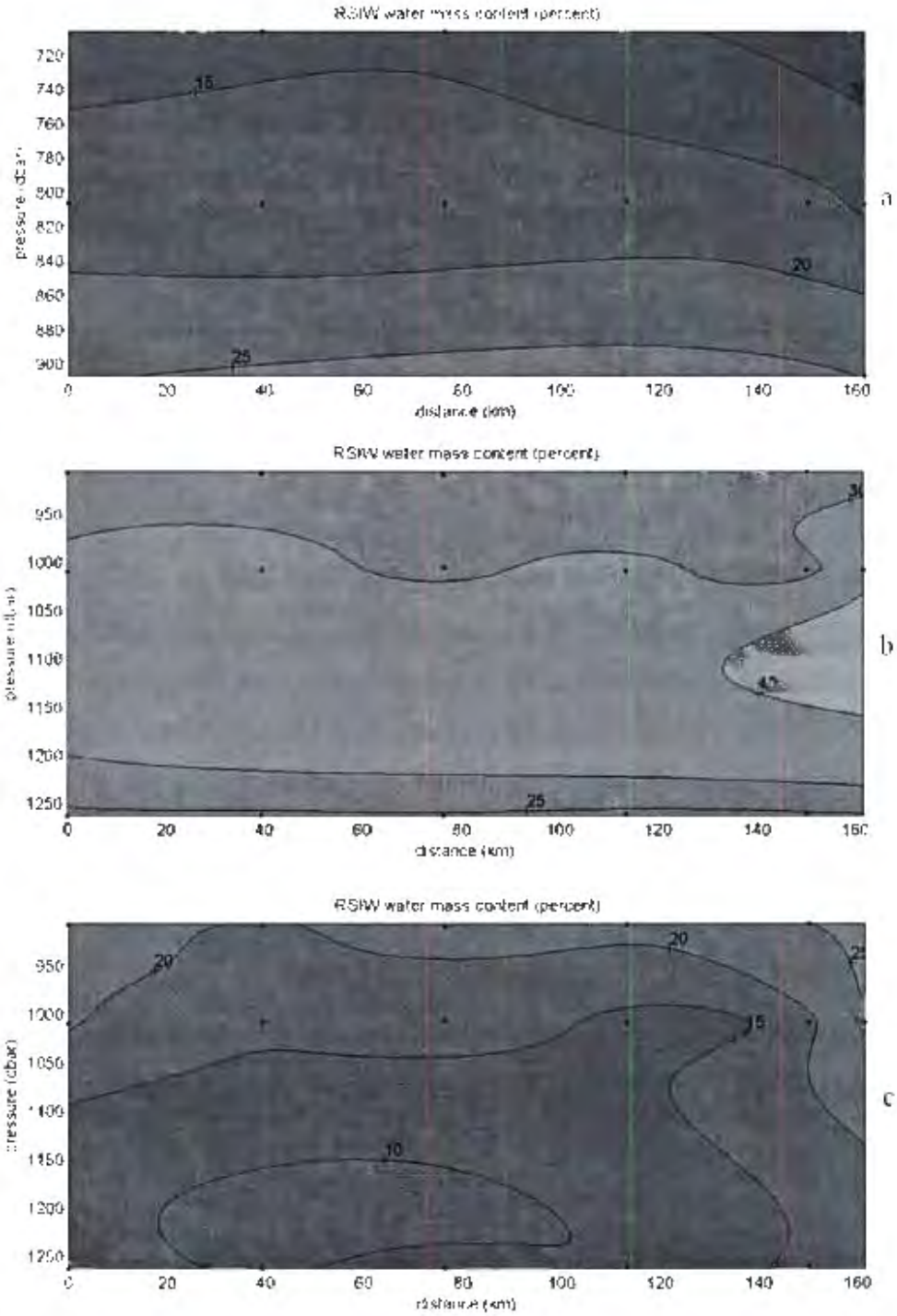

Fig 22 (i): a) RSIW contribution over the density range σ_n=27.25-27.40 (b) RSIW contribution without NIDW in the source water matrix over the range σ_n=27.40-27.70 (c) RSIW contribution with NIDW in the source water matrix over the range σ_n=27.40-27.70 along section B7 (see figure 14). Dots indicate bottle sample locations.

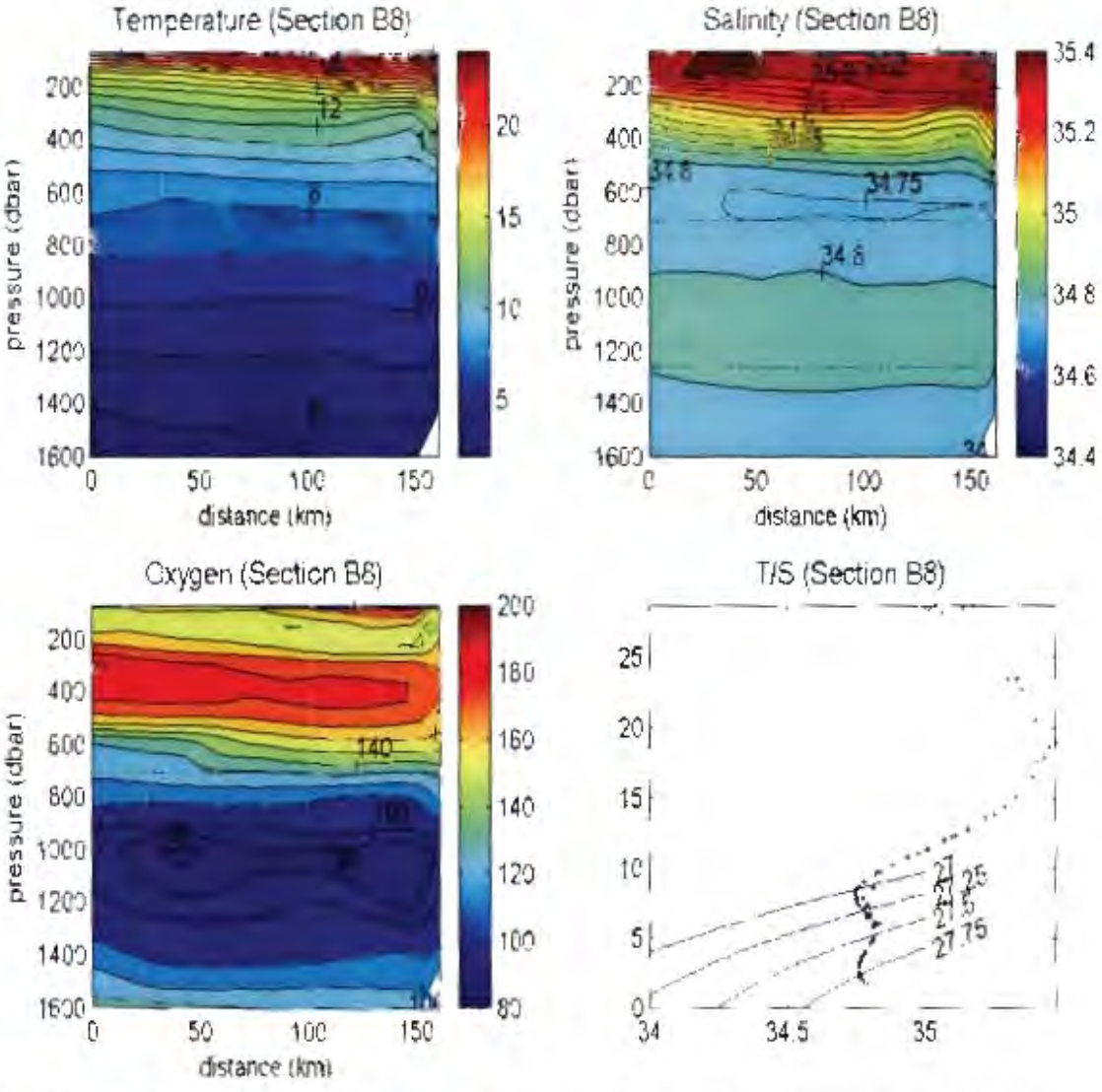

Fig 22 (ii): Property plots along section B8 (see figure 14) of temperature, salinity, oxygen and a T/S plot

Historical section

Section B9

Along this historical section the downward slope of the isotherms and isohalines suggests southward flow along the African continental slope (figure 22(i)). Compared to the other sections described above RSIW contributed 20-25% of the water sample at its core over the density range 27.25-27.40 (figure 22(ii)a). This is slightly higher than the 15-20% detected along the WOCE I04 line (section B6) and the ACSEX I section (section B5) at the southern exit of the Mozambique Channel. Also unlike the abovementioned sections the highest RSIW fraction is found in both the upper and lower density range similar to section B4 rather than in the 27.40-27.70 range. Over the 27.40-27.70 range only two data points were available. These two data points were associated with stations 1 and 2 in the upper density range. In fact over the entire density range the distribution of data points is very sparse. This means that except for an indication of the maximum contribution of RSIW of available data points no other conclusions can be drawn from this section. In both density ranges the RSIW is concentrated along the continental slope (figures 22(ii)a and b). This correlates well with the higher salinity and lower oxygen values observed along the slope and seen in the T/S diagram (figure 22(i)). The 20-25% contribution of RSIW observed in the lower density range compares well with the other sections at the southern exit of the channel. No NIDW was observed in the two water samples analysed in the lower density range.

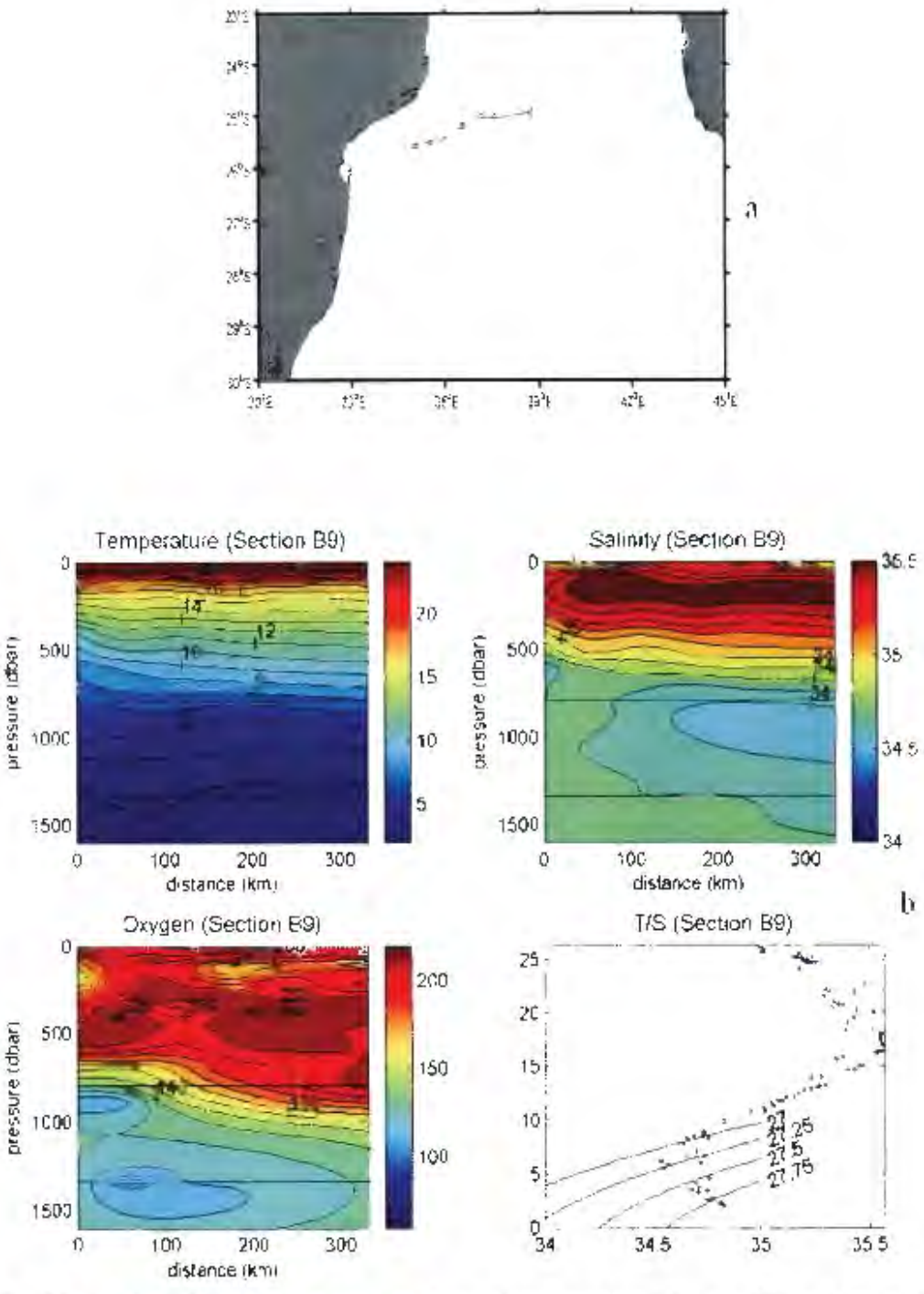

Fig 23(i): Map showing station positions along section B9 (see figure 14) (a) with property plots of temperature, salinity, oxygen and a T/S plot (b).

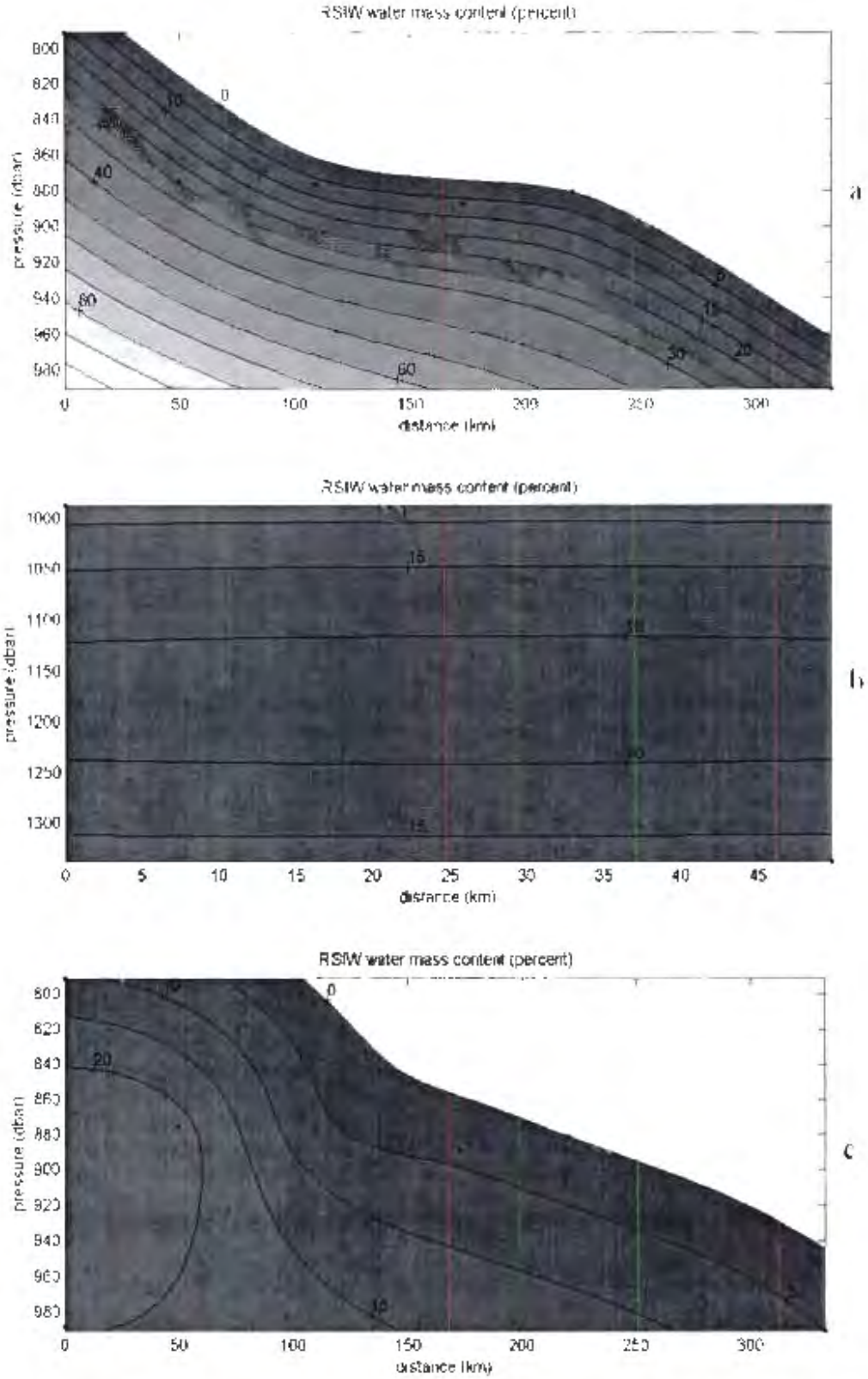

Fig 23 (ii): a) RSIW contribution over the density ranges 27.25-27.40 (b) 27.40-27.70 (b) and 27.25-27.45 along section B9 (see figure 14). Dots indicate bottle sample locations.

4.3) Region C: Northern Agulhas Current

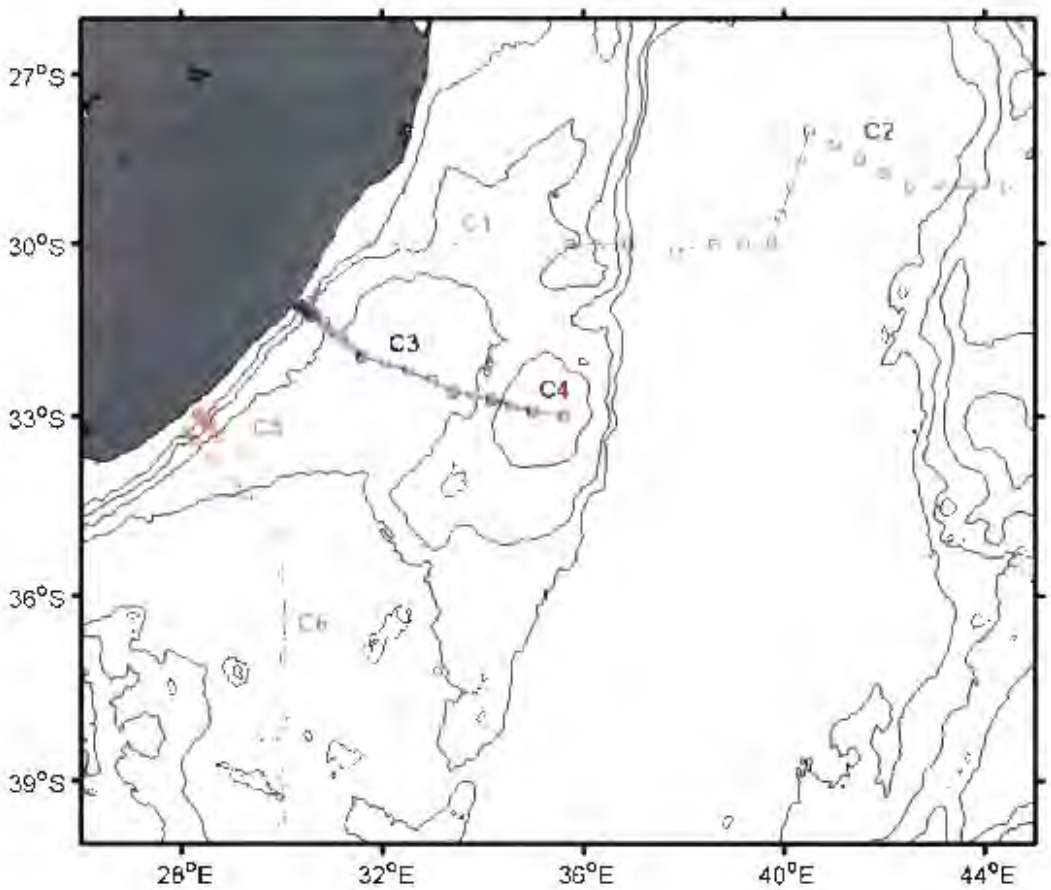

Fig 24: Map showing the positions of the cruise tracks of the sections investigated in this region. C1 and C2 are ACSEX II sections whilst sections C3 to C6 were completed as part of the WOCE program.

4.3) Section C (northern Agulhas Current)

ACSEX II sections

Section C1

This section stretched ~225 km from the African continental slope into the northern Natal Valley. The isotherms and isohalines (figure 25(ii)) suggest southward flow along the slope as would be expected with the Agulhas Current hugging the slope (Bryden and Beal, 2001). Offshore however the dome shape of the isotherms and isohalines suggests the presents of a cyclonic eddy about 200 km from the slope (figure 25(ii)).

Over the density range 27.25-27.40 RSIW at its core constituted between 10-15% of the water sample which as in the case of the abovementioned two sections was situated along the continental slope (figure 25(i)a). This core was not distinct but formed part of the underlying layer of RSIW (figure 25(i)b). Considering that east of Madagascar RSIW was almost absent in this density range it would thus appear that the RSIW observed in this density range came from the Mozambique Channel. Although this 10-15% RSIW contribution compared well to values found along sections B5 and B6 this is less than what was found along section B9 just north of it. Over the density range 27.40-27.70 RSIW contributed between 10-15% of the water sample at its core that now is observed as a layer across the Natal Valley (figure 25(i)b). This value is only slightly higher when NIDW is introduced into the water source matrix. When this was done RSIW contributed between 15-20% to the water sample situated close to the continental shelf (figure 25(i)c). Both the above two source water matrix configuration results were below that observed in the southern exit of the Mozambique Channel. As is the case in the upper density range the maximum RSIW contribution indicates the RSIW seen in this density range to have come from the Mozambique Channel. Also similar to abovementioned sections further north the RSIW spreading range was greater than the neutral density 27.6. The total net transport of RSIW across this section was -0.67 Sv. This is almost similar to that along section B5 but much higher than that observed along section B6.

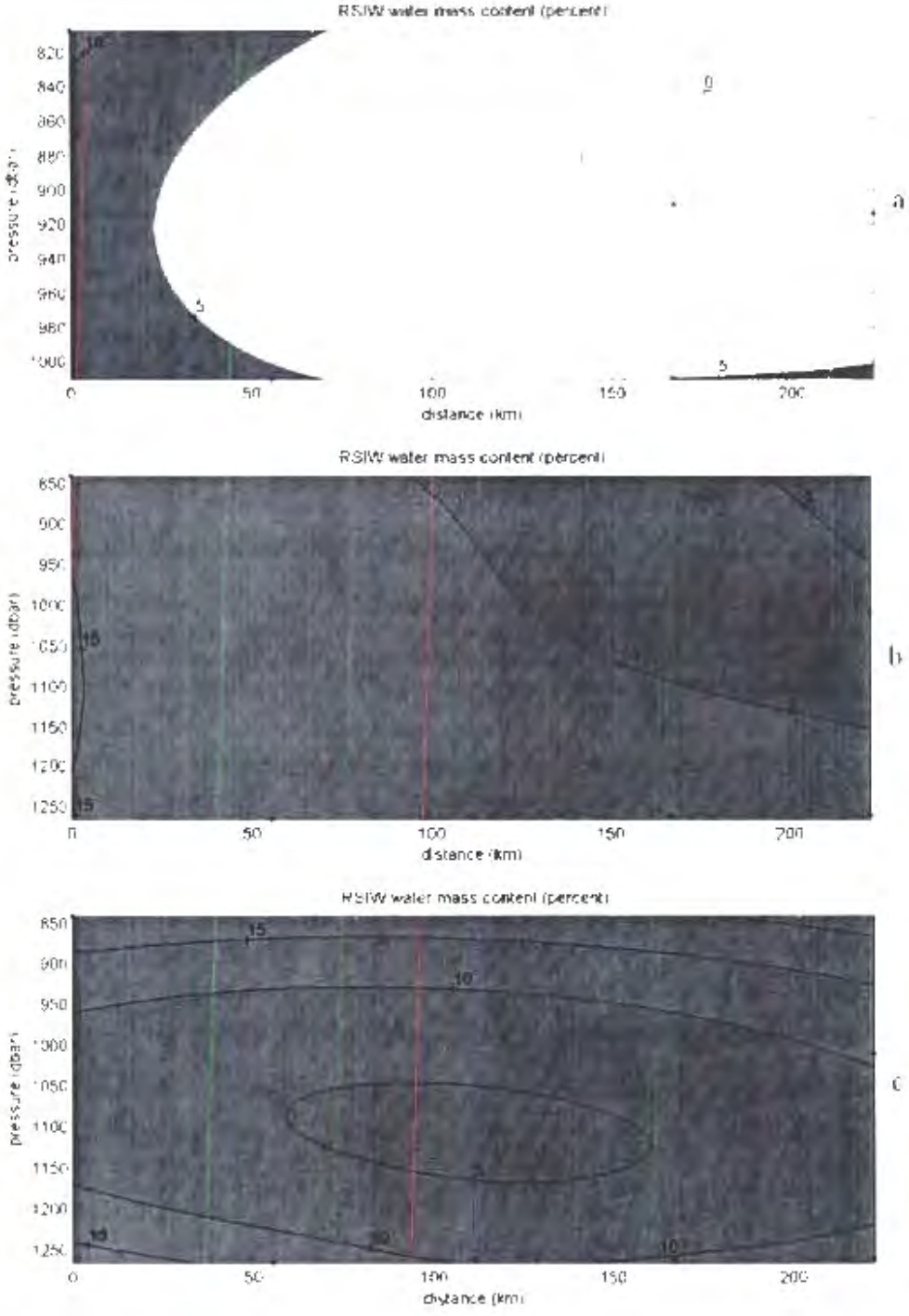

Fig 25 (i): a) RSIW contribution over the density range σ_n=27.25-27.40 (b) RSIW contribution without NIDW in the source water matrix over the range σ_n=27.40-27.70 (c) RSIW contribution with NIDW in the source water matrix over the range σ_n=27.40-27.70 along section C1 (see figure 24). Dots indicate bottle sample locations.

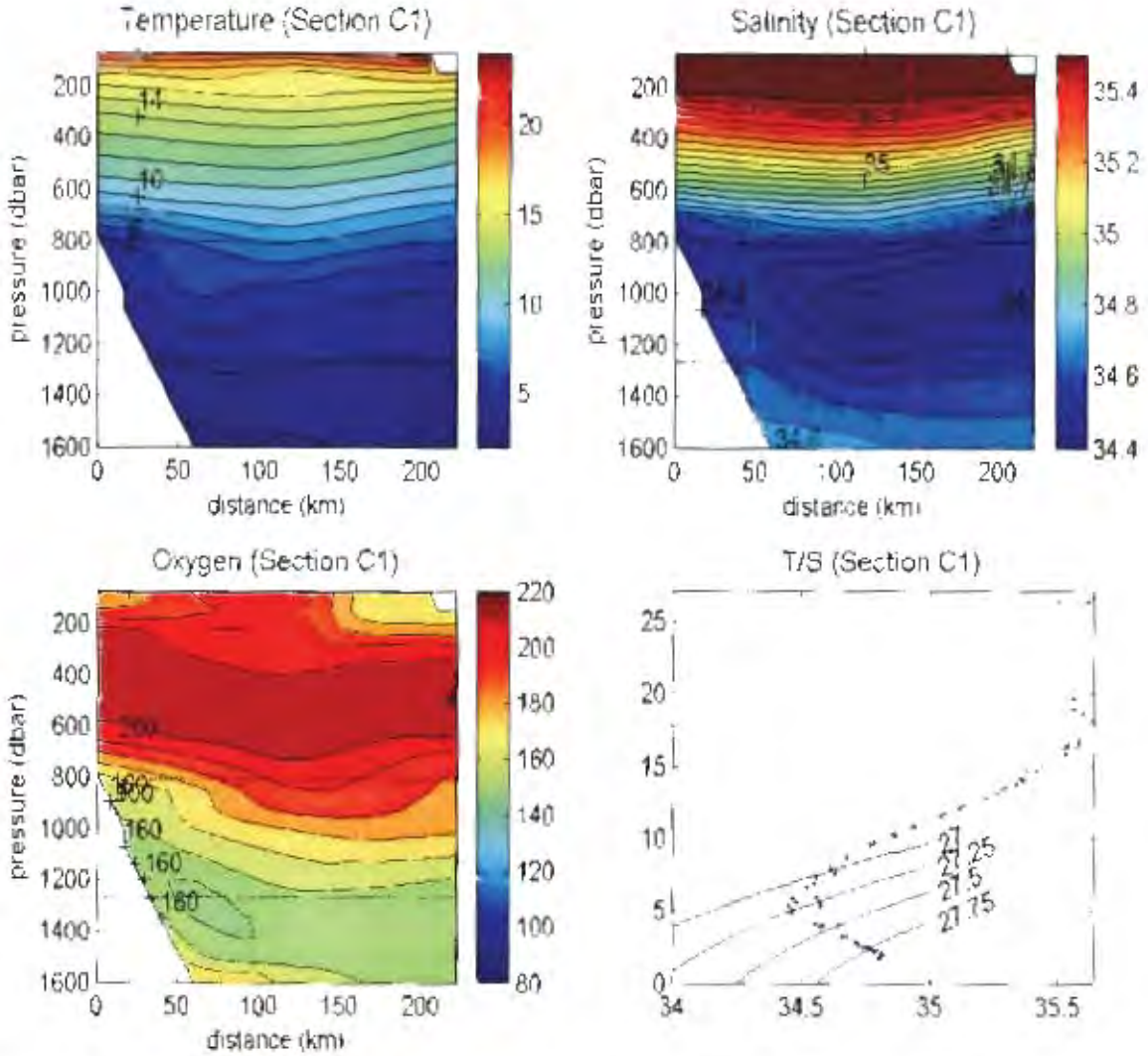

Fig 25 (ii): Property plots along section C1 (see figure 24) of temperature, salinity, oxygen and a T/S plot

Section C2 (Eddie dipole)

This section crosses a cyclone between two anti-cyclonic eddies situated in the Mozambique basin and across part of the Madagascar Plateau. These eddies were spawned south of Madagascar where the East Madagascar Current separates from the shelf (de Ruijter et al., 2004). The divisions between the different eddies (figure 26(i)) were obtained from de Ruijter et al. (2004). The three eddies can also clearly be seen in the bowl like structure and doming of the isohalines, isotherms and oxygen contours (figure 26(ii)).

From the distribution of RSIW cores over the density range 27.40-27.70 it would appear if RSIW contributed to both the cyclonic and to the anti-cyclonic eddies. The highest contribution of RSIW in terms of purity appears to be in the anti-cyclonic eddies. This is also seen in the oxygen minima with the extreme oxygen minima observed in the anti-cyclones (figure 26(ii)). IIW was only observed in the cyclonic eddy which would probably indicate its water to originate from the inshore part of the East Madagascar Current. The intermediate water of the anti-cyclonic eddies was observed to be mostly siAAIW found in the offshore environment. Over this density range RSIW contributed between 15-20% of the water sample in the different cores. This result correlates well with other sections east and south of Madagascar. However unlike most sections in that region, with the introduction of NIDW, RSIW contributions is only slightly reduced and still contributed 15% of the water sample concentrated in the western anti-cyclonic eddy. Considering its spawning position and somewhat higher purity to that observed along the east Madagascar slope it is possible that this core came through the Mozambique Channel. This is not conclusive as along section A2 RSIW still contributed around 15% of water sample along the slope. Little to no RSIW is visible in the density range 27.25-27.40 similar to what was found east of Madagascar (figure 26(i)a and b). The absence of RSIW is also clearly illustrated in the T/S diagram (figure 26(ii)) with only a single data point indicating highly saline water in this intermediate density range compared to the other intermediate water masses.

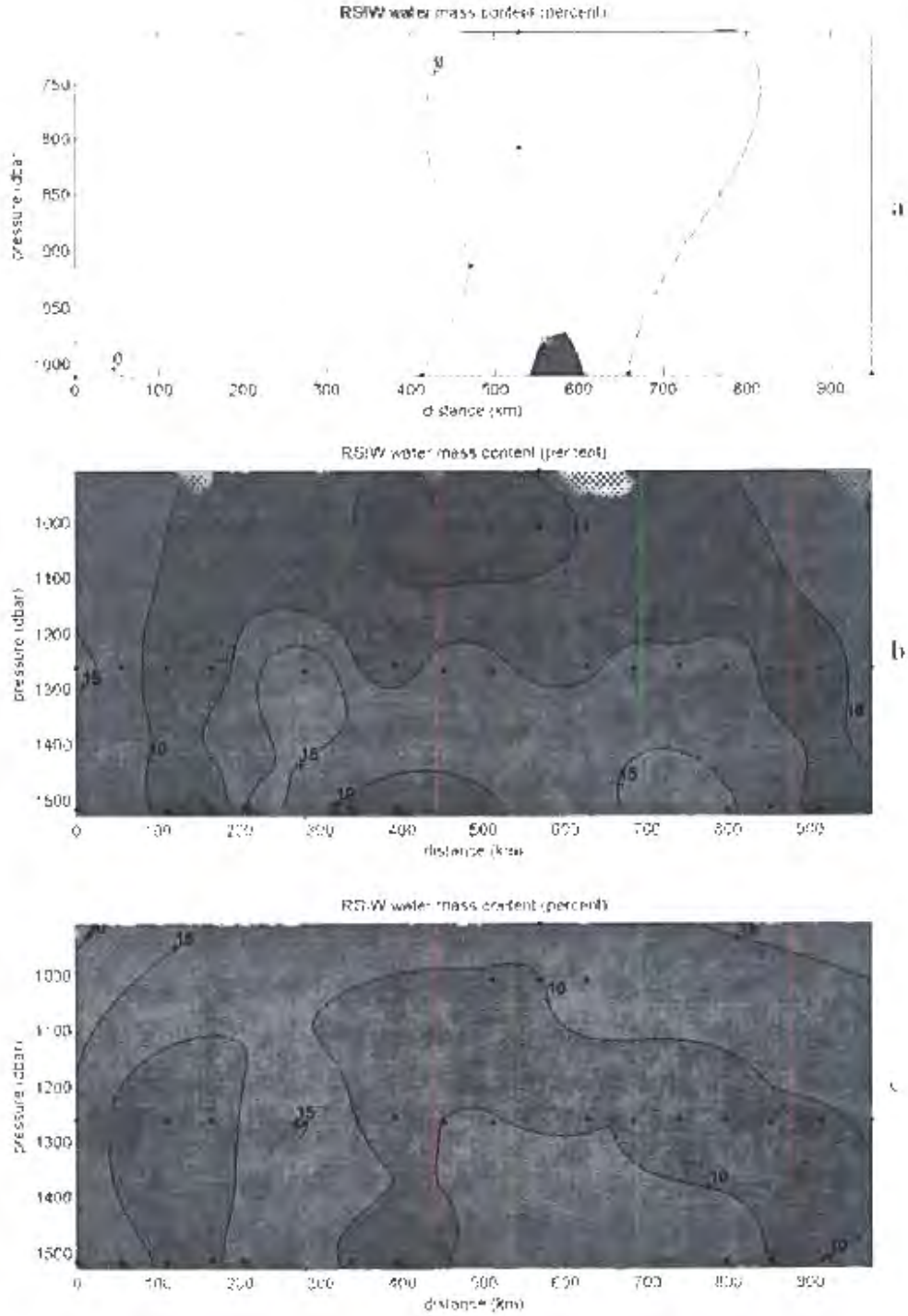

Fig 26 (i): a) RSIW contribution over the density range σ_θ=27.25-27.40 (b) RSIW contribution without NIDW in the source water matrix over the range σ_θ=27.40-27.70 (c) RSIW contribution with NIDW in the source water matrix over the range σ_θ=27.40-27.70 along section C2 (see figure 24). Dots indicate bottle sample locations.

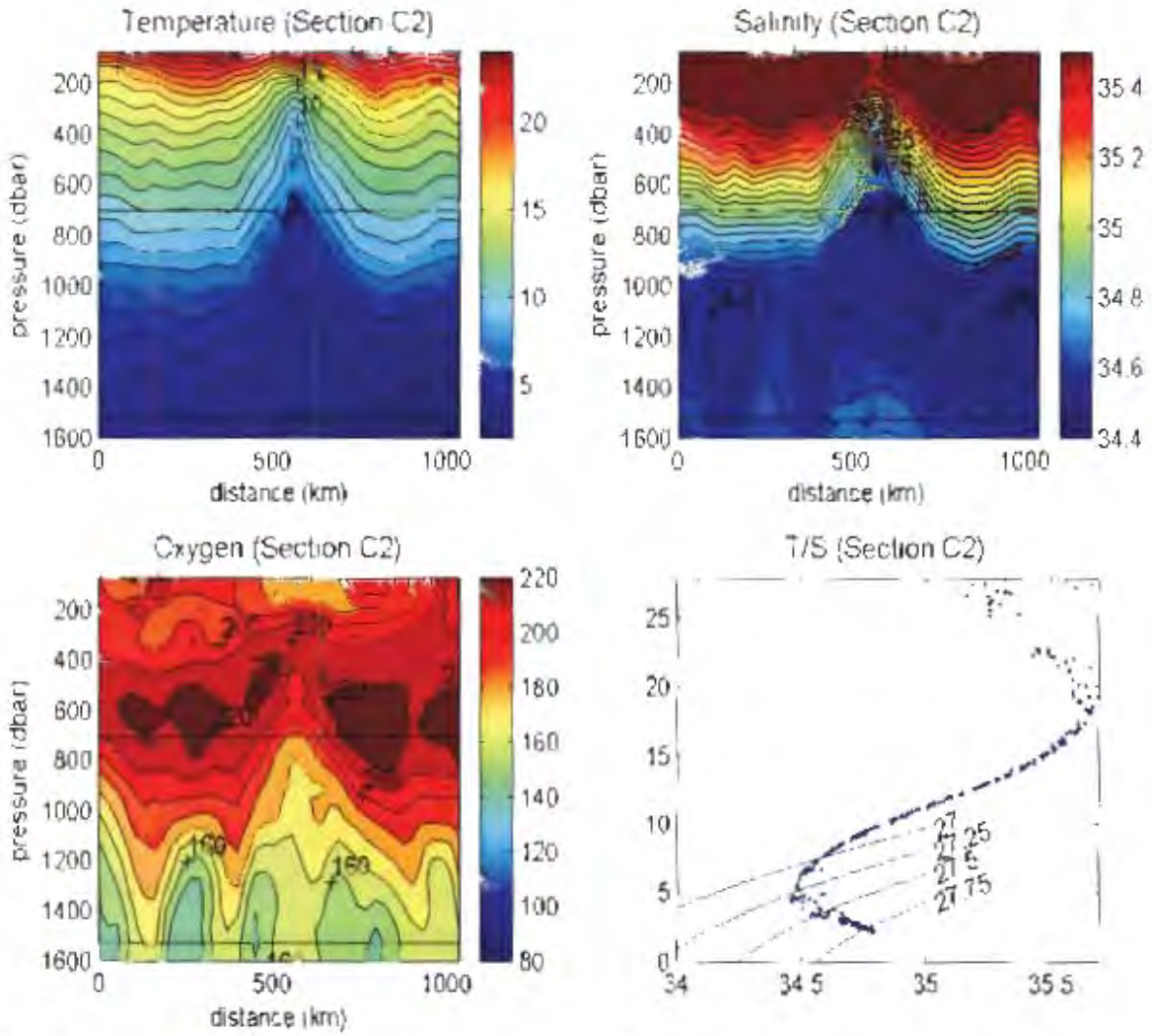

Fig 26 (ii): Property plots along section C2 (see figure 24) of temperature, salinity, oxygen and a T/S plot

WOCE sections

Section C3 (I05)

Crossing the Agulhas Current and a surface intensified eddy on the oceanic side of the current (Donohue and Toole, 2003) this section stretches from the African coast across the Natal Valley to the Mozambique Plateau. The circulation features can also be seen in the isolines in the downward slope along the continental slope and dome structure further offshore (figure 27(ii)).

Over the density range 27.25-27.40 two separate RSIW cores are visible, one along the African continental slope and the other offshore between the current and the surface-intensified eddy (figures 27(i)a and 27(ii)). RSIW would thus appear to flow on both the inside and on the outside of the Agulhas Current. In the core along the shelf RSIW contributed nearly 20% of the water sample whilst in the offshore core its contribution was slightly less, amounting to 15-20%. The slope core result compares well with what was observed along section B9 at the southern mouth of the Mozambique Channel. Both cores appear distinct with the introduction of NIDW in the source water matrix (figures 27(i)a and 27(i)c). As was the case along section C1 the RSIW observed in the inside and outside cores would have had to have come from the Mozambique Channel when comparing it to the RSIW water mass fractions of sections east of Madagascar. With both the inshore and offshore water masses originating from the Mozambique Channel it would appear if the water mass distribution as described by Harris (1972) does not hold for this section. Over the density range 27.40-27.70 RSIW contributes 20-25% of the water samples found in two cores situated on the landward side of the Agulhas Current and under the current even when NIDW is introduced into the source water mass matrix (figure 27(i)b and c). This value is considerably higher than the value found along section C1 just north of it and section B6 in the southern Mozambique Channel. The RSIW distribution discussed is also clearly visible from both the salinity and oxygen sections with the high salinity (also seen in the T/S diagram) and low oxygen cores visible on both sides of the Agulhas Current (figure 27(ii)). The net transport of RSIW across this section was -1.39 Sv which is higher than any value measured at the southern mouth of the Mozambique Channel. This can however be attributed to the higher current speeds of the Agulhas Current.

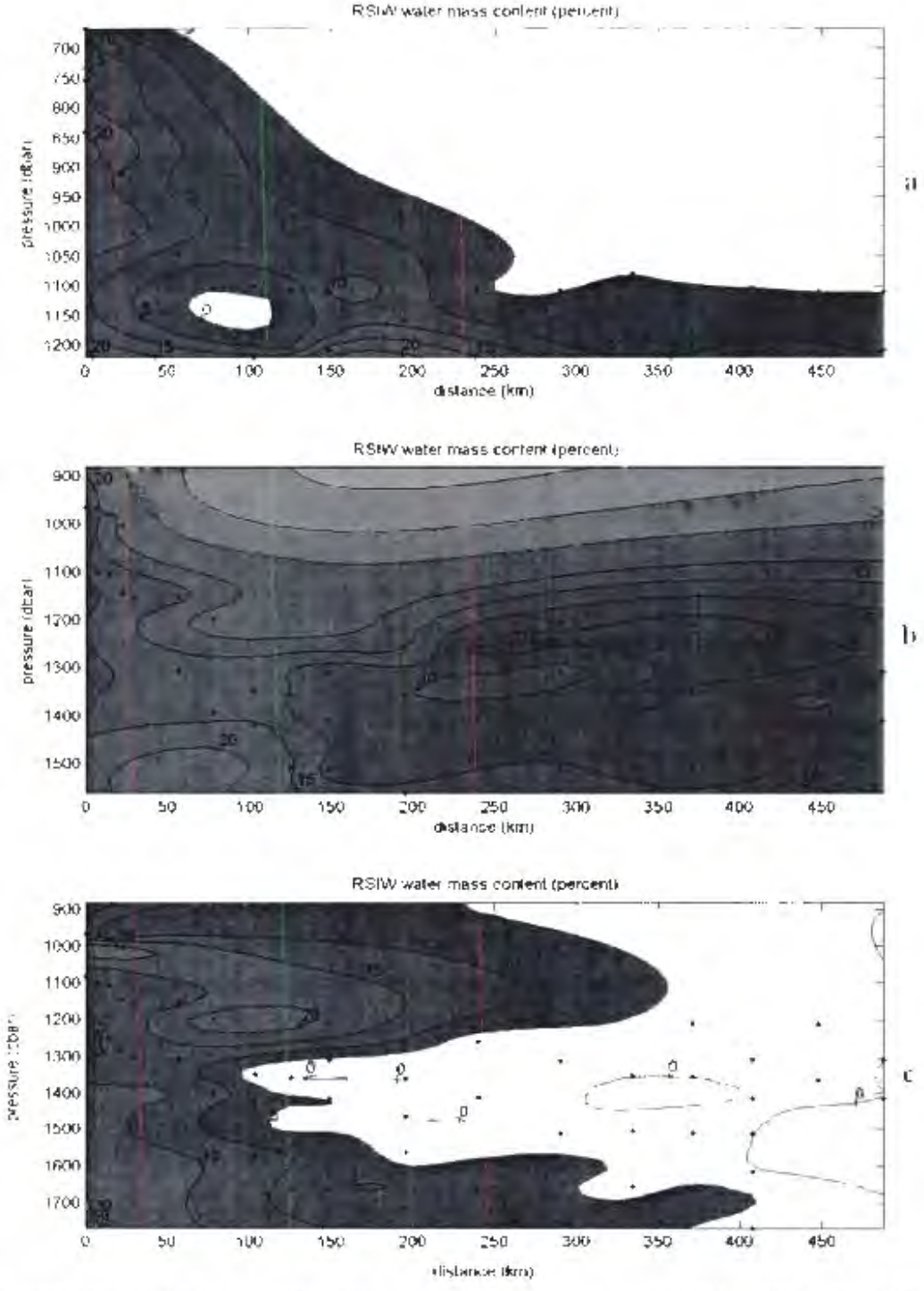

Fig 27 (i): a) RSIW contribution over the density range σ_n=27.25-27.40 (b) RSIW contribution without NIDW in the source water matrix over the range σ_n=27.40-27.70 (c) RSIW contribution with NIDW in the source water matrix over the range σ_n=27.40-27.70 along section C3 (see figure 24). Dots indicate bottle sample locations.

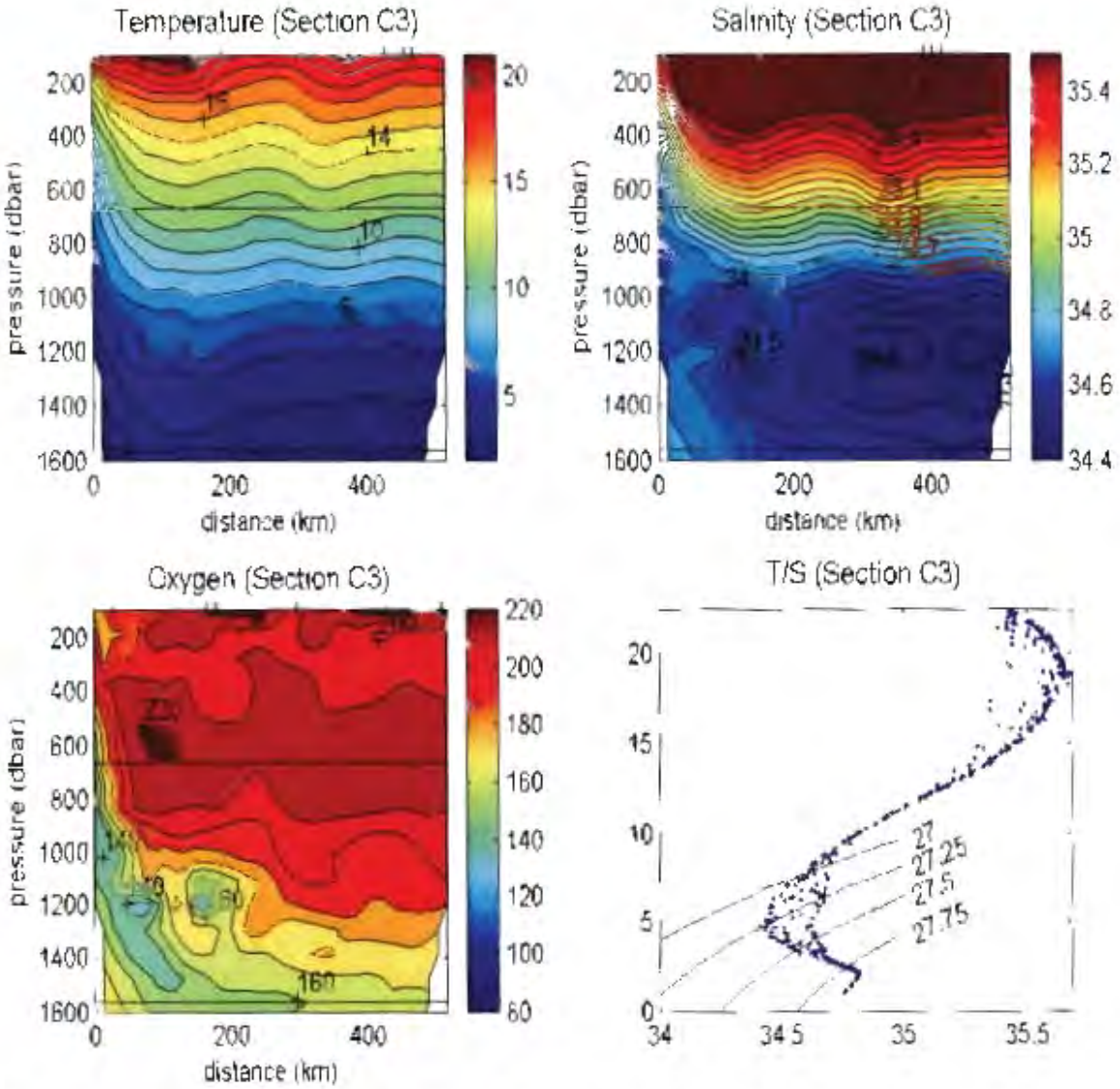

Fig 27 (ii): Property plots along section C3 (see figure 24) of temperature, salinity, oxygen and a T/S plot

Section C4 (105p)

This section covers much the same station positions as the above section also extending to the Mozambique Plateau. In terms of the flow regime the Agulhas Current is still along the continental slope but unlike the previous section we do not have the surface intensified eddy offshore of the current (Toole and Warren, 1993). The flow regime is also clearly depicted in the slopes of the isolines (figure 28(ii)).

Over the density range 27.25-27.40 RSIW at its core contributed just under 10% of the water sample situated along the slope. This value is considerably lower than the nearly 20% in the previous section (figure 28(i)a). The core does not appear to be separate from RSIW found in the underlying layer (figure 28(i)b and c). Offshore RSIW contributed only 5-10% to the water sample which is similarly much less than that observed in the previous section. This reduction in the water mass percentage is also observed in the higher oxygen minimum observed in this density range (figure 28(ii)). The reduced RSIW core value is also observed over the density range 27.40-27.70 (figure 28(i)b and c). Here RSIW contributed only between 10-15% of the water mass samples at its core compared to 20-25% observed in the previous section. This difference was also observed when NIDW was included in the source water matrix figure 28(i)c). With the inclusion of NIDW RSIW is almost exclusively found along the continental slope compared to it's almost layer like distribution. However in combination with the upper density range this layer appear to consist of two cores situated on either side of the current that co-inside with the two oxygen minimum cores (figure 28(ii)). From these two sections it would thus appear that although RSIW is a consistent part of the Agulhas Current System just south Durban there seems to be some variability in its source water contribution. The presence of RSIW in the absence of offshore eddies seems to be restricted mostly to the inside of the Agulhas Current when NIDW is included in the source water matrix. RSIW is detected as deep as the neutral density surface 27.66 around 250 km offshore and 27.63 along the slope where it still contributed above 10% of the water sample. The variability in its contribution is also observed in the net transport of RSIW which now amounted to only -0.75 Sv. This is a considerable reduction compared to the previous section.

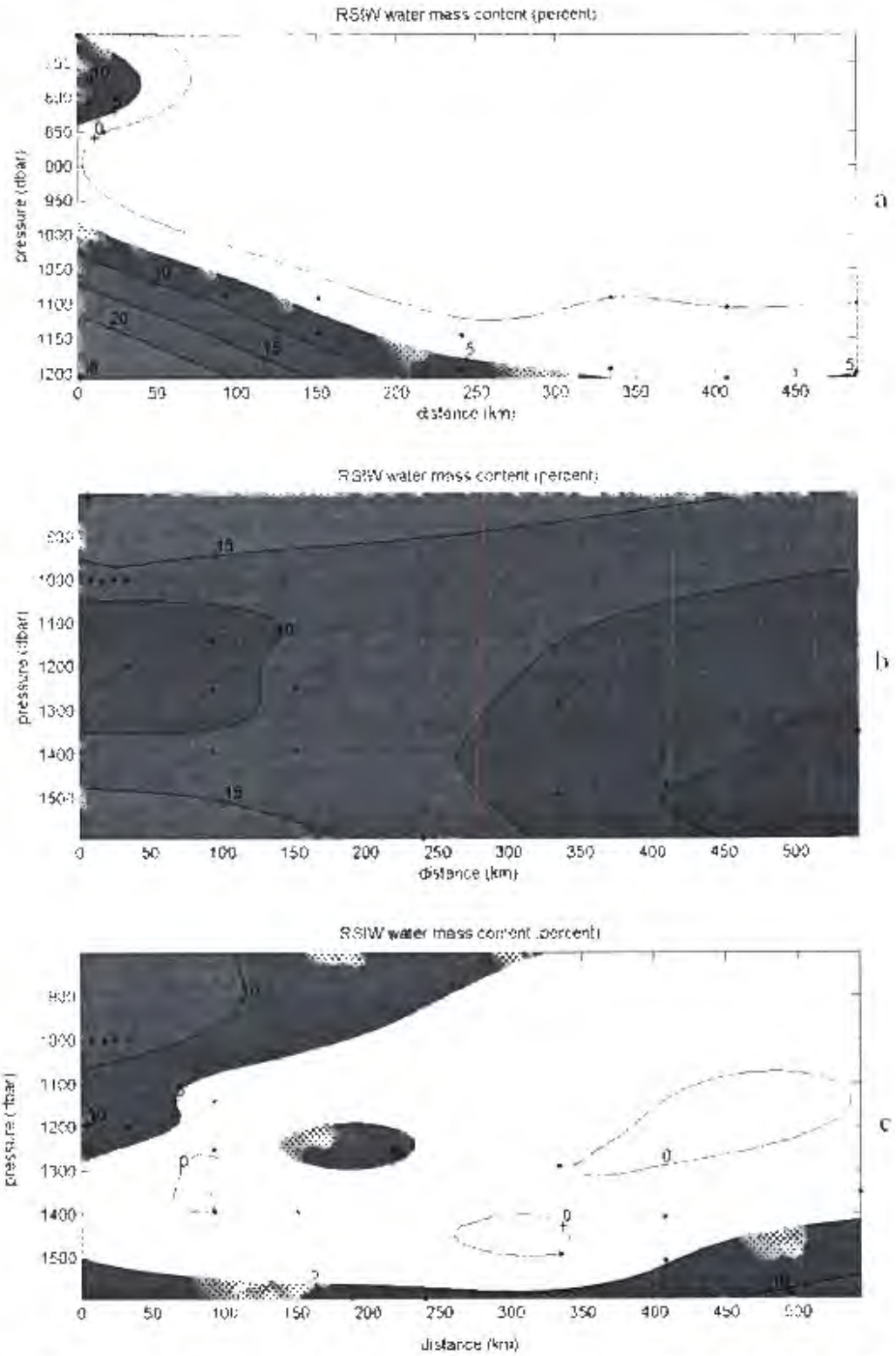

Fig 28 (i): a) RSIW contribution over the density range σ_n=27.25-27.40 (b) RSIW contribution without NIDW in the source water matrix over the range σ_n=27.40-27.70 (c) RSIW contribution with NIDW in the source water matrix over the range σ_n=27.40-27.70 along section C4 (see figure 24). Dots indicate bottle sample locations.

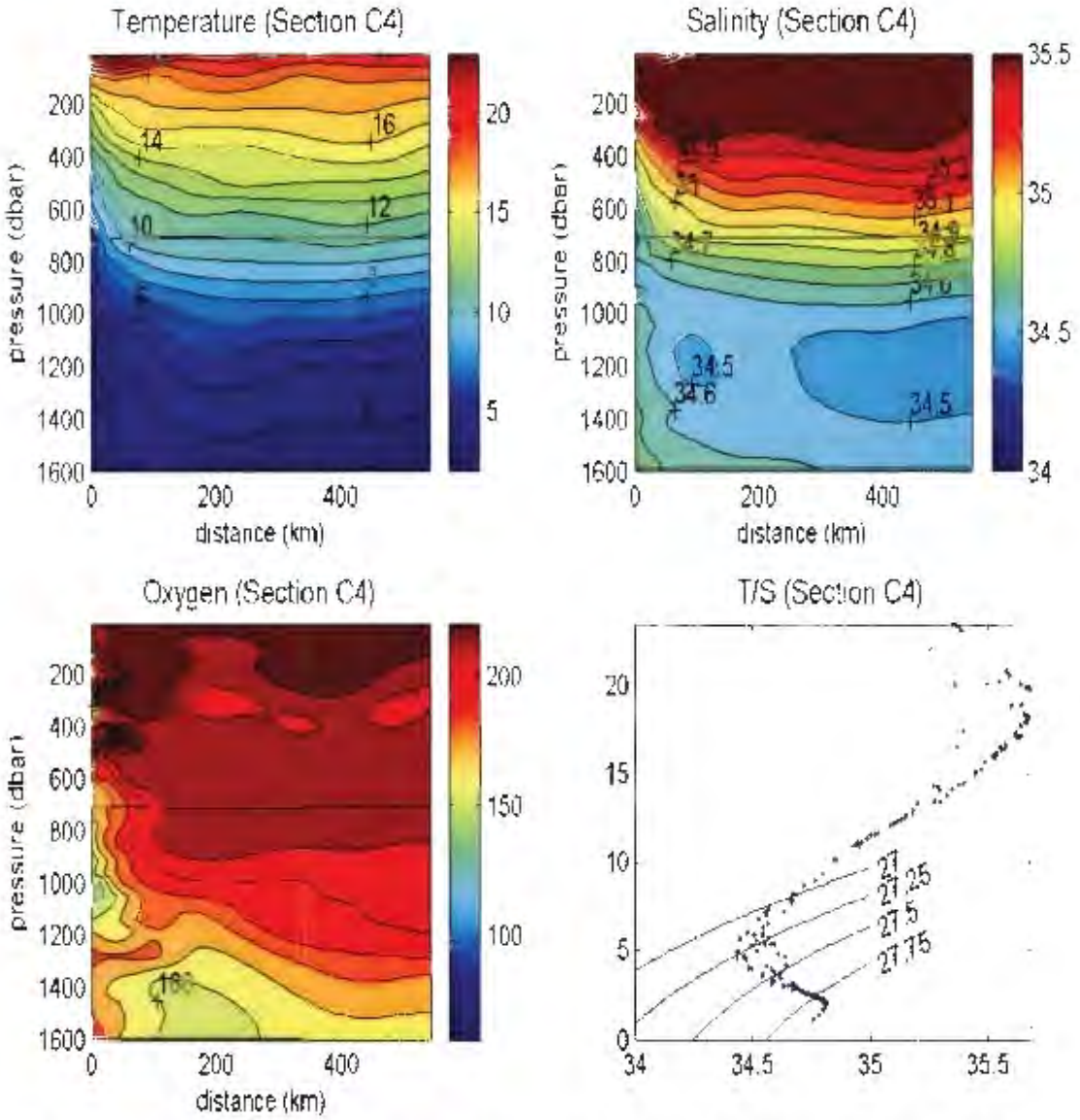

Fig 28 (ii): Property plots along section C4 (see figure 24) of temperature, salinity, oxygen and a T/S plot

Section C5

This section stretched only 45 km offshore from the African continental slope and would thus cover only the inshore half of the Agulhas Current (figure 29(ii)). Slightly different to previous source water matrices we introduced ICW into the source water matrix and made the upper neutral density surface 27.20. This was done to introduce two more data points that lay just shallower than the 27.25 surface. RSIW at it core contributed 10-15% of the water sample in the density range 27.20-27.40 (figure 29(i)a). This is comparable with that found along section C4 even though it was 3 degrees of latitude further south. Over the density range 27.40-27.70 RSIW constituted 20-25% of the water sample at its core even when NIDW was introduced into the source water mass matrix concentrated around 15-20 km offshore of the continental slope (figure 29(i)a and b). It needs to be noted that the deepest density surface was shallower than the 27.6 surface or potential density surface 27.5 (figure 29(ii)). This is considerably higher than what was found along section C4 further north but comparable with that of section C3 at the same latitude as section C4. This would suggest variable input of RSIW into the Agulhas Current System.

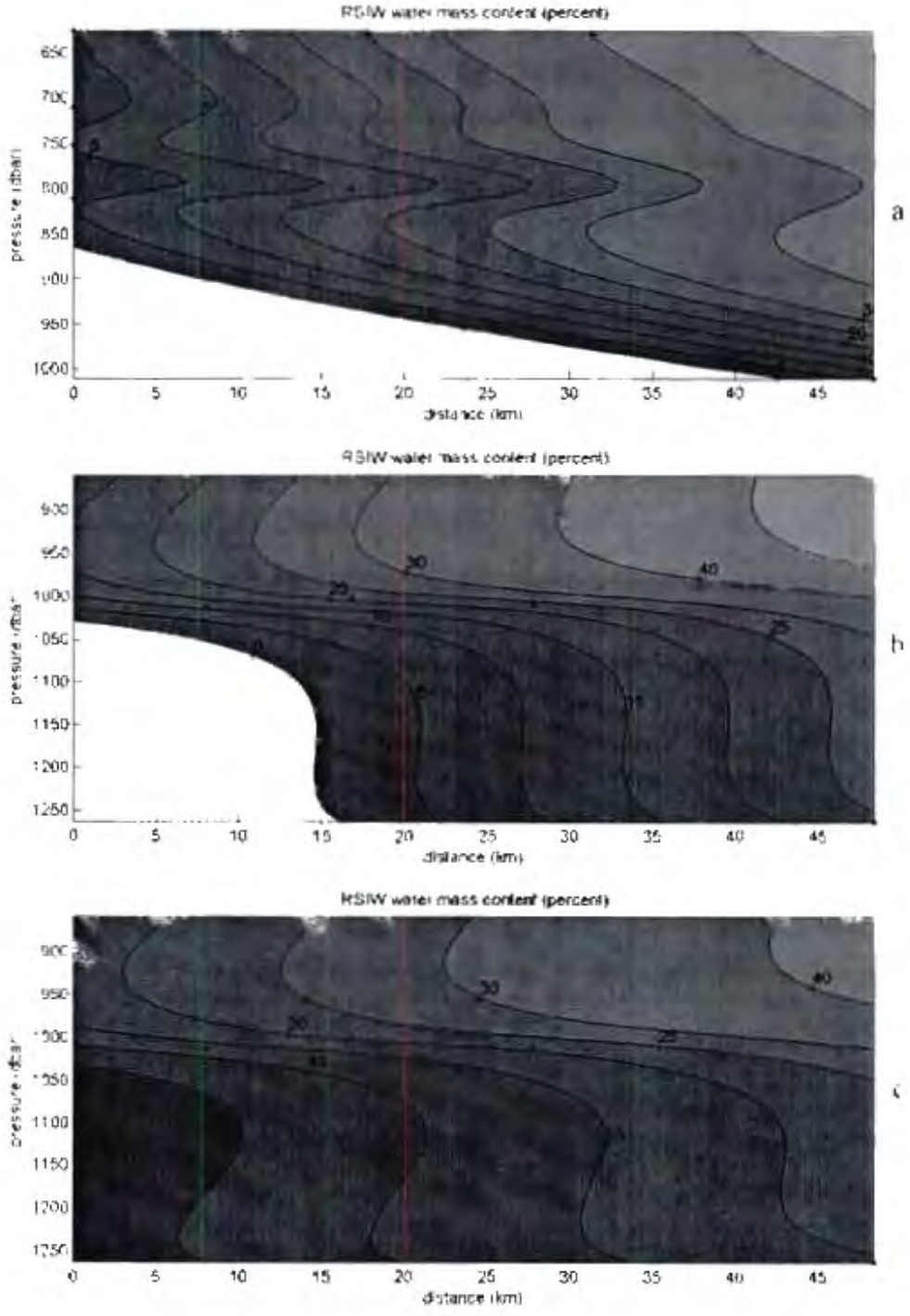

Fig 29 (i): a) RSIW contribution over the density range σ_n=27.25-27.40 (b) RSIW contribution without NIDW in the source water matrix over the range σ_n=27.40-27.70 (c) RSIW contribution with NIDW in the source water matrix over the range σ_n=27.40-27.70 along section C5 (see figure 24). Dots indicate bottle sample locations.

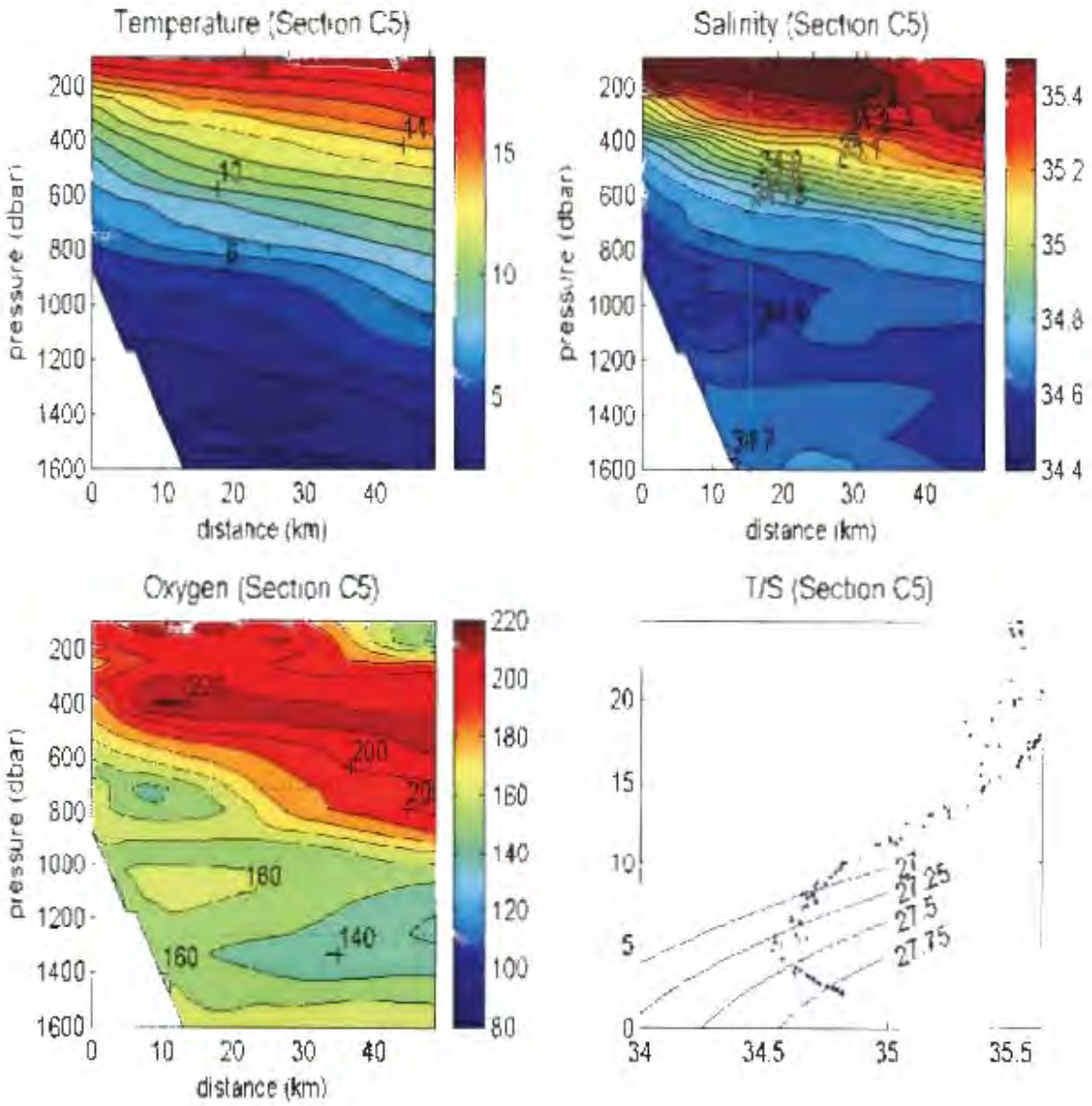

Fig 29 (ii): Property plots along section C5 (see figure 24) of temperature, salinity, oxygen and a T/S plot

Section C6 (106)

This section extended from the African continent across the Agulhas Current as far south as the Subtropical Convergence (figure 30(ii)). From the isolines and oxygen contours it is clear that the flow along this section was dominated by the Agulhas Current along the continental slope and a cyclonic eddy further south seen in the doming of the isotherms, isohalines and the upwelling of the oxygen minimum (figure 30(ii)). RSIW contributed only slightly over 5% of the water sample at its core over density range 27.25-27.40 (figure 30(i)a). This is slightly less than the abovementioned section but much reduced compared to sections further north. As would be expected with the smaller RSIW contribution we now find that much of the water along the slope in this density range is below 34.6 psu as opposed to above it as was the case further north (figure 30(ii)). Over density range 27.40-27.70 the RSIW core was situated along the continental shelf. The RSIW contribution was 15-20% of the water sample with and without NIDW as part of the source water matrix. This is only slightly less than the over 20-25% in the above section (figure 30(i)b). Similar to section C3 an offshore core is observed with RSIW contributing just over 5% of the water sample in the core. This core was observed just north of a cold core eddy with Southern Ocean water masses at its core. The 5% observed in the core of the eddy is not considered as its mass conservation residual fit was greater than 1%. Just south of the eddy the Agulhas Return Current was flowing eastward (Park et al. 2001). The maximum depth upon which RSIW was detected was on the 27.66 neutral density surface. Along this section the net RSIW transport amounted to -0.63 Sv

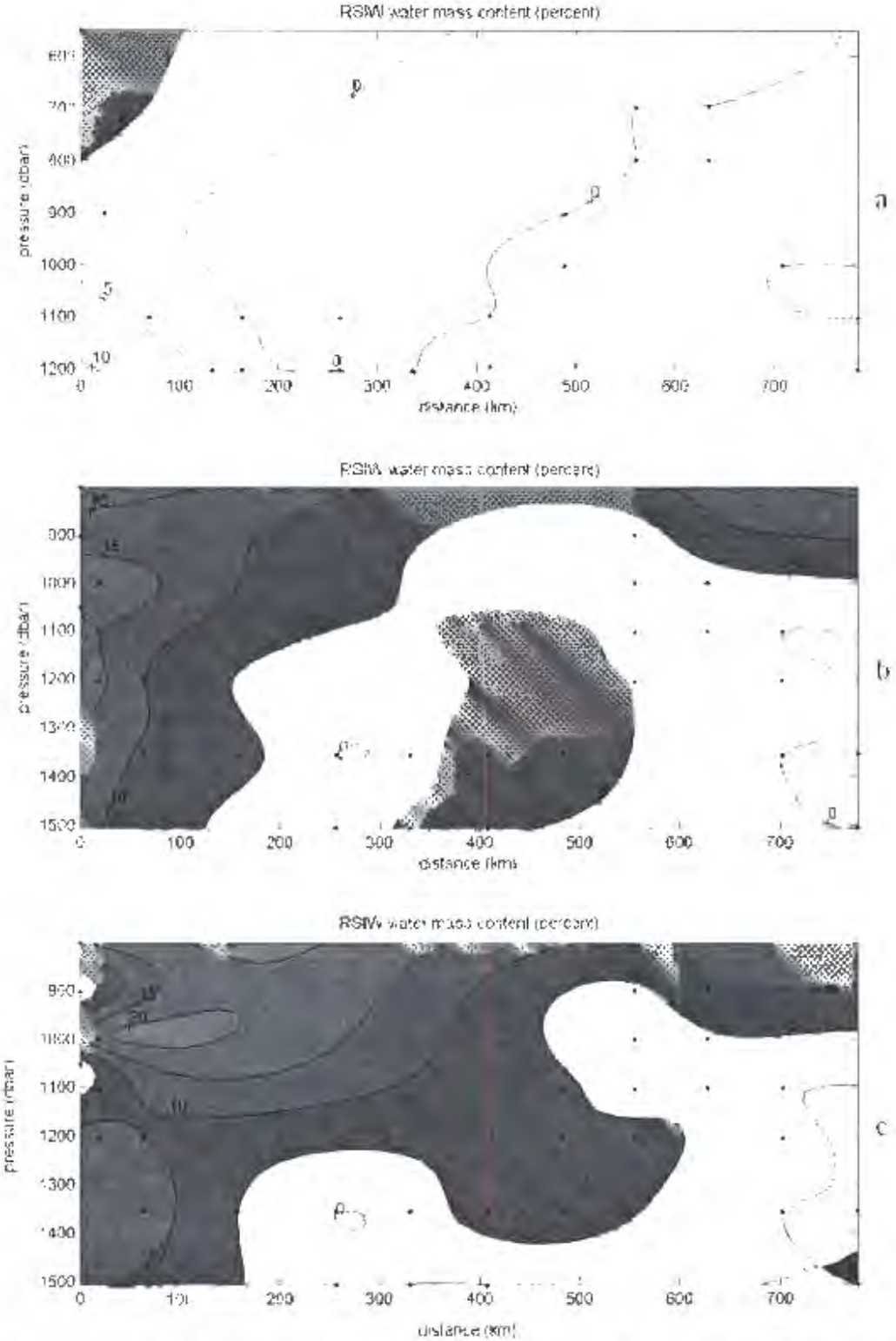

Fig 30 (i): a) RSIW contribution over the density range σ_n=27.25-27.40 (b) RSIW contribution without NIDW in the source water matrix over the range σ_n–27.40-27.70 (c) RSIW contribution with NIDW in the source water matrix over the range σ_n–27.40-27.70 along section C6 (see figure 24). Dots indicate bottle sample locations.

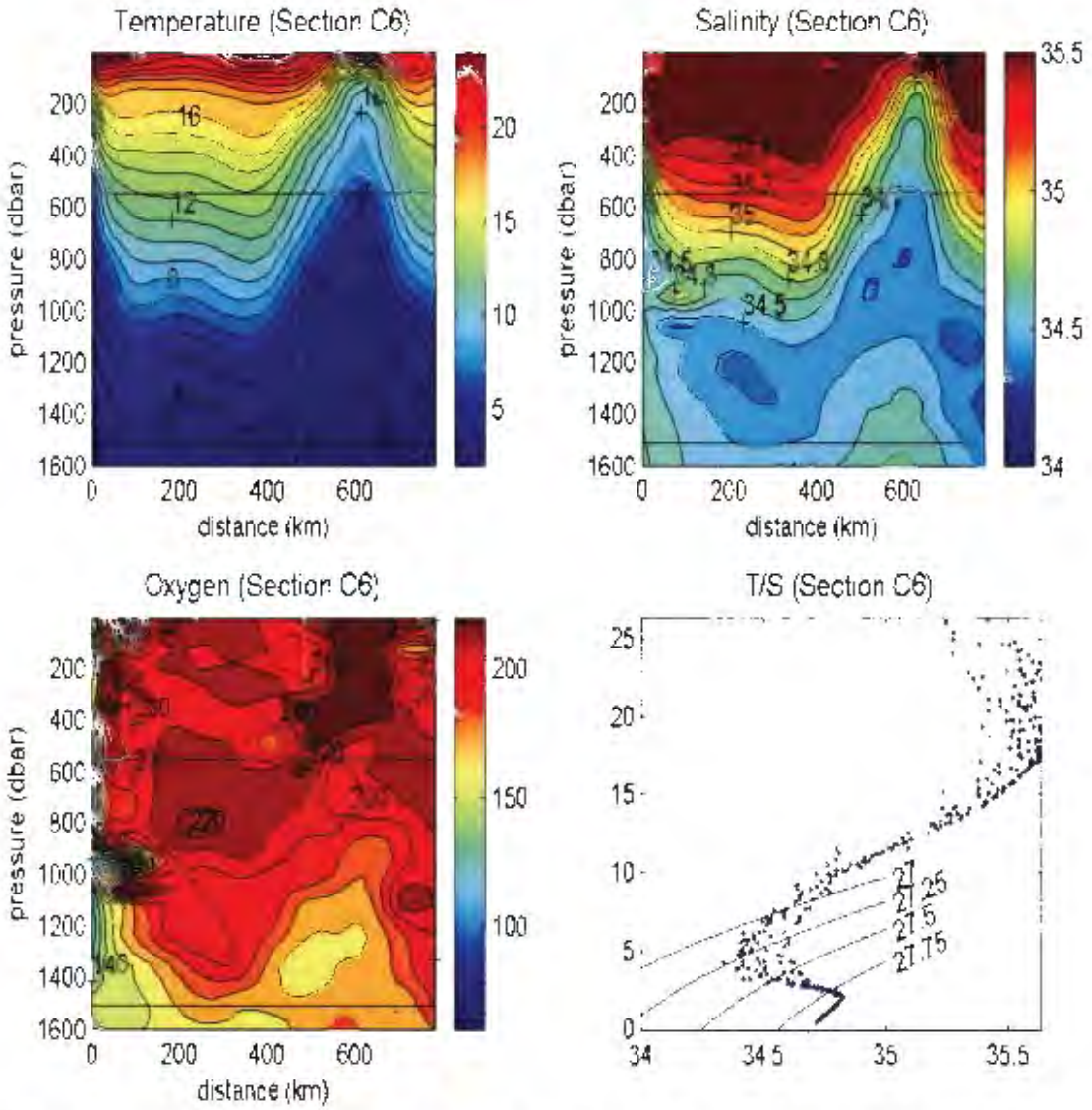

Fig 30 (ii): Property plots along section C6 (see figure 24) of temperature, salinity, oxygen and a T/S plot

4.4) Region D: Southern Agulhas Current

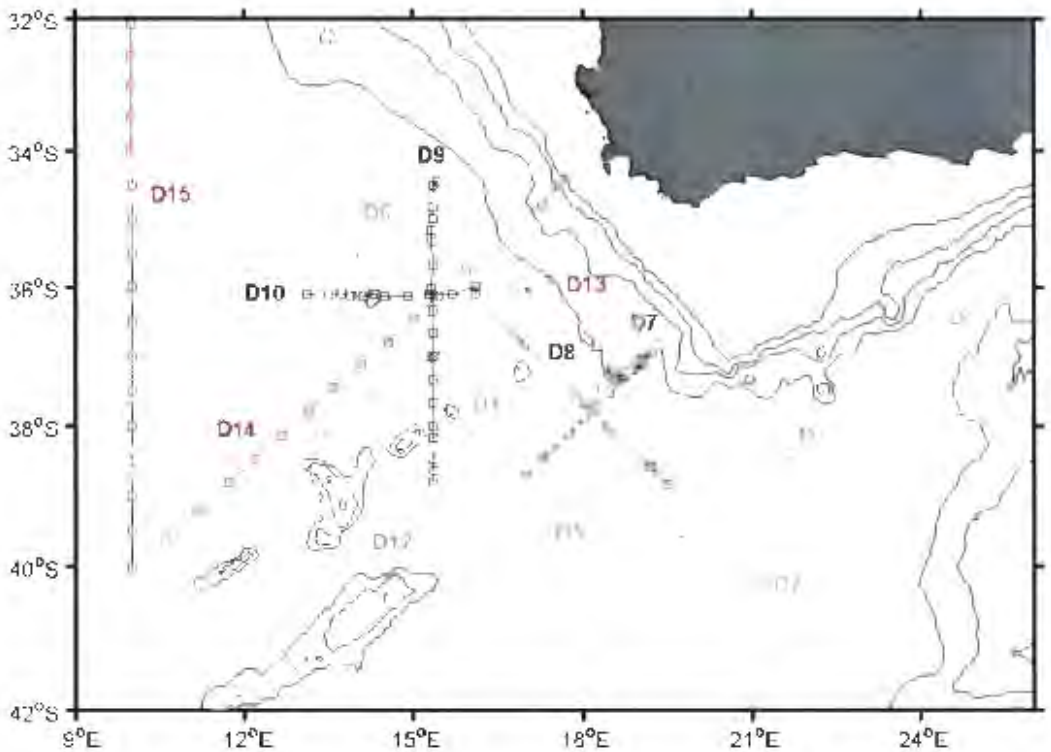

Fig 31 : Map showing the sections investigated in region D. Cruise tracks D1-D6 (magenta) were completed as part of the ARC cruise, tracks D7-D10 are the MARE I and MARE II cruise tracks and D11-15 were WOCE program cruise tracks.

4.4) Section D (southern Agulhas Current)

Agulhas Return Current sections

Section D1 (see figure 31)

This hydrographic section extended from the African coast as far south as 42°S, close to the Subtropical Convergence. It crossed the Agulhas Current and then the Agulhas Return Current at about 250 km from the start of the section as well as a meander in the Agulhas Return Current at 400 km and 600 km distance (Gordon et al., 1987). This threefold crossing is clearly seen in the changing slopes of the isolines and to a degree in the oxygen contours (figure 32(ii)).

Over the density range 27.25-27.40 RSIW was observed on both sides of the Agulhas Current as was the case off Durban but not seen in section C6. At its core RSIW contributed between 15-20% (figure 32(i)a) of the water sample. This was greater than that observed along sections C5 and C6 along which its contributions ranged between 5-10% and 10-15% respectively indicating considerable variability in the amount of RSIW transported down the current over this density range. In the offshore core RSIW only contributed 5-10% of the water sample which is comparable with that observed offshore of Durban along section C4 but much reduced compared to that observed along section C3. The RSIW core along the slope is not distinct but form part of the RSIW core along the continental slope observed in the underlying density range (figure 32(i)b and c) when NIDW is introduced in the source water matrix. Over the density range 27.40-27.70, RSIW have very similar distribution patterns and water sample contributions to that of section C6 just to the north of it. At its core RSIW contributed between 15-20% of the water sample along the continental slope (figure 32(i)b). In the core underneath the Agulhas Current its contribution to the water sample was 10-15%. The total transport of RSIW along this section was -1,36 Sv. This was nearly twice as much as that transported along section C6. The biggest difference is observed in the neutral density range 27.25-27.40 where the difference in transport between the two sections is 0.56 Sv. This was due to the fact that the RSIW water mass contribution along this section is more than twice that along section C6 in the upper density range.

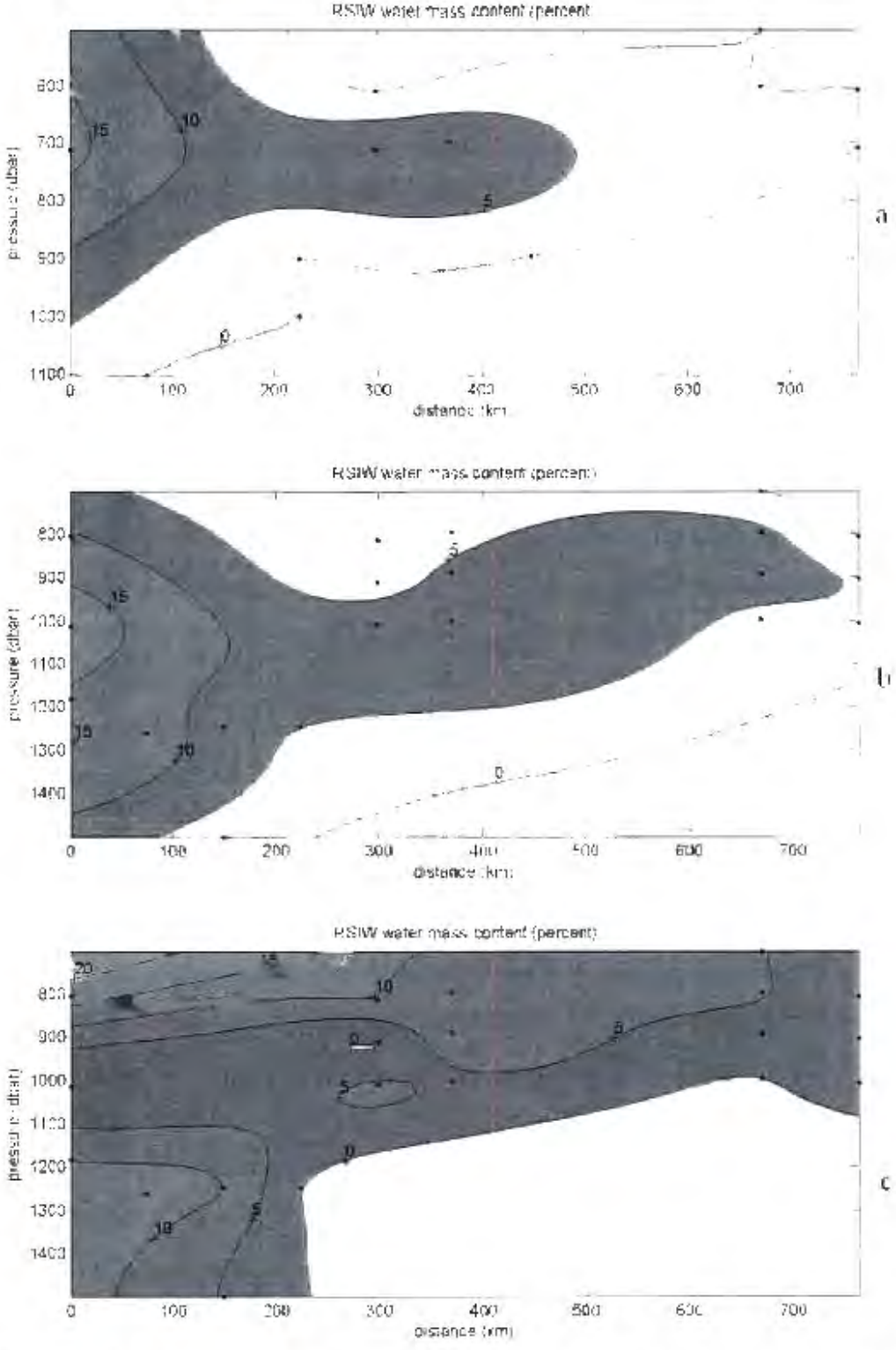

Fig 32 (i): a) RSIW contribution over the density range σ_n=27.25-27.40 (b) RSIW contribution without NIDW in the source water matrix over the range σ_n=27.40-27.70 (c) RSIW contribution with NIDW in the source water matrix over the range σ_n=27.40-27.70 along section D1 (see figure 31). Dots indicate bottle sample locations.

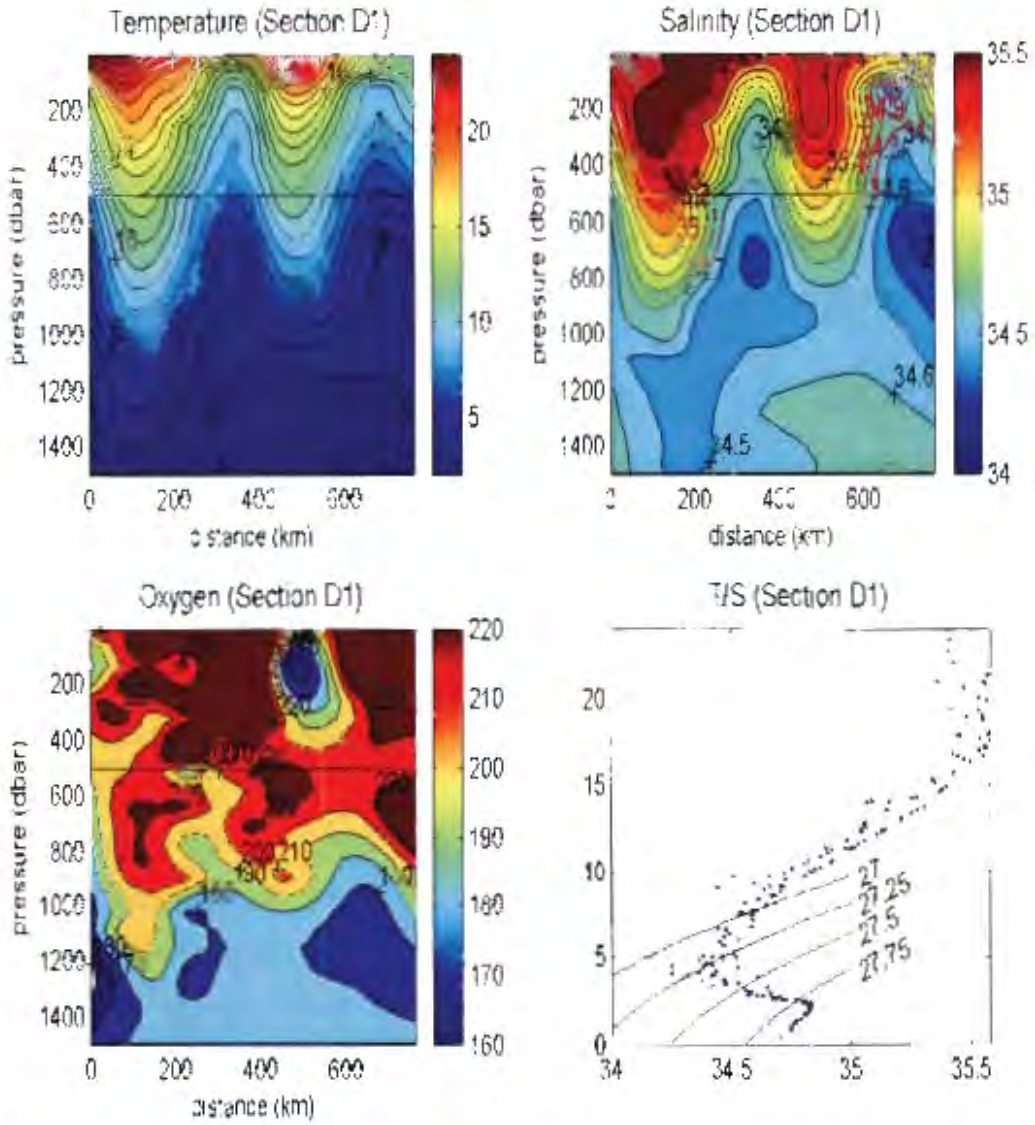

Fig 32 (ii): Property plots along section D1 (see figure 31) of temperature, salinity, oxygen and a T/S plot

Section D2 (see figure 31)

This section at the Agulhas Retroflection along 21°E crossed the Agulhas Current, the Agulhas Return Current and part of an Agulhas ring to the south (Gordon et al., 1987). At this point the temperature and salinity sections indicate that the Agulhas Current had moved some distance offshore (figure 33(ii)). The water mass found along the slope is now has a salinity minimum and highly oxygenated compared to further upstream which would indicate it to be AAIW (figure33 (ii)).

Over the density range 27.25-27.40 (figure 33(i)a) hardly any RSIW is observed inshore of the Agulhas Current. In fact the only strong RSIW signal is found south of the Agulhas Return Current associated with the ring where RSIW contributed between 5-10% of the water sample at its core. This core appears to be distinct from the underlying RSIW only when NIDW is not a part of the source water matrix (figures 33(i)b and c). The stronger inshore core compared to offshore seen further upstream of the Retroflection region is thus not observed across this section. Over the density range 27.40-27.70 we find strong RSIW cores almost directly under the Agulhas Current, on the landward side of the Agulhas Current, on the offshore side of the Agulhas Return Current and on the one side of the Agulhas ring where it contributed between 10-15% of the water samples at each of the cores (figures 33(i)b and c, figure 33(ii)). This would thus indicate that RSIW rounds the Agulhas Retroflection and flows east along the Agulhas Return Current. Also evident is that RSIW seems to be closely associated with the Agulhas Current as its movement offshore is also observed in the distribution of the RSIW cores. When NIDW is introduced the RSIW contribution to the ring is slightly reduced but its distribution remained more or less the same. The net transport in the upper density range was eastward amounting to 0.047 Sv. In the lower density range -0.13 Sv was associated with the Agulhas Current, 0.11 Sv with the Agulhas Return Current and -0.079 Sv with the Agulhas ring resulting in a net transport of -0.099 Sv. The total net transport of RSIW over the combined range was a mere -0.052 Sv.

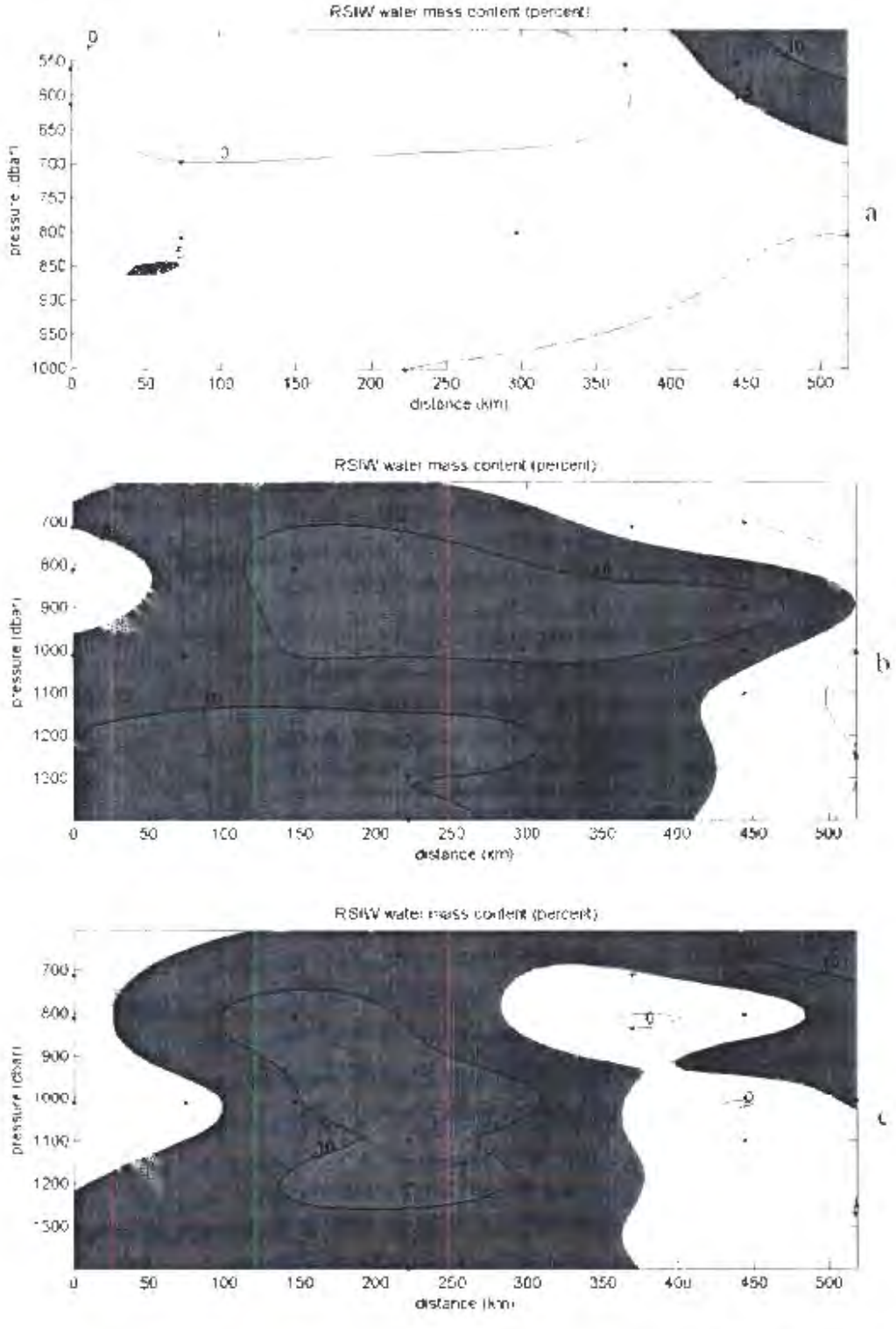

Fig 33 (i): a) RSIW contribution over the density range σ_n=27.25-27.40 (b) RSIW contribution without NIDW in the source water matrix over the range σ_n=27.40-27.70 (c) RSIW contribution with NIDW in the source water matrix over the range σ_n=27.40-27.70 along section D2 (see figure 31). Dots indicate bottle sample locations.

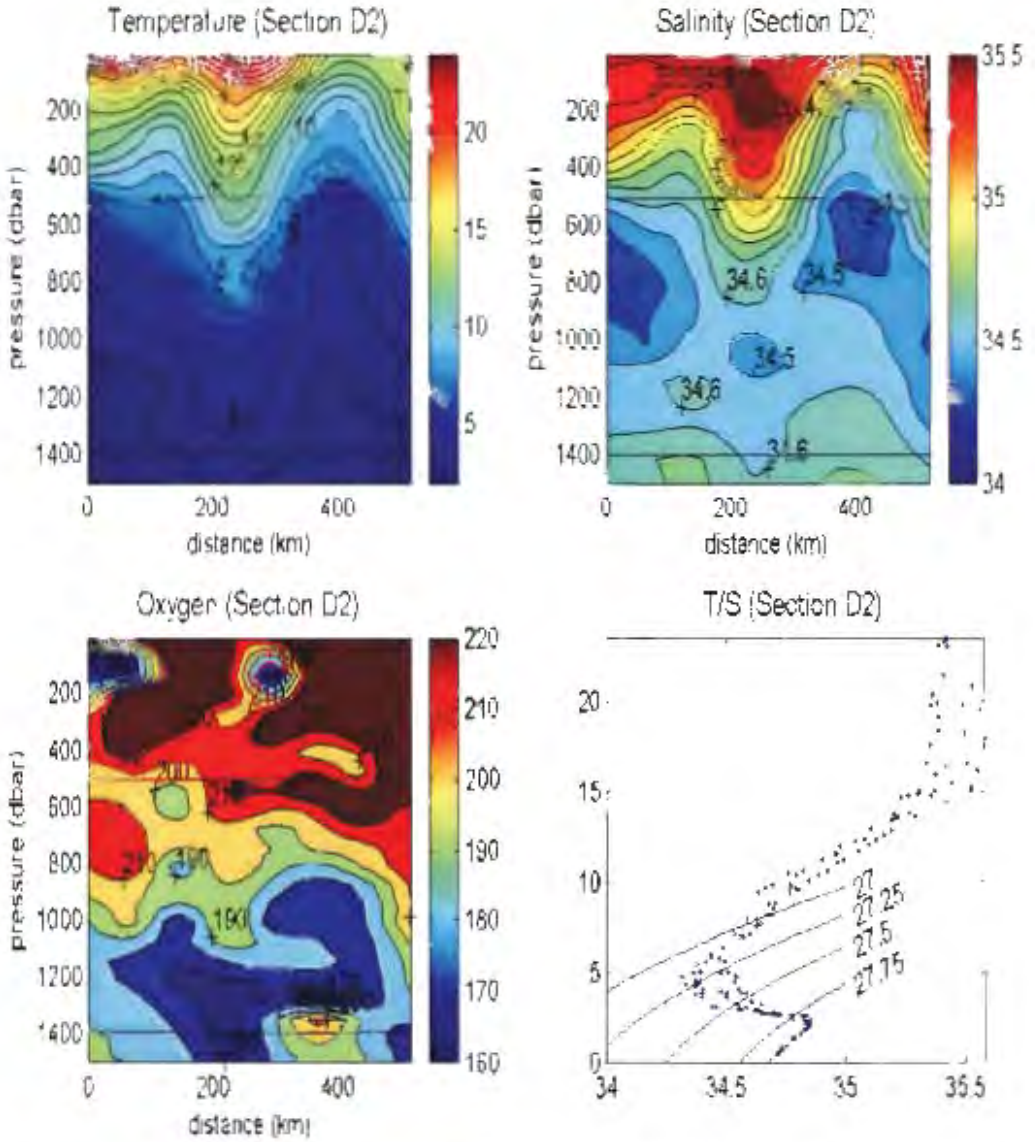

Fig 33 (ii) Property plots along section D2 (see figure 31) of temperature, salinity, oxygen and a T/S plot

Sections D3, D4, D5 (see figure 31)

Section D3 crossed the western half of the Agulhas Current as it retroflected at around 400 km and a recently shed ring just to the west of it seen as a bowl like structure in the isotherms and isohalines (figure 34c). Unlike in the previous section where almost no RSIW was observed over the density range 27.25-27.40 on the landward side of the Agulhas Current, RSIW now contributed 5-10% of the water sample at its core (figure 34a) that could only have came from the landward side of the current. The core was associated with the underlying RSIW (figure 34b). No RSIW was detected in the water samples associated with the Agulhas ring to the west. But it has to be noted that the upper density range was poorly sampled and that the above finding is thus not conclusive. Sections D4 and D5 also crossed the abovementioned ring. RSIW presence along these two sections varies from almost absent to contributing between 5-10% of the water sample at its core enforcing the perceived variability previously mentioned in this density range (figures 35a and 36a). As the downward slope of the isolines (figures 35c and 36c) would indicate these two sections were both done across the western half of the Agulhas ring (figure 34c).

Over the density range 27.40-27.70 RSIW contributed 10-15% of the water sample at its core along section D3 (figure 34b). The cores along this section are associated with the Agulhas Current as it retroflects and the ring to the west of it. The core associated with the ring appears only on one side which would suggest that RSIW is not continuous around the ring. However this is not conclusive as the vertical resolution of data points on the eastern side is somewhat less than that on the western side of the ring. Sections D4 and D5 (figures 35b and 36b) through the same ring reveal that RSIW does seem to be continuous around the ring. Its variable contributions which ranged between 5-10% and 10-15% indicate small variability's in the amount of RSIW at different positions around the ring (figures 35b and 36b). This variability seen around the ring is consistent with what was observed in the Agulhas Current proper.

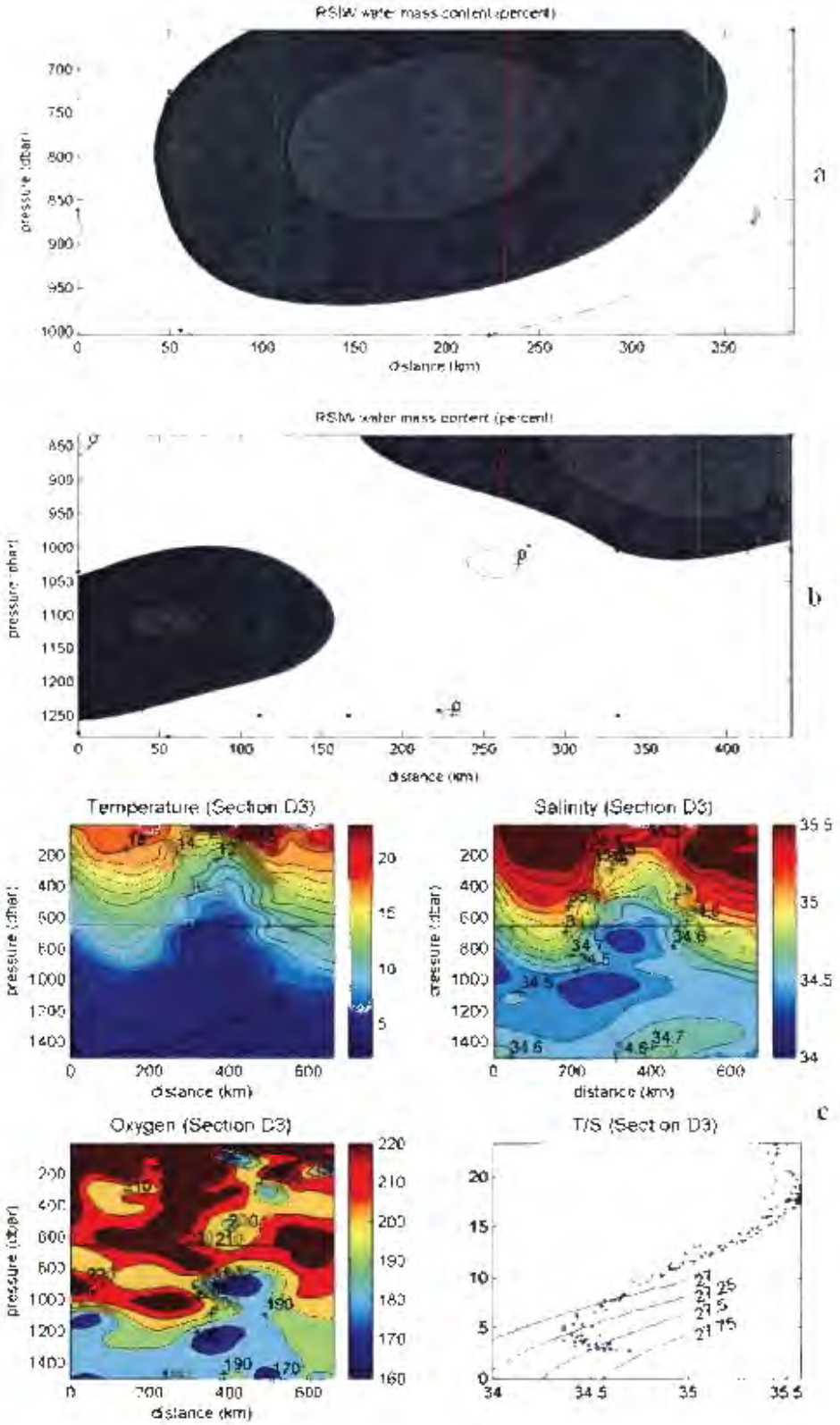

Fig 34: a) RSIW contribution over the two densities 27.25-27.40 and (b) 27.40-27.70 and (c) property distributions of temperature, salinity oxygen with a T/S plot along section D3 (see figure 31). Dot indicate bottle sample locations

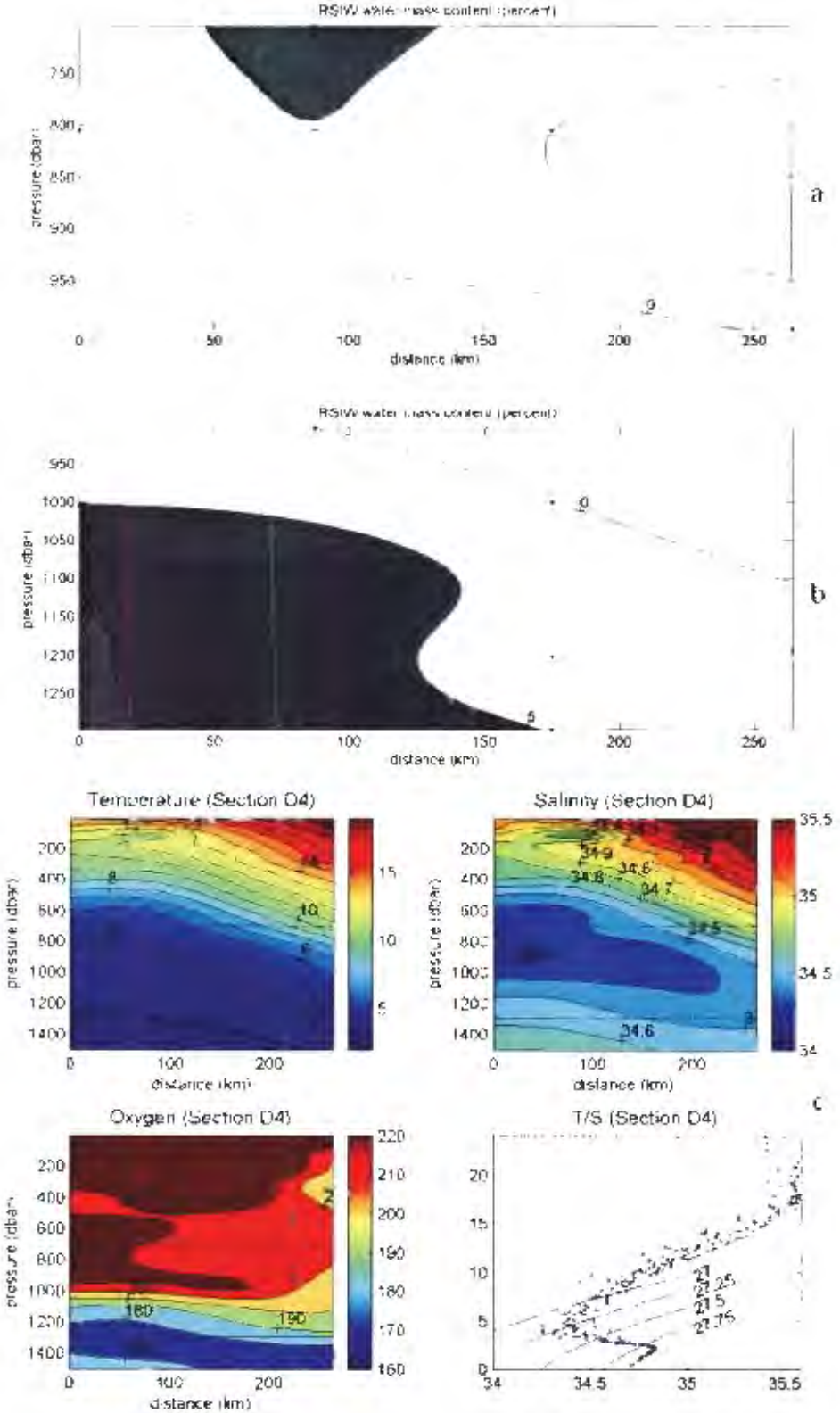

Fig 35: a) RSIW contribution over the two densities 27.25-27.40 and (b) 27.40-27.70 and (c) property distributions of temperature, salinity oxygen with a T/S plot along section D4 (see figure 31). Dots indicate bottle sample locations.

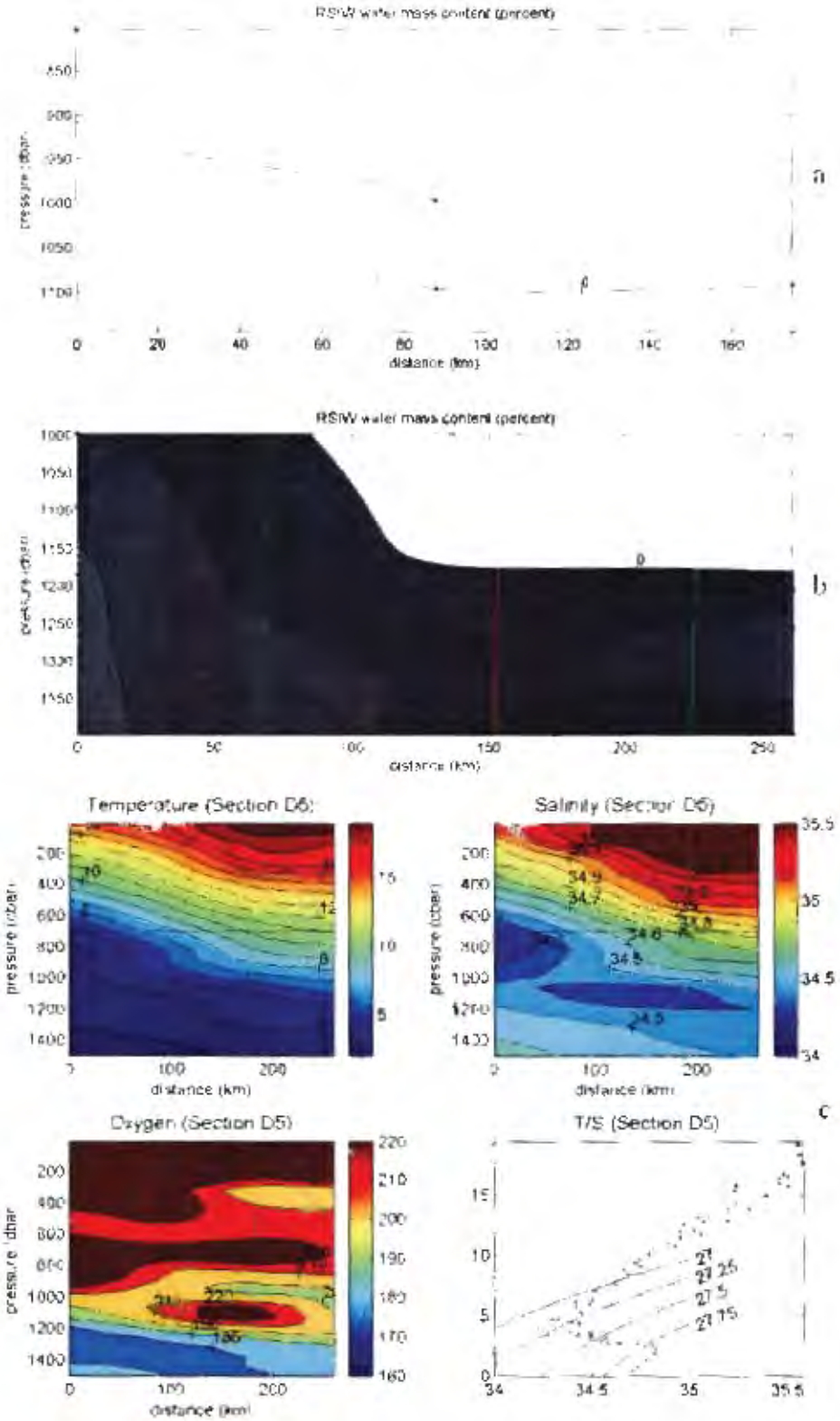

Fig 36: a) RSIW contribution over the two densities 27.25-27.40 and (b) 27.40-27.70 and (c) property distributions of temperature, salinity oxygen with a T/S plot along section D5 (see figure 31). Dots indicate bottle sample locations.

Section D6 (see figure 31)

This north-south section ran through what appears to be the eastern edge of an older (relative to abovementioned ring) Agulhas ring just west of Cape Town (Gordon et al., 1987). The dimensions and slightly shallower isotherms and isohalines indicating the greater age of the ring are shown in figure 37c. Over the density range 27.25-27.40 RSIW is almost absent as was the case along some sections in the abovementioned ring just west of the Retroflection (figure 37a). Over density range 27.40-27.70 RSIW contributed just over 5% in the two water samples compared to the 10-15% in the newly shed ring (section D3) just south east of it (figure 37b). The absence or small contribution of RSIW to the intermediate depths along this section can also be clearly seen in the T/S diagram (figure 37c).

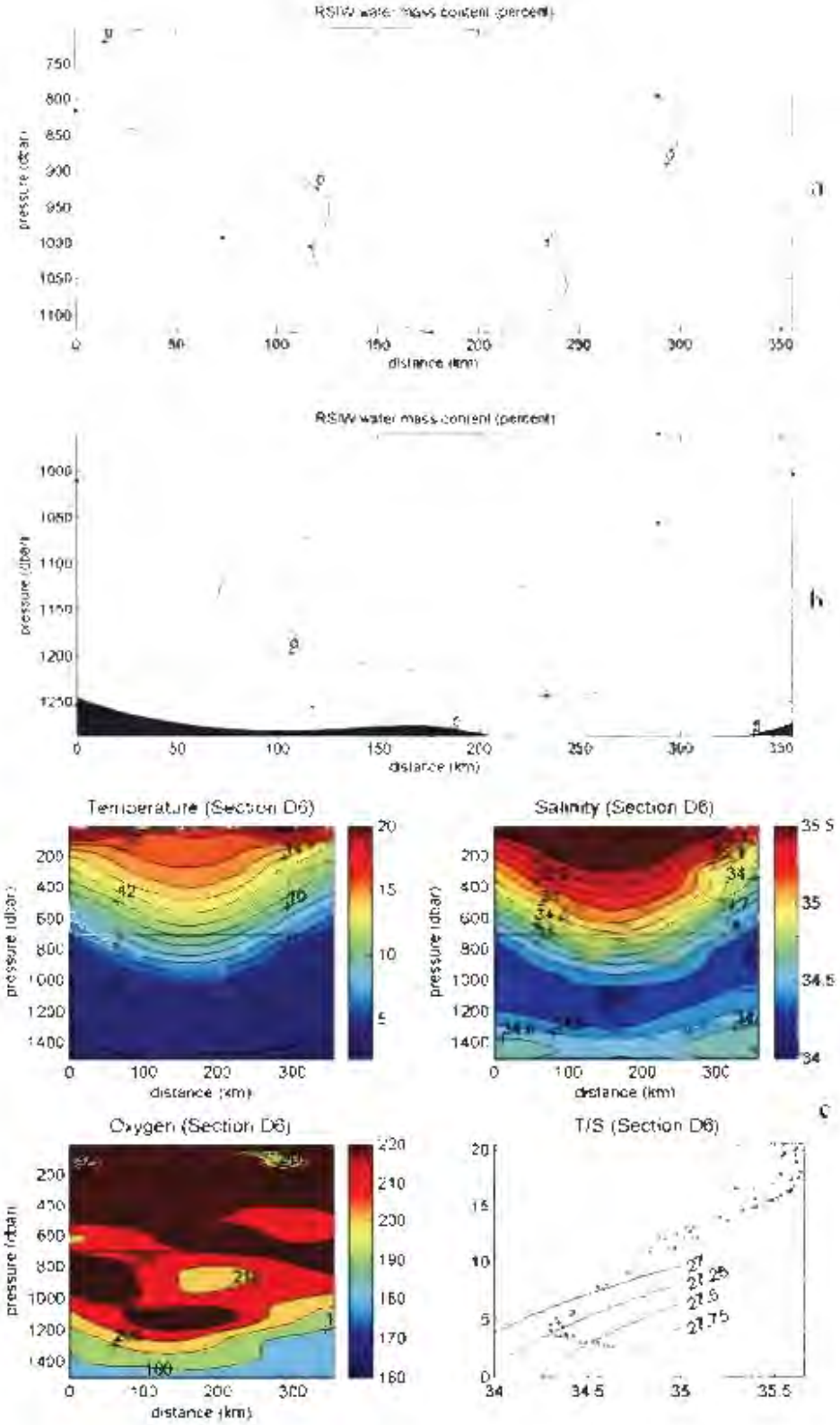

Fig 37: a) RSIW contribution over the two densities 27.25-27.40 and (b) 27.40-27.70 and (c) property distributions of temperature, salinity oxygen with a T/S plot along section D6 (see figure 31). Dots indicate bottle sample locations.

Sections D7 and D8 (MARE I, see figure 31)

These two hydrographic sections were made across a two month old ring just west of the Agulhas Retroflection (figures 38(i)c and 39(i)c). Compared to sections D3, D4 and D5 the T/S diagram associated with D7 and D8 would indicate somewhat less saline intermediate and thus a smaller amount of RSIW contribution (figures 38(i)c, 39(i)c, 34c, 35c and 36c). OMP analysis of section D7 resulted in the loss of a considerable amount of data points in the 27.25-27.40 range when potential vorticity was included as a parameter. It was thus decided to exclude it from the source water mass matrix for section D7 to maximize the vertical and horizontal resolution. Because of the limited number of oxygen samples results are shown for source water mass matrix configurations when using initial phosphate and NO as well as when using non-conservative phosphate and nitrate. This is done for comparative purposes and to increase the number of data points that would otherwise be excluded due a lack of oxygen data. Using You's (1998) argument that the rate of water mass spreading occurs at a far greater rate than nutrient regeneration and oxygen consumption we will assume the sections comparable with each other.

Over the 27.25-27.40 density range for section D7, RSIW contributed only 5-10% of the water sample at its core situated in the middle of the ring (figure 38(i)a) when using conservative initial phosphate and NO as parameters. It needs to be noted however that the distribution of data points over this density range are poor with most of the data points around 27.30 neutral density surface making any conclusions on RSIW content and distribution impossible. This value is slightly higher (10-15%) when using non-conservative phosphate and nitrate (figure 38(ii)a). Over the neutral density range 27.40-27.70 potential vorticity was once again introduced into the source water matrix as a parameter. For the water samples analysed RSIW was almost completely absent. Its maximum contribution was less than 5% (figure 38(i)b). Again due to the poor distribution of data points any conclusions on the presence and distribution of RSIW will be inconclusive. As would be expected from the water mass fractions of RSIW, the total transport of RSIW was a mere -0.0056 Sv.

For section D8 the maximum contribution of RSIW was around 5% (figures 39(i)a). This increases to 10-15% at station 1 when non-conservative phosphate and nitrate are used as parameters (figures 39(ii)a). As the differences in distance covered would

indicate, station 1 is excluded when using the conservative parameters of initial phosphate and NO due to the lack of a oxygen measurement. The other data points would thus lend support to You's (1998) assumption. This higher RSIW contribution is much higher than was found along any other section at the Retroflection in this density range except for section D7 (figure 38(ii)a). Similar to that found in the density range 27.25-27.40, RSIW in density range 27.40-27.70 showed very similar distribution patterns and maximum contribution values when comparing results obtained from the two water mass matrix configurations. In this density range RSIW seems to be circulating the ring contributing 5-10% of the water sample at its core (figure 38 (i)b). This is slightly higher than that observed along the previous section. Although RSIW is observed on both sides of the ring the net transport of RSIW was 0.11 using the contributions obtained from the use of non-conservative phosphate and nitrate as parameters.

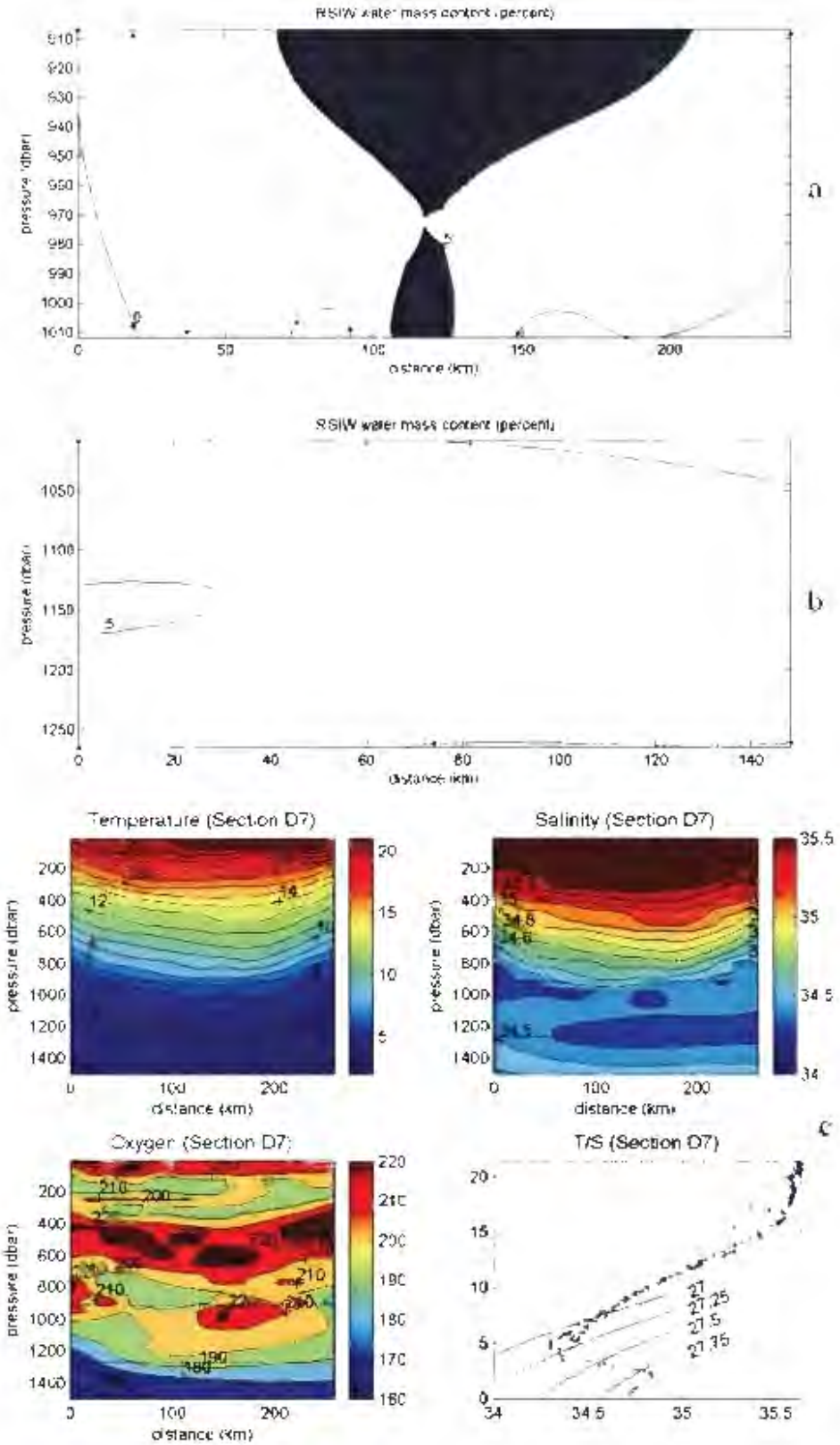

Fig 38(i): a) RSIW contribution over the two densities 27.25-27.40 and (b) 27.40-27.70 and (c) property distributions of temperature, salinity oxygen with a T/S plot along section D7 (see figure 31). Dots indicate bottle sample locations.

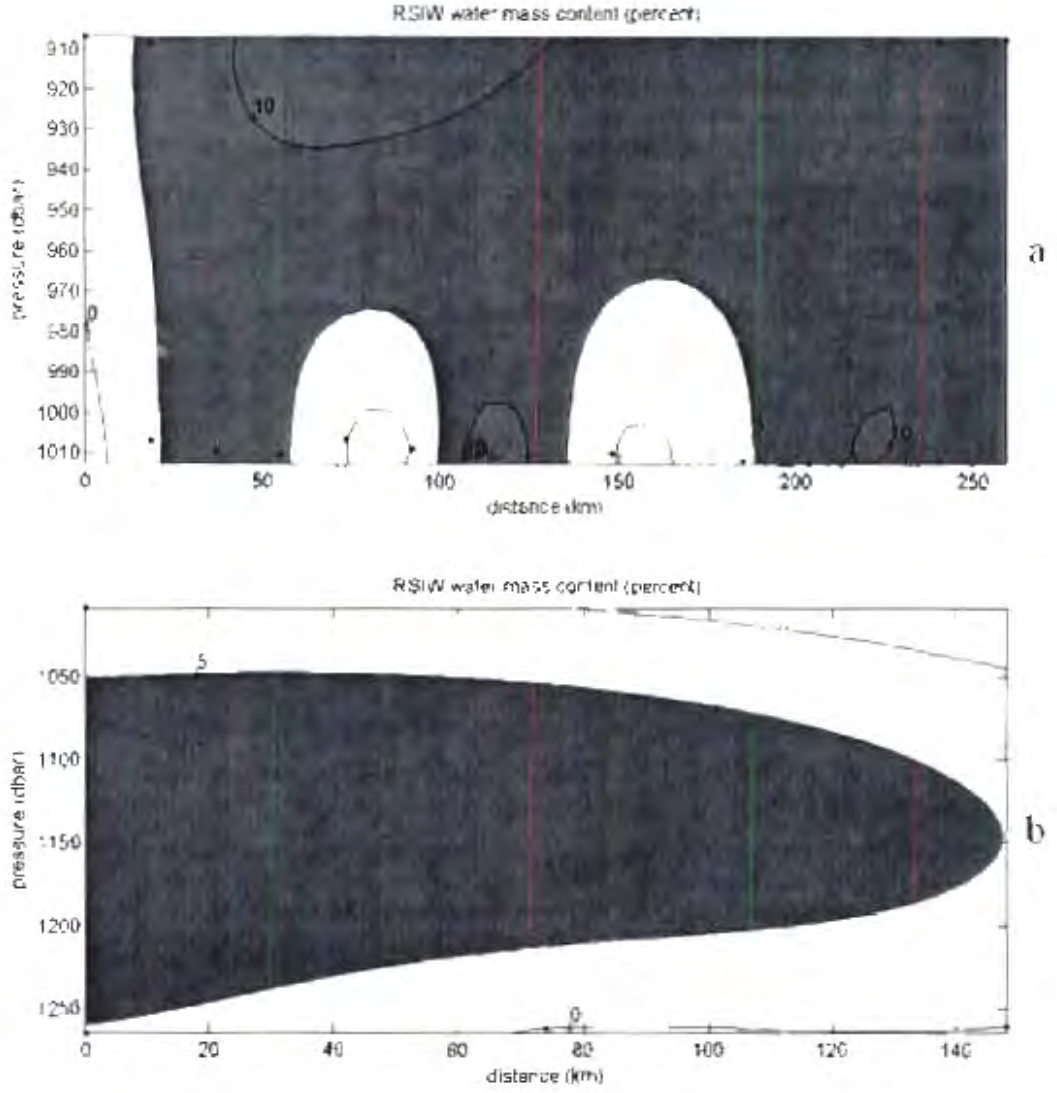

Fig 38(ii): a) RSIW contribution over the two neutral density ranges 27.25-27.40 and (b) 27.40-27.70 using non-conservative nitrate and phosphate and no potential vorticity for the upper density range along section D7 (see figure 31). Dots indicate bottle sample locations.

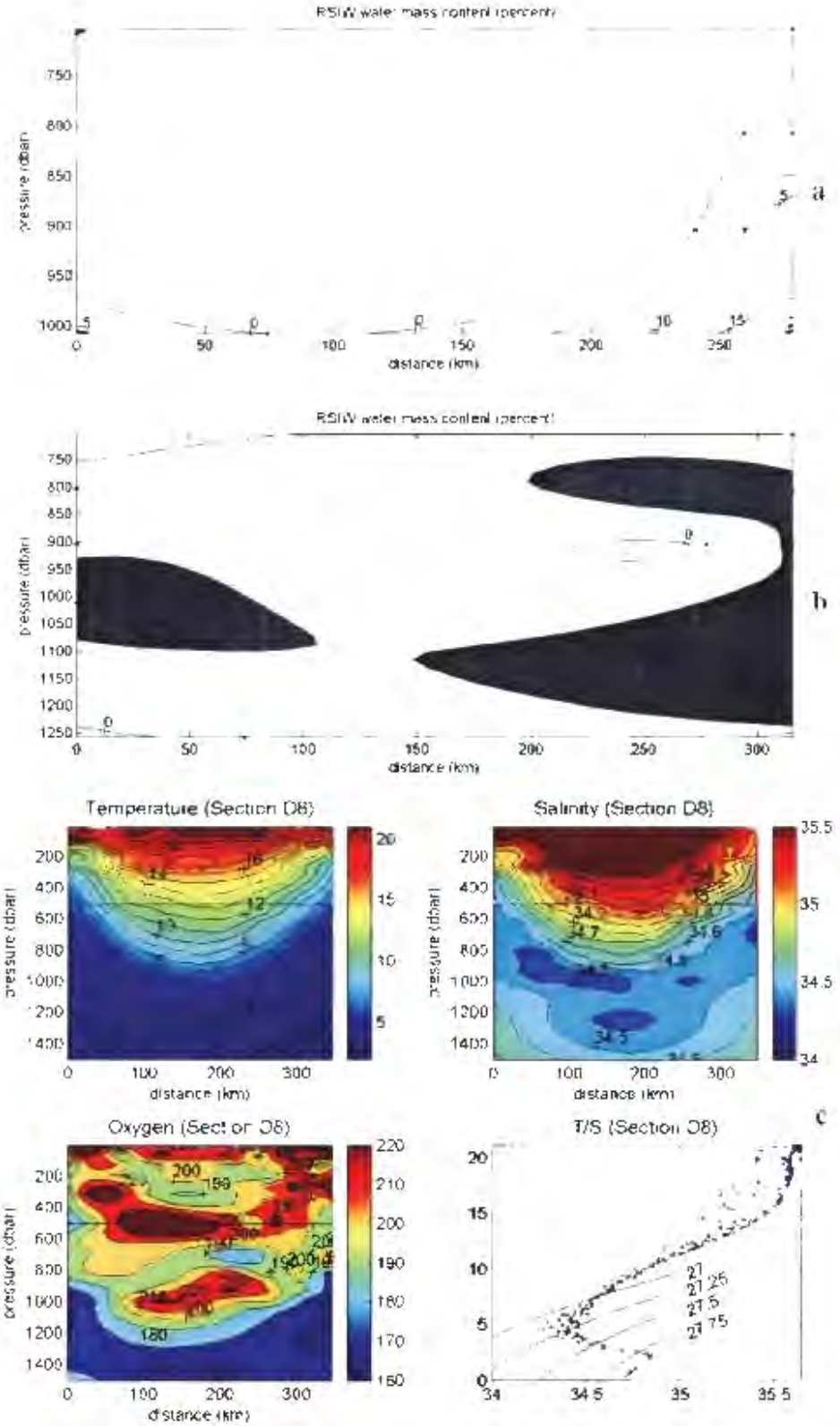

Fig 39(i): a) RSIW contribution over the two densities 27.25-27.40 and (b) 27.40-27.70 and (c) property distributions of temperature, salinity oxygen with a T/S plot along section D8 (see figure 31). Dots indicate bottle sample locations.

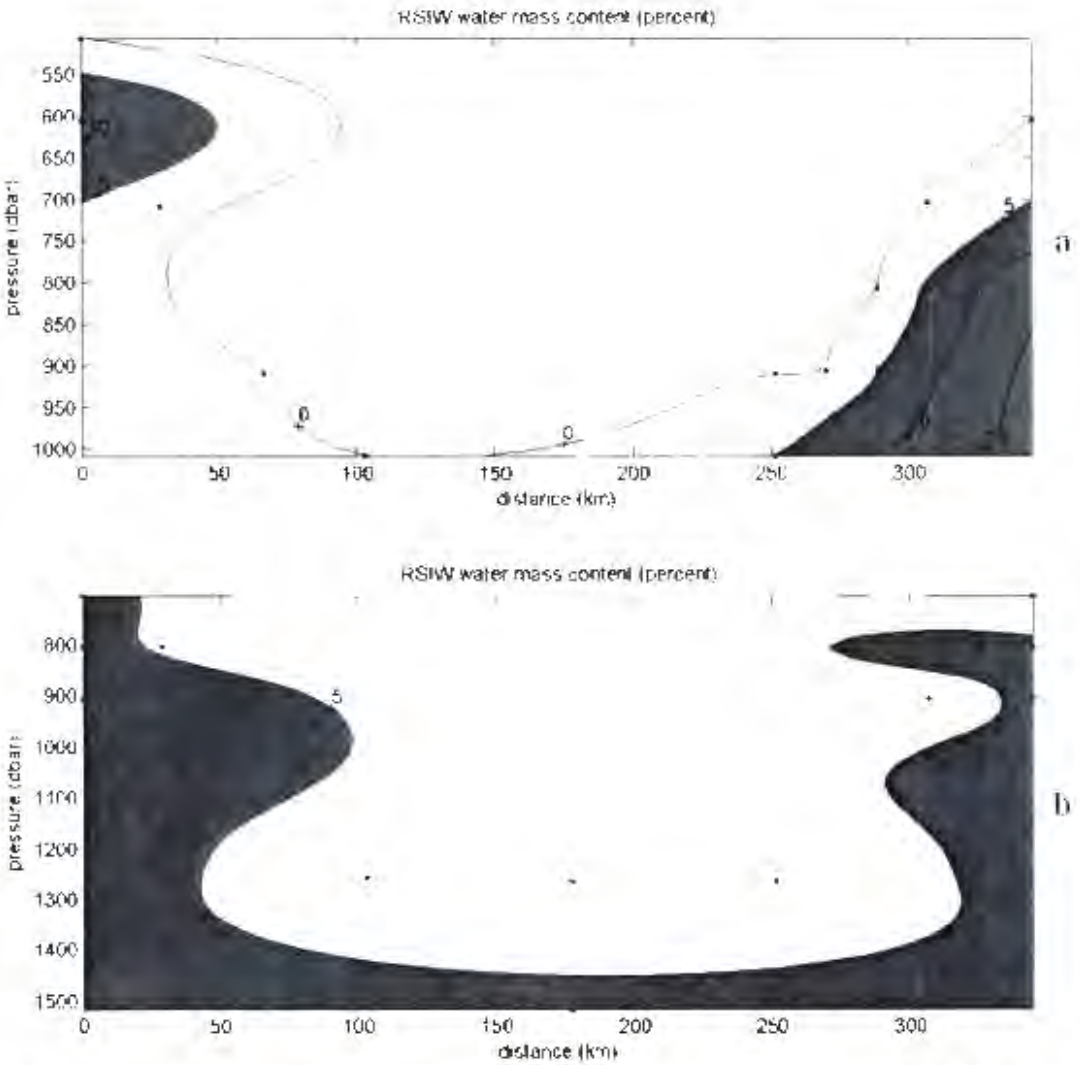

Fig 39(ii): a) RSIW contribution over the two neutral density ranges 27.25-27.40 and (b) 27.40-27.70 using non-conservative nitrate and phosphate and no potential vorticity in the upper density range along section D7 (see figure 31). Dots indicate bottle sample locations

Sections D9 and D10 (MARF II, see figure 31)

These two sections were done 5-6 months after sections D7 and D8 crossing the same ring. The centre of the ring had now crossed into the Cape Basin and it is clear that considerable mixing had taken place resulting in a much reduced bowl like structure seen in the isolines (figures 40c and 41c). Because of the limited number of oxygen samples I used the non-conservative phosphate and nitrate to keep the vertical resolution. As was the case along section D8, RSIW still contributed a maximum 10-15% of a water sample in density range 27.25-27.40 (figure 40a) along section D9. Along section D10 it only contributed 5-10% of the water sample at its core situated almost near the middle of the ring as was the case along section D7 (figure 41a). Over the density range 27.40-27.70 RSIW still seems to be circulating the ring along section D9 contributing 5-10% of the water sample at its core (figure 40b). This does not seem to be the case along section D10 with RSIW only found on one side of the ring (figure 41b). The coarse vertical resolution along these two sections makes definite conclusions on the maximum water mass contribution of RSIW difficult. The contributions were however comparable to those previously observed in the ring.

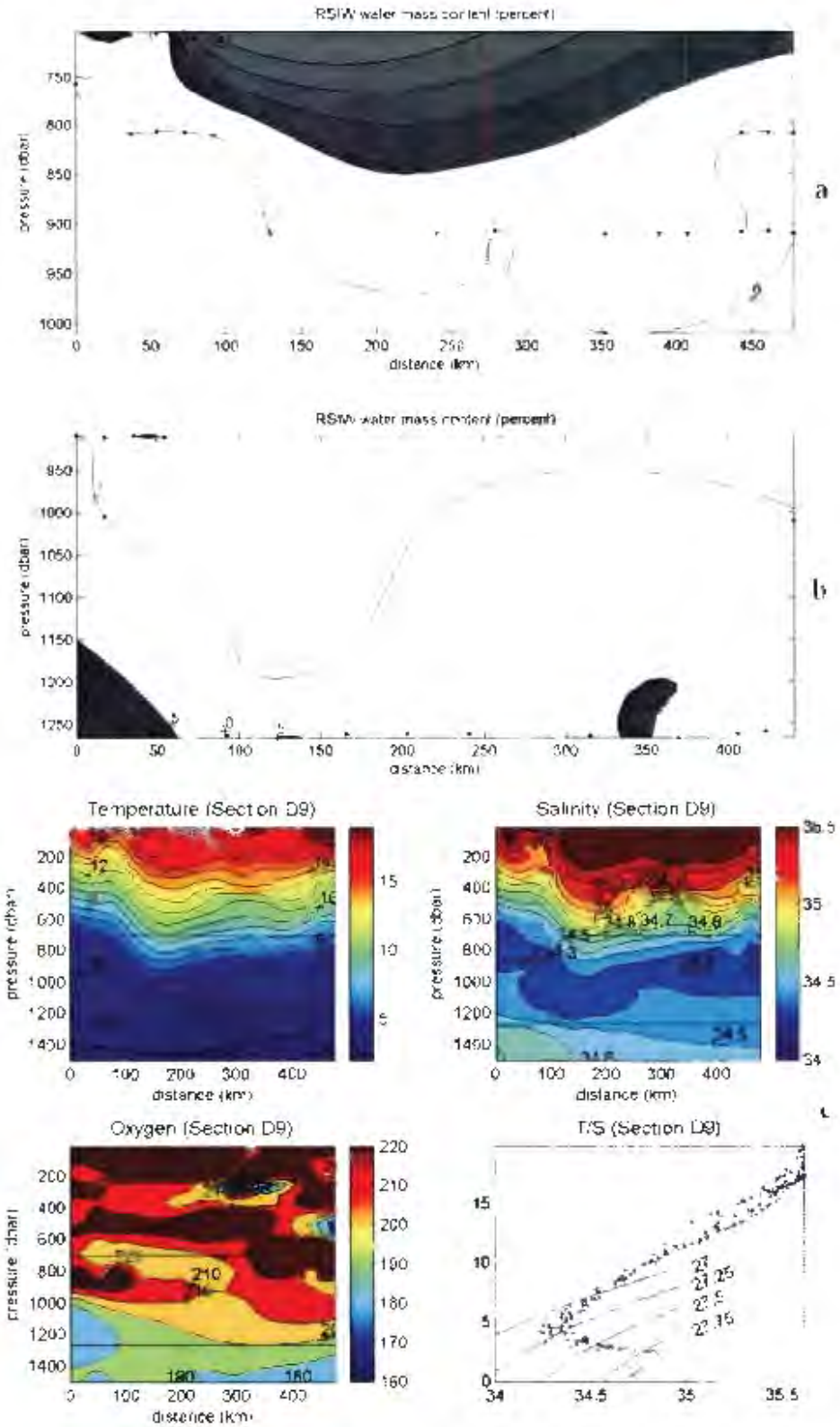

Fig 40: a) RSIW contribution over the two densities 27.25-27.40 and (b) 27.40-27.70 and (c) property distributions of temperature, salinity oxygen with a T/S plot (c) along section D9 (see figure 31). Dots indicate bottle sample locations.

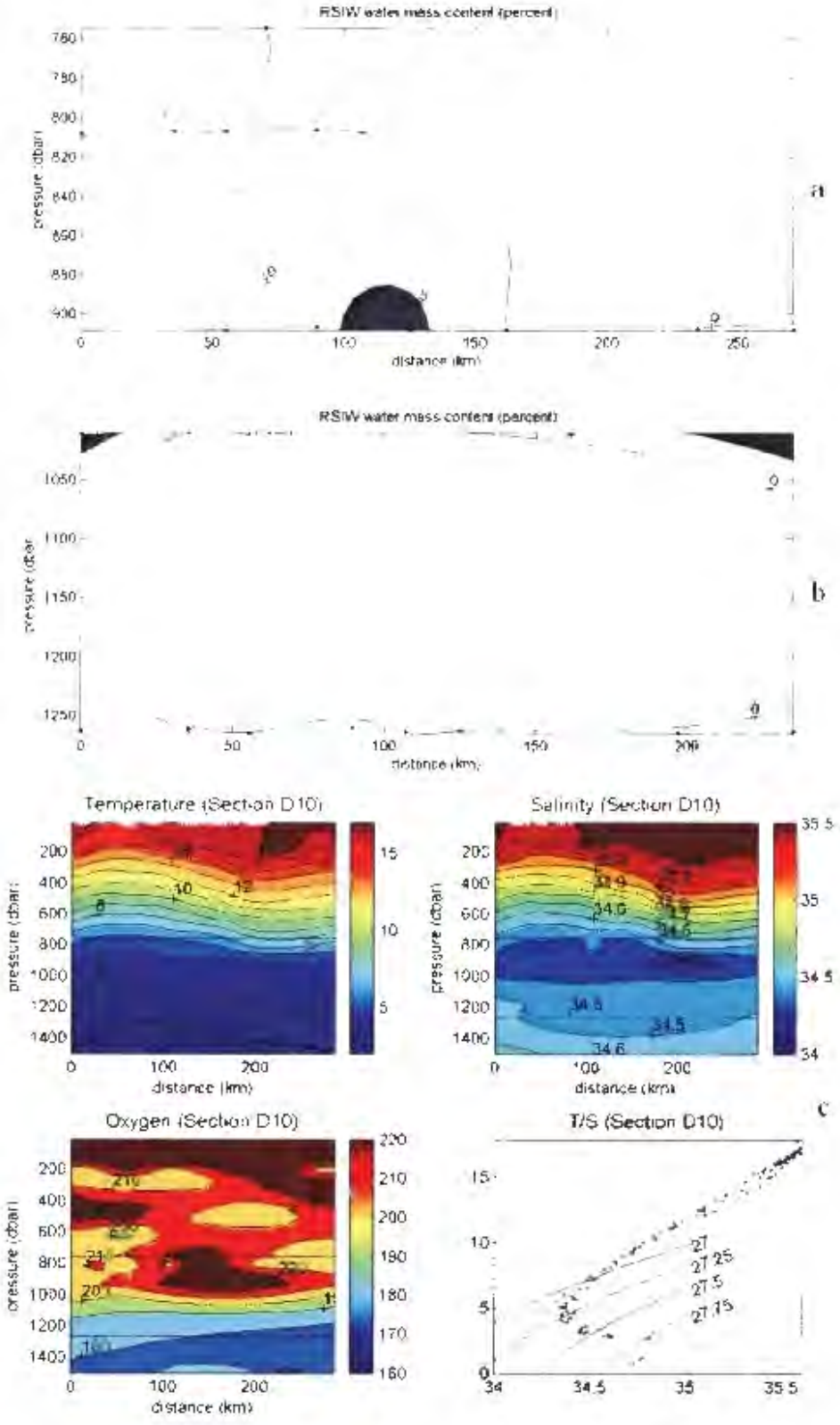

Fig 41: a) RSIW contribution over the two densities 27.25-27.40 and (b) 27.40-27.70 and (c) property distributions of temperature, salinity oxygen with a T/S plot along section D10 (see figure 31). Dots indicate bottle sample locations.

Sections D11 and D12 (SR02 WOCE sections, see figure 31)

These two sections were completed along the World Ocean Circulation Experiment repeat line SR02. Since we are interested only in RSIW these sections were shortened and only extended from the African continent to the Subtropical Convergence around 42°S. Along section D11 the isolines indicate the presence of two Agulhas rings whilst along D12 only one ring is observed (figures 42c and 43c). No significant amounts of RSIW (contributions of ~5% of the water samples) are observed along section D11 in density range 27.25-27.40 consistent with many other sections in this area (figure 42a). Over density range 27.40-27.70 of the same section the core with the greatest RSIW contribution is observed right under the northern ring. Under the ring it contributes ~10% of the water sample at its core whereas around the sides of the ring it contributed only 5-10% to the water samples analysed (figure 42b). Since it is found on both sides of the ring it would appear to be a continuous annulus around the ring unlike what appeared to be the situation around the MARE ring. This continuous annulus is also observed around the southern ring along this section where RSIW still contributed 5-10% of the water sample in its core.

Along section D12 RSIW is nearly completely absent in both density ranges 27.25-27.40 and 27.40-27.70 (figure 43a and b). Its maximum contribution in both density ranges was now less than 5% in the samples it was detected. Whilst the vertical resolution along this section was much better compared to section D11, the horizontal resolution of 100 km makes it very hard to draw any solid conclusions. At most you would only get three stations through a ring with that resolution. Although we cannot say that RSIW is completely absent we can confirm its patchy distribution around Agulhas rings. The net RSIW transport amounted to -0.046 Sv along section D11 whilst along section D12 it was only -0.024 Sv. This is an order of magnitude smaller than that observed by You et al. (2003).

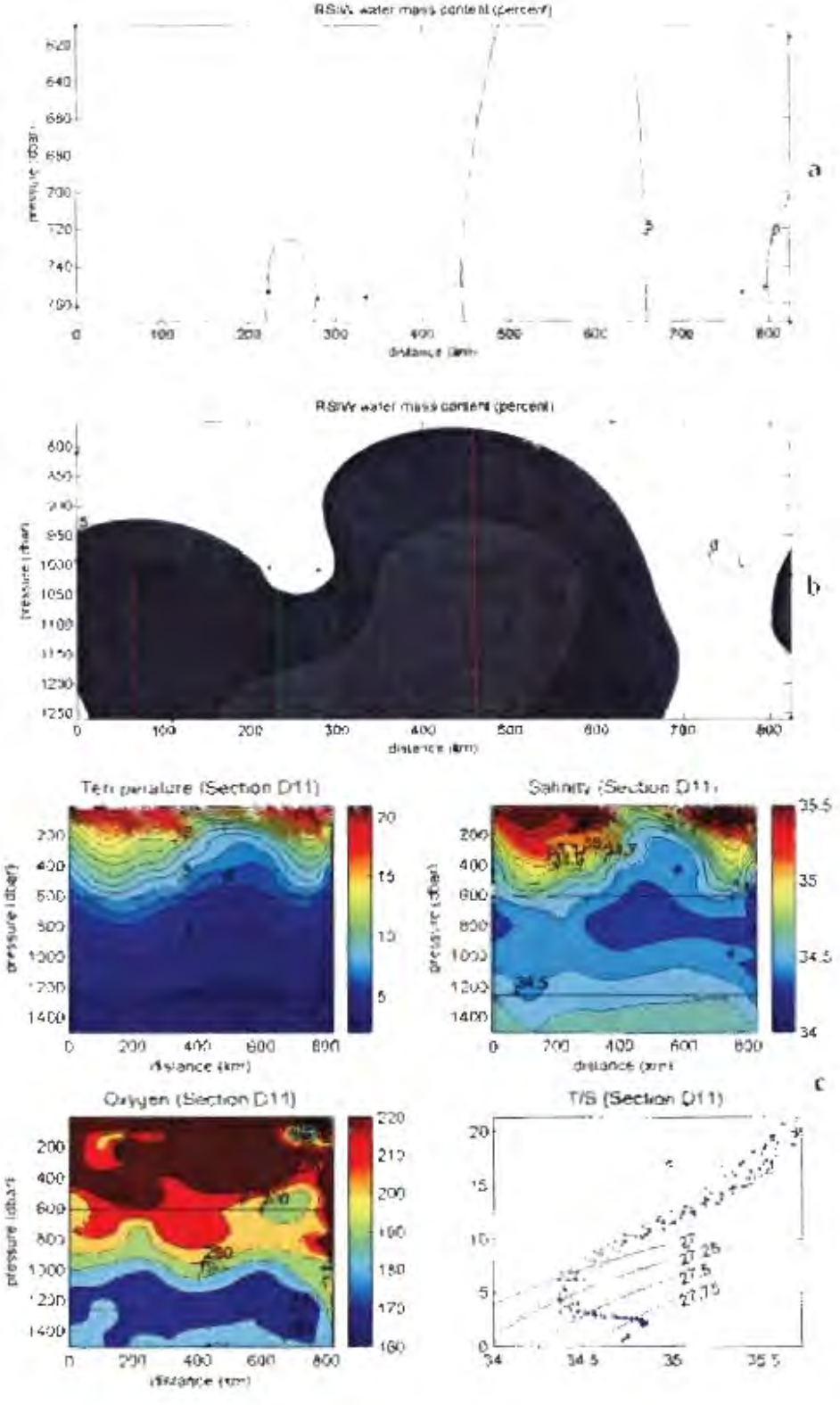

Fig 42: a) RSIW contribution over the two densities 27.25-27.40 and (b) 27.40-27.70 and (c) property distributions of temperature, salinity oxygen with a T/S plot along section D11 (see figure 31). Dots indicate bottle sample locations.

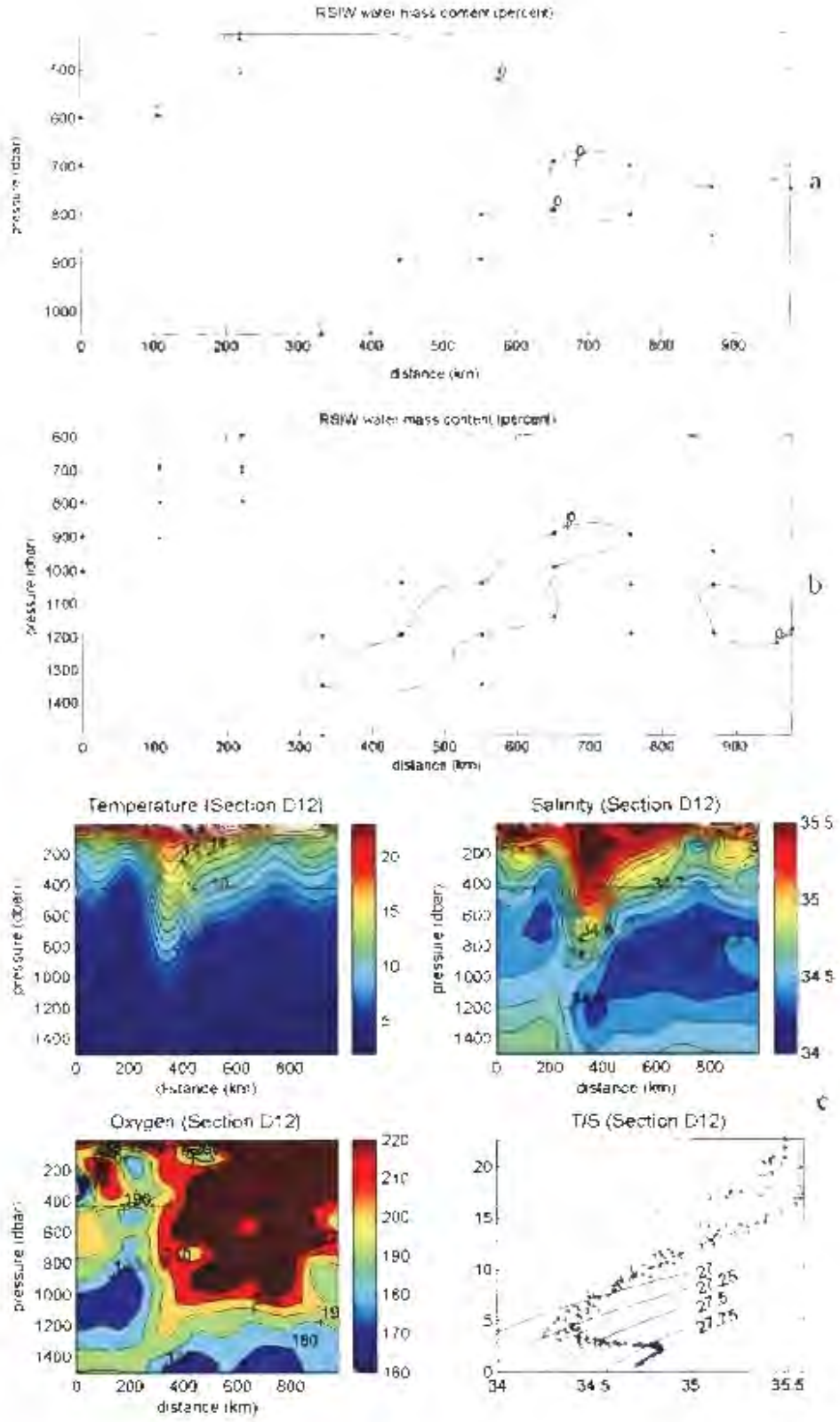

Fig 43: a) RSIW contribution over the two densities 27.25-27.40 and (b) 27.40-27.70 and (c) property distributions of temperature, salinity oxygen with a T/S plot along section D12 (see figure 31). Dots indicate bottle sample locations.

D13 (A12 WOCE section, see figure 31)

This section covers much the same ground track as the abovementioned two sections. The temperature section (figure 44c) would indicate that this section does not cross an Agulhas ring or at least not through the middle as the 10°C isotherm is much shallower than observed along the other two ring sections mentioned above. Two bowl like structures are however observed around 300 km and 600 km in the isolines with the doming between them indicating cyclonic motion. The T/S diagram (figure 44c) does however indicate somewhat more saline water in the intermediate water mass range than what was observed along the two abovementioned sections. Over density range 27.25-27.40 RSIW contributed only 5-10% of the water sample in the two cores observed higher than that observed along sections D11 and D12 (figure 44a).

Over the density range 27.40-27.70 this value is slightly higher with RSIW contributing as much as 10-15% of the water sample at its core (figure 44b). This core appears to be associated with an Agulhas ring which was only partially sampled along this section. Limited horizontal resolution along the northern part of the ring makes any conclusion of its content variability around the ring impossible. RSIW does however appear to be continuous around the ring. Geostrophic velocities indicate that this section at least partially crossed another ring to the south of the abovementioned ring around which RSIW contributes only 5-10% of the water samples at its core observed on both sides of the ring. Along this section the net transport of RSIW was significantly greater than along the previous two sections amounting to -0.14 Sv which is of similar order of magnitude as that of You et al. (2003) but still lower than values put forward in their paper for this region.

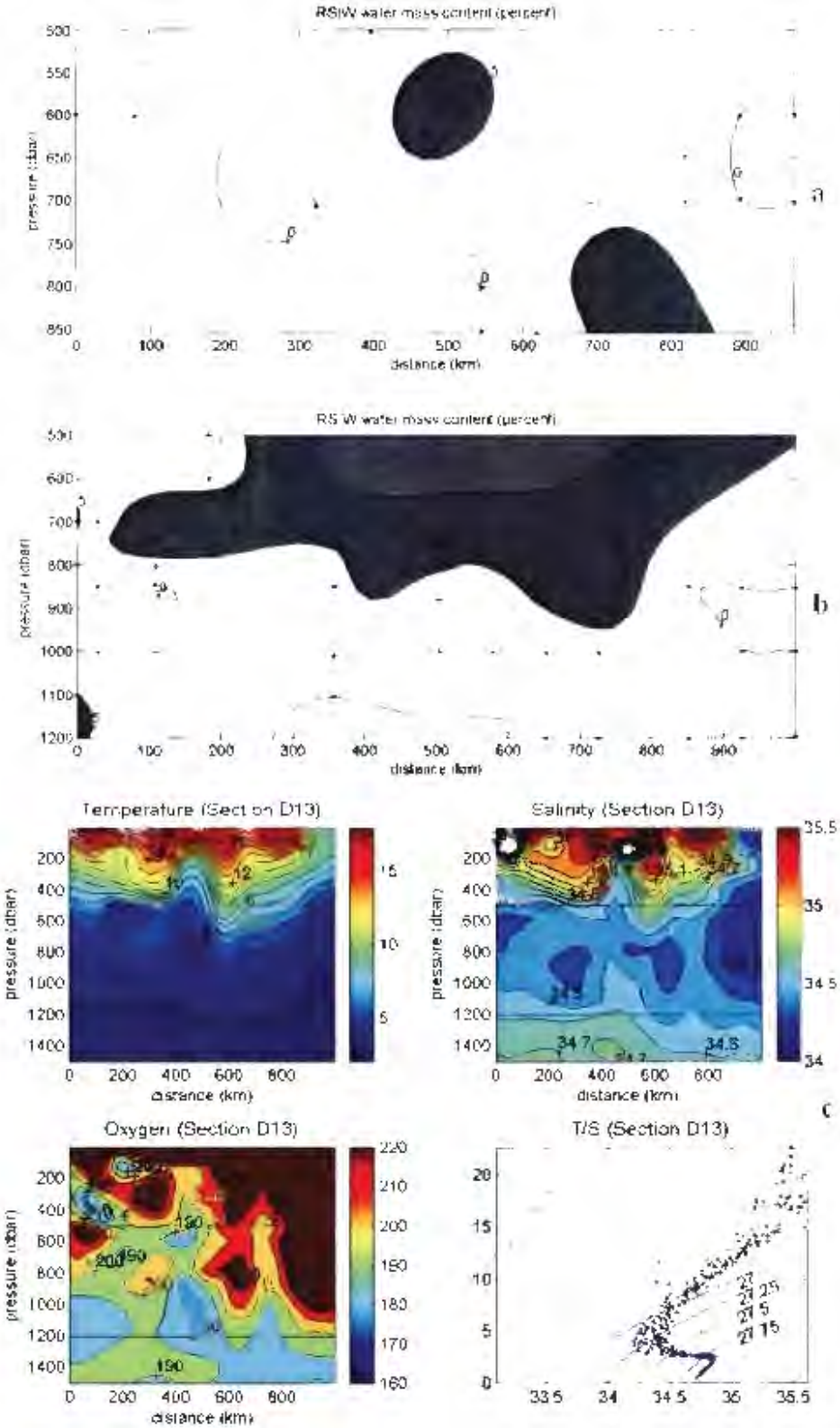

Fig 44: a) RSIW contribution over the two densities 27.25-27.40 and (b) 27.40-27.70 and (c) property distributions of temperature, salinity oxygen with a T/S plot along section D13 (see figure 31). Dots indicate bottle sample locations

D14 (A13a WOCE section, see figure 31)

Geographically along almost the same line as the other WOCE sections this section probably gives the most accurate distribution and water mass fractions of RSIW in the southwest Atlantic Ocean in terms of its vertical and horizontal resolutions. Along this section Arhan et al. (1999) indicated one anti-cyclone through which the section goes though roughly the middle at around 800 km. The isolines indicate partial crossings of at least two other anti-cyclones (figure 45b) to the north which is also observed in the sea surface height anomaly shown in Arhan et al (1999). The southern Agulhas ring has undergone considerable modifications which are visible in the surface temperature and oxygen concentrations. Over the density range 27.25-27.40 no RSIW was observed whilst over density range 27.40-27.70 RSIW contributed 5-10% of the water samples in two separate cores (figure 45a). Both cores appear to be associated with the two Agulhas rings that were only partially sampled. No RSIW signal is observed in the water samples associated with the southern ring. This may be as a result of the water mass modifications indicated by Arhan et al. (1999). The net transport of RSIW water across this section was -0.0761 Sv which as in the case of all the above sections is lower than that observed by You et al. (2003).

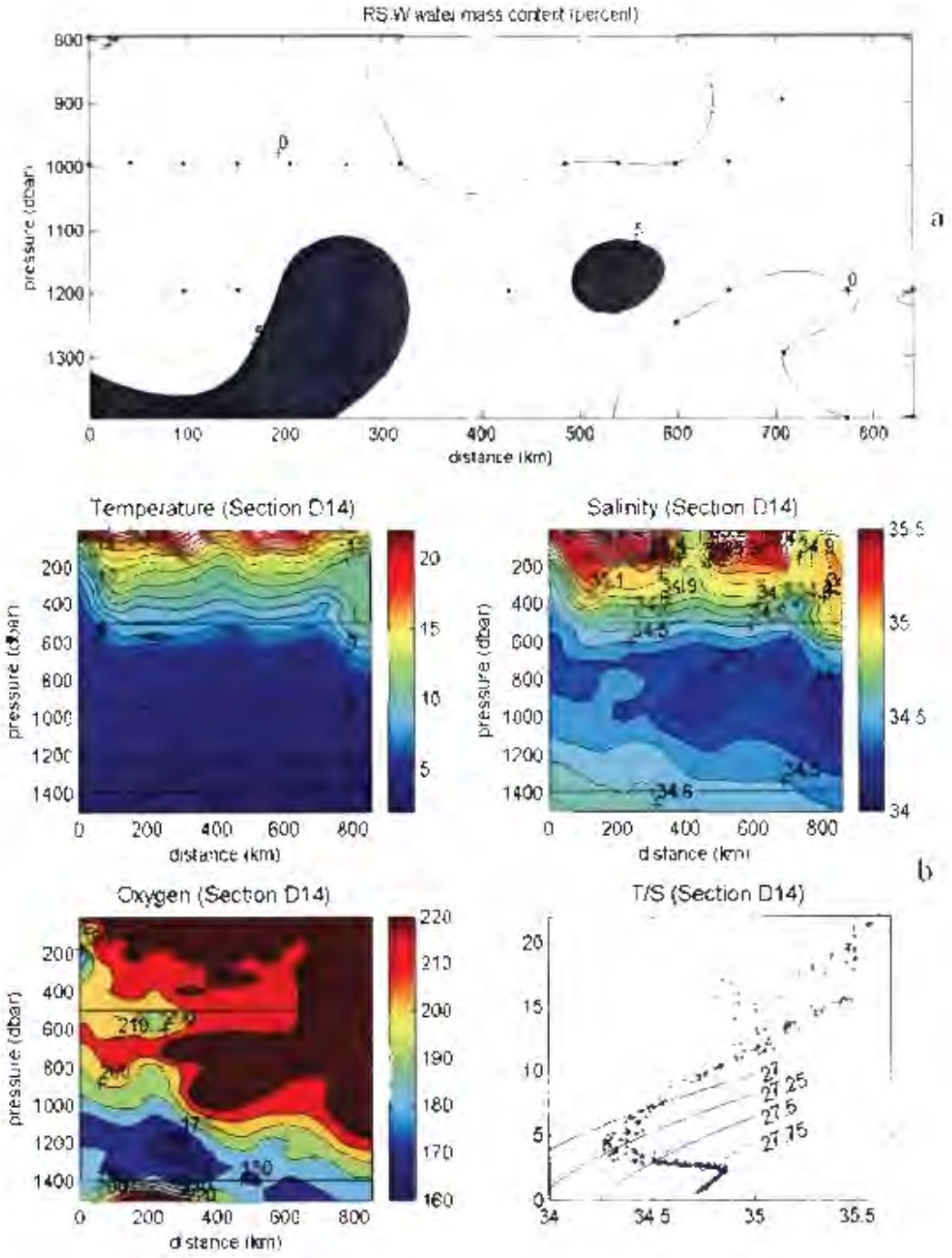

Fig 45: a) RSIW contribution over the neutral density range 27.40-27.70 and (b) property distributions of temperature, salinity oxygen with a T/S plot along section D14 (see figure 31). Dots indicate bottle sample positions.

Section D15 (A13b WOCE section, see figure 31)

This is the north-south section of the A13 line along 10°E, does not cross any Agulhas rings directly through the middle but as indicated by Arhan et al. (1999) we do have two rings lying just west of the section. The temperature and salinity sections do however only indicate one eddy like structure along the section (figure 46b). It was decided to limited the length of the section to 32°S as going further north would mean the introduction of aged AAIW as a water mass in the source water mass matrix. This was not possible due to the limitations imposed by the limited number of parameters. As was the case in the above section RSIW was not present in density range 27.25-27.40 whilst over the density range 27.40-27.70 it contributed less than 5% of the water samples analysed (figure 46a). This is slightly less than what was observed in the abovementioned section.

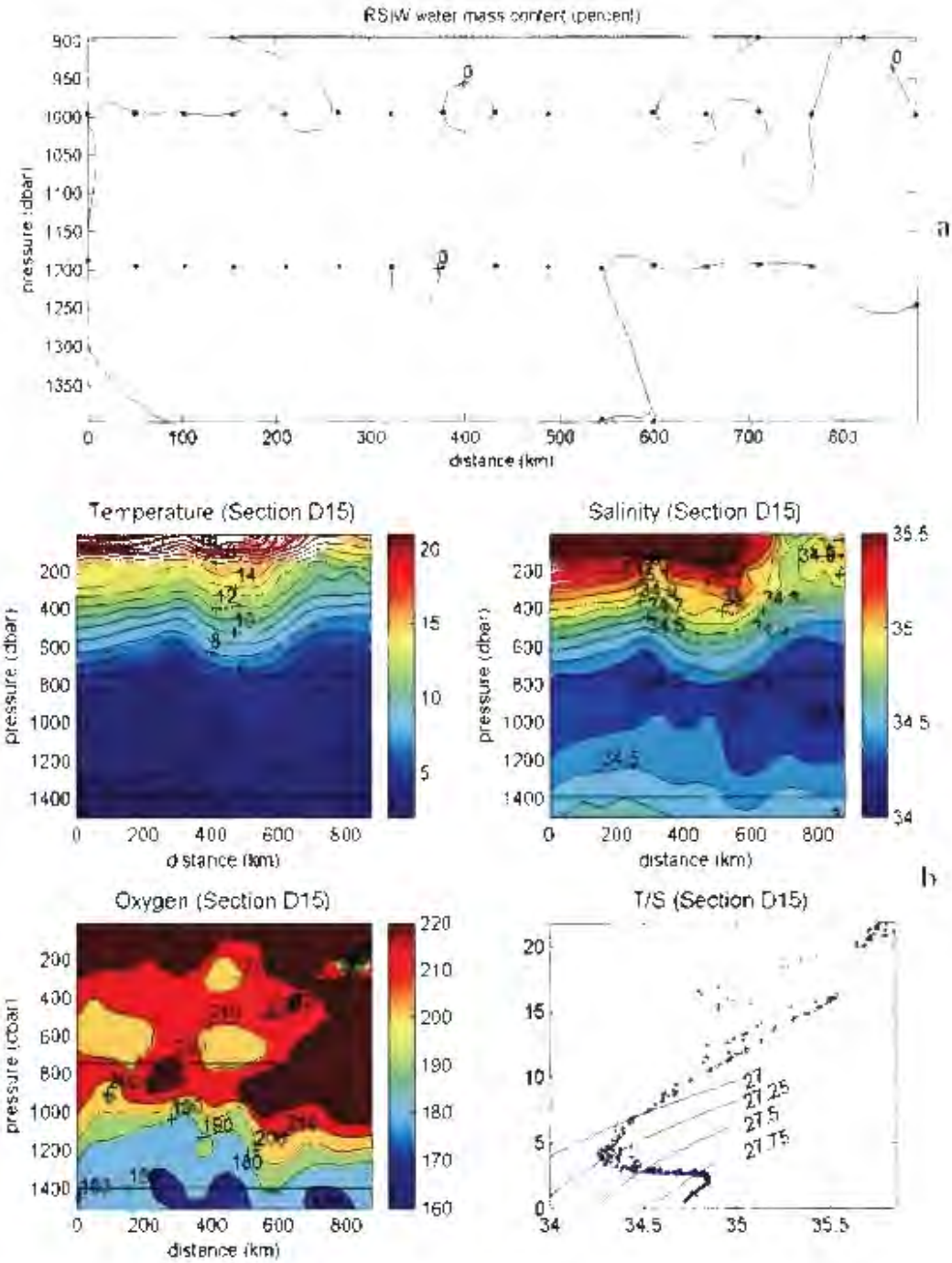

Fig 46: a) RSIW contribution over the neutral density range 27.40-27.70 and (b) property distributions of temperature, salinity oxygen with a T/S plot along section D15 (see figure 31). Dots indicate bottle sample locations.

Chapter 5

Discussion

East of Madagascar

East of Madagascar the maximum RSIW contribution was exclusively found in the density range 27.4-27.7 whereas in the density range 27.25-27.4 it was either completely absent or it made up a very small percentage of the water mass contribution. This would indicate much more vigorous mixing taking place between RSIW, IIW and AAIW over the density range 27.25-27.4 as compared to the density range 27.40-27.70. In the neutral density range 27.25-27.4 its maximum contribution ranged from 0% (completely absent) to around 9% at the southern tip of Madagascar. This would either indicate a variable mixing regime or variable input from the north. At the southern tip of Madagascar RSIW was almost exclusively found along the continental slope in the sections in which it was detected. In the lower density range its maximum contribution was either in the range 0-5% or 15-20% when using conservative initial phosphate and NO as parameters. The section along which its contribution was 0-5% did, however, not extend deeper than the 27.5 neutral density level and can thus not be considered when determining variability. When NIDW was introduced into the source water matrix (which means we used non-conservative phosphate and nitrate) the maximum RSIW contribution was just under 15% and ranged between 6-15% at the southern tip of Madagascar. Thus although its contribution to water mass mixture was relatively small, variability of about 100% was observed when NIDW is introduced in to the water mass matrix. In terms of its distribution, the RSIW core was observed along the slope as was the case in the upper density range. The offshore RSIW cores at the southern tip of Madagascar were found to flow in the opposite direction to that observed along the slope, i.e., equatorward.

The observed maximum RSIW contributions for this region were similar to that presented by You et al. (2003) and You (1998) when using conservative parameters. The introduction of NIDW into the source water matrix on the other hand showed their results in most cases to be an overestimate. In terms of the full spreading range of RSIW, it is clear that RSIW was still detectable below the neutral density surface 27.6 even when NIDW was part of the source water matrix. However its contribution to the oxygen minimum water mass at the southern tip of Madagascar was in most cases just over 5% on this level (except for along section A2), with most of the oxygen minimum water mass being classified as NIDW (>20%). How much RSIW flows down the east coast of Madagascar is thus highly dependent on the definition of

RSIW or more specific, your density range and source water matrix. It is clear from the hydrographic sections analyzed herein that most of the low oxygen, high salinity water observed in this region is more likely to be NIDW than RSIW as it is portrayed in some publications.

Mozambique Channel

Unlike the ocean region east of Madagascar, the RSIW content of some of the water samples in the northern Mozambique Channel was still greater than 25% over the neutral density range 27.25-27.4. In this part of the channel its maximum contribution ranged between 15-20% (section B7) to 25-30% (sections B1 and B2) resulting at most in a variability of 60% in the aforementioned density range. However, compared with historical sections (sections B11, B12 and B13 in addendum; figures 48(ii)a, 49(ii)a and 50(ii)a) the observed variability in the maximum RSIW contribution was in excess of 100%. This variability was also observed at the southern mouth of the channel where the maximum observed variability was 100% when comparing the RSIW content of sections B6 and B9. The maximum RSIW contributions for these two sections at the southern mouth of the channel were 10-15% and 20-25% respectively. Although slightly less than observed in the northern part of the channel, this was a much larger contribution than observed east of Madagascar over this density range. In terms of its distribution over this density range RSIW spreading appears layer-like in the northern part of the channel whilst in the southern part it appears confined to the edges of the channel (section B6). This conclusion is supported by section B15 (addendum) which does not extent to the slope. Along this section no RSIW was detected in the upper density range.

The maximum RSIW content ranged from 25-30% (sections B2, B7, B8) to 30-40% (sections B1 and B3) resulting in a variability of around 30% in the northern part of the channel. At the southern mouth, the maximum RSIW contributions ranged from 15-20% (section B6) to 25-30% (section B5). This resulted in variability of around 60% which was also observed in the total transport. This would indicate variable input of RSIW into the Agulhas Current proper over the complete density range. The variability observed in the western half of the channel (sections B5 and B6) was also

observed in the eastern half when comparing section B6 and section B15 in the addendum (figure 52(ii)c). As mentioned above, the variability observed in the maximum RSIW was also observed in the net transport of RSIW. At the northern entrance of the channel, the net transport between the two channel crossings differed by as much as 0.16 Sv whilst at the southern mouth the difference was 0.31 Sv. It needs to be noted that in terms of the total transport, water mass contribution is not the only determining factor as flow and distribution also plays an important role in determining the net transport across a section. As was the case in the upper density range, RSIW spreading in the lower density range in the northern part of the channel appears layer–like. In the south, however, RSIW spreading in the lower range appears strongly associated with anti-cyclonic and cyclonic eddies. Comparing cyclonic and anti-cyclonic eddies it appears that the highest RSIW water mass contributions was associated with anti-cyclonic eddies. Much of the low oxygen and high salinity water associated with the cyclonic eddies was found to be NIDW. Section B6 shows RSIW circulating around the outside of the cyclonic eddies, and having variable contributions at different positions around the rings.

In terms of its maximum density range it is evident that RSIW in the Mozambique Channel is detectable as deep as the 27.69 neutral density surface. One does have to be cautious along section B6 where most of the low oxygen and high salinity water was found to be as NIDW rather than RSIW. Along that section all the high salinity, low oxygen water below the 27.6 neutral density surface was found to be NIDW in the western half of the channel. We find the maximum RSIW contribution to be similar to that calculated by You et al. (2003) and Beal et al. (2000) if a 40% dilution is taken into account at the point where the above water types were defined.

Northern Agulhas Current

Sections along the continental slope between the Mozambique Channel and just south of Durban indicate considerable variability in the maximum RSIW contribution over the density range 27.25-27.40. The observed variability was about 100% with the maximum RSIW contributions just off Durban (sections C3 and C4) ranging from 10-15% to 20-25%. This variability is also seen when comparing sections C3 and C1. Section C1 was completed north of section C3 but had the lower RSIW content of the two. In the southern part of region C, the contribution of RSIW (sections C5 and C6)

reaches its lowest value. The contributions range from 5-10% to 10-15% which still resulted in a variability of around 100%. The variability seen in the southern mouth of the Mozambique Channel can thus still be seen in the Agulhas Current proper. Indications in this density range for the sections C1, C3, C4, C5 and C6 (Agulhas Current) were that the RSIW came from the Mozambique Channel as opposed to east of Madagascar if you consider the water mass contributions associated with those areas. For section C2 it is clear that the water mass mixture in the aforementioned density range came from east of Madagascar considering the 5-10% RSIW contribution that far north. It is unclear how eddies spawned south of Madagascar interact with the northern Agulhas Current but for the sections analysed it would appear that the water carried in these eddies flows down the current on the offshore side. This is however not conclusive considering the high offshore RSIW content observed along section C3. As was the case east of Madagascar, the highest RSIW water mass contributions were observed along the continental slope. However, RSIW spreading was not confined exclusively to the slope as offshore cores were observed associated with eddies.

The variability observed in the density range 27.25-27.4 was also clearly visible in the density range 27.4-27.7. Off Durban (sections C3 and C4) the difference in maximum contributions was around 10% and ranged between 10-15% and 20-25% even when NIDW was introduced into the source water matrix. This again resulted in variability of about 100%. This variability as (was the case in the upper density range) was also observed when comparing section C3 with section C1 further north. The variability seen in the maximum RSIW water mass contributions was, as would be expected, also observed in the total transport of these three sections. Off Durban, as the maximum RSIW contributions would suggest, the total transport of RSIW along section C3 was almost double that calculated for section C4, whilst compared to section C1 it was also more than twice the volume. The transport of RSIW for sections C1 and C4 was comparable. In the southern part of region C (sections C5 and C6) the maximum RSIW contributions over this density range were 20-25% and 15-20% even when NIDW was included into the source water mass matrix. This would result in a variability of around 35% which is much smaller than is observed further north. Even so, this would support the observed variable input of RSIW if you consider that these values were higher than that observed along sections C4 and C1 further north. The net

transport of RSIW between sections C6, C4 and C1 were however not very different from each other. The unexpected low transport of RSIW along section C6 considering its maximum RSIW concentration can be largely ascribed to the smaller maximum contribution of RSIW in the upper density range. As observed in the upper density range, RSIW spreading occurs both onshore and offshore of the Agulhas Current. Unlike east of Madagascar, this spreading occurs in one general spreading direction, namely, south-westward. In terms of the maximum range of RSIW spreading it was still observed on the 27.69 neutral density surface even when NIDW was part of the source water mass matrix. In some cases its maximum contribution on this surface was greater than 15% of the water sample. However for section C4, the maximum neutral density upon which RSIW was detected was 27.66 upon which its concentration was just over 5%.

Southern Agulhas Current

In the density range 27.25-27.4 the variability seen in the northern sections was also observed in the southern Agulhas Current. RSIW contribution to its core water sample along the eastern most section (section D1) was at least 10% higher than that found along section C6, the southern-most section analysed in the above region. Also (as was the case further north along section C3) an offshore core was observed along this section. According to the flow pattern this core, although much reduced, is south of the Agulhas Return Current. It cannot be said for certain whether this core rounded the Agulhas Retroflection further west or simply crossed the Agulhas Return Current in the east. The maximum RSIW contribution, as is the case further north, is still concentrated along the continental slope. At the Agulhas Retroflection and in the southeastern South Atlantic, the maximum water mass contribution of RSIW varied mostly between 0-5% to 5-10% except in the case of the MARE sections where in some cases RSIW contributed 10-15% of its water to the sample. If you consider sections D2 and D3, along which the maximum RSIW contribution associated with Agulhas Current ranging from 0-5% to 5-10%, it can be concluded that RSIW contributions in this region vary by as much as 100%. The sparse distribution of data points does however not lend a lot of weight to the above conclusion. Better sampled WOCE sections (sections D12, D13 and D14), other ARC sections (sections D4, D5, D6) and the MARE sections on the other hand do lend support to variable transport of RSIW down the Agulhas Current if we assume a steady mixing regime.

In the density range 27.4-27.7 no variability was observed in the maximum contribution of RSIW associated with the Agulhas Current at the retroflection (sections D2 and D3). Along the two sections analysed its maximum contribution was in the range 10-15%. Indications from the other ARC sections that sampled Agulhas rings (sections D2, D3, D4 and D5) do on the other hand suggest variability in the deeper density range. This was well supported by observations along other sections that crossed Agulhas rings, namely, the MARE I sections (sections D7 and D8) and WOCE sections (sections D11 and D12) where RSIW was almost absent along the one section or side of a ring but still contributed 5-10% in some of the water samples along the other section or side. Rings shed by the Agulhas Current showed the maximum contribution of RSIW at the Agulhas Retroflection and southeastern South Atlantic to range from 0-5% to 10-15% in the aforementioned density range. RSIW spreading in the south-east Atlantic appears strongly associated with Agulhas rings. Its distribution in some cases also appears very patchy with the transport of RSIW mostly mirroring its water mass contribution (compare for example sections D7 and D8). This is not true for sections D11 and D13 along which the maximum water mass contribution of RSIW was in both cases 10-15%. Along these sections the circulation was the determining factor. It can however be concluded that the transport of RSIW into the southeastern South Atlantic is highly variable due to a number of factors. This variability and more important its patchy distribution was not considered by You et al. (2003) and we find their total transport of RSIW to be somewhat over-estimated. In some cases the difference was an order of magnitude. Not all the RSIW transported down the Agulhas Current ends up in the South Atlantic Ocean. The indication from section D2 is that in the absence of ring shedding, RSIW is transported back east via the Agulhas Return Current.

Chapter 6
Conclusions

1) What is the flow pattern of RSIW in the greater Agulhas Current System and is the flow intermittent?

The East Madagascar Current transports the least amount of RSIW towards the Agulhas Current. At most RSIW contributed 10-15% to some of the water samples when NIDW was part of the source water matrix at the southern tip of Madagascar. Despite its small water mass contribution, considerable variation in RSIW contribution was observed in both the 27.25-27.40 and 27.40-27.70 neutral density ranges. With the maximum credible RSIW content east of Madagascar ranging from 6% to 15-20% the resulting observed variability was in excess of 100%. The southward transport of RSIW at the southern tip of Madagascar was mostly confined to the Madagascar continental slope along which the highest RSIW contributions were observed. The offshore cores were observed to be moving either northward or eastward. Recent observations show the transport of water from the East Madagascar Current to the Agulhas Current at least in part to occur via eddies. From the dipole eddies we investigated it would appear, as would be expected, that the eddy formed in the lee of the island has the highest RSIW content. As the section through the eddy dipole and other sections at the southern tip of Madagascar would indicate, most of this transport is confined to the lower density range 27.40-27.70 as opposed to the upper range 27.25-27.40.

In the northern Mozambique Channel, RSIW distribution in the absence of a strong boundary current appears layer-like, with RSIW contributions observed in both the upper and lower density ranges. The presence of cyclonic and anti-cyclonic eddies across the narrowest part of the channel meant that although the net transport of RSIW was southward, not all the RSIW in this layer was moving in the same direction. As the distribution would indicate, this southward transport occurred over the entire density range considered. Further south the, southward spreading of RSIW appears strongly associated with eddies, both cyclonic and anti-cyclonic. The highest RSIW content was found to be associated with anti-cyclonic eddies. In the cyclonic eddies analysed RSIW appears to be circulating around the outside half of the ring. Its distribution around the cyclonic rings also appears variable if you compare the northward and southward flowing limbs of the cyclones. The above conclusions are however strongly dependant on the source water matrix. When NIDW was excluded the highest RSIW content water samples were not associated with the cyclonic eddies.

In terms of content the maximum contribution of RSIW in the northern Mozambique Channel was more than twice that observed East of Madagascar. Using modern data, the variability in the maximum contribution observed east of Madagascar was less clear in the northern part of the channel. When compared to the historical data however, considerable variations in the maximum contribution of RSIW were observed across the narrowest part of the channel as well as to the north of it. The maximum RSIW content ranged from 15-20% to 30-40% in this area which results in an observed variability of about 100%. Whilst there was some variability in the maximum RSIW contribution and transport, the flow southward across the narrowest part of the channel does not appear to be intermittent even though the flow regime differed from being anti-cyclonic to being cyclonic. Variability in the maximum water mass contribution of RSIW observed in the northern Mozambique Channel was also evident at the southern mouth of the channel. The variability was however slightly less extreme compared to that observed further north, and was in the order of around 60% with the highest RSIW content ranging from 15-20% to 25-30%. The variability in the maximum contribution also strongly correlated with the total net transport of RSIW at the southern mouth of the channel.

In the northern Agulhas Current, as was the case east of Madagascar, the highest RSIW content was observed along the continental slope with the occasional lesser offshore core. Different however was the fact that the offshore cores moved in the same general direction as that onshore. As shown in other publications most of the RSIW observed in the Agulhas Current comes from the Mozambique Channel and spreads southward in both the upper and lower density ranges. One of the abovementioned offshore cores was even observed south of the Agulhas Return Current. In terms of RSIW content variability, the northern Agulhas Current displayed similar characteristics as its source water regions. Variability in water mass contributions of RSIW was again about 100% which as in the above cases was also observed in the total net transport of RSIW. The maximum RSIW contribution ranged from 10-15% to 20-25% in this region. The observed variability in the maximum contributions and net transports in the Agulhas Current east of the Agulhas Retroflection thus strongly suggest variable transport of RSIW. No intermittency was however observed. At the Agulhas Retroflection the distribution of RSIW was patchy and in most cases, although much reduced compared to further upstream, observed in

both the upper and lower density ranges. The two sections through the Agulhas Current at the retroflection do not support the conclusion of variable RSIW contributions along the length of the current. Sections through Agulhas rings shed by the current show a different picture with variations in the maximum RSIW contribution observed at different positions around rings. The maximum RSIW content in the rings ranged from 0-5% to 10-15% resulting variability in excess of 100%.

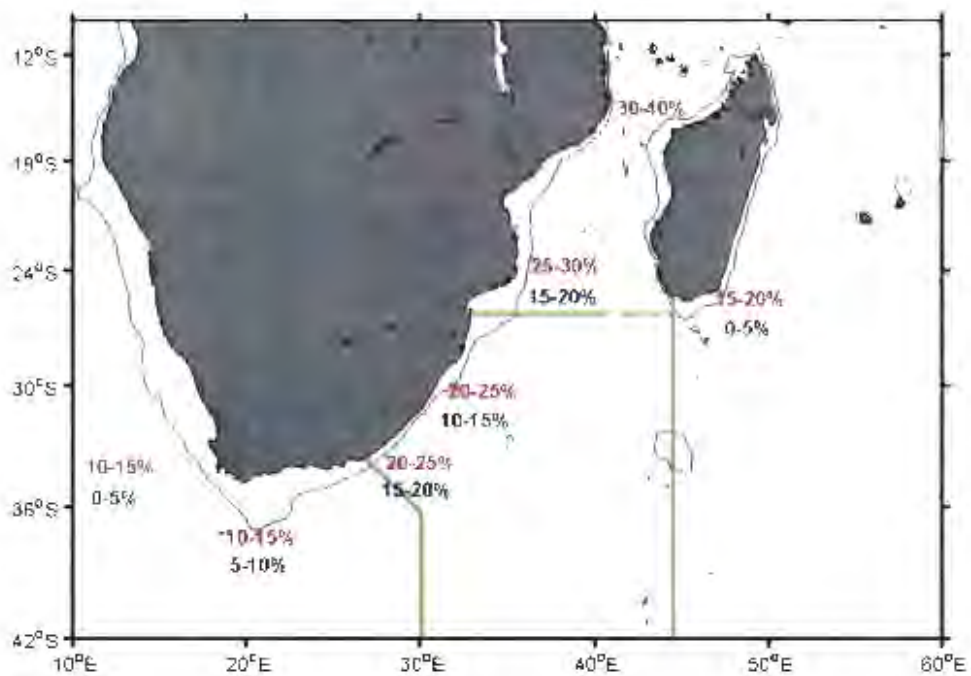

Figure 47(i): Maximum (red) and minimum (blue) RSIW contributions observed at the southern tip of Madagascar, northern part of the Mozambique Channel, southern mouth of the Mozambique Channel, off Durban at 30°S, around 27°E, the Agulhas Retroflection and in the southwest Atlantic Ocean.

From the sum of all the sections analysed it can thus be concluded based on both its maximum water mass contribution as well as the net transport (figure 47(ii)) that the transport of RSIW through the greater Agulhas Current system is highly variable. Inter-ocean fluxes of RSIW can thus only be established along a single hydrographic section or on a meticulously detailed observation of an Agulhas Ring.

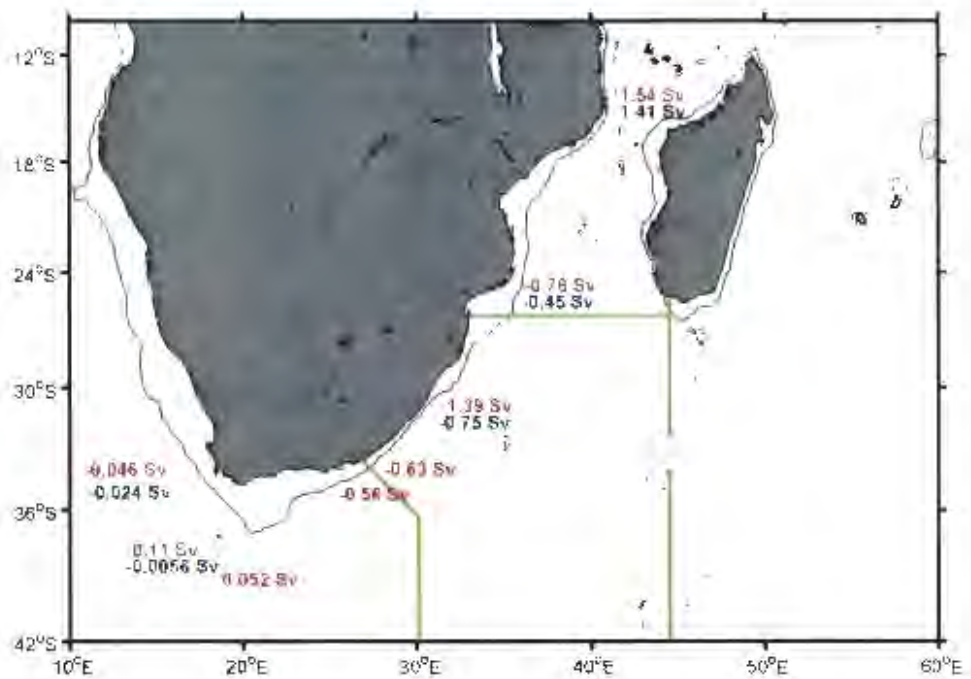

Figure 47(ii): Maximum (red) and minimum (blue) RSIW transports observed at the southern tip of Madagascar, northern part of the Mozambique Channel, southern mouth of the Mozambique Channel, off Durban at 30°S, around 27°E, the Agulhas Retrollection and in the southwest Atlantic Ocean.

2) ***What is the full spreading range of RSIW in the south-west Indian Ocean?***

From the sections analysed it was clear that not all high salinity, low oxygen water observed at intermediate depths along the different sections was RSIW. RSIW does, however, appear to occur as deep as the 27.7 neutral density surface in the south-western Indian Ocean. Its maximum contribution on this surface east of Madagascar can be as low as 5-10%; the remainder of the high salinity, low oxygen water is NIDW (>20% of the water mass content). This was also observed at the southern mouth of the Mozambique Channel along section B6 where most of the high salinity, low oxygen water was NIDW. From the sections analysed in the greater Agulhas Current system it thus clear that without a multi-parameter analysis it would be very difficult to state the origin of high salinity, low oxygen water in the south-western Indian Ocean. This result calls into question much of the earlier work that has been

done in which RSIW and NIDW were not distinguished from one another. In conclusion it can be said that although we cannot say which of the two water masses has the greatest water mass contribution, RSIW will almost always have made some contribution to the low oxygen, high salinity water even as deep as the 27.7 neutral density surface.

References

Arhan, M., Mercier, H., Lutjeharms, J. R. E., 1999. The disparate evolution of three Agulhas rings in the South Atlantic Ocean. Journal of Geophysical Research 104, 20987-21005.

Beal, L. M., Bryden, H., 1997. Observations of an Agulhas undercurrent. Deep-Sea Research I 44, 1715-1724.

Beal, L. M., Bryden, H., 1999. The velocity and vorticity structure of the Agulhas Current at 32°S. Journal of Geophysical Research 104, 5151-5176.

Beal, L. M., Ffield, A., Gordon, A. L., 2000. The spreading of Red Sea overflow waters in the Indian Ocean. Journal of Geophysical Research 105, 8549-8564.

Beal, L. M., Chereskin, T. K., Bryden, H. L., Ffield, A., 2003. Variability of water properties, heat and salt fluxes in the Arabian Sea, between the onset and wane of the 1995 southwest monsoon. Deep Sea Research II 50, 2049-2075.

Boebel, O., Lutjeharms, J. R. E., Schmid C., Zenk, W., Rossby, T., Barron, C., 2003. The Cape Cauldron: a regime of turbulent inter-ocean exchange. Deep-Sea Research II 50, 57-86.

Bower, A. S., Hunt, H. D., Price, J. F., 2000. Character and dynamics of the Red Sea and Persian Gulf. Journal of Geophysical Research 105, 6387-6414.

Bower, A. S., Fratantoni, D. M., Johns, W. E., Peters, H., 2002. Gulf of Aden eddies and their impact on Red Sea Water. Geophysical Research Letters 29, 2025, doi:10.1029/2002GL015342.

Bower, A. S., Johns, W. E., Fratantoni, D. M., Peters, H., 2005. Equilibration and circulation of Red Sea Outflow Water in the western Gulf of Aden. Journal of Physical Oceanography 35, 1963-1985.

Bray, N. A., Wijffels, S. E., Chong, J. C., Fieux, M., Hautala, S., Meyers, G., Morawitz, W. M. L., 1997. Characteristics of the Indo-Pacific throughflow in the eastern Indian Ocean. Geophysical Research Letters 24, 2569-2572.

Bryden, H. L., Beal, L. M., 2001. Role of the Agulhas Current in the Indian Ocean circulation and associated heat and freshwater fluxes. Deep-Sea Research I 48, 1821-1845.

Broecker, W. S., Takahashi, T., 1985. Sources and flow patterns of deep-ocean waters as deduced from potential temperature, salinity, and initial phosphate concentration. Journal of Geophysical Research 90, 6925-6939.

Byrne, D. A., Gordon, A. L., Haxby, W. F., 1995. Agulhas eddies: A synoptic view using Geosat ERM data. Journal of Physical Oceanography 25, 902-917.

Chapman, P., Di Marco, S. F., Davis, R. E., Coward, A. C., 2003. Flow at intermediate depths around Madagascar based on ALACE float trajectories. Deep-Sea Research II 50, 1957-1986.

Cember, R. P., 1988. On the sources, formation and circulation of Red Sea deep water. Journal of Geophysical Research 93, 8175-8191.

de Ruijter, W. P. M. and Boudra, D. B., 1985. The wind-driven circulation of the South Atlantic-Indian Ocean—I. Numerical experiments in a one-layer model. Deep-Sea Research **32**, 557–574.

de Ruijter, W. P. M., Biastoch, A., Drijfhout, S. S., Lutjeharms, J. R. E., Matano, R. P., Pichevin, T., van Leeuwen, P. J. and Weijer, W., 1999. Indian-Atlantic inter-ocean exchange: dynamics, estimation and impact. Journal of Geophysical Research **104**, 20885–20910.

de Ruijter, W. P. M., Ridderinkhof, H., Lutjeharms, J. R. E., Schouten, M. W., Veth, C., 2002. Observations of the flow in the Mozambique Channel. Geophysical Research Letters 29(10), 1401-1403.

de Ruijter, W. P. M., van Aken, H. M., Beier, E. J., Lutjeharms, J. R. E., Matano, R. P., Schouten, M. W., 2004. Eddies and dipoles around South Madagascar: formation, parthways and large-scale impact. Deep-Sea Research I 51, 382-400.

DiMarco, S. F., Chapman, P., Nowlin, W. D., Jr., 2000. Satellite observations of upwelling on the continental shelf south of Madagascar. Geophysical Research Letters 27, no. 27, 3965-3968.

DiMarco, S. F., Chapman, P., Nowlin, W. D., Jr., Hacker, P., Donohue, K., Luther, M., Johnson, G.C., Toole, J., Nowlin, J., 2002. Volume transport and property distributions of the Mozambique Channel. Deep-Sea Research. II 49, 1481-1511.

Donohue, K. A., Beal, L. M., Firing, E., 2000. Comparison of three velocity sections of the Agulhas Current and Agulhas Undercurrent. Journal of Geophysical Research 105, 28585-28593.

Donohue, K. A., Toole, J. M., 2003. A near-synoptic survey of the Southwest Indian Ocean. Deep-Sea Research II 50, 1893-1931.

Eshel, G., Cane, M. A., Blumenthal, M. B., 1994. Modes of subsurface, intermediate, and deep water renewal in the Red Sea. Journal of Geophysical Research 99, 15941-15952.

Fine, R. A., 1993. Circulation of Antarctic intermediate water in the South Indian Ocean. Deep-Sea Research I 40, 2021-2042.

Fisher, J., Schott, F., Stramma, L., 1996. Currents and transports of the Great Whirl-Socotra Gyre system duting the summer monsoon, August 1993. Journal of Geophysical Research 101, 3573-3587.

Gordon, A. L., Lutjeharms, J. R. E., Gründlingh, M. L, 1987. Stratification and circulation at the Agulhas Retroflection. Deep-Sea Research 34, 565-599.

Gründlingh, M. L., 1983. On the course of the Agulhas Current. South African Geographic Journal 65, 49-57.

Gründlingh, M. L., 1985. Occurrence of Red Sea water in the southwestern Indian Ocean. Journal of Physical Oceanography 15, 207-212.

Gründlingh, M. L., 1987. Cyclogenesis in the Mozambique Ridge Current. Deep-Sea Research 36, 149-153.

Gründlingh, M. L., 1993. On the winter flow in the southern Mozambique Channel. Deep-Sea Research I 40, 409-418.

Harris, T. F. W., 1972. Sources of the Agulhas Current in the spring of 1964. Deep-Sea Research 19, 633-650.

Jean-Baptiste, P., Fourré, E., Metzl, N., Ternon, J. F., Poisson, A., 2004. Red Sea deep water circulation and ventilation rate deduced from the 3He and 14C tracer fields. Journal of Marine Systems 48, 37-50.

Lutjeharms, J. R. E., 1988. On the role of the East Madagascar Current as a source of the Agulhas current. South African Journal of Science 84, 236-238.

Lutjeharms, J. R. E., Ansorge, I. J., 2001. The Agulhas Return Current. Journal of Marine Systems, 30, 115-138.

Lutjeharms, J. R. E., Bang, N. D., Duncan, C. P., 1981. Characteristics of the Currents East and South of Madagascar. Deep-Sea Research 28, 879-899.

Lutjeharms, J. R. E., Catzel, R., Valentine, H. R., 1989. Eddies and other boundary phenomena of the Agulhas Current. Continental Shelf Research 9, 597-616.

Lutjeharms, J.R.E., Cooper, J., 1996. Interbasin leakage through Agulhas current filaments. Deep-Sea Research I, 43 , 213-238.

Lutjeharms, J. R. E., Gordon, A. L., 1987. Shedding of an Agulhas ring observed at sea, Nature, 331, 251-254.

Lutjeharms, J. R. E., Machu, E., 2000. An upwelling cell inshore of the East Madagascar Current. Deep-Sea Research I 47, 2405-2411.

Lutjeharms, J. R. E., Roberts, H. R., 1988. The Natal Pulse: An extreme transient on the Agulhas Current. Journal of Geophysical Research 93, 631-645.

Lutjeharms, J. R. E., Valentine, H. R., 1988. Evidence for persistent Agulhas rings south-west of Cape Town. South African Journal of Science 84, 781-783.

Lutjeharms, J. R. E., Valentine, H. R., 1988. Eddies at the subtropical convergence south of Africa. Journal of Physical Oceanography 18, 761-774.

Lutjeharms, J. R. E., van Ballegooyen, R. C., 1984. Topographic control in the Agulhas Current system. Deep-Sea Research 31, 1321–1337.

Lutjeharms, J. R. E., van Ballegooyen, R. C., 1988. The retroflection of the Agulhas Current. Journal of Physical Oceanography 18, 1570-1583.

Maillard, C., 1974. Fromation d'eau profonde en Mer Rouge, in La Formation des Eax Oceaniques Profondes, pp. 115-125, Cent. Natl. de la Rech. Sci., Paris.

Mantyla, A. W., Reid, J. L., 1995. On the origins of deep and bottom waters of the Indian Ocean. Journal of Geophysical Research 100, 2417-2439.

Matano, R. P., 1996. A numerical study of the Agulhas retroflection: The role of bottom topography. Journal of Physical Oceanography 26, 2267-2301.

McCarthy, M. S., 1977. Subantarctic mode water. Deep-Sea Research 24, suppl., 103-119.

McDonagh, E. L., Heywood, K. J., Meredith, M. P., 1999. On the structure, paths, and fluxes associated with Agulhas rings. Journal of Geophysical Research 104, 21007-21020.

Menaché, M., 1963. Premier Campagne Océanographique du "Commandant Robert Giraud" dans le canal de Mozambique, 11 Octobre–28 Novembre 1957. Cahiers Océanographiques XV, 224–249 (in French).

Morcos, S. A., 1970. Physical and chemical oceanography of the Red Sea. Oceanography and Marine Biology: Annual Review 8, 73-202.

Murray, S. P., Johns, W., 1997. Direct observations of seasonal exchange through the Bab el Mandab Strait. Geophysical Research Letters 24, 2557-2560.

Olson, D. B., Evans, R. H., 1986. Rings of the Agulhas Current. Deep Sea Research 33, 27-42.

Ou, H. W., de Ruijter, W. P. M., 1986. Seperation of an inertial boundary current from an irregular coastline. Journal of Physical Oceanograpy 16, 280-289.

Piola, A. R., Gordon, A. L., 1989. Intermediate water in the southwest South Atlantic. Deep-Sea Research I 36, 1-16.

Poole, R., Tomczak, M., 1999. Optimum multiparameter analysis of the water mass structure in the Atlantic Ocean thermocline. Deep-Sea Research I 46, 1895-1921.

Privett, D. W., 1959. Monthly charts of evaporation from the North Indian Ocean, including the Red Sea and the Persian Gulf. Quarterly Journal of the Royal Meteorological Society 85, 424-428.

Quadfasel, D. R., Schott, F., 1982. Water-mass distribution at intermediate layers off the Somali coast during the onset of the southwest monsoon, 1979. Journal of Physical Oceanography 12, 1358-1372.

Quadfasel, D. R., Swallow, J., 1986. Evidence of a 50-day period planetary waves in the South Equatorial Current of the Indian Ocean. Deep-Sea Research I 33,1307-1312.

Quartly, G. D., Srokosz, M. A., 2002. SST Observations of the Agulhas and East Madagascar retroflection by the TRMM microwave imager. Journal of Physical Oceanography 32, 1585-1592.

Ridderinkhof, H., de Ruijter, W. P. M., 2003. Moored current observations in the Mozambique Channel. Deep-Sea Research II 50, 1933-1955.

Schott, F. A., Fieux, M., Kindle, J., Swallow, J., Zantopp, R., 1988. The boundary currents east and north of Madagascar. 2. Direct measurements and model comparison. Journal of Geophysical Research 93, 4963-4974.

Schott, F. A., Fisher, J., 2000. Winter monsoon circulation of the northern Arabian Sea and Somali Current. Journal of Geophysical Research 105, 6359-6376.

Schouten, M. W., de Ruijter, W. P. M., Van Leeuwen, P. J., 2002. Upstream control of Agulhas Ring Shedding. Journal of Geophysical Research 107, 21913-21925

Schouten, M. W., de Ruijter, W. P. M., Van Leeuwen, P. J., Lutjeharms, J. R. E., 2000. Translation, decay and splitting of Agulhas Rings in the south-east Atlantic Ocean. Journal of Geophysical Research 105, 21,913-21,925.

Schouten, M. W., de Ruijter, W. P. M., Van Leeuwen, P. J., Ridderinkhof, H., 2003. Eddies and variability in the Mozambique Channel. Deep-Sea Research. II 50, 1987-2003.

Shapiro, G. I., Meschanov, S. L., 1991. Distribution and spreading of Red Sea Water and salt lens formation in the northwest Indian Ocean. Deep-Sea Research I 38, 21-34.

Shapiro, G. I., Meschanov, S. L., Polonsky, A. B, 1994. Red Sea water lens formation in Arabian Sea. Oceanology 34 , 26-31.

Shenoi, S. S. C., Saji, P. K., Almeida, A. M., 1999. Near-surface circulation and kinetic energy in the tropical Indian Ocean derived from Lagrangian drifters. Journal of Marine Research 57, 885-907.

Spencer, D., Broecker, W. S., Craig, H., Weiss, R. F., 1982. GEOSECS Indian Ocean Expedition, vol. 6, Section and profiles, 140 pp., National Science Foundation, Washington, D. C.

Sofianos, S. S., Johns, W. E., Murray, S. P., 2002. Heat and freshwater budgets in the Red Sea from direct observations at Bab el Mandeb. Deep-Sea Research II 49,1323-1340.

Stramma, L., 1992. The South Indian Ocean Current. Journal of Physical Oceanography 22, 421-430.

Stramma, L., Lutjeharms, J. R. E., 1997. The flow field of the subtropical gyre of the South Indian Ocean. Journal of Geophysical Research 102, 5513-5530.

Toole, J. M., Warren, B. A., 1993. A hydrographic section across the subtropical South Indian Ocean. Deep-Sea Research I 40, 1973-2019.

Swallow, J., Fieux, M., Schott, F., 1988. Boundary currents east and north of Madagascar. 1. Geostrophic currents and transport. Journal of Geophysical Research 93, 4951-4962.

Tchernia , P., 1980. The Indian Ocean. In: Descriptive Regional Oceanography. Pergamon Marine Series 3, pp. 171–215.

Tomczak, M., 1999. Some historical, theoretical and applied aspects of quantitative water mass analysis. Journal of Marine Research 57, 275-303.

Tomczak M., Large, D. G. B., 1989. Optimum Multiparameter Analysis of Mixing in the Thermocline of the Eastern Indian Ocean. Journal of Geophysical Research 94, 16141-16149.

Valentine, H. R., Lutjeharms, J. R. E., Brundrit, G. B., 1993. The water masses and volumetry of the southern Agulhas Current region. Deep-Sea Research I 40, 1285-1305.

van Aken, H. M., van Veldhoven, A. K., Veth, C., de Ruijter, W. P. M., van Leeuwen, P. J., Drijfhout, S. S., Whittle, C. P., Rouault, M., 2003. Observations of a young Agulhas ring, Astrid, during MARE in March 2000. Deep-Sea Research II 50, 167-195.

van der Vaart, P. C. F., de Ruijter, W. P. M., 2001. Stability of western boundary currents with an application to pulselike behavior of the Agulhas Current. Journal of Physical Oceanography 31, 2625-2644.

van Leeuwen, P.J., de Ruijter, W.P.M. and Lutjeharms, J.R.E., 2000. Natal Pulses and the formation of Agulhas Rings. Journal of Geophysical Research **105**, 6425–6436.

Veronis, G., 1973. Model of the world ocean circulation: I. Wind-driven, two layer. Journal of Marine Research 31, 228-288.

Warren, B. A., 1981. Transindian hydrographic section at lat. 18°S: property distributions and circulation in the South Indian Ocean. Deep-Sea Research 28, 859-864.

Warren, B. A., 1992. Circulation of North Indian Deep Water in the Arabian Sea. Oceanography of the Indian Ocean. Edited by B. N. Desai, Oxford and IBH, New Delhi.

Warren, B. A., Johnson, G. C., 1992. Deep currents in the Arabian Sea in 1987. Marine Geology 104, 279-288.

Warren, B. A., Sommel, H., Swallow, J. C., 1966. Water masses and patterns of flow in the Somali Basin during the southwest monsoon of 1964. Deep-Sea Research 13, 825-860.

Weijer, W., de Ruijter, W. P. M., Dijkstra, H. A., van Leeuwen, P. J., 1999. Impact of interocean exchange on the Atlantic overturning circulation. Journal of Physical Oceanography 29, 2266-2284.

Weijer, W., de Ruijter, W. P. M., Dijkstra, H. A., 2001. Stability of the Atlantic overturning circulation: competition between Bering Strait freshwater flux and Agulhas heat and salt sources. Journal of Physical Oceanography 31, 2385-2402.

Wijffels, S., Sprintall, J., Fieux, M., Bray, N., 2002. The JADE and WOCE I10/IR6 Throughflow sections in the southeast Indian Ocean. Part 1: water mass distribution and variability. Deep-Sea Research II 49, 1341-1362.

Woelk, S., Quadfasel, D., 1996. Renewal of deep water in the Red Sea during 1982-1987. Journal of Geophysical Research 101, 18155-18165.

Wyrtki, K., 1971. Oceanographic Atlas of the International Indian Ocean Expedition, National Science Foundation, Washington, D. C.

Wyrtki, K., 1974. On the deep circulation of the Red Sea, in La Formation des Eax Oceaniques Profondes, pp. 91-106, Cent. Natl. de la Rech. Sci., Paris.

You, Y., 1998. Intermediate water circulation and ventilation of the Indian Ocean derived from water-mass contributions. Journal of Marine Research 56, 1029-1067.

You, Y., 1999. Dianeutral mixing, transformation and transport of the deep water of the Indian Ocean. Deep-Sea Reseach I 46, 109-148.

You, Y., 2000. Implications of the deep circulation and ventilation of the Indian Ocean on the renewal mechanism of North Atlantic Deep Water. Journal of Geophysical Research 105, 23895-23926.

You, Y., 2002. Quantitative estimate of Antarctic Intermediate Water contributions from the Drake Passage and the southwest Indian Ocean to the South Atlantic. Journal of Geophysical Research 107, 10.1029/2001JC000880.

You, Y., Lutjeharms, J. R. E, Boebel, O., de Ruijter, W. P. M., 2003. Quantification of the interocean exchange of intermediate water masses around southern Africa. Deep-Sea Research II 50, 197-228.

Addendum

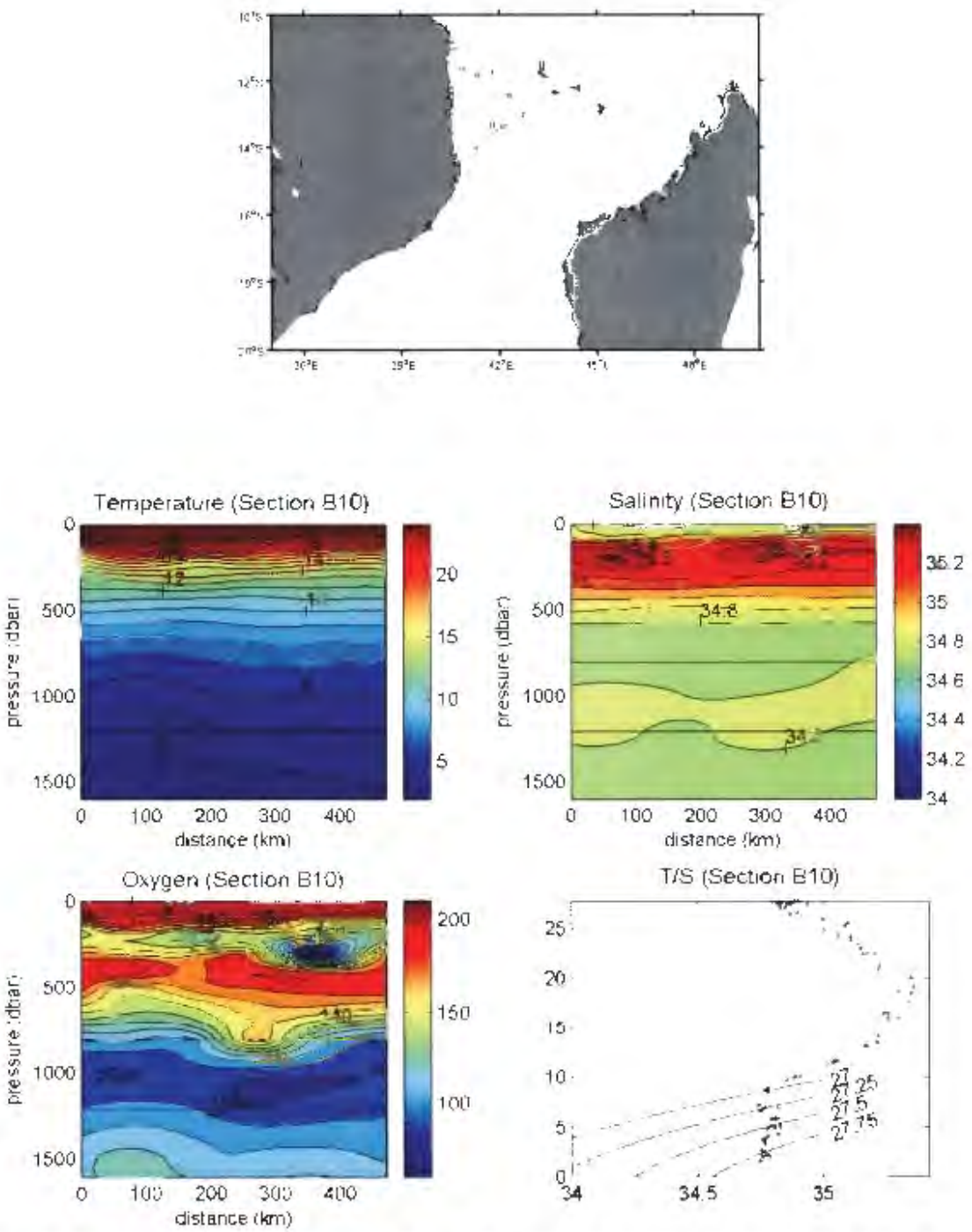

Fig 48(i): Map showing station positions of section B10 (a) with property plots of temperature, salinity, oxygen and a T/S plot.

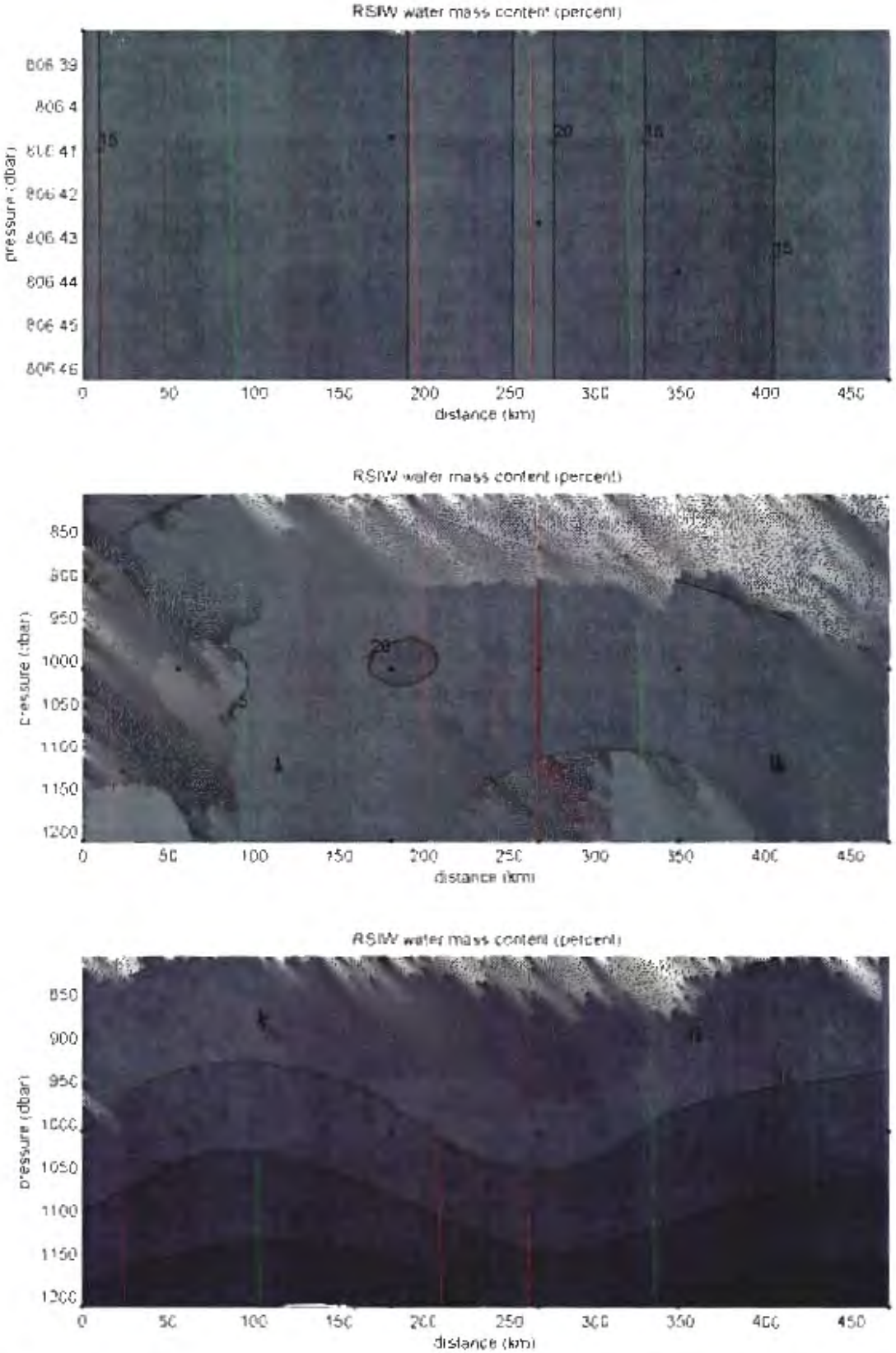

Fig 48 (ii): RSIW contribution over the density range 27.25-27.40 (a) as well as RSIW contribution without (b) and with (c) NIDW in the source water matrix over the density range 27.40-27.70 along section B10

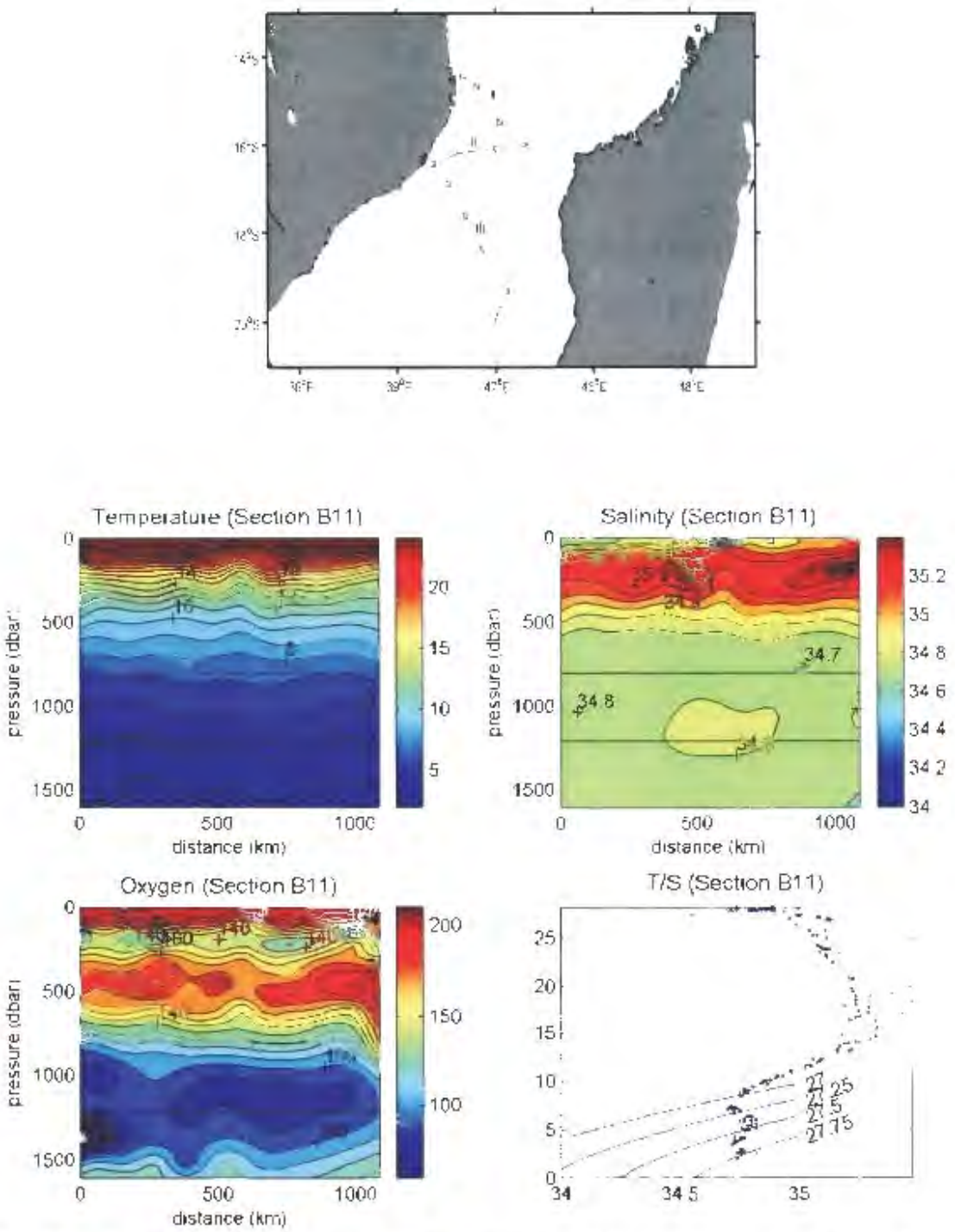

Fig 49(i): Map showing station positions of section B11 (a) with property plots of temperature, salinity, oxygen and a T/S plot.

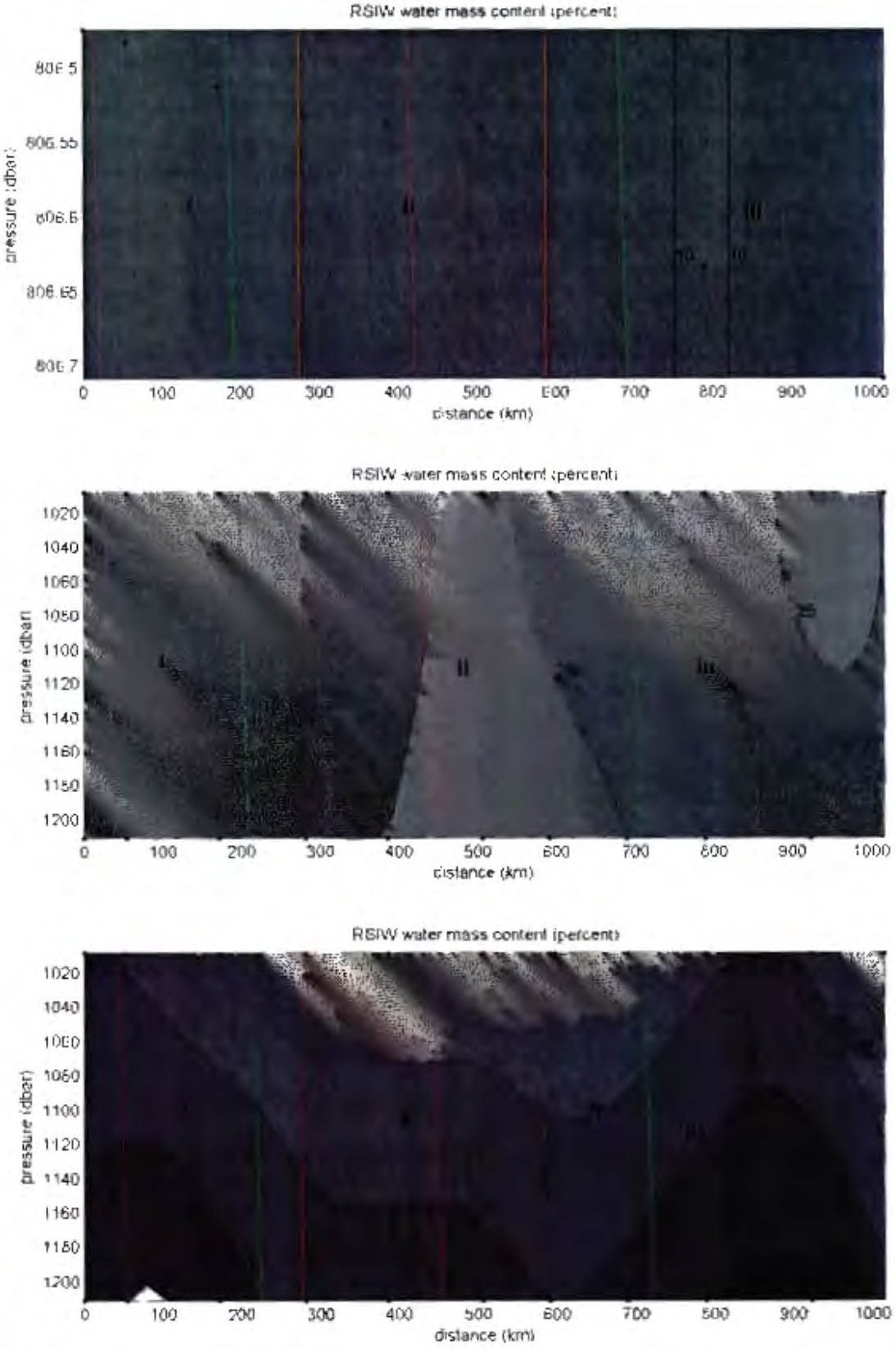

Fig 49 (ii): RSIW contribution over the density range 27.25-27.40 (a) as well as RSIW contribution without (b) and with (c) NIDW in the source water matrix over the density range 27.40-27.70 along section B11

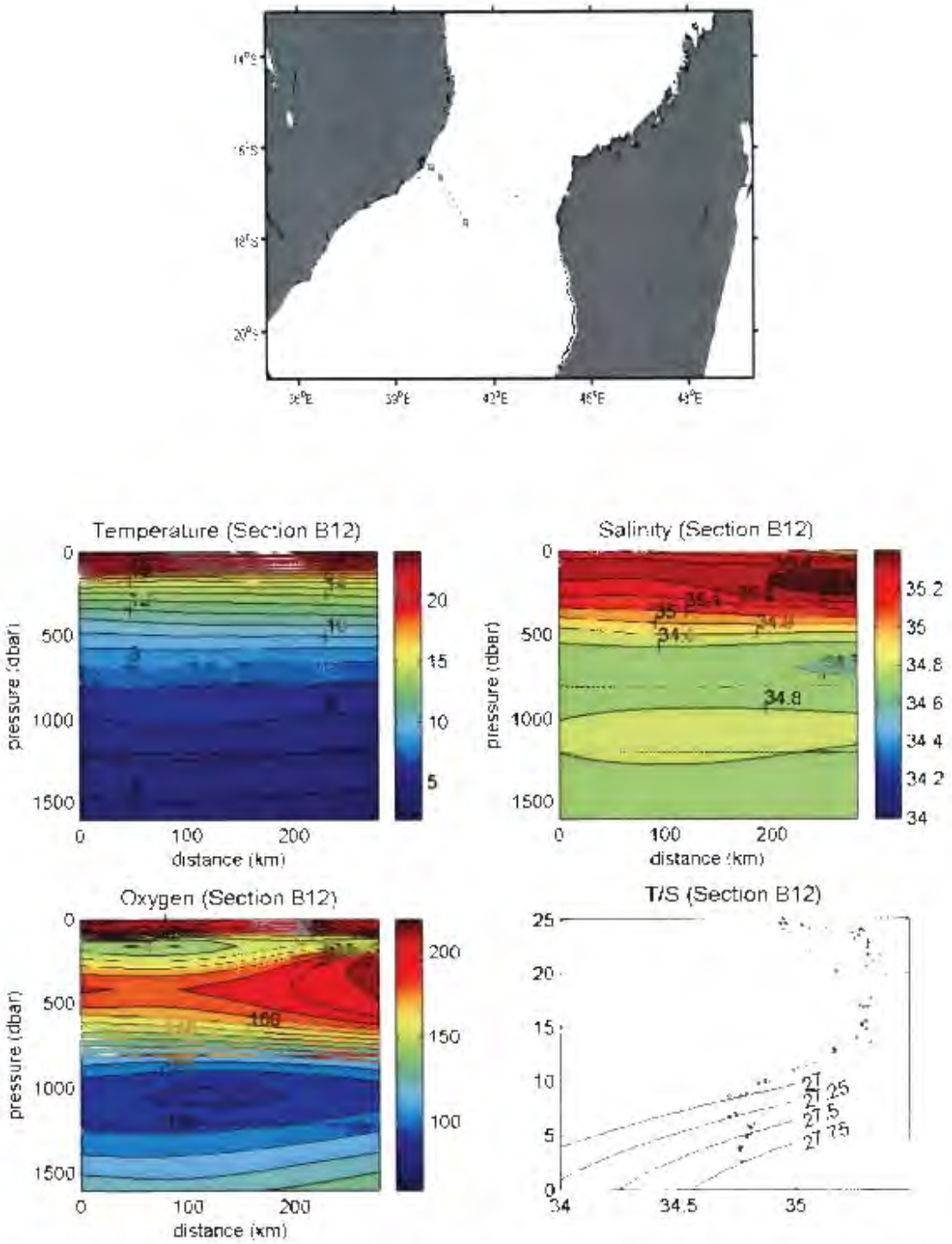

Fig 50(i): Map showing station positions of section B12 (a) with property plots of temperature, salinity, oxygen and a T/S plot.

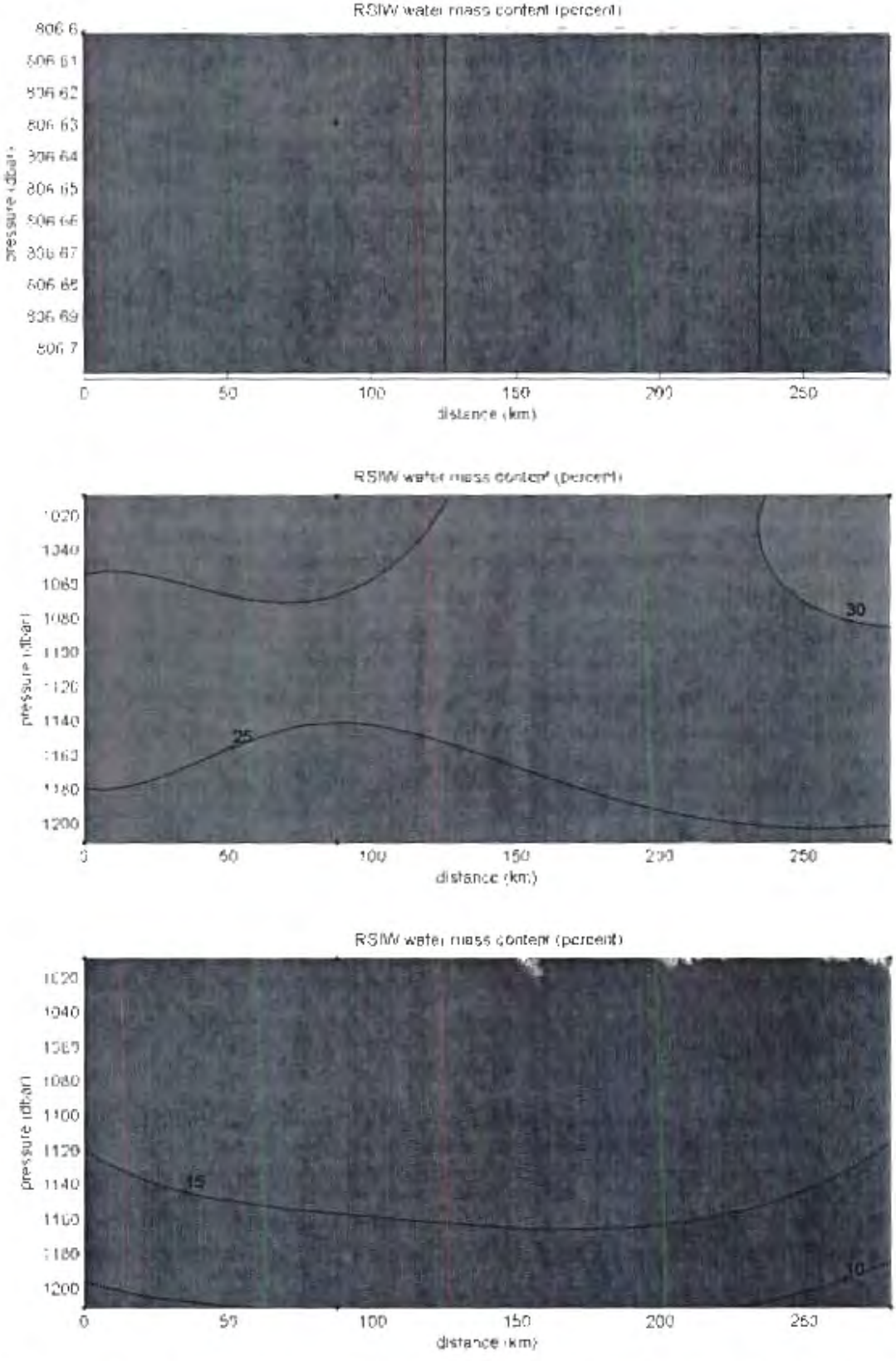

Fig 50(ii): RSIW contribution over the density range 27.25-27.40 (a) as well as RSIW contribution without (b) and with (c) NIDW in the source water matrix over the density range 27.40-27.70 along section B12

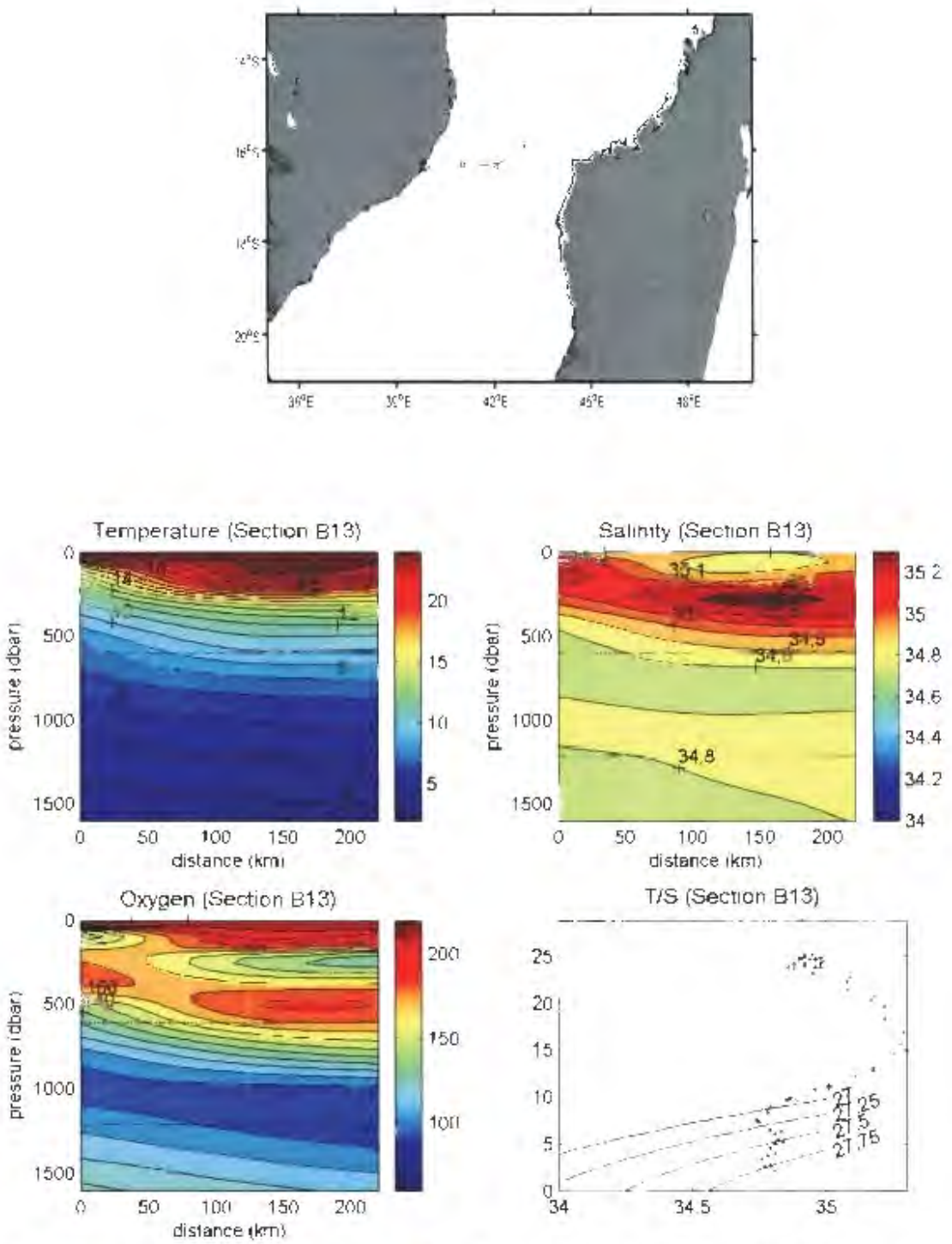

Fig 51(j): Map showing station positions of section B13 (a) with property plots of temperature, salinity, oxygen and a T/S plot.

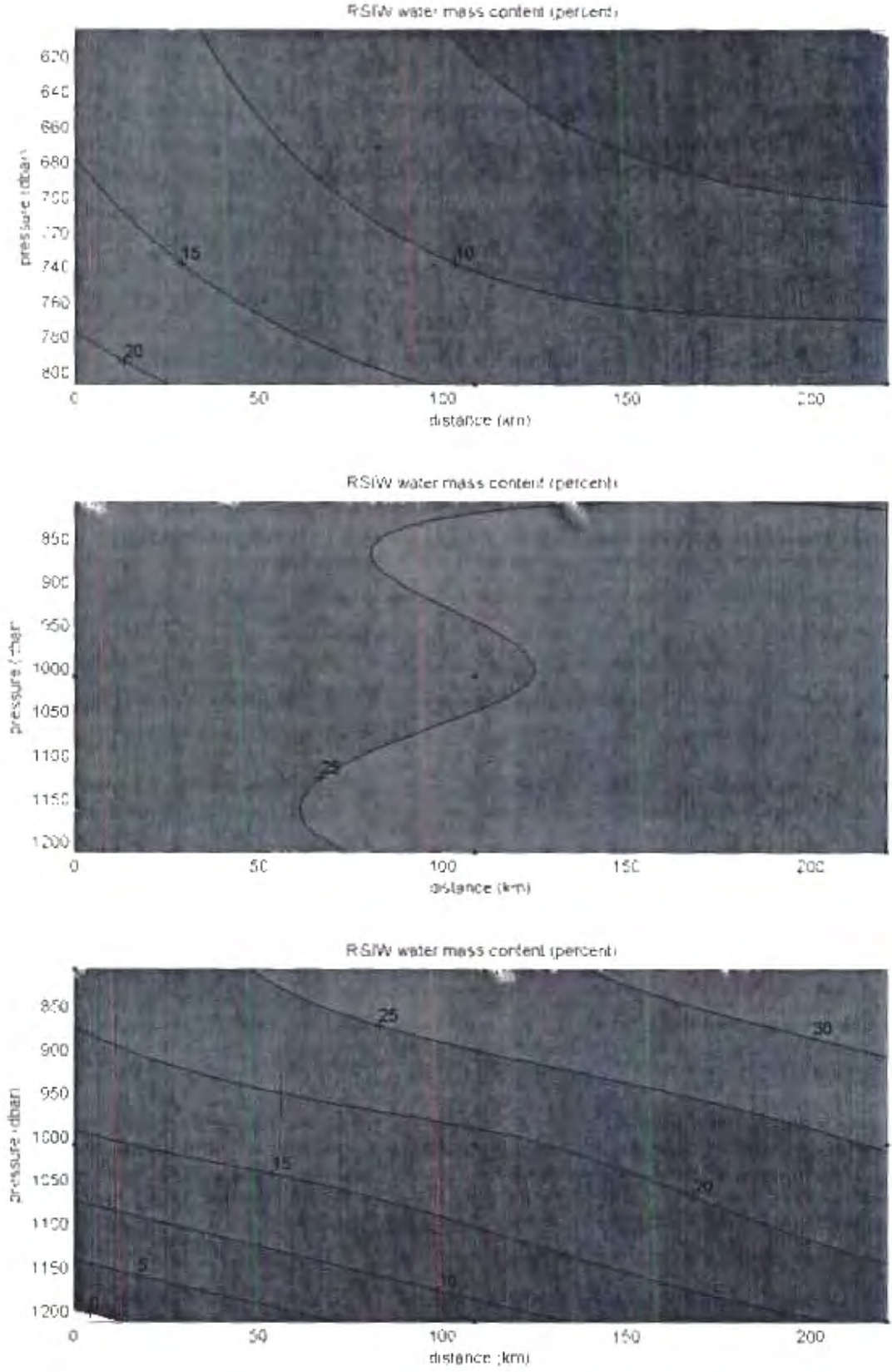

Fig 51(ii): RSIW contribution over the density range 27.25-27.40 (a) as well as RSIW contribution without (b) and with (c) NIDW in the source water matrix over the density range 27.40-27.70 along section B13

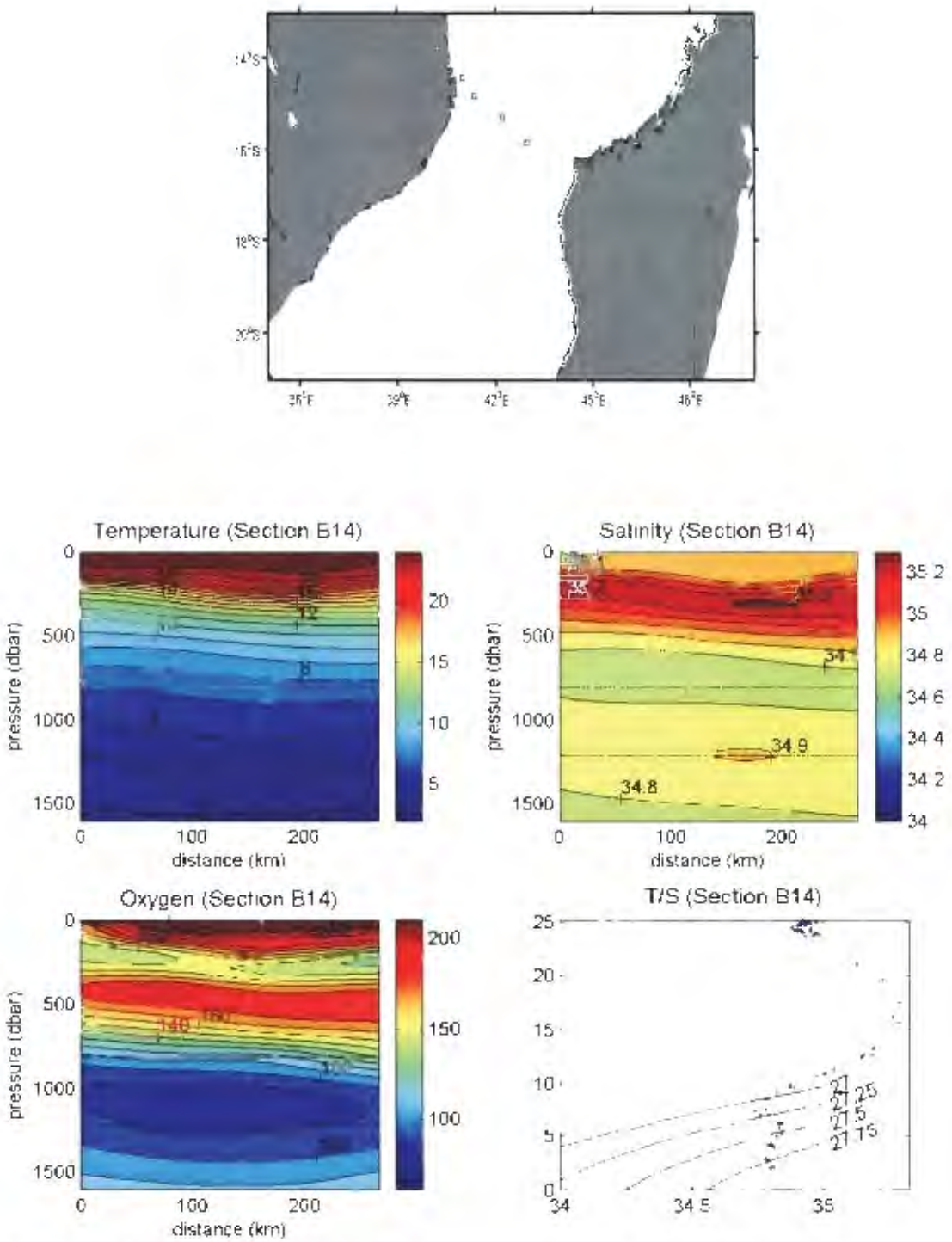

Fig 52(i): Map showing station positions of section B14 (a) with property plots of temperature, salinity, oxygen and a T/S plot.

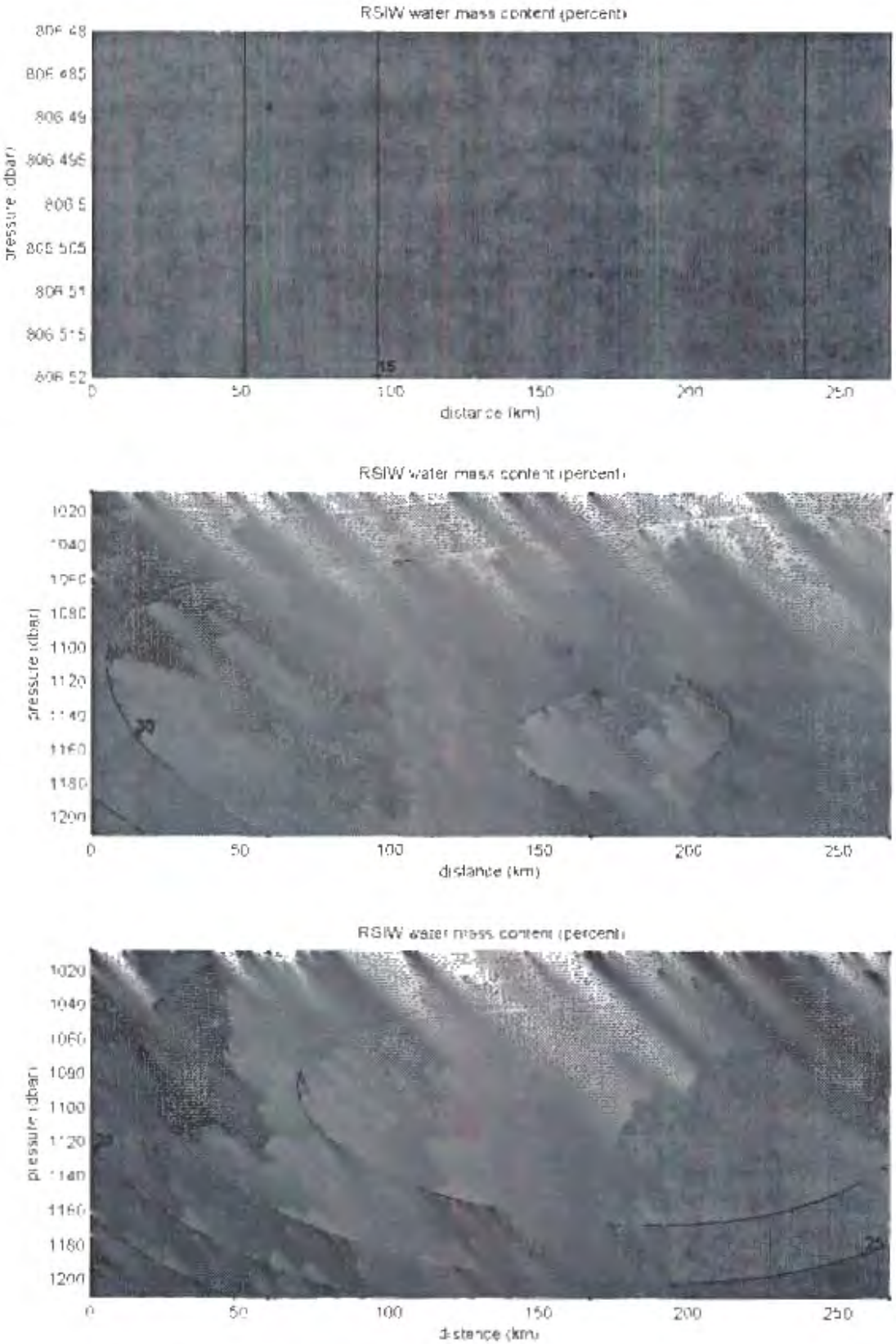

Fig 53(a): RSIW contribution over the density range 27.25-27.40 (a) as well as RSIW contribution without (b) and with (c) NIDW in the source water matrix over the density range 27.40-27.70 along section B14

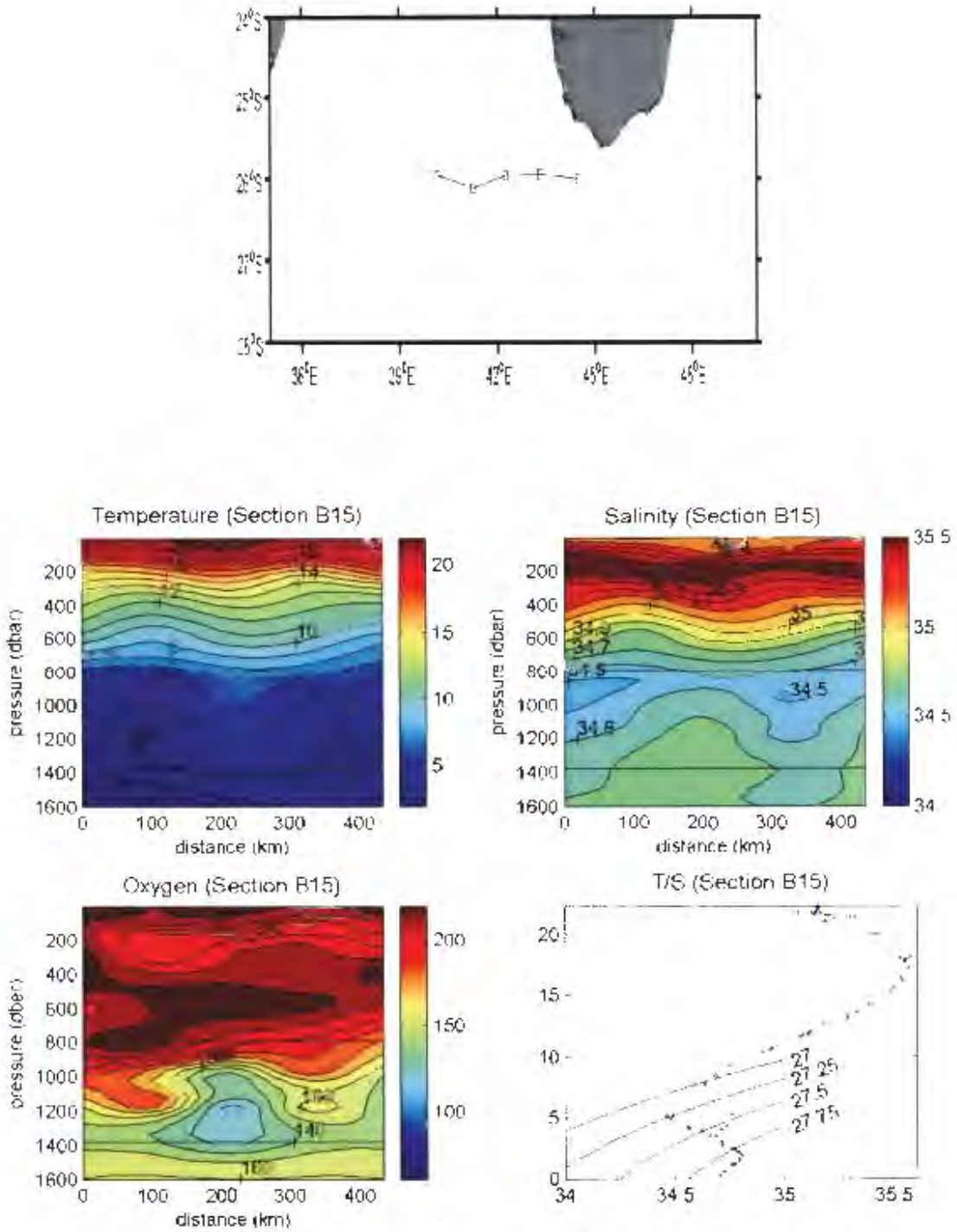

Fig 53(i): Map showing station positions of section B15 (a) with property plots of temperature, salinity, oxygen and a T/S plot.

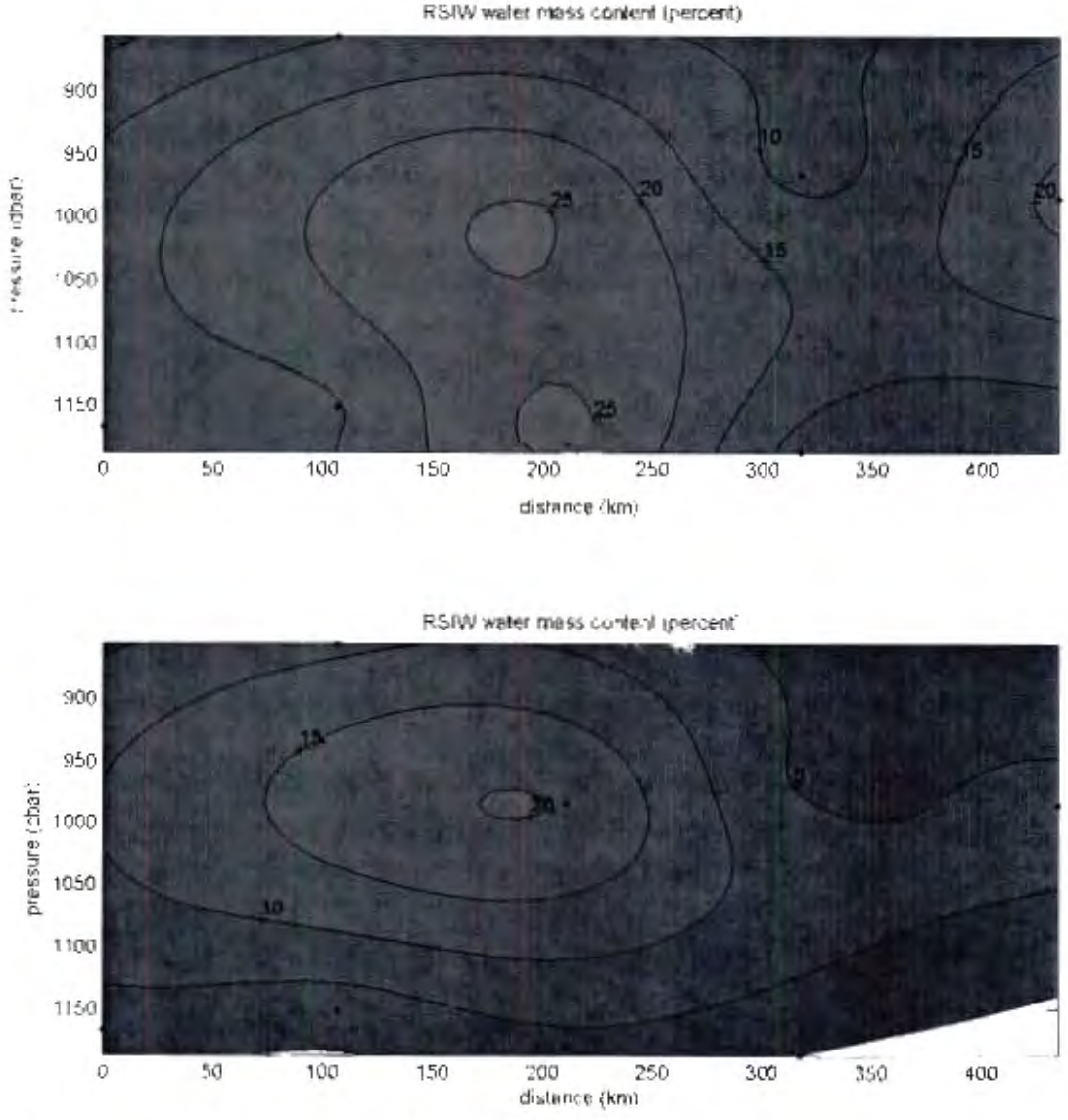

Fig 53(ii): RSIW contribution without NIDW as a source water (a) as well as RSIW contribution with NIDW in the source water matrix over the density range 27.40-27.70 along section B15